THE INFLUENCE OF SLURRY VISCOSITY ON HYDROCYCLONE PERFORMANCE

Jason G. Waters

August 2012

CENTRE FOR MINERALS RESEARCH

THE INFLUENCE OF SLURRY VISCOSITY ON HYDROCYCLONE PERFORMANCE

By

Jason Waters

Thesis presented for the degree of Master of Science in Engineering
in the Department of Chemical Engineering

AUGUST 2012

STATEMENT OF ORIGINALITY

I declare that this thesis, submitted for the degree of Master of Science in Engineering at the University of Cape Town, is my own work and has not been submitted prior to this for any degree at this university or any other institution. I know the meaning of plagiarism and declare that all the work in the document, save for that which is properly acknowledged, is my own.

Jason Waters

SYNOPSIS

Many of the empirical hydrocyclone cut size models available consider the feed solids content to be an important variable in determining the efficiency and resultant classification. However, feed viscosity as a whole is admittedly a more accurate variable to consider as it can be affected by many factors, including solids content, particle size distribution, particle size, mineralogy, pulp chemistry, particle shape and carrier fluid temperature. Earlier theoretical models did try to incorporate slurry viscosity but were developed for very low solids content systems due to the difficulty in measuring slurry viscosity at higher concentrations. Current hydrocyclone models being applied in industry have difficulty in predicting rheological fluctuations at constant solids content, for example with an increase in feed clay content. Investigations, focussed on expanding the studies of previous researchers in this area, were conducted.

Experiments involved the design and operation of two test rigs incorporating three hydrocyclone sizes (75,100, 165 mm), with two different ore types (platreef ore, copper ore) from a secondary stage operation used as the feed material. A change in relative viscosity was investigated by altering the viscosity of the carrier fluid (water) by the addition of sucrose, and modification of the slurry temperature. Hydrocyclone feed flow rate and solids content were also modified. A custom made on-line tube rheometer allowed viscosities of feed concentrations of up to 43% (by vol.) to be measured over a range of shear rates (200/s to 1500/s). The slurries under investigation were found to be settling in nature, and therefore a decision was made to exclude data below the critical settling velocity of the tube. Rheological characterisations revealed both ore types exhibited Bingham plastic behaviour. A concentration versus viscosity relationship was determined from the rheological data and the resultant viscosity values were then linked to hydrocyclone efficiency.

The significant findings of this work included the following:

- Increased pulp viscosity achieved by 1) sucrose addition and 2) decreased slurry temperatures resulted in a drop in hydrocyclone performance attributed to the combined effect on the partition curve parameters namely - an increased cut size (d_{50c}), decreased water split to O/F (C) and reduced value of alpha.

- Increased pulp viscosity achieved by 3) feed solids content had dissimilar effects on the partition curve parameters. An optimum viscosity point was reached for water

split to O/F and alpha parameters, however cut size increased with increased pulp viscosity.

- Rheological effects on the cut size parameter appeared more significant for the largest of the three cyclone body diameters used in the study. This can be attributed to the decreased tangential velocities inside the larger cyclone radius.

The combined rheology and hydrocyclone data from this thesis will provide useful validation data for the new hydrocyclone models currently being developed as part of the P9 project. The models are to be incorporated in the JKSimMet simulation package and consider the effects of viscosity in their equations for cut-size and water split.

ACKNOWLEDGEMENTS

I wish to acknowledge the following persons who contributed either directly or indirectly to this thesis reaching its completion:

Firstly, to my supervisors Dr Aubrey Mainza and Dr Indresan Govender. I thank you for all your valuable input during the thesis and for sharing your wealth of expertise in the relevant fields. One less thesis at 30,000 feet Aubrey.

To Mr. Andre van der Westhuizen and Mrs Jenni Sweet for their inputs and for allowing me the time to enable the thesis to progress during my day job.

To Prof. Malcolm Powell, for demonstrating the enthusiasm required when working in this industry.

To Prof. Dee Bradshaw for how it all began, for the early inspiration and positive reinforcement provided for me to proceed along this path.

To Mr. Lawrence Bbosa for helping preserve my sanity in the office with MOTD discussions and fantasy league rivalries.

To the Centre for Minerals Research laboratory staff for their assistance and humour, in particular to Mr. Rubin van Schalkwyk for his assistance with the hydrocyclone tests and sample processing.

To the workshop staff who assisted with the building of the test rigs, Mr. David Bramble at UCT and Mr. Jannie Barnard at Stellenbosch University.

To Mr. Elton Thyse and Mr. Alvin Peterson at the Stellenbosch University for their assistance with the logistics and in getting the hydrocyclone test rig operational.

To my parents Shirley and Adrian, thanks for always believing, and for encouraging me to take on the challenge.

Last, but certainly not least to all my special girls: To my wife Helouise, and daughters Skye and Summer. My sincere gratitude to Helouise for your belief and patience throughout the years, and for your understanding during the write-up period. I could not have done it without you.

YNWA

CONTENTS

LIST OF FIGURES

LIST OF TABLES

NOMENCLATURE AND ABBREVIATIONS

The symbols most commonly used in the thesis are defined here. Specialized terms and constants that are only used in specific equations are defined in the text itself. In certain cases the same symbol is used with multiple definitions. In that case the equation number is provided.

A : cone angle in Asomah model (degrees)

B1-B4 : Asomah model system constants

C : water split fraction to overflow $=1 - R_f$

C_m : mass concentration (%)

C_v : solids volume fraction

C_w : feed mass fraction, in Lynch/Rao model (%)

d : particle size in efficiency curve

d_i : particle size in size fraction i (µm)

d_P : particle diameter (µm)

d_{50} : 50% cut size (µm)

d_{50c} : corrected cut size (µm)

D : pipe/tube diameter

D_c : hydrocyclone cylinder inside diameter (mm)

D_i : hydrocyclone inlet equivalent inside diameter (mm)

D_o : hydrocyclone vortex finder inside diameter (mm)

D_u : hydrocyclone spigot inside diameter (mm)

E_{oa} : actual efficiency to overflow

E_{oc} : corrected efficiency to overflow

Eu : dimensionless Euler number $= 2 \Delta P / v_i^2 \rho$

f_i : size fraction i in hydrocyclone feed

f_v : feed solids volume fraction in Narasimha/Mainza cyclone model

F_L : empirical constant in Durand equation

F_{80} : size 80% of feed material passes

F1,F3,F4: feed size effect constants in Flintoff/Plitt models

Fr : dimensionless Froude number = $(g*D_c)/v_i^2$

g : gravitational acceleration (m/s^2)

h : distance between apex and vortex finder in Plitt model (cm)

k : constant in equilibrium orbit theory equation

K : hydrodynamic constant in Flintoff/Plitt cut-size model

K1-K6 : empirical constants in Lynch/Rao models

K_{Do} : Nageswararao's d_{50c} equation constant

K_{D1} : constant in Narasimha/Mainza cut-size model

K_{Qo} : Nageswararao's throughput equation constant

K_{Q1} : constant in Narasimha/Mainza throughput model

K_{W1} : Nageswararao's water split equation constant, eq.*2.22*

K_{W1} : constant in Narasimha/Mainza water split model, eq.*2.35*

L : tube rheometer tube length (m)

L' : total hydrocyclone length (m)

L_c : hydrocyclone cylinder length (mm)

LZVV : locus of zero vertical velocity

Mo,Mf : solids mass flowrates of overflow and feed streams

n : hindered settling exponent in Turian equation, eq.*2.8*

n : hydrodynamic constant, eq.*2.10*

n' : parameter in Rabinowitsch-Mooney shear rate equation

o_i : size fraction i in hydrocyclone overflow

O/F : cyclone overflow stream

P : cyclone feed pressure (kPa)

P_{40} : size 40% feed material passes, in Asomah model (cm)

Q : hydrocyclone feed throughput (m^3/h)

Q_F : feed volumetric flow rate in Asomah model (m^3/h)

R : cyclone radius (cm)

Re : cyclone Reynold's number = $(v_i * \rho_p * D_i)/ \mu_p$, eq.*2.23*

Re : cyclone Reynold's number = $(v_i * \rho_p * D_c)/ \eta$, eq.*2.4 & 2.34*

Re_P : pulp Reynold's number = $(v_i * D_c * (\rho_s - \rho_p))/ \mu_{sl}$, eq.*2.27-2.29*

Re_p : particle Reynold's number = $(\rho_p * v_i * d_p)/ \mu$, eq.*2.3*

R_f : water split fraction to underflow

Rmax : radius at maximum tangential velocity (mm)

s : ratio of solid to liquid density in Turian equation

u_i : size fraction i in hydrocyclone underflow

U/F : cyclone underflow stream

v_i : hydrocyclone inlet velocity (m/s)

v_c : critical velocity/minimum transport velocity (m/s)

V : tube rheometer slurry velocity = $4Q / \pi D^2$ (m/s)

VF : vortex finder

V_H : hindered settling velocity, in Castro model (m/s)

V_r : radial velocity of particle in cyclone (m/s)

V_s : feed solids volume fraction (in Asomah cut-size model)

V_t : tangential velocity of particle in cyclone (m/s)

V_T : free settling terminal velocity (m/s)

V_z : axial velocity of particle in cyclone (m/s)

WF : mass flow of water in cyclone feed in Lynch/Rao model.

W_{oi}, W_{fi}: mass of material of size i in overflow and feed solids

Symbols

α : alpha, sharpness of separation

β : Whiten fish hook function

β^* : Whiten fish hook function – preserves definition of d_{50c}

Φ : feed volume solids concentration (%)

$\emptyset$: volume fraction solids

$\emptyset_m$: maximum packing fraction

η : pulp viscosity (cP)

η_a : pulp apparent viscosity (cP)

η_o : fluid viscosity, in Krieger-Dougherty equation (cP)

θ : cyclone cone angle (degrees)

θ : cyclone inclination from vertical in Asomah model (degrees), eq.*2.27-2.30*

λ : hindered settling term in Nageswararao model = $C_v^3/(1-C_v)^2$

ρ : liquid density (kg/m^3)

ρ_l : fluid density (kg/m^3)

ρ_p : pulp density (kg/m^3)

ρ_s : solids density (kg/m^3)

γ : shear rate (s^{-1})

γ_w : pseudo shear rate (s^{-1})

τ : shear stress (Pa)

τ_o : yield stress (Pa)

τ_w : wall shear stress (Pa)

μ : dynamic viscosity of the fluid, water at 20°C (Pa.s)

μ : slurry viscosity in eq. *2.16*

μ_m : pulp viscosity in Narasimha/Mainza water split model (cP)

μ_p : pulp apparent viscosity, in Castro model (Pa.s)

μ_{sl} : viscosity of slurry, in Asomah alpha model (cP)

μ_w : viscosity of water at 20°C (Pa.s)

1. INTRODUCTION

This chapter provides the introduction to the thesis which deals with the influence of viscosity on the operation of the hydrocyclone. The hydrocyclone is a classification device used in mineral processing to separate particles on the basis of particle size, shape, and density. A description of the method of separation is given. The subject of characterisation of suspensions is then discussed, before a motivation for this thesis is presented.

1.1 The Hydrocyclone

The purpose of any minerals processing comminution circuit is to produce a product which conforms to certain size-related criterion. The ability to control this product is made possible by devices such as screens and hydraulic classifiers, which are an integral part of any circuit. One such a device is the hydraulic cyclone or 'hydro' cyclone, so called as it is usually water which is the suspending fluid medium. The hydrocyclone remains one of the foremost classification devices used in the mining industry today. Despite the fact that they have been in operation since the beginning of the 20th century, there is much that is still not fully understood regarding the principle and mechanism of separation and their fluid flow profiles.

The hydrocyclone as a solids-liquid classifier classifies material by size, shape, and density. The device consists of a cylindrical upper section and a conical lower section, with openings at the top and bottom, see Figure 1-1. The feed material (generally particulate solids suspended in a fluid) is fed into the hydrocyclone tangentially at high pressure and the material is hereby subjected to high centrifugal forces which are the driving force behind the separation process, (Svarovsky, 1984). These centrifugal forces (Fc) generate a vortex which causes the heavier and/larger particles to migrate to the walls of the cyclone and they travel downwards towards the apex of the cone. At the same time the constriction at the apex (spigot) causes the generation of an upward flow vortex which passes through what is termed the vortex finder. The lighter particles are then entrained into this upward vortex of fluid and pass through the vortex finder (with most of the fluid). Certain authors, Bradley (1965), Svarovsky (1984) have suggested that these particles are subjected to drag forces (Fd) towards the centre. This could be considered misleading as the drag force is generally greater as the particle size is increased and is applicable when the fluid is considered to have a uniform pressure and velocity field. A detailed description of the likely forces involved is discussed in Kraipech *et al.* (2005).

The fact that the outlets are open to the atmosphere creates an area of low pressure inside the hydrocyclone and an air core develops which is stabilised by the vortex finder. The product leaving the bottom through the apex or spigot is the underflow (U/F) and consists of mainly coarse material with a high solids percentage (generally 60-80% by mass). The product leaving the top through the vortex finder is the overflow (O/F) and is mainly fine material with a lower solids percentage (generally 20-40% by mass). The material in the O/F is usually the desired product to be sent for further downstream processing. For closed circuit operations it is important that the liberated valuable minerals leave the O/F at this stage to avoid over grinding, (Wills & Napier-Munn, 2006).

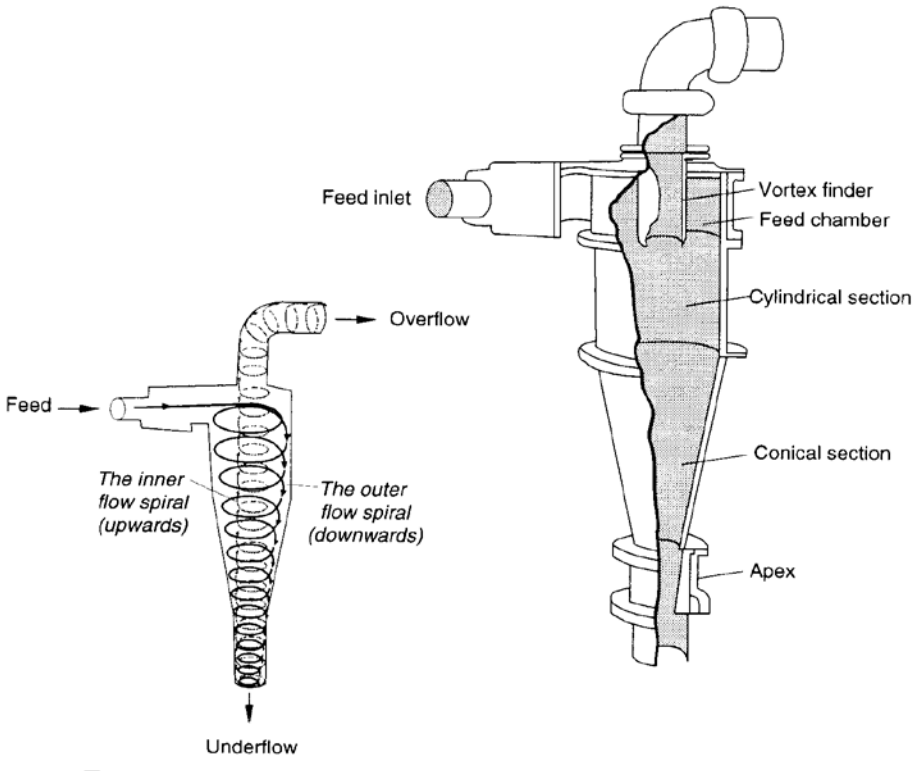

Figure 1-1. The hydrocyclone, Napier-Munn *et al.* (1996).

As in all classifiers, separation is never ideal and there exists a certain amount of short circuiting in the cyclone which negatively affects the efficiency. Short circuiting can occur as a result of coarse particles being carried into the O/F stream, or as is generally the case, fine particles being entrained into the bed of coarse particles travelling to the apex. The fact that the majority of fine particles follow the water flow is the predominant reason that the water in the U/F should be minimised, although certain operations require a more dilute U/F stream.

The viscosity of the feed stream is considered to be an important factor in the operation of the hydrocyclone and it is this aspect which will be dealt with in this thesis. Specifically the influence of the change in viscosity on the hydrocyclone efficiency curve parameters.

The quality of separation in the hydrocyclone is represented by an efficiency curve, also called a grade efficiency or partition curve. The formulation of a partition curve was originally discussed by Tromp (1973) and later by Svarovsky (1984). The efficiency curve is an extremely useful tool is observing the performance of the hydrocyclone as it depicts three important pieces of information on just a single line. The efficiency curve will be discussed further in Chapter 2.

Hydrocyclones are still widely used in industry today and besides their role in classification their application also includes slurry thickening (or dewatering), liquid degassing, solids washing, and also separation of liquid from liquid such as water from oils. Their use on mineral processing concentrators is only threatened by the recent advances in wet screening technology, although it is unlikely that their operation will ever be discontinued. Instead they will be used in conjunction with alternative classification equipment to streamline operations, reduce unnecessary recycle and therefore contribute towards a reduction in energy and cost.

1.2 Suspension characterization

The study of the properties of mineral processing circuit suspensions is important in understanding how the circuit might behave. As soon as the dry ore enters the wet milling stage the properties undergo changes as a slurry is created. This slurry is subjected to numerous processing stages on its way to the final product or tailings dam – from milling to classification to flotation or leaching, to thickening and filtration. The influence of the properties of this slurry as it enters the hydrocyclone stage is considered an important factor on the operation and performance of the hydrocyclone, (Bradley, 1965).

Brown & Heywood (1991) classified slurries in terms of their physical properties (particle density, solids concentration, particle size and size distribution, particle shape), and their flow properties (rheology). They classified suspensions according to the criteria in Table 1-1.

Table 1-1. Classification of solid/liquid systems, Brown & Heywood (1991)

<table>
<tr><td colspan="4">PHYSICAL DESCRIPTION</td></tr>
<tr><td>SINGLE-PHASE
liquid</td><td colspan="3">TWO-PHASE
solid-liquid mixture</td></tr>
<tr><td colspan="4">FLOW REGIME</td></tr>
<tr><td>TRUE HOMOGENEOUS</td><td>PSEUDOHOMOGENEOUS</td><td>HETEROGENEOUS</td><td>FULLY SEGREGATED</td></tr>
<tr><td colspan="2">FLOW STRUCTURE</td><td colspan="2">FLOW PATTERN</td></tr>
<tr><td colspan="2">LAMINAR and TURBULENT</td><td colspan="2">VARIOUS</td></tr>
<tr><td colspan="4">RELATION BETWEEN SHEAR RATE AND SHEAR STRESS</td></tr>
<tr><td colspan="2">NEWTONIAN FLUID
directly proportional & linear</td><td colspan="2"></td></tr>
<tr><td colspan="2">NON-NEWTONIAN FLUID
not directly proportional & linear</td><td colspan="2"></td></tr>
</table>

According to the table, only true homogeneous and pseudohomogeneous suspensions can be characterized by their flow structure. A class of the heterogeneous group are the so-called dense phase slurries. Dense phase slurries are those which result in a clear water surface on standing. These slurries are typical in the mining industry and are termed “settling slurries”. They are usually extremely difficult to characterize by their rheological properties alone. The slurries used in this thesis were obtained from secondary circuit Platreef and Copper

concentrator operations. The samples were collected on-site from the hydrocyclone feed streams and were thus considered as being two-phase heterogeneous and settling in nature.

If suspensions exhibit a settling nature the characterization of viscosity is not straight forward. The viscosity usually needs to be defined in terms of a relative viscosity and is determined by the viscosity of the carrier fluid (or suspending medium including the suspended fine particles) and the densities of the phases forming the suspension. Generally the coarser size fractions do not contribute to viscosity when dealing purely with particle size effects. The size below which particles do contribute to viscosity has been the focus of many studies in the past, (Jinescu, 1974). There is a general view in industry amongst equipment suppliers, Multotec (2010), that 38 or 32 µm is a suitable size to use as the 'cut-off point' when studying the effects of rheology on hydrocyclone operation as this is often the final screen size used during standard particle size determination. Hydrocyclones positioned in secondary circuit operations could thereby receive a more viscous feed than those situated in primary circuits, but this may ultimately depend on many factors. A finer feed will contain particles which may have a greater rheological influence on the carrier fluid and will therefore result in an increased viscosity, but the size distribution of these particles will also play a role.

The continued depletion of high grade mineral reserves has meant that mining companies are being forced to mine more rheologically complex ore bodies. This together with the introduction of the mainstream ISAMill technology for finer grinding has meant that industry may be faced with a shift in rheology of their process streams. These changes will need to be anticipated in order for the process to continue providing the required thoughput, efficiency and recovery. An understanding of the rheology of the ore body is essential in determining how the ore will behave once it is introduced to the wet process and it is expected that rheological characterisations will become more commonplace in the near future. The issues just mentioned have contributed to the motivation behind this work.

1.3 Motivation

In terms of plant applications the successful operation of the hydrocyclone depends largely on: 1 - the quantity of material that they can treat in the equipment (tonnage), and 2 - the quality of separation that can be achieved. The JKSimMet mineral processing simulator developed at the Julius Kruttschnitt Mineral Research Centre (JKMRC) in Brisbane, is used on a number of mining concentrators for simulation studies. The commonly used hydrocyclone model contained in the package is based on the work of Nageswararao (1978) who developed a dimensionless empirical model based on earlier work of Lynch & Rao (1975a). The model contains equations to predict cyclone performance that include partition curve properties and capacity. However the models predictive capabilities encounter problems when treating slurries with a significant clay content and those with a high proportion of fine material. It has also been shown to only be applicable to slurries with a solids content above 30% by weight, (Castro, 1990). The model only accounts for changes in slurry rheology by the inclusion of a feed solids concentration term and viscosity influence is only implied. Slurry viscosity is dependent on many other factors besides solids concentration. If a slurry is initially behaving like a Newtonian fluid, and then by a change in its properties shifts towards a non-Newtonian regime, the viscosity of the two slurries could show a marked difference. Despite this they may be processed at the same conditions (inlet velocities, shear rates) inside the cyclone.

As a result, a new hydrocyclone model for inclusion in JKSimMet has been developed by researchers at the University of Cape Town Centre for Minerals Research and the JKMRC under the P9O project, and includes the effect of viscosity explicitly. The aim of this thesis was then to generate suitable viscosity data using two ore types for testing the influence of viscosity in classification using three hydrocyclone sizes. The experimental work in this thesis therefore involved rheological characterisation and laboratory scale hydrocyclone test work under changing rheological conditions. These rheological conditions were quantified and then linked to the performance of the hydrocyclone. Suitable data arising from the thesis may well be used for validation of the new cyclone model.

2. REVIEW OF THE LITERATURE

This chapter provides a review of the previous research dealing with the influence of slurry rheology on the operation and efficiency of the hydrocyclone, and also the measurement of viscosity and interpretation of rheological data. The influences of specific variables on the hydrocyclone efficiency curve parameters are initially discussed. Thereafter, the physical parameters influencing pulp viscosity are described, before a review of the previous work relating to the inclusion of viscosity in hydrocyclone testwork is given. Finally, the theoretical and empirical hydrocyclone models relevant to this subject are introduced.

The study of suspension rheology and hydrocyclones has generated significant interest in the past, with both research areas resulting in countless scientific papers being published. Despite this however, there are still elements of both which are not fully understood. In particular, the measurement and interpretation of rheological data, and understanding flow patterns and velocity profiles in the hydrocyclone. The combination of rheology and hydrocyclones is an area which has been the focus of specific research in the past but questions still remain regarding the effect of a change in the former on the resulting efficiency and performance of the latter.

2.1 The Hydrocyclone

2.1.1 Design

The conventional hydrocyclone has the advantage of no moving parts, a high throughput, and a relatively small footprint compared to other classification devices such as vibrating screens or spirals. They also have fairly low maintenance requirements with the spigot and vortex finder the main wear components which can easily be changed. Standard designs were based on the original designs of Driessen (1951), and Rietema (1960). The alteration of cyclone internals is also an important advantage to have on mineral processing plants as changes to plant flow rates and ore type/size distributions sometimes require a different set of cyclone internal geometries to achieve a similar cut size. Lilge & Plitt (1968) related the ratio of spigot & vortex finder diameter (termed cone force ratio) to cut size. Feed arrangements have become consistently rectangular in shape (especially for larger cyclones as it ensures the particles are closer to the wall on entry), and involute (Figure 2-1) to reduce turbulence and energy requirements, (Svarovsky, 1984).

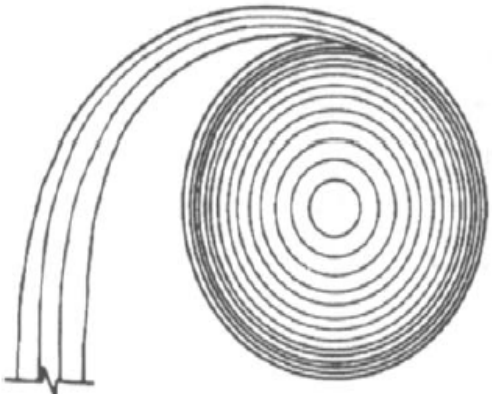

Figure 2-1. Involuted feed arrangement, Wills & Napier-Munn (2006).

Linings of hydrocyclones are also important, and are application dependent. Operations with highly abrasive ore-types require wear resistant linings and internals, and polyurethane or silicon carbide have become popular in these cases, (Svarovsky, 1984).

2.1.2 Operation

The correct operation of an installed cyclone or cluster of cyclones is important in ensuring that maximum benefit is attained from the equipment. The correct procedures for the installation and operation of standard hydrocyclones are published in Bradley (1965), Mular & Jull (1980), Svarovsky (1984), and Wills & Napier-Munn (2006). The important criterion, especially when constructing and operating a single cyclone test rig, is to ensure that there is minimum disruption to the 'steady state' flow of material or stability. This can be achieved by ensuring the following:

- Any bends or elbows situated before the feed must be of a large radius, and must be positioned at a distance from the inlet which is greater than or equivalent to the entire length of the hydrocyclone itself.
- The O/F discharge pipe should also be of a large radius and should be open the atmosphere. It should also discharge at a point above the line of the feed entry point to ensure no siphoning effects can occur. The overflow receiver design of Trawinski (1976) was adopted in this thesis.
- Centrifugal pumps should always be used to provide a constant feed flow to the hydrocyclone.

- A pressure gauge/device should be situated as close as possible (ideally a distance of about one feed pipe diameter) to the inlet to ensure an accurate pressure drop reading.

2.1.3 Efficiency

The hydrocyclone efficiency is measured by an efficiency curve Figure 2-2 which is a plot of efficiency to underflow (U/F) or overflow (O/F) against log size. Since the overflow is generally the final product in mineral processing, it is the preferred choice for the efficiency curve, although many previous authors have preferred to represent U/F efficiency. It is therefore the proportion of material of a given size, which will report to the O/F or U/F. Most O/F efficiency curves will never reach 100% at zero size. This is due to the proportion of fine material which does not pass through the O/F but passes with the water and coarse solids to the U/F. The measure of efficiency is represented by three partition curve properties - alpha (α), cut-size (d_{50}), and water split (R_f or C). Alpha is the sharpness of separation and represents the slope of the curve – the steeper the slope, the greater the alpha, and the more efficient the separation. C is the term that is given to the water split to the O/F and this 'bypass' fraction is then 100-C. The actual curve in Figure 2-2 is the type of curve which would be expected from the experimental data. The corrected curve is then the efficiency due to classification only, or the probability of a particle of a specific size reporting to the O/F.

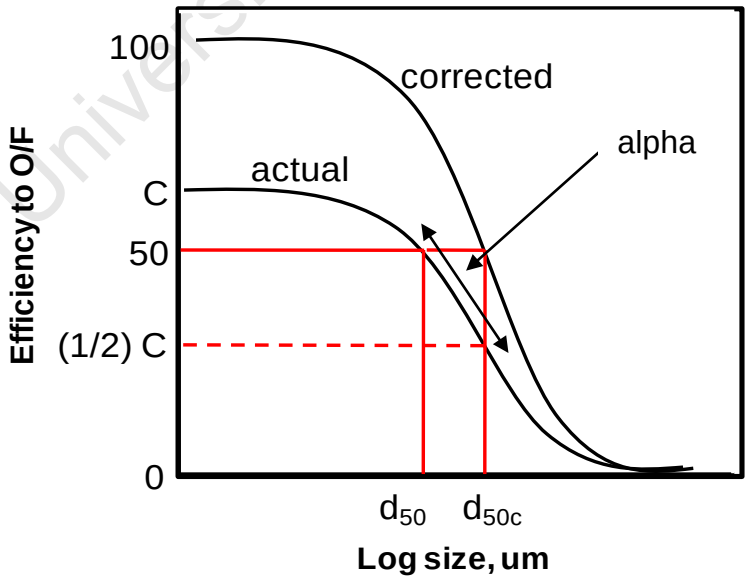

Figure 2-2. Efficiency curve to O/F, Napier-Munn *et al.* (1996)

The d_{50} parameter is defined as the cut-size and is the size whereby 50% of the material will either report to the O/F or U/F. The corrected cut size (d_{50c}) is therefore the size which divides equally by classification forces only and represents the mean of the curve.

Yoshioka & Hotta (1955) first proposed a dimensionless normalised (or 'reduced') efficiency curve whereby the corrected efficiency curve is plotted against the ratio of particle size (d_i) to d_{50c}. The reduced efficiency curve has been found to be generally independent of hydrocyclone diameter and operating conditions, Lynch & Rao (1975a), assuming geometrical similarity between cyclones. However, feed characteristics e.g. feed size, mineralogy and **viscosity**, may have a significant effect on the curve.

In order to obtain a smooth partition curve which would fit the cyclone experimental data, a mathematical function for the curve was derived by Whiten in 1966 (equation *2.1*). He derived the exponential sum expression where he included an efficiency parameter (α) in his equation for reduced efficiency.

$$E_{oa} = C\left[\frac{\exp(\alpha)-1}{\exp(\alpha x)+\exp(\alpha)-2}\right]; \quad where\ x = \frac{d}{d_{50c}} \qquad [2.1]$$

2.2 Fish-hook effect

In certain cases an anomaly at the fine end of the efficiency curve is noted - commonly termed a 'fish-hook' by Finch and Matjiwenko (1977), and shown in Figure 2-3. There have been various investigations on the subject conducted in the literature, and there are conflicting theories for its appearance.

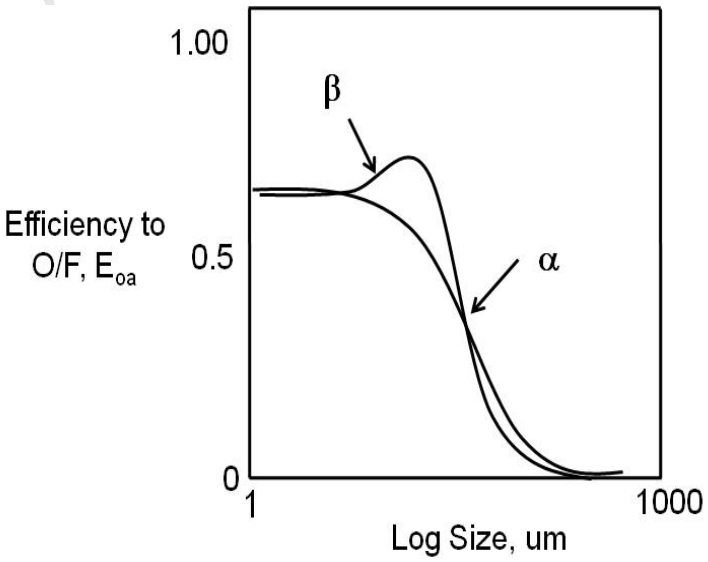

Figure 2-3. Efficiency curve with 'fish-hook', Napier-Munn *et al.* (1996).

It was suggested by Finch (1983) that it is caused by entrainment of the finer particles in the water. Flintoff *et al.* (1987) believed the fish-hook effect occurred as a result of poor experimental procedures and/or fines agglomeration onto the coarser particles. Roldan-Villasana *et al.* (1993) believed that data reconciliation and sub-sieve analysis could help to identify the fish hook phenomenon. Nageswararao (2000) conducted a detailed critical analysis of the effect and he concluded the following:

- The actual efficiency precision of measurement has been overlooked when reporting the fish hook effect. There is a need to be able to predict the conditions which will favour a fish hook and its reproducibility.
- Kelsall's bypass hypothesis is regarded as a mathematical transformation and the theories for size dependent bypass for a fish hook explanation are also refuted.
- There is a need to establish the cause of the fish hook phenomenon if it does in fact occur.
- The fact that the exclusion of the fish hook from simulation models shows little effect implies that it is of theoretical interest only.
- Future work is necessary to assist in quantifying the measurement precision for efficiency.

Nageswararao stated that whether the fish hook is real or not, the research into its cause and effect will advance the understanding of the hydrocyclone classification process, and the predictive capability of the empirical models.

Additional studies on the subject include the work of LaPlante & Finch (1984), Neesse *et al.* (1997), Patil & Rao (2001), Kraipech *et al.* (2002), Schubert (2003) and Majumder *et al.* (2003). It is important to note that the presence of a fish hook will only occur if sub sample sizing is carried out as any presence of a fish hook will usually occur in the sub 30 µm region. Studies that claim to show evidence of a fish-hook without sizing in this range need to ensure that there are no errors present in their experimental procedure or data analysis methods.

Whiten accommodated this factor in his efficiency equation by including an additional parameter, **β** which controls the initial rise in the curve on the fine end. The **β*** term was introduced to preserve the definition of d_{50c} , Napier-Munn *et al.* (1996) The Whiten equation (equation *2.2*) is the form of the equation that is used in JKSimMet:

$$E_{oa} = C\left[\frac{(1+\beta*\beta*x)(\exp(\alpha)-1)}{\exp(\alpha*\beta*x)+\exp(\alpha)-2}\right]; \quad where \;\; x=\frac{d_i}{d_{50c}} \quad \ldots\ldots\ldots\ldots\ldots\ldots\ldots\ldots\ldots\ldots\ldots\ldots [2.2]$$

2.3 Separation in the hydrocyclone

The complex flow fields inside a hydrocyclone have been the focus of many studies in the past as researchers try to understand the principles behind the operation of this relatively 'simple' device. Two of the earliest researchers to perform fundamental studies on the hydrocyclone were Kelsall (1952); and Dahlstrom (1954).

2.3.1 Velocities

Separation of particles in the hydrocyclone is imparted by the magnitude of the various velocities of the carrier fluid. Kelsall was the first to propose a locus of zero vertical velocity (LZVV) as the location where a particle in the hydrocyclone is theoretically at rest and has no motion in the vertical direction (see Figure 2-4). He described this point as the point where a particle has an equal chance of reporting to the U/F or O/F (d_{50}). In reality it is not a single location but rather an envelope. All particles on the inside of this envelope will report to the O/F and all particles on the outside should then report to the U/F. Particles which lie on this envelope should then have an equal chance of reporting to either the O/F or U/F. Kelsall conducted experiments using optical methods and concluded that there were three velocity vectors that contributed to the separation process – axial (or vertical), radial (or horizontal) and tangential velocities.

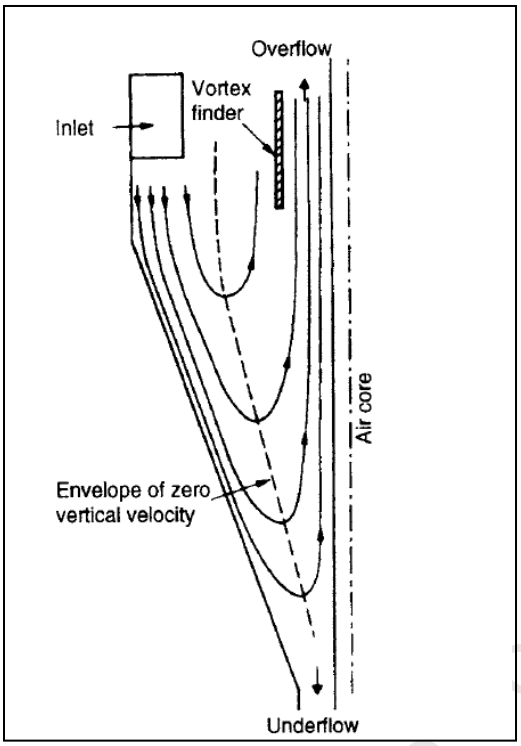

Figure 2-4. Distribution of the radial and vertical velocities in a hydrocyclone. The dotted line signifies the LZVV, Wills & Napier-Munn (2006).

Dahlstrom recognized that understanding the velocity components was key to understanding the classification in the hydrocyclone. He stated that the tangential velocity component was the one responsible for supplying the centrifugal force for classification and that the axial velocity component influenced the magnitude of the vortices within the cyclone body. He suggested that the radial velocity appeared to be the current against which the coarser particles had to settle due to the centrifugal forces at play.

Bradley (1965) reported that tangential velocities increase with a decrease in the radius of the cyclone. Any alteration in the density of the carrier fluid in the hydrocyclone will have an effect on the separation as the fluid flow patterns and velocities will change. An increase in the feed flow rate will lead to an increase in the centrifugal forces (and tangential velocities) and will reduce the viscosity of any shear thinning slurry. Stokes Law (which relates drag force to liquid viscosity, particle/fluid velocity and particle size) has previously been used for prediction of particle movement within a rotational field by equating the terminal settling velocity in an outward direction to the inward radial velocity of the liquid. Many researchers have used the law as a basis for their theoretical models. However it is well known that Stokes Law can only be applied to very dilute suspensions of spherical particles under laminar flow conditions, none of which are found on mineral processing classification

circuits. Richardson & Zaki (1954) modified the equation by including a hindered settling velocity and a voidage term to account for increased concentrations. The main focus in determining the interaction between particle and fluid though has been the use of dimensionless numbers.

2.3.2 Dimensionless numbers

The particle Reynolds number (equation *2.3*), which relates the inertial to viscous forces, is an important yet complex dimensionless number to apply to hydrocyclones as a single Reynolds number cannot be used in flow calculations due to the range of shear rates that exist within the cyclone.

$$\mathrm{Re}_P = \frac{\rho * v_i * d_P}{\mu} \quad \text{.....} [2.3]$$

Previous literature making use of the particle Reynolds number restricted its use to the radius at the LZVV, Lilge & Plitt (1968), so that the particle diameter (d_P) must be the cut size at this point. An approximate average particle density (ρ) and liquid viscosity (μ) still have to be used however and this will vary from point to point in the hydrocyclone. Svarovsky (1984) stated that the centrifugal force is proportional to the particle volume and the drag force is proportional to the particle size which explains the strong dependence of particle settling velocities within the cyclone on particle size. A cyclone Reynolds number (equation *2.4*) using measured values (of pulp density, inlet feed velocity, cyclone body diameter and pulp viscosity) is sometimes also used.

$$\mathrm{Re} = \frac{\rho_p * v_i * Dc}{\eta} \quad \text{.....} [2.4]$$

Another important number used in hydrocyclone research is the Euler number (equation *2.5*) which relates the pressure drop across the cyclone to the pressure arising from the velocity in the cyclone.

$$Eu = \frac{\Delta P}{\left(\frac{\rho * v_i^{\,2}}{2}\right)} \quad \text{.....} [2.5]$$

There exists a relationship between the Reynold's number and the Euler number in hydrocyclones as shown in the log-log plot in Figure 2-5. The Euler number has been found

to reach a minimum at a Reynold's number of just above 1000 due to the increase in centrifugal head, (Van Kooy, 1958). Below this minimum the vortex is not considered to be fully developed yet. The decrease in Euler number at very high Reynold's numbers was considered by Svarovsky to be due to the highly turbulent conditions that may have developed inside the cyclone.

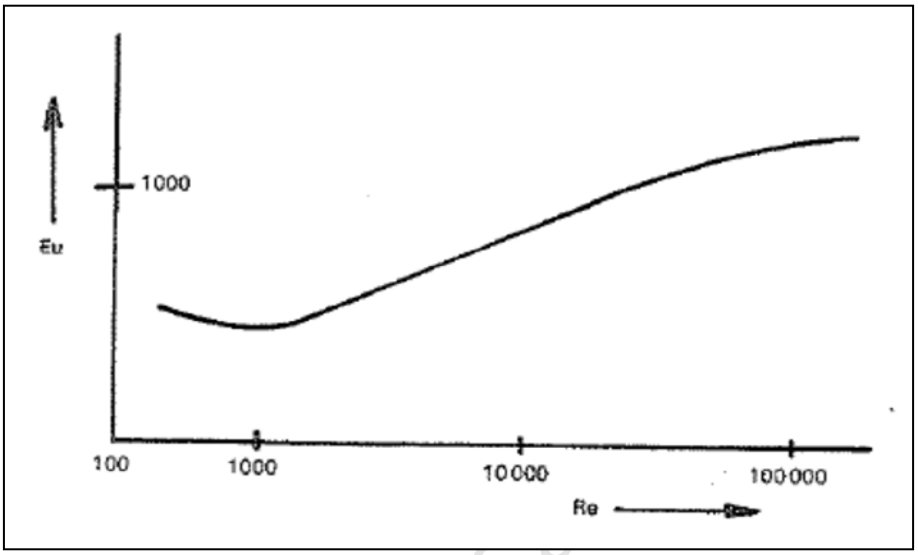

Figure 2-5. Relationship between Re # and Eu # in hydrocyclones, Svarovsky (1984)

Studies on large hydrocyclones have sometimes made use of the Froude number (equation *2.6*) which relates the gravitational and inertial forces.

$$Fr = \frac{g * D_c}{v_i^{\,2}} \quad \text{.....} [2.6]$$

Gravity does not normally play a significant role during cyclone operation as axial velocities are greatly affected by hindered settling at higher particle concentrations. It may only be applicable therefore in larger cyclones which receive coarse material in the feed stream.

2.3.3 Separation of multi component ore types

Multi-component minerals exhibit different behaviour in the hydrocyclone in that denser components cut finer than the rest of the material. This is the main reason that problems are often encountered in hydrocyclones when treating mixed minerals ore types and ore types with a significant proportion of dense material, eg. the UG2 ore type from the Bushveld Complex. The UG2 ore has a significant chromite proportion and because of its high density compared to the silicates, chromite tends to report to the U/F even if it is fine enough to pass

to the O/F and to flotation. A possible solution is the application of a three-product cyclone which has an inner and an outer vortex finder – the outer vortex finder separates the so-called middling's product. Comprehensive studies of the device have been carried out by Obeng (2003) and Mainza (2006).

Multi-component ore types exhibit different efficiency curves for the different mineral components and an average or 'bulk' efficiency curve is normally taken when considering the cyclone performance. Studies by Lynch & Rao (1975a) and Weedon *et al.* (1990) have considered the effect of so-called mixed minerals on hydrocyclone operation. Weedon showed that the corrected cut-sizes in a classification circuit increased with a decrease in mineral density and as a result the dense materials generated larger recirculating loads which could result in overgrinding of already liberated material.

2.3.4 Computational Methods

A considerable amount of work has been conducted in the area of computational fluid dynamics (CFD) and hydrocyclones - Narasimha *et al.* (2004), Nowakowski *et al.* (2004), Delgadillo & Rajamani (2007). Results thus far have been very promising in that researchers have been able to identify the changing velocity profiles under variable conditions of flow and pressure drop, as depicted in Figure 2-6. Work has been mainly conducted in 2-phase systems, but more recently 3-phase studies have been investigated - Brennan *et al.* (2007), albeit with a low density feed. The rapid progression in computing power means that the computational research into cyclones will continue to grow in the near future.

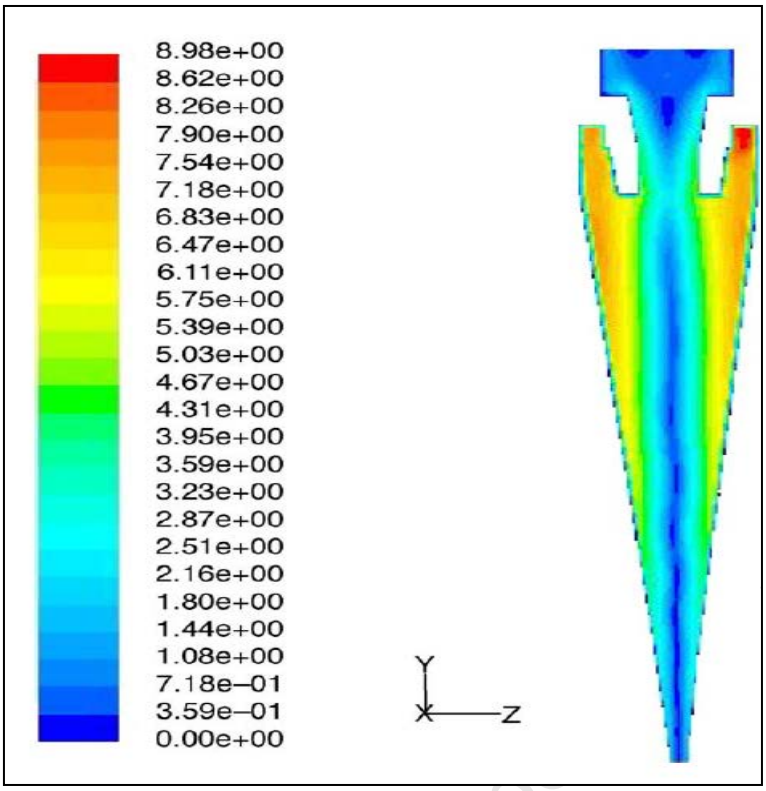

Figure 2-6. Tangential velocity contours in the hydrocyclone, Narasimha *et al.* (2004).

In addition to CFD the recent application of positron emission particle tracking (PEPT) to mineral processing systems has opened up an exciting avenue of research. PEPT has indeed already been applied to a fluidised bed cyclone, Chan *et al.* (2009) and a hydrocyclone, (Chang *et al,.* 2011). The high tangential velocities (and corresponding short residence times) in smaller cyclones are possibly the biggest challenge to overcome for PEPT in hydrocyclones.

2.4 Effect of hydrocyclone operating variables on efficiency

Many factors play a role in the successful operation of the hydrocyclone and various authors – (Bradley, 1965), (Lynch & Rao, 1975a), (Svarovsky, 1984), (Napier-Munn *et al.*,1996), (Wills & Napier-Munn, 2006) have all discussed the effects of variables on hydrocyclone efficiency parameters.

A summary is presented in Table 2-1, outlining the effects of changes in cyclone geometry and feed slurry conditions. The table is a summary compiled by the author to capture what has been reported in the literature thus far by the authors listed above, amongst others. The relationships are the generally accepted outcomes; there are of course always exceptions. At times contradictory statements have been made by different authors, especially regarding the influence of pulp viscosity. It is hoped that the data generated during this work would be able to provide insight into some of these contradictory findings, and provide a new source of reference related to the subject.

Table 2-1. Effect of variables on hydrocyclone operation

Variable, Change		Throughput	Fines eff. (α)	d_{50c}	R_f	C
* Feed Q (P)	↑	↑	↑	↓	↓	↑
	↓	↓	↓	↑	↑	↓
* Feed η	↑	↑↓	↓	↑	↑	↓
	↓	↓↑	↑	↓	↓	↑
* Feed %	↑	↑ **up to 18%v/v**	↓↑	↑	↑	↓
	↓	↓ **from 18%v/v**	↑↓	↓	↓	↑
Dc	↑	↑	↓	↑		
	↓	↓	↑	↓		
Du	↑	↑		↓	↑	↓
	↓	↓		↑	↓	↑
Do	↑	↑		↑	↓	↑
	↓	↓		↓	↑	↓
Lc	↑	↑	↑	↓		
	↓	↓	↓	↑		
Di	↑	↑	↓	↑		
	↓	↓	↑	↓		
Θ (constant Lc)	↑	↑	↓	↑		
	↓	↓	↑	↓		
Θ (changing Lc)	↑	↓	↓	↑		
	↓	↑	↑	↓		
F_{80}	↑	↓	↓	↑		
	↓	↑	↑	↓		
VF length	↑		↓	↑	↓	↑
	↓		↑	↓	↑	↓
Incline Angle	↑		↓	↑	↓	↑
	↓		↑	↓	↑	↓

modified in this work.

2.5 Rheology

Rheology is the study of the flow and deformation of matter. When the rheological properties of fluids are measured, a flow curve or rheogram is obtained which is a plot of shear stress, τ, vs shear rate, γ. Shear stress (SS) is the force applied parallel to the surface/unit area (Pa) and shear rate (SR) is the rate of deformation of a fluid element (s^{-1}) Viscosity is defined as the rate of resistance to deformation (Pa.s). Absolute viscosity is only obtainable in Newtonian fluids. For non-Newtonian fluids, which are sometimes encountered in mineral processing, the apparent viscosity (η_a) is the shear stress divided by the shear rate (τ/γ), measured at a single point. The viscosity is therefore a function of shear rate and in certain cases is also time dependent. An example of the type of rheograms obtained for non-Newtonian suspensions is shown in Figure 2-7 below.

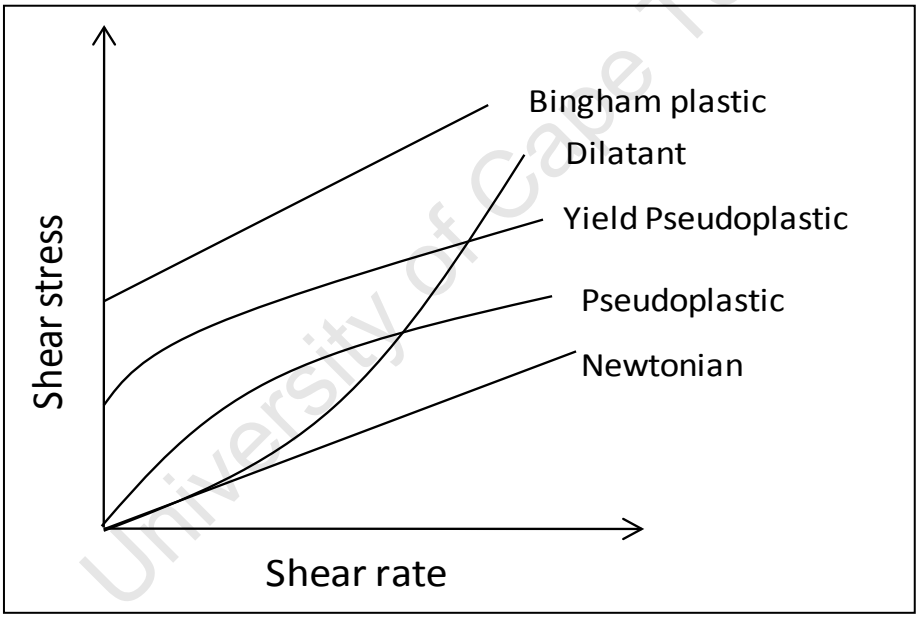

Figure 2-7. Typical rheograms, adapted from Kelly & Spottiswood (1982)

Curves that exhibit an increase in SS with SR (ie. dilatant) are termed shear thickening and those who show a decrease with SR (ie. pseudoplastic) are termed shear thinning. Suspensions that deviate from the origin on the y-axis exhibit what is termed a yield stress (τ_o). This is the minimum force that needs to be applied to generate flow, and no flow will occur below this point. Many factors can influence the rheological properties of slurries and the effect of these factors and their interactions determines the final rheology of the slurry. According to Cheng (1980), the specific interactions can be divided into three main categories:

- Hydrodynamic interaction between the liquid and the dispersed solids.
- Inter-particle attraction, which promotes the formations of flocs, aggregates, agglomerates or structure.
- Particle-particle contact.

All of the above interactions can play a role in the hydrocyclone classification process, although the second one is generally not applicable due to the presence of the fairly high shear rates generated by the centrifugal forces on entry to the hydrocyclone, especially in smaller diameter cyclones.

2.6 Measurement of viscosity

The difficulty in obtaining an accurate and reliable viscosity measurement, particularly for settling slurries remains an ongoing problem. This unreliability of measurement has been one of the reasons behind the exclusion of viscosity in models used in minerals processing and the hydrocyclone models are no exception.

Methods employed to date have been the use of: viscometers – instruments used to obtain a viscosity measurement at a single shear rate, and rheometers – instruments used to obtain a full rheogram covering a range of shear rates. The two main measurement techniques that have been applied to the measurement of mineral suspensions are the rotational (couette flow) device and capillary or tube (Hagen-Poiseuille flow) device. The standard bench top rotational viscometer which is found in many laboratories cannot be used for settling slurries as it does not keep the slurry in suspension during the measurements. Besides the difficulty in measurement, the other issue is accurately interpreting what is measured.

Various authors have attempted to modify rotational viscometers to allow them to be suited to settling slurries. The advantage of rotational viscometers is that continuous measurements at a given shear rate can be made for extended time periods thereby indicating the time-dependent nature of the fluid, (Van Wazer *et al.,* 1963). Reeves (1985) was the first to apply a dedicated on-line Debex viscometer to suspensions. Castro (1990) too used a modified Debex on-line viscometer to obtain measurements for his thesis (Figure 2-8). This instrument consisted of a cup with a submerged rotating bobbin. An annular section between the cup and the bobbin allowed for continuous flow of the pulp from the bottom out the top. The measurement output related bobbin angular velocity to motor speed and torque. These readings were then converted to apparent viscosity data. The instrument was found to give

consistent measurements only for Newtonian suspensions and its limitations for application to non- Newtonian fluids was admitted.

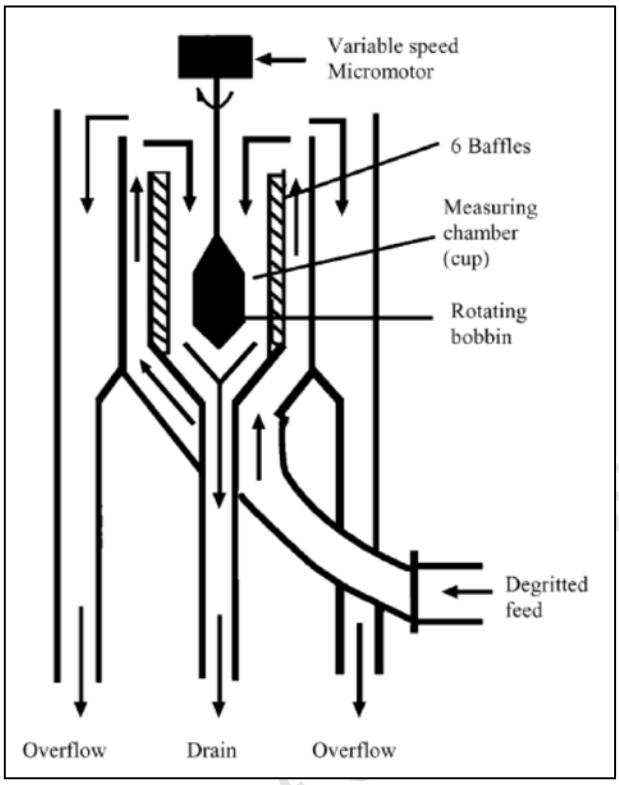

Figure 2-8. Schematic of the Debex viscometer, Shi & Napier-Munn (1996a).

The same device was later used by Shi & Napier-Munn (1996a) and they presented a method of extracting a corrected rheogram from the instrument. Kawatra & Bakshi (1996) used a vibrating sphere viscometer with a specially designed slurry presentation device to measure the viscosity of a fine silica slurry (80% passing 65 μm) at various solids concentrations. Unfortunately they provide no indication of accuracy or reproducibility for their viscosity results and make no mention of whether the instrument was capable of non-Newtonian measurements. Other techniques that have been employed include an online pressure vessel rheometer - Kawatra *et al.* (1999), a helical flow device for continuous online measurements - Akroyd & Nguyen (2003), and a parallel plate rheometer - Chryss & Pullum (2007). A large number of early viscometer types are described by Van Wazer *et al.* (1963). The rheometer used in this thesis is a custom made tube rheometer, its design and operation are described on page 55.

Another issue with measurement of viscosity is the issue of wall slip in the capillary and rotational (concentric cylinder) viscometers. This can occur at low shear rates as the fluid forms a thin film on the wall surface and results in the main body of slurry moving at a

greater velocity than this film. The result is a decreased shear stress at a specific shear rate as shown in Figure 2-9 from Boger (2009).

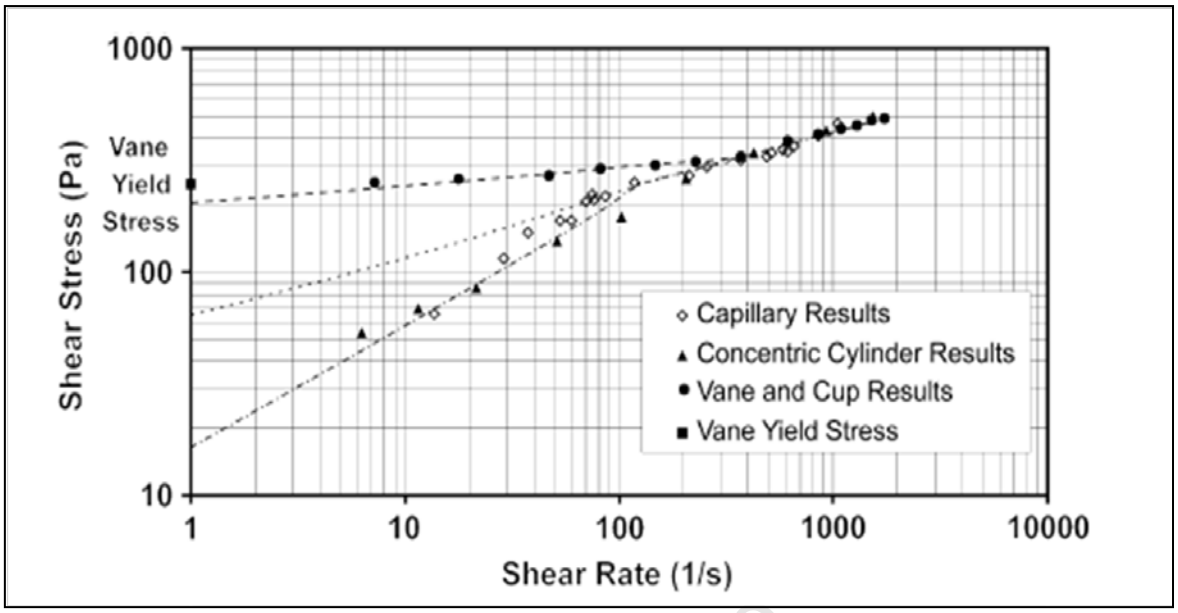

Figure 2-9. Influence of slip on capillary and concentric cylinder viscometers, Boger (2009).

Many researchers have also pointed out both the importance and difficulty of obtaining a true yield stress measurement, (He *et al.,* 2001). The capillary rheometer is not capable of obtaining accurate measurements at low shear rate values (below 200/s) and thus the true yield stress cannot be obtained by extrapolation. Yield stress is an important measurement when a shear is applied to a suspension at rest. If characterisation of a suspension which is already subjected to shear is required, then the yield stress is less important (as in the case of a hydrocyclone). The Bingham yield stress value is often reported although it is no reflection of the true yield of the suspension. Figure 2-9 reflects the differences that can be obtained when trying to obtain a value for yield stress. A new type of rheometer – the bucket rheometer- was discussed by Boger (2009). It is simply a portable rotating vane device with a torque measuring head which can obtain effective measurements of shear stress and shear rate in the absence of slip. It is admittedly not suitable for low viscosity Newtonian fluids as the vane type rheometer is specifically designed for the measurement of yield stress.

Care must also be taken when characterising a slurry under turbulent conditions as the effect can be similar to that of a dilatant flow curve, (Castro, 1990) and (Chryss & Pullum, 2007). They warn against the dangers of classifying a slurry as being shear thickening and state that these are generally exhibited by suspensions of complex submicron particles. Shi & Napier-

Munn (1996b) devised a turbulence correction factor for tests with a rotational type viscometer to negate against the influence of turbulence on the data. However, flow curves depict the ore as tending towards being shear thickening at higher rates of shear and at dilute concentrations, and it is not clear whether this data had been corrected.

Rheograms are only generally applicable to laminar flow conditions and the included difficulty in characterising a settling slurry is that they will tend to settle out under laminar flow conditions. Analysis of any rheological data should therefore only include the portion of the curve where the slurry is maintained in suspension (higher shear rates), ie. above the critical particle velocity, v_c. Critical velocity is defined as the minimum velocity that must be maintained to prevent the settling out of solids in a pipe. Durand (1953) formulated an equation for v_c, (equation *2.7)*, based on work with sand and coal for pipe diameters from 40 to 700 mm and for concentrations of up to 15 volume percent.

$$v_c = F_L\left[\frac{2gD\left(\rho_s-\rho_l\right)}{\rho_l}\right]^{0.5} \quad \text{.....} [2.7]$$

**Where: v_c is the minimum transport velocity, F_L is an empirical constant that varies between 0.4 and 1.5 depending on the particle size and concentration, ρ_s is the solids density, ρ_l the fluid density and D is the pipe/tube diameter.*

A more recent correlation for v_c was proposed by Turian *et al.* (1987), equation *2.8*. It included the effect of volume concentration (C_v) and fluid viscosity. Turian conducted a comprehensive study of the available correlations at the time and concluded the following –

- The dependence of v_c on pipe diameter is almost proportional to $D^{0.5}$
- For slurries composed of large settling particles, v_c is virtually independent of particle size.
- The v_c versus C_v relationship possesses a maximum (about 0.25 to 0.30 C_v for their work).

$$\frac{v_c}{2gD\left(s-1\right)^{0.5}} = 1.67\left[C_v\left(1-C_v\right)^{2n-1}\right]^{0.53}\times\left[\frac{D\rho\left[gD\left(s-1\right)\right]^{0.5}}{\mu}\right]^{0.067} \quad \text{.....} [2.8]$$

**Where:* *n is the hindered settling exponent as in Richardson & Zaki (1954) and lies in the range 2< n <5*

D is the pipe diameter (m)

s is the ratio of solid to liquid density (ρ_s / ρ_L)

C_v is the solids volume fraction

ρ is the liquid density (kg/m^3)

μ is the liquid viscosity (Pa.s)

The equation is very sensitive to changes in *n*, with the highest value corresponding to the lowest Reynolds Stokes' law region.

This method of excluding the viscosity data below a certain shear rate range is acceptable as hydrocyclones subject the entering slurry to higher rates of shear due to the centrifugal forces involved. Results from the calculation using the Turian equation are discussed in Chapter 4.

2.7 Effect of physical factors on slurry rheology

The rheology of suspensions (or slurries) is a complex subject and there are certain inconsistencies in the literature regarding the effect of certain factors on slurry rheology. The discrepancies are due to the fact that suspension rheology is affected by the interaction of a combination of these factors and usually not by one factor alone. When dealing with a mineral slurry the factors which are thought to have an effect on the rheological properties include solids concentration, particle size, particle size distribution, chemical environment, temperature, particle shape and mineralogy. Each of these will now be discussed.

2.7.1 Solids Concentration

Solids concentration is probably the greatest contributor to the viscosity of slurry, but only once it has reached a critical value or critical concentration, (Clarke, 1967). This point varies depending on the type of material. The viscosity of a suspension will increase with increasing solids concentration (assuming a constant particle size) due to the physical particle interactions taking place. At low to medium solid concentrations hydrodynamic interactions are important. At medium to high concentrations particle frictional contact and interparticle attraction and repulsion becomes important and for relatively high solids concentrations the particle effect predominates over the hydrodynamic effects leading to increased viscosity, (Jinescu, 1974). Rutgers (1962) showed that viscosity increased linearly with increased solids concentration until a maximum concentration was obtained (approx 47% by volume, 70% by mass, for an ore density of 2.65); thereafter the increase was exponential.

The flow behaviour can also shift from Newtonian to non-Newtonian at increased concentrations, (Cheng, 1980). This is obviously also dependent on shear rate. Hydrocyclone feed solids concentration varies depending on the application and location of the cyclone in the circuit, but is generally always within the range of 30 to 70% by mass. By simply plotting the raw viscosity data from various copper ore tests by Nageswararao, a sharp increase in viscosity at a solids concentration above 65% by mass (Figure 2-10) can be observed. This trend has been demonstrated by Jinescu (1974) and Tangsathitkulchai & Austin (1988). Feed solids concentration was a variable in this study.

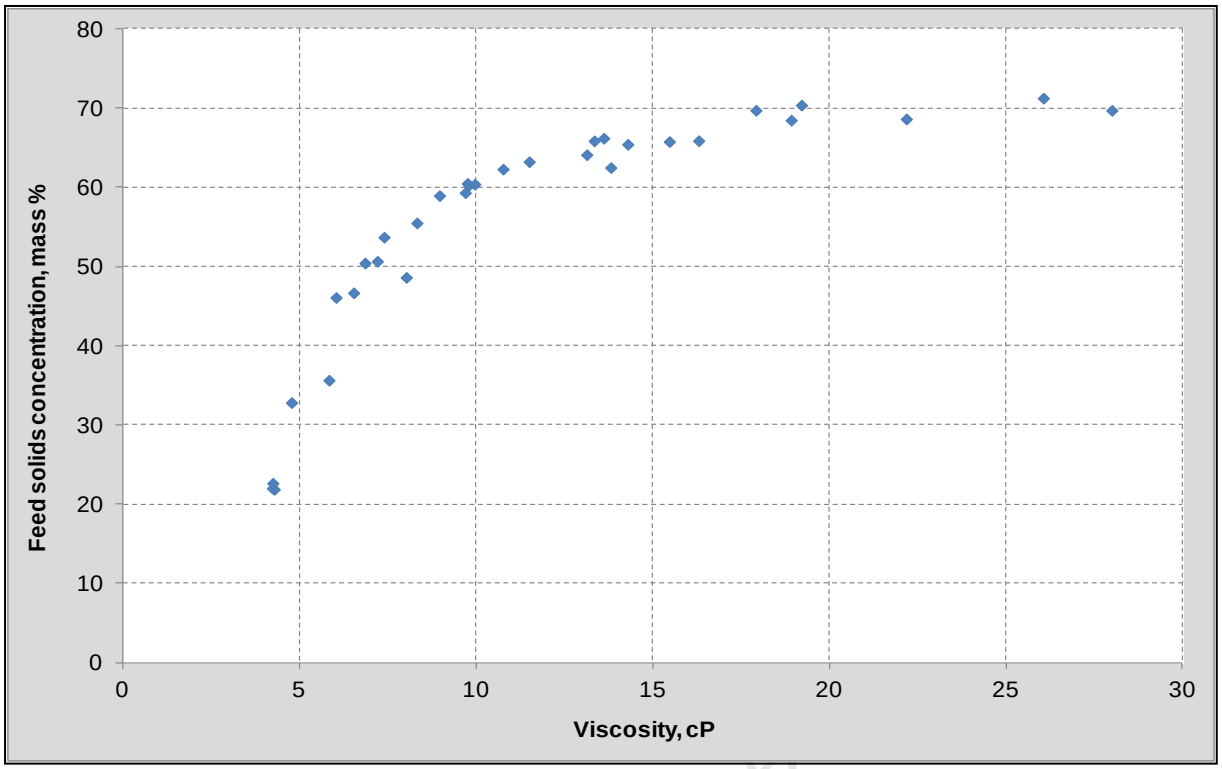

Figure 2-10. Effect of solids concentration on viscosity.

2.7.2 Particle Size

Clarke (1967) initially showed that viscosity increased with particle diameter due to the inertial effects of the particles resulting in energy dissipation. However, he stated that it appears that there exists a size (about 16 µm) above and below (due to surface effects) which viscosity could increase. This was reiterated by Jinescu (1974), although he stated the size to be 10 µm. The finding that viscosity will increase at sizes larger than the 16 µm contradicts what other researchers observed, Kawatra & Eisele (1988), Castro (1990) and Shi & Napier-Munn (1996b). They found that a reduction in particle size in general resulted in an increase in slurry viscosity and this is generally the accepted outcome. Clarke did not use actual mineral particles in his work and there is some doubt over his experimental technique. The increase in viscosity with a reduction in particle size can be attributed to the binding of water molecules due to increased surface area (this results in less water available for flow and hence increases viscosity).

As soon as particles are small enough to remain in suspension, they contribute largely to the viscosity of the slurry, (Olhero & Ferreira, 2004). This is the case for clay slurries (suspensions containing phyllosilicates) as the term ‘clay’ often refers to particles below one

or two µm according to the British Standards Institute, (Brown & Heywood, 1991). Generally for a constant volume fraction, when the particle size decreases the number of particles in suspension increases which leads to increased particle-particle interaction and increased viscosity, (Malvern, 2009). Particle-particle interactions are considered weak forces and the increased viscosity is observed more at the lower shear rate range. Conversely an increase in particle size will result in a lower viscosity due to less particle interactions, (Malvern, 2009). This again contradicts what was found by Jinescu who stated that since the energy dissipated is proportional to the mass, viscosity will tend to increase with particle diameter. The feed size to a hydrocyclone can vary depending on the application. The particle sizes used in this study were those generated naturally during the specific concentrator operations. Particle size was not a variable in this study.

2.7.3 Particle Size Distribution (PSD)

The packing density (and maximum attainable solids concentration) for spheres differs depending on the size distribution, (Hudson, 1949). As the size distribution widens the voidage between particles decreases and less water is necessary to fill these voids. As a result, adding the same volume of fluid increases the distance between particles and the viscosity decreases due to assisted shear, (Castro, 1990). This is dependent on the particle size range, as addition of excess fine particles to widen the distribution could have the opposite effect and result in an increased viscosity. This means that a higher solids concentration can be achieved at the same viscosity by widening the size distribution. This is evident when looking at the Krieger Dougherty equation (equation *2.9*). This shows that the relative viscosity (η) can be reduced by increasing the maximum packing fraction ($Ø_m$).

$$\frac{\eta}{\eta_o} = \left(1 - \frac{\phi}{\phi_m}\right)^{-[\eta]\phi_m} \quad [2.9]$$

Another representation of this is shown in Figure 2-11, from Laskowski (2001). This diagram shows the reduction in relative viscosity (line P→Q) as one moves from a mono to a bi-modal suspension. This effect becomes more pronounced at a solids concentration of above 50% by volume. Line P→S again illustrates the increase in solids content that can be achieved (at the same viscosity) when changing the particle size distribution. Hydrocyclones generally operate more effectively with a wide feed size distribution, as an absence of material in a certain size fraction could result in abnormalities in the efficiency curve. The particle size distribution of the ore types used in this thesis were considered to be similar

enough so as to not include the effects of size distribution, although small differences in the specific test feed samples did exist.

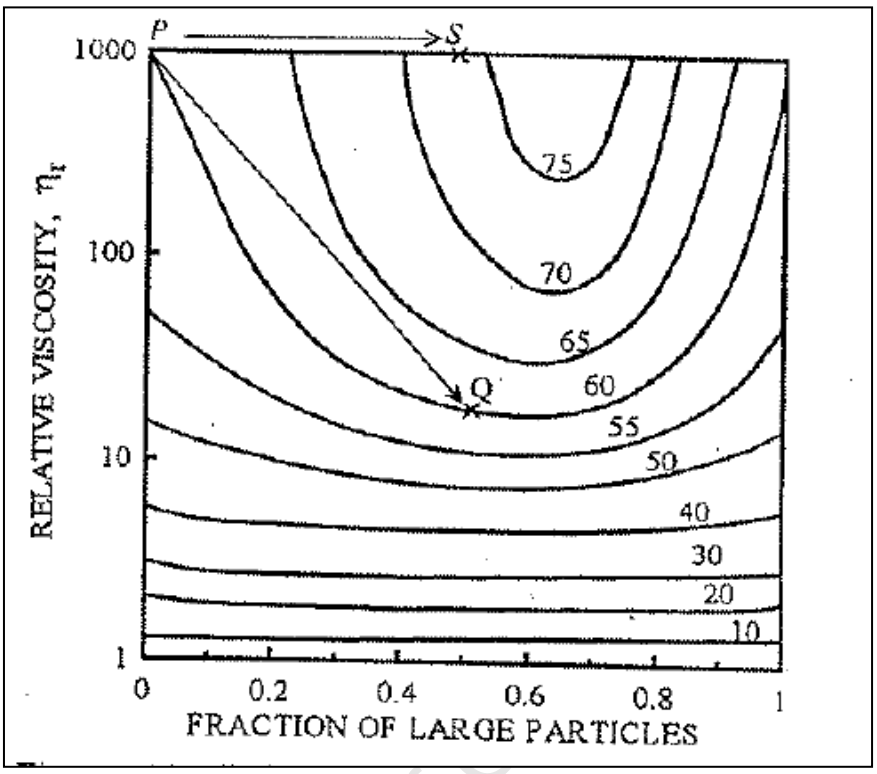

Figure 2-11. Relative viscosity of a bimodal suspension containing coarse and fine particles, Laskowski (2001).

2.7.4 Chemical environment

The chemistry of slurries can have a significant influence on their viscosity. The influence will be more significant for suspensions of ultra fine (colloidal) particles (sub-micron). These are small enough to not be affected by gravity and their interactions will be controlled by a range of inter particles forces including Van der Waals and electrical double layer forces, structural (hydration) forces, and hydrophobic forces, (Cheng, 1980).

An increase in the magnitude of the zeta potential (+'ve or –'ve) will lead to an increase in the viscosity at low shear rates. Zeta potential is a measure of the magnitude of the repulsive forces between particles. The particles here repel each other and are thus prevented from flowing freely. For dispersions with particles >1 µm, gravity has a greater effect at high concentrations and a decrease in zeta potential to the point of zero charge (iso-electric point) can introduce a yield stress to the suspension, (Malvern, 2009). The iso-electric point is the point of maximum Van der Waals attraction and coincides with the maximum yield stress for concentrated suspensions, (Boger, 2009). The suspension pH is also very important here as

discussed by He *et al.* (2001). He showed that zeta potential is directly dependent on the pH value of the suspension, and that dispersants are beneficial to fine grinding as they can eliminate the yield stress. Gravity forces on large particles will generally override any charge effects, however if conditions within the pulp favour particle attraction, flocculation may occur. When a dispersant is added, the surface nature of particles will change resulting in the inter-particle forces being repulsive and this could result in decreased viscosity as well. Solids concentration effects would generally be expected to override the effects of pulp chemistry, although this is also situation specific. The high shear environment that exists in a hydrocyclone can be beneficial for certain applications in that any surface charge effects will effectively be counteracted, resulting in the breakdown of any flocs or agglomerates, (Franks *et al.*, 2005).

Plant water can also influence the viscosity of suspensions as this can have a high mineral salt content due to the leaching out of both organic and inorganic material and this may keep recirculating and accumulating throughout the process, (Lambert, 2010). This high salt content can influence the fine particles present in the slurry.

2.7.5 Temperature

A change in slurry temperature has little effect on the physical interactions between the slurry components, (Jinescu, 1974). Viscosities of suspensions however have been shown to decrease with increasing temperature, (Kawatra *et al.*, 1988). This is mainly due to the decreased molecular cohesion forces in the carrier fluid (mainly water) which reduces liquid viscosity. Temperature should therefore always be kept constant or closely monitored during experimental work. Temperature fluctuations in hydrocyclone operations are significant as they are often fed by the mill discharge streams. These streams can vary by up to 20 degrees seasonally, (Yopps *et al.*, 1987), depending on the location of the operation. The carrier fluid in typical classification circuits is water and it is the change in the water viscosity which affects the relative viscosity of the suspension. The change in water viscosity with temperature is shown in APPENDIX A. Yang *et al.* (2001) did work on titanium dioxide suspensions (Figure 2-12) and interestingly found that the yield stress decreased with an increase in temperature up to a point, thereafter it increased again, indicating that there is an optimum temperature for rheology of certain suspensions.

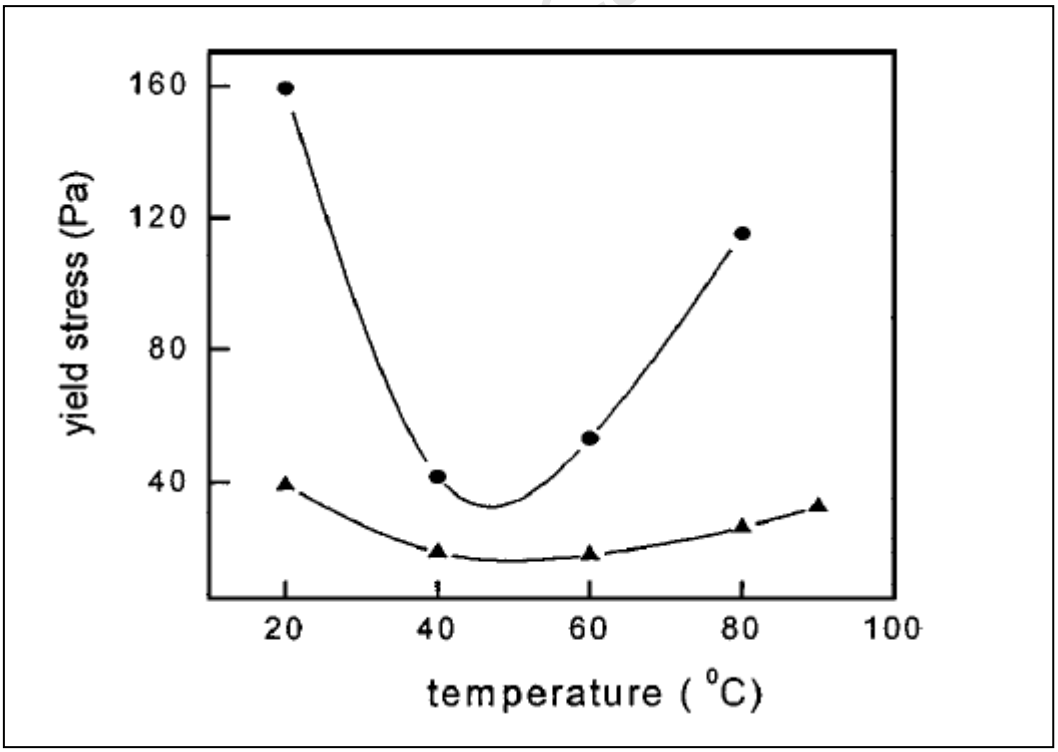

Figure 2-12. Yield stress at different temperatures:●, Cv=0.282; ▲, Cv=0.238.Yang *et al.* (2001).

The hydrocyclone feed temperature was a variable in this study as it was necessary to quantify the effects of changing fluid viscosity on the cyclone operation.

2.7.6 Particle Shape

Shape is another factor that can have an influence on suspension rheology. A deviation from spherical particle shape may result in increased viscosity due to less efficient packing and increased physical interactions between particles, (Clarke, 1967) and (Peronius & Sweeting, 1985). Non-spherical particles, especially those elongated on one edge, will also tend to have a higher viscosity at the low shear rate range due to a random orientation being a barrier. At the higher shear rates however these particles may align themselves to the direction of flow resulting in a lower viscosity (shear thinning behaviour). This viscosity could in fact be lower than that of a suspension of spherical same size particles, (Malvern, 2009). This is in contradiction with Jinescu who stated that an alignment of non-spherical particles will increase viscosity due to interparticle collisions. The slurries encountered in minerals processing will rarely consist of spherical particles due to the size reduction process, as the grinding mills produce fragments/chips, (Brown & Heywood, 1991). The effect of particle shape was not included in this work, however the sphericity of particles for the ore types used in this thesis are determined in Chapter 5.

2.7.7 Ore Mineralogy

Ore mineralogy has an influence on viscosity due to mineral composition and mineral surface charge effects. There has been little work done on characterizing the effects of ore mineralogy on slurry rheology. Mixed mineral ore types (multicomponent ores) are often encountered in mineral processing and these may possess unusual rheological qualities, depending on the mineral composition and method of characterisation. The major influence on viscosity in terms of mineralogy is the content of phyllosilicates (clay minerals) in the ore which may also relate to particle size effects, (McFarlane *et al.*, 2006). Phyllosilicates are known to increase suspension viscosity due to their platey, sheet-like nature and the charges which exist on their surfaces. Studies by Ndlovu *et al.* (2011) on the rheological behaviour of pure minerals have shown that significant changes to the yield stress occur with increased concentration of certain phyllosilicate materials. However, the phyllosilicate levels investigated were far greater than exist in the ore types studied in this thesis. Hence it is believed that mineralogy will not be responsible if significant differences in hydrocyclone performance are observed between the ore types under investigation. The mineralogy of the two ore samples used in this work is shown in Chapter 5.

2.8 Rheological Models

The most common available models for rheological prediction are tabulated in Table 2-2. All the models are conceptually similar to the Newtonian model. These models only apply to non-Newtonian suspensions under laminar flow conditions and cannot normally be used where the flow profile is in the turbulent regime unless a turbulent correction procedure has been applied, as in Shi & Napier-Munn (1996b).

Table 2-2. Rheogram models.

Newtonian	$\tau = \eta * \gamma$	Only for Newtonian fluids, $\tau \infty \gamma$
Ostwald / de Waele	$\tau = C * \gamma^{P}$ C = consistency index P = Power index	For shear thickening or thinning fluids with NO yield stress, P>1: Shear thickening, P<1: shear thinning, P = 1: Newtonian
Bingham	$\tau = \tau_{\mathbf{B}} + \eta_B * \gamma$ τ_B = Bingham yield stress η_B = Bingham viscosity	Approximates yield point, no account for shear thickening/thinning
Casson	$\sqrt{\tau} = \tau_C + \sqrt{\eta_C * \gamma}$ τ_C = Casson yield stress η_C = Casson viscosity	Gives improved approximation of yield point, assumes shear thinning behaviour
Herschel-Bulkley	$\tau = \tau_{HB} + C * \gamma^{P}$ τ_{HB} = Herschel-Bulkley yield stress C = flow coefficient P = HB index	Similar to Bingham but also indicates whether shear thickening/thinning. P: criteria same as for Ostwald de Waele

The most common types of non-Newtonian mineral suspensions can be modelled using the Bingham or Herschel-Bulkley models. Bingham type behaviour is characterised by an initial yield stress and then a straight line. The apparent viscosity of a Bingham fluid is constant at

different shear rates for parallel flow lines due to its straight line behaviour. The Herschel-Bulkley model will fit a flow curve that exhibits either shear thickening (i.e. dilatant) or shear thinning (i.e. pseudoplastic) behaviour.

The study of rheological influences on minerals processing equipment has been the subject of numerous articles in the past. The research specific to hydrocyclones will now be discussed in the following section.

2.9 Rheology and hydrocyclones

Rheological properties of suspensions coupled with fluid dynamics have been known to play an important role in the performance and operation of hydrocyclones, but as yet there has been no quantitative study outlining all the possible effects this may have. The complex nature of mineral slurries, as well as the difficulties associated with rheological measurements has led to viscosity being accounted for in many hydrocyclone models by feed solids content.

Most slurries below 70% by mass, Kawatra *et al.* (1996) are considered Newtonian in nature (or possess Newtonian-like characteristics). However, there are cases where the slurry exhibits Non-Newtonian properties below this concentration, (Shi & Napier-Munn, 1996a). The treating of Non-Newtonian slurries within the hydrocyclone becomes significant as the viscosity and flow behaviour is now dependent on shear rate. Upon entry into the cyclone body at the feed inlet the slurry experiences an increase in shear rate which reaches a maximum at the point of maximum tangential velocity. This point is close to the centre of the cyclone, Bradley (1965), at a radius of approximately one eighth of the cyclone body radius. Smaller cyclones exhibit greater tangential velocities (and hence greater rates of shear) due to their decreased radius. A slurry which exhibits pseudoplastic behaviour (thixotropy) will tend to show a decrease in viscosity once it attains a rate of shear which is greater than that which it experienced before entry to the cyclone, (Castro, 1990). Slurry with dilatant characteristics (rheopexy) would have its viscosity increased by these higher shear rates, (Van Wazer *et al.*, 1963).

Shear rate is however not the only factor that influences the flow behaviour of the slurry inside the hydrocyclone. At concentrations above 30% by volume, hindered settling becomes important and viscosity will increase due to increased particle-particle interactions, (Cheng, 1980). As the concentration profile in the hydrocyclone increases (moving towards the apex), the velocities (shear rates) will decrease, in turn affecting the rheology. A Newtonian slurry entering a hydrocyclone will not experience any significant alteration of its flow behaviour, and the viscosity should remain fairly constant throughout. However concentration profiles can still have an effect on Newtonian fluids. There has been much debate whether flow in a hydrocyclone is in the laminar or turbulent regime, with some researchers in agreement that there is an intermediate zone which exists between the two. Reynolds numbers are extremely difficult to quantify within the cyclone as different areas possess different velocity profiles; (Kelsall, 1953), (Bradley, 1965). Previous researchers have explored different aspects of the

effect of rheology on hydrocyclones. A chronological review of some of these will now be given.

Lilge *et al.* (1957) performed experiments with heavy media and assigned apparent viscosity values to the cyclone using rotational viscometer shear rate data and anemometer/stroboscope data for shear rate estimations. They showed how the viscosity (shear rate range) in the cyclone (75 mm, 150 mm) can vary by plotting viscosity versus shear rate and viscosity versus position in the cyclone for media of different densities. It is clear from their data that a pseudoplastic suspension will show a decreased viscosity towards the centre of the cyclone as the shear rate increases. Alternately a dilatant suspension (ferrosilicon) will show an increase in viscosity at the same point.

Rietema (1960) in his series of papers conducted test work on a 75mm hydrocyclone using glycerol to alter the viscosity of the carrier fluid. This was one of the earliest cases of viscosity alteration in a hydrocyclone. His focus was however on pressure drop correlations and he found that at low Reynold's numbers frictional losses will dominate, and at higher Reynold's numbers centrifugal head will dominate the pressure drop. He saw the static pressure drop as determined by the centrifugal head which was in turn determined by the tangential velocity. Higher viscosities resulted in lower tangential velocities.

Fontein *et al.* (1962) conducted an extensive investigation involving tests on a range of cyclone sizes (15 mm to 120 mm) using liquids with different viscosities (water, potato starch, corn starch). For tests with a Newtonian fluid at varied temperatures (30 mm,60 mm cyclone), he found that the capacity of a cyclone increased with an increase in liquid viscosity up to a point and then it remained fairly constant. He reasoned that an increase in fluid viscosity reduces the tangential velocity which lowers the pressure drop in the cyclone. This lower pressure drop enables a higher capacity to be reached. Eventually the rotational flow will be retarded by the increased viscosity and the liquid will be forced through the cyclone. The influence of feed viscosity was investigated using potato starch in water in a 15mm cyclone, varying viscosity by means of solids content and suspension temperature. An improved efficiency (clarification number) was obtained for tests at higher temperature due to the decreased viscosity resulting in increased centrifugal forces and decreased drag (entraining) forces. Bradley (1965) also reported that the throughput of a hydrocyclone will increase with an increase in slurry viscosity to a point, but then start to decrease. He proposed that this was due to the fact that the pressure drop occurring as a result of the viscous drag is more important than the pressure drop due to the centrifugal head change.

Agar & Herbst (1966) performed experiments using quartz in a sugar solution medium in a small 30 mm hydrocyclone. They tried to determine the relationship between cut size and fluid viscosity. They only performed 6 experiments and deduced that d_{50c} was proportional to $\mu^{0.58}$.

Mizrahi & Cohen (1966) did tests on a 60 mm cyclone using water and tetrabromoethane when studying the effect of feed rate on the U/F. The tetrabromoethane increased the viscosity tenfold (the density tripled) but they stated that no significant change was seen in the relationship between feed rate, and the U/F and O/F flow rates at these conditions which was contrary to the findings of Fontein.

Lilge & Plitt (1968) in developing their cone force equation acknowledged that the viscosity of the suspending medium has a large influence on the operation of the hydrocyclone. They found that the apparent viscosity became prohibitively high when above 45% by volume. Due to the fact that the shear rate on particles varies in the hydrocyclone depending on the position, they deduced that one point needs to be taken for the calculation of a specific shear rate. They decided on the LZVV and excluded the influence of axial velocity. This meant that all shear at this point would be due to the difference between the tangential and radial velocities.

Klimpel (1981) investigated how a chemical dispersant would affect the sizing performance of a 24-inch hydrocyclone operating with a copper ore slurry. He found an increase in fines bypass to U/F, cut size and sharpness of separation with increased addition of XFS-4272 (a Dow company wet grinding aid). It is assumed that the grinding aid should reduce the feed viscosity to the cyclone although no mention of a change in viscosity is made and viscosity was also not measured in this case. This increase in cut size was in contradiction to other research which found decreased cut size with decreased viscosities, and it is suspected that this was possibly a result of experimental issues as no sub-sieve analysis was conducted and the cut-size difference was very small (considering the size of cyclone under investigation). A possibility of a fish-hook effect was mentioned but unfortunately no sub-sieve size analysis was done to investigate this further.

Yopps *et al.* (1987) conducted tests on a 4-inch hydrocyclone using fine silica sand. They altered the rheology of the slurry using sodium lignin sulfonate, and temperature. They found that increasing the viscosity by reducing the slurry temperature increased R_f and decreased the sharpness of separation (α). The lignin addition was found to initially increase the suspension viscosity but then decrease it. At increased viscosity conditions, the fines bypass

fraction to underflow decreased, as in Klimpel (1981). They attributed this to the increase in inlet pressure (although there is no mention of pressure values) that occurs with a decreased feed viscosity. This does not agree with previous findings as an increased inlet pressure would be expected to lead to a decrease in the bypass fraction, (Napier-Munn *et al.*, 1996). It is believed that the chemical alteration of viscosity may have additional effects on the hydrocyclone operation which need to be quantified.

Horsley & Allen (1987) studied the effect of yield stress on hydrocyclone (4-inch) performance by the addition of volclay (kentonite) to a fine (d_{50} of 33 μm) silica suspension. They stated that smaller particles become trapped in flocs at a higher yield stress (viscosity) and therefore get carried to the U/F reducing efficiency. The presence of flocs is not normally expected in a cyclone due to the high centrifugal forces involved but this can also depend on the feed material. When dealing with suspensions with large amounts of fine particles, surface effects come into play and the authors explained this by referring to colloidal theory. Whether the surface effects override the hydrodynamic and inertial forces is under question for this size distribution of silica particles. At an increased viscosity they found an increase in R_f,. The term R_f here was given as the underflow to throughput ratio. Their tests were performed with only 10% silica by mass in the feed, which is not conducive to accurate hydrocyclone operation.

Perhaps the most comprehensive study of the influence of rheology on hydrocyclone efficiency and model performance under realistic conditions was carried out by Castro (1990). He demonstrated the effect of changing slurry concentration and fluid viscosity on the performance of hydrocyclones at pilot plant and industrial scale. His pilot scale tests involved using limestone on a 250 mm cyclone. Viscosity was modified by particle size, solids concentration and sucrose addition. The plant testwork was carried out on a copper ore concentrator on a 500 mm cyclone, in order to validate the conclusions from the pilot scale work. Despite the fact that his data resulted in some very peculiar efficiency curves, he was able to demonstrate that cut-size was predicted much more accurately using an apparent viscosity term rather than a solids concentration term in the Nageswararao and Plitt hydrocyclone models still currently in use today. He related the sharpness of separation to the degree of pseudoplasticity of the slurry and stated that viscosity will affect α due to hindered settling in the cyclone. He proposed a modified Nageswararao model (equations *2.23 to 2.26*), including a viscosity term in place of solids concentration.

Kawatra *et al.* (1996) studied the effect of slurry viscosity on classification by varying solids content and slurry temperature, using fine silica sand in a 100 mm cyclone. They proposed a new cut size model incorporating these rheological changes. The authors found that d_{50} and R_f increased with an increase in slurry viscosity, but the sharpness of separation (α) was not significantly affected.

Tavares *et al.* (2002) investigated the rheological effects of an ultrafine suspension of phosphate ore (non-Newtonian) on small diameter (25 mm and 50 mm) cyclones. They tested the effects of adding a dispersant PSA (polycarboxylic sodium salt), and a thickening agent (glycerine) to alter the rheology. They also derived an equation for the calculation of plastic viscosity at any radial point in the cyclone. Their findings agreed with those of previous researchers in that viscosity has a major influence on cut-size, however they found no impact of viscosity on cyclone capacity, water split, or sharpness of separation under the conditions studied. These fact that there was no effect on water split may be due to the combined effect of small cyclone size and ultrafine feed material which could have created unique rheological conditions inside the cyclone.

A few of the researchers mentioned settling slurry as an issue when measuring the viscosity of the suspensions. For settling slurries viscosity has to be measured in terms of a relative viscosity. Relative viscosity is defined as the viscosity of the slurry relative to the viscosity of the suspending medium/fluid. In addition, many of these studies were carried out using very fine suspensions at very low solids concentrations which can differ greatly from the reality of suspensions dealt with in the mineral processing industry.

Viscosity has been identified as an important parameter in the modelling of hydrocyclones. From the earliest theories to the latest empirical models, there has been some measure of a viscosity descriptor present. Hydrocyclone modelling is presented in the following section; an emphasis has been placed on models related to viscosity inclusion.

2.10 Hydrocyclone models

2.10.1 Theoretical Models

The section reviews the physical theoretical equations of the hydrocyclone efficiency correlations. The theories were classified by Svarovsky (1984) into four groups: the equilibrium orbit theory, the residence time theory, the turbulent two-phase flow theory and the crowding theory. These theories were all physical models developed using first principles. Many of the equations contained viscosity as a parameter which is an indication of the importance of slurry viscosity in hydrocyclone modelling. Some could predict the cut size, and some of them the entire efficiency curve. Unfortunately many were derived for low feed solids concentration conditions (less than 1% by volume) which made them unsuitable for practical applications.

2.10.1.1 Equilibrium Orbit Theory

The theory was based on the concept of an equilibrium radius, originally proposed by Driessen (1951) and Criner (1950). This concept stated that a particle of a certain size will attain an equilibrium radial orbit position inside the cyclone when the terminal settling velocity equals the radial velocity of the liquid (when the centrifugal force equals the drag force). This coincides with the so-called LZVV (locus of zero vertical velocity) and is the position at which a particle has an equal chance of reporting to the O/F or U/F. The best known approach to the theory reported in Napier-Munn *et al.* (1996) is that developed by Bradley & Pulling (1959), which is more of an empirical relationship:

$$d_{50} = k\left(\frac{D_C{}^3 * \eta}{Q_f\left(\rho_s - \rho_l\right)}\right)^n \quad \text{.....} [2.10]$$

Where n is a hydrodynamic constant (0.5 for laminar flow), and k is a constant incorporating mainly cyclone geometry factors.

The equilibrium orbit theories appeared to give reasonable predictions of cyclone performance for low solids concentrations, but did not consider particle residence time or the effect of turbulence which are important factors in hydrocyclone operation. Certain particles may not have the opportunity to reach the equilibrium position before exiting the cyclone. Turbulence is known to affect internal flow patterns and hence can affect the separation.

2.10.1.2 Residence time theory

Rietema (1961) proposed that non-equilibrium conditions exist in the cyclone due to the short particle residence time. He assumed a homogeneous distribution of particles across the cyclone inlet. The cut size (d_{50}) was then defined as the size of that particle located at the midpoint of the cyclone inlet on entry which will manage to reach the cyclone wall in residence time T. His expression for d_{50} was as follows:

$$\frac{{d_{50}}^2(\rho_s - \rho)L'^*\Delta P}{\mu^*\rho^*Q} = \frac{36^*V_z^*R}{\pi^*V_t^*D_i} \quad \text{.....[2.11]}$$

He argued that the RHS of the equation should be constant for constant cyclone dimensions (V_z/V_t is constant) and termed it the 'characteristic cyclone number' $C_{y50.}$ Rietema's theory did not account for radial fluid flow, inertial effects, or hindered settling at high concentrations. It also strangely did not include the effect of either pulp density, or pulp viscosity as his experiments were conducted at a single low concentration of quartz fines in water. The relationship assumed that the residence time of the particle would not be affected by slurry concentration and only changes in carrier fluid viscosity and solids/liquid density were included. An increased feed solids concentration has an influence on the pulp viscosity and on separation in the hydrocyclone as has been mentioned in Svarovsky (1984).

A later version of the theory was proposed by Holland-Batt (1980). He made the important contribution in his cut-size equation of including a factor to allow for hindered settling effects, as well as a shape factor to allow for the influence of irregularly shaped particles.

2.10.1.3 Crowding theory

Fahlstrom (1963) proposed that the cut size is dependent on the capacity of the underflow orifice and the particle size distribution of the feed. The crowding effect, or hindered discharge through the apex (spigot), was said to be related to particle mass and density – coarser/heavier particles therefore have a higher probability of passing through. He proposed that the differences between actual and corrected cut size was simply a function of size and the recovery of solids to the underflow. This is now known to be incorrect as the difference is due to the change in shape of the efficiency curve. More recently Bloor *et al.* (1980), using a relationship for slurry **viscosity** as a function of solids concentration, modelled the flow in the boundary layer. Their work showed the effect of increased feed solids on the boundary layer

– an increase was shown to thicken the layer and the underflow would have to increase to accommodate this. The model by Bloor *et al.* does not provide an equation for cut size, but does give direct proof of the crowding theory.

2.10.1.4 Turbulent two-phase flow theory

This theory tried to explain the effect of turbulence on hydrocyclone separation. Rietema (1961) estimated the turbulent **viscosity** by making use of tangential velocity profiles measured by Kelsall (1952). He derived theoretical tangential velocity profiles by solving Navier-Stokes equations and assumed the turbulent viscosity to be independent of radial position. A large amount of research in this area has been ongoing, including the work of Bloor & Ingham (1975), Schubert & Neesse (1980), and Van Duijn & Rietema (1983). Bloor & Ingham derived a **viscous** turbulent model based on Prandtl mixing length theory and related turbulent **viscosity** to the strain rate in the main cyclone flow. The distribution of eddy viscosities with radial distance at various cyclone levels was also derived.

The majority of the theoretical models show that for geometrically similar cyclones the product of the Stokes number (Stk) and the Euler number (Eu) is a constant. The advantages of theoretical equations based on fluid dynamics is that they would allow a measure of the effect of a change in slurry properties. Unfortunately most equation solutions result in non linear partial differential equations which cannot easily be solved. Numerical methods are therefore required to solve these problems which further complicates the process. Empirical models which are based on actual hydrocyclone test data have thus become more favourable and their origin and development will now be discussed.

2.10.2 Empirical Models

Due to the mathematical constraints of the theoretical models and their limitations in dealing with high solids concentrations, more practical models had to be developed for studying the hydrocyclone efficiency and throughput. Of the first empirical models to be used were those developed by Lynch & Rao (1975a). Later two general-purpose empirical hydrocyclone models (still the most widely used for simulation in the mineral processing field) were developed: the Plitt model, Plitt (1976) - modified by Flintoff, Flintoff *et al.* (1987), and Nageswararao models Nageswararao (1978). Of these models, the Nageswararao model was found to be most useful for scale-up purposes and was incorporated into the JKSimMet mineral processing simulator. Since then there has been continued research into this area, and the influence of viscosity has been included in models from Castro (1990) and Asomah (1996) in particular. New models are currently being developed as part of the P9 project, and one such model is also introduced. The models discussed below are concerned with the prediction of cut size, water split, throughput, and on occasion the alpha parameter.

2.10.2.1 Lynch/Rao Models

The earliest empirical models which found use in the industry were those of Lynch & Rao (1975a). The models were based strongly around the cyclone geometry factors as well as feed flow rate and percentage solids. They developed equations (equations *2.12 to 2.14*) designed for scale-up and specific to limestone ore. It was recommended that their model constants be modified depending on the ore type to be used. They did not propose a model for alpha (sharpness of separation). Their equations for cut size, throughput and water split were as follows:

$$\log_{10} d_{50c} = K_1 * D_o - K_2 * D_u + K_3 * D_i + K_4 * C_w - K_5 * Q_f + K_6 \quad \text{.....} [2.12]$$

Where :K_1 - K_6 are empirical constants.

$$Q_f = K * D_o^{0.73} * D_i^{0.86} * P^{0.42} \quad \text{.....} [2.13]$$

Where: K = 6 for limestone

$$R_f = K_1 * \left(\frac{D_u}{WF}\right) - \left(\frac{K_2}{WF}\right) + K_3 \quad \text{.....} [2.14]$$

Where: WF is the mass flow rate of water in the feed, and for limestone tests K_1=193, K_2=271.6, K_3=1.61.

2.10.2.2 Plitt Models

Plitt (1976) proposed the expression for cut size (equation *2.15*) using data from the work of Lynch in 1966 and then Rao (cyclone sizes 150 mm to 500 mm), and then also his own data from three different cyclone sizes (32 mm to 150 mm). He did the majority of his tests however at very low solids concentrations (13% by mass). He also incorrectly assumed a constant bypass (mass recovery of water to U/F) and his models were not dimensionless.

$$d_{50c} = \frac{50.5 * D_c^{0.46} * D_i^{0.6} * D_o^{1.21} * e^{0.063\Phi}}{D_u^{0.71} * h^{0.38} * Q^{0.45} * (\rho_s - \rho_l)^{0.5}} \quad \ldots\ldots [2.15]$$

The model allowed for a volume concentration input (Φ) and considered the density effects of the solid and liquid phases. This model was later modified (eq. *2.16*), by Flintoff *et al.* (1987), to include a slurry viscosity term and a hydrodynamic exponent (K) and incorporated a constant (F1) which could consider feed size effects:

$$d_{50c} = \frac{F1 * 39.7 * D_c^{0.46} * D_i^{0.6} * D_o^{1.21} * \mu^{0.5} * e^{0.063\Phi}}{D_u^{0.71} * h^{0.38} * Q^{0.45} * ((\rho_s - 1)/1.6)^K} \quad \ldots\ldots [2.16]$$

Plitt developed an expression for throughput using the same data as follows:

$$Q = \frac{0.70 * P^{0.56} * D_c^{0.21} * D_i^{0.53} * h^{0.16} * (D_u^2 + D_o^2)^{0.49}}{e(0.0031\Phi)} \quad \ldots\ldots [2.17]$$

He again included a feed concentration term (V_p). The equation was later modified, Flintoff *et al.* (1987), to include a calibration parameter (F3) which accounted for feed size effects:

$$Q^{1.78} = \frac{P * D_c^{0.37} * D_i^{0.94} * h^{0.28} * (D_u^2 + D_o^2)^{0.87}}{1.88 * F3 * e(0.0055\Phi)} \quad \ldots\ldots [2.18]$$

The modified Plitt expression for flow split included a pulp density effect and a size effect constant (F4) as follows:

$$S = \frac{F4 * 18.62 * \rho_p^{0.24} * \left(\frac{D_u}{D_o}\right)^{3.31} * h^{0.54} * (D_u^2 + D_o^2)^{0.36} * e^{(0.0054\Phi)}}{(P^{0.24} * D_c^{1.11})} \quad \ldots\ldots [2.19]$$

2.10.2.3 Nageswararao Models

The Nageswararao model (1978) consists of empirical equations developed using data gathered by Nageswararao and Rao (Lynch and Rao, 1975). Nageswararao conducted numerous tests on a range of hydrocyclone sizes and ore types. He formulated an expression for throughput (Q) based on the well known throughput versus pressure relationship. Besides geometrical factors, he considered the pulp density to be an important input and included a feed material constant (K_{Qo}):

$$\frac{Q}{D_{c^2}\sqrt{\frac{P}{\rho_p}}} = K_{Qo}\left\{D_c{}^{-0.10}\right\}\left(\frac{D_o}{D_c}\right)^{0.68}\left(\frac{D_i}{D_c}\right)^{0.45}\left(\frac{L_c}{D_c}\right)^{0.20}\theta^{-0.10} \quad \text{.....} [2.20]$$

His cut-size (d_{50c}) relationship was based on the product of the Euler and Froude numbers. He also included a hindered settling factor term (λ) based on the expression proposed by Steinour in 1944 to account for the influence of feed solids concentration. A feed material constant K_{Do} was again included:

$$\frac{d_{50c}}{D_c} = K_{Do}\left\{D_c{}^{-0.65}\right\}\left(\frac{D_o}{D_c}\right)^{0.52}\left(\frac{D_u}{D_c}\right)^{-0.47}\left(\frac{D_i}{D_c}\right)^{-0.50}\left(\frac{L_c}{D_c}\right)^{0.2}\theta^{0.15}\left(\frac{P}{\rho_p g D_c}\right)^{-0.22}\lambda^{0.93} \quad \text{....} [2.21]$$

$$\rightarrow Where: \lambda = \left[\frac{(C_v)^3}{(1-C_v)^2}\right]$$

The Nageswararao expression for water recovery to the underflow (R_f) was identical to his cut size model in terms of input variables, but the exponents differed in magnitude and a new feed material constant (K_{W1}) was included:

$$R_f = K_{W1}\left(\frac{D_o}{D_c}\right)^{-1.19}\left(\frac{D_u}{D_c}\right)^{2.4}\left(\frac{D_i}{D_c}\right)^{-0.50}\left(\frac{L_c}{D_c}\right)^{0.22}\theta^{-0.24}\left(\frac{P}{\rho_p g D_c}\right)^{-0.53}\lambda^{0.27} \quad \text{….....} [2.22]$$

Nageswararao (2001) found that water split was a more accurate prediction than actual flow split. He also stated that previous researcher's equations were considered too site specific and the Plitt and Svarovsky, (Svarovsky, 1996), models did not consider the influence of feed material characteristics which were found to be significant.

As it stands the Nageswararao model only accounts for influence of feed solids on rheology via the ρ_p (feed pulp density) and the λ terms (feed volume solids fraction). It does not take into account the various other factors which influence the rheology ie. carrier fluid viscosity, particle size distribution, particle size. Nageswararao also did not incorporate alpha into his models.

2.10.2.4 Castro Models

Castro (1990) reviewed some of the weaknesses of the Nageswararao model and reported that the model was found to be unsuitable for slurries with pulp densities below 30% by mass. He showed that the model reflected deviations in cut size and pressure prediction when applied to hydrocyclones treating viscous pulps (clayey) due to the omission of a viscosity term. Plots of cut size against % solids and apparent viscosity using pilot plant data also showed improved trends when using apparent viscosity over % solids (Figure 2-13). Castro therefore continued to modify the existing models with the inclusion of viscosity terms.

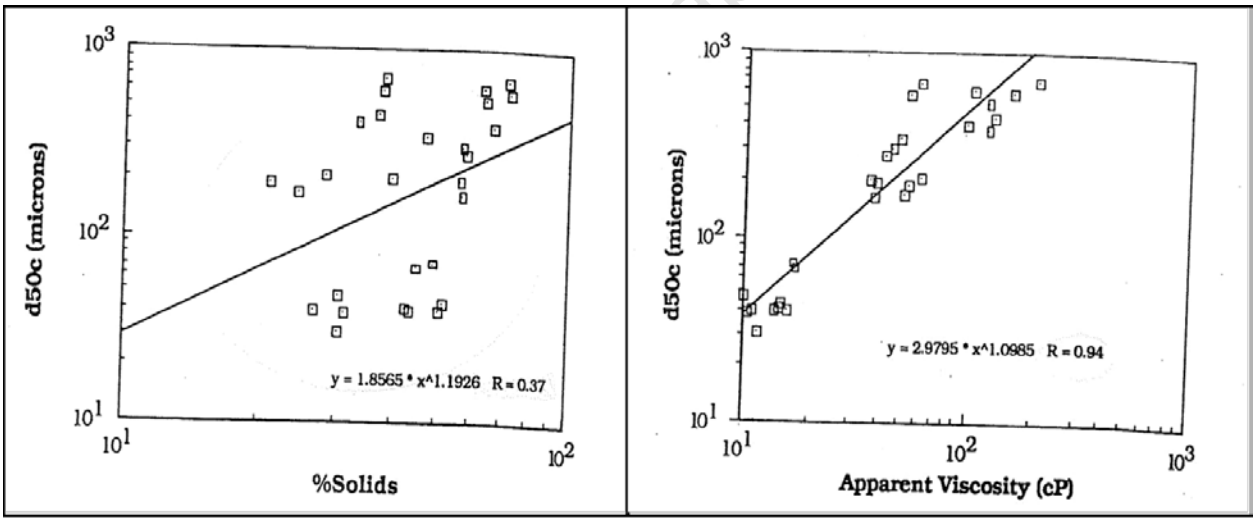

Figure 2-13. Improvement of prediction of d_{50c} using apparent viscosity (right) compared to using % solids (left), Castro (1990).

He developed models using the same methodology as Nageswararao, based on the data from pilot plant and plant scale test work. His Euler number equation (equation *2.23*) was based on the Nageswararao throughput equation which incorporated the products of the Euler (relates static pressure drop to dynamic pressure calculated from the velocity) and Froude (relates gravitational to inertial forces) numbers as independent variables. Castro brought in the relative viscosity term (pulp viscosity over carrier fluid viscosity, in this case water) and a cyclone Reynold's number term to incorporate viscosity as follows:

$$E_u = 10^{-2.903}\left(\frac{D_o}{D_c}\right)^{0.5831}\left(\frac{\mu_p}{\mu_w}\right)^{-0.6900}\left(\frac{D_i}{D_c}\right)^{0.3298}\mathrm{Re}^{0.7525} \quad \ldots\ldots\ldots\ldots\ldots\ldots\ldots\ldots\ldots\ldots [2.23]$$

Castro's cutsize equation (equation *2.24*) included the relative viscosity term as well as a term to account for the change in solids, pulp and fluid density:

$$\frac{d_{50c}}{Dc} = \frac{10^{-9.586}\left(\frac{\mu_p}{\mu_w}\right)^{-0.6465}}{\left(\frac{P}{\rho_p g D_c}\right)^{0.8313}\left(\frac{D_u}{D_c}\right)^{1.792}\left(\frac{\rho_s-\rho_p}{\rho_l}\right)^{1.596}} \quad \ldots\ldots\ldots\ldots\ldots\ldots\ldots\ldots\ldots\ldots\ldots\ldots\ldots\ldots\ldots\ldots [2.24]$$

His equation for water split (R_f) also incorporated a Reynold's number term and feed volume concentration term:

$$1-\frac{R_f}{100} = \frac{\left(\frac{d_{50c}}{D_c}\right)^{0.06305}\left(\frac{P}{\rho_p g D_c}\right)^{0.1589}\mathrm{Re}^{0.08345}}{C_V{}^{0.1063}\left(\frac{D_u}{D_c}\right)^{0.5792}} \quad \ldots\ldots\ldots\ldots\ldots\ldots\ldots\ldots\ldots\ldots\ldots\ldots\ldots\ldots\ldots\ldots [2.25]$$

Castro found that the hindered settling term (λ) in Nageswararao's equations did not match his data well (inaccurate below 30% solids) and so excluded this from his final model equations. He decided to use a simple exponential model to relate the hindered and terminal velocities:

$$\left(\frac{V_H}{V_t}\right) = e^{-k C_v} \quad \ldots\ldots\ldots\ldots\ldots\ldots\ldots\ldots\ldots\ldots\ldots\ldots\ldots\ldots\ldots\ldots\ldots\ldots [2.26]$$

2.10.2.5 Asomah Models

Work on the development of hydrocyclone models with the view of incorporating a viscosity term continued and in 1996 a thesis was published by Asomah for his PhD at the JKMRC, (Asomah, 1996). His work mainly looked at the effect of the angle of inclination of hydrocyclones but he also included a slurry viscosity term in his models, (Asomah & Napier-Munn, 1997). He modified the Nageswararao models to include slurry viscosity which was incorporated into a modified Reynold's number term. This Reynolds number term (termed pulp Reynold's number) also accounted for the change in feed density. He also included a

relative viscosity term in the equation for alpha. The models for cut-size (d_{50c}), water split, sharpness of separation and pressure drop developed by Asomah are given in equations *2.27* to *2.30*:

Cut-size -

$$d_{50c} = D_c^{\,0.229}\left(\frac{P_{40}}{D_o}\right)^{-0.457}\left(\frac{D_o}{D_u}\right)^{0.948}\left(1-V_s^{(1-\theta/180)}\right)^{-2.941}\mathrm{Re}_p^{\,-0.155}*$$
$$(A)^{0.719}\exp\left(-1.392\frac{\theta}{180}\right)B1 \quad , default\ B1=0.2278 \qquad \ldots\ldots\ldots\ldots\ldots\ldots\ldots\ldots [2.27]$$

Water split -

$$1-C = D_c^{\,0.471}\left(\frac{P_{40}}{D_o}\right)^{0.214}(1-V_s)^{-0.825}\left(\frac{D_o}{D_u}\right)^{-1.806}\left(\frac{L_c}{D_c}\right)^{0.287}\mathrm{Re}_p^{\,-0.175}*$$
$$(A)^{-0.478}\exp\left(-1.357\frac{\theta}{180}\right)B2 \quad , default\ B2=10.16 \qquad \ldots\ldots\ldots\ldots\ldots\ldots\ldots\ldots [2.28]$$

Sharpness of separation (alpha) -

$$\alpha = D_c^{\,-0.148}\left(\frac{D_o}{D_c}\right)^{1.046}\left(\frac{D_u}{D_c}\right)^{-0.161}\left(\frac{u_{sl}}{u_w}\right)^{-0.854}\left(\frac{\rho_s-\rho_p}{\rho_s}\right)^{-2.182}\mathrm{Re}_p^{\,-0.107}*$$
$$(A)^{0.429}\exp\left(-0.094\frac{\theta}{180}\right)B3 \quad , default\ B3=25.59 \qquad \ldots\ldots\ldots\ldots\ldots\ldots\ldots\ldots [2.29]$$

Pressure drop -

$$P = Q_F^{\,2.0}D_c^{\,-1.478}\,\rho_p(1-V_s)^{0.435}\left(D_{i*}\,D_o\right)^{-1.538}\left(\frac{L_c}{D_c}\right)^{-0.455}*$$
$$(A)^{0.246}\exp\left(-0.133\frac{\theta}{180}\right)B4 \quad , default\ B4=714.5 \qquad \ldots\ldots\ldots\ldots\ldots\ldots\ldots\ldots\ldots\ldots [2.30]$$

The B parameters were system constants which accounted for any changes in variables which were not well quantified such as feed properties. Unfortunately these constants needed to be fitted to each new condition. His models also required many inputs to extract the efficiency parameters.

In terms of other modelling work, Kawatra *et al.* (1996) using the same data, modified first the original Lynch/Rao cut-size model, and then Plitt's cut-size model to include a viscosity

term. They determined the viscosity/cut-size relationship by plotting d_{50c} vs viscosity on a log-log scale (Figure 2-14) and then deduced that the d_{50c} was proportional to the 0.35^{th} power of the slurry viscosity.

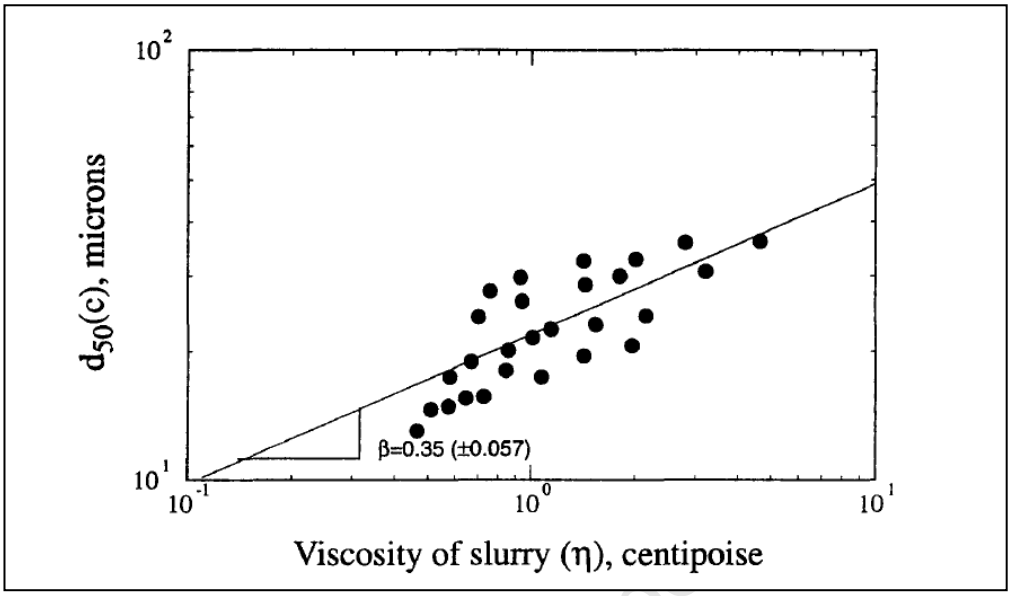

Figure 2-14. Determination of the exponent of viscosity, Kawatra *et al.* (1996).

Figure 2-14 shows the data to be quite variable and the best fit is not necessarily the correct relationship. Nevertheless they proposed new models based on their work as follows: The modified version of the Lynch/Rao model (eq. *2.12*) became-

$$\log_{10} d_{50c} = 0.41 \log_{10} \Phi - 0.0695 * D_u + 0.0130 * D_o + 0.0048 * Q + 0.35 \log_{10} \eta + K_3 \quad \text{.....} [2.31]$$

The modified version of the Plitt cut-size model (eq. *2.15*) became-

$$d_{50c} = \frac{50.5 * {D_c}^{0.46} * {D_i}^{0.6} * {D_o}^{1.21} * \Phi^{0.41} * \eta^{0.35}}{{D_u}^{0.71} * h^{0.38} * Q^{0.45} * (\rho_s - \rho_l)^{0.5}} \quad \text{.....} [2.32]$$

2.10.2.6 Narasimha-Mainza cyclone model

More recently in 2011, Narasimha & Mainza developed a new model for use in JKSimMet. The model has taken into account the effect of a change in relative viscosity. The modified capacity equation incorporated the effect of feed solids concentration (λ) and also spigot diameter (D_u) as shown in equation *2.33:*

$$\frac{Q}{D_c^2\sqrt{P/\rho_p}} = K_{Q1}\left(\frac{D_i}{D_c}\right)^{0.45}\left(\frac{D_o}{D_c}\right)^{0.826}\left(\frac{D_u}{D_c}\right)^{0.11}(1/\tan\left(\frac{\theta}{2}\right))^{0.33}\left(\frac{L_c}{D_c}\right)^{0.406}(\lambda)^{-0.0535} \quad \text{.....[2.33]}$$

The cut size equation (equation *2.34*) incorporated a parameter that accounts for the hindrance of particles, proposed by Steinhour (1944), and also used in Castro (1990). It includes a feed pulp Reynolds number term which has slurry viscosity as the denominator. This Reynold's number incorporates the cyclone body diameter as an input as opposed to the particle diameter and so does not link directly to particle size:

$$\frac{d_{50c}}{D_c} = K_{D1}\left(\frac{D_o}{D_c}\right)^{0.88}\left(\frac{D_u}{D_c}\right)^{-0.687}\left(\frac{(1-fv)^2}{10^{(1.82*fv)}}\right)^{-0.911}(\mathrm{Re})^{0.042}\left(\frac{D_i}{D_c}\right)^{-1.058}\left(\frac{L_c}{D_c}\right)^{0.2}\left(\frac{1}{Tan(\theta)}\right)^{-0.163} \quad \text{..[2.34]}$$

The modified water split equation (equation *2.35*) included a term to quantify the G-forces inside the cyclone in terms of tangential velocities and gravitational forces imposed. It also included the addition of the viscosity ratio (μ_m/μ_w) and a term accounting for the percentage of material passing 38 µm in the feed stream (F_{-38um}).

$$R_f = K_{W1}\left(D_o/D_c\right)^{-0.37}\left(D_u/D_c\right)^{1.86}\left(V_t^2/R_{\max}g\right)^{-0.71}\left(1/\tan(\theta)\right)^{-0.15}\left(\mu_m/\mu_w\right)^{0.434}\left(Lc/D_c\right)^{1.28} \quad \text{...[2.35]}$$

$$where\ u_m = u_w * \left(1-\frac{f_v}{0.62}\right)^{-1.55} * \left(F_{-38um}\right)^{0.39},\ and\ V_t = 4.5\left(\frac{D_i}{D_c}\right)^{1.13} V_i$$

The ongoing development of empirical models is bound to continue as new model validation data becomes available. Ultimately though, the key to understanding the mechanism of separation and hence being able to provide an accurate predictive model must lie in the basic physics of fluid flow and this area is also currently generating research interest once again.

2.11 Summary of effects of viscosity on hydrocyclone efficiency parameters

2.11.1 Effect on cut size, d_{50}

There is general consensus that viscosity will affect cut-size, a lower feed viscosity generally decreases the cut-size and vice versa. There may be other factors which will influence cut-size and may override the effects of viscosity but there is a direct relationship between viscosity and d_{50} (d_{50} α η^k), where k is a constant. Various authors have come up with different values for k, ranging from 0.3 to 0.6. A few of these are listed in Table 2-3, although these consider the carrier fluid viscosity rather than the actual slurry viscosity.

Table 2-3. Historical exponents of carrier fluid viscosity, adapted from Castro (1990).

AUTHORS	VISCOSITY POWER
Yoshioka and Hottta, 1955	0.50#
Haas *et al*, 1957	0.50#
Rietema, 1961	0.50#
Agar and Herbst, 1966	0.58*
Williamson, Kumar *et al*, 1984	0.48*
Svarovsky, 1987	0.50#
Kawatra, 1988	0.53*
Castro, 1990 – pulp viscosity	0.65*

*# Theoretical derivation, * Experimental Work*

2.11.2 Effect on sharpness of separation, α

The effect of viscosity on the α parameter is less clear and more difficult to quantify. The effect on α thus far has either been no significant change, or a decrease in α with an increase in suspension viscosity.

2.11.3 Effect on water split to O/F, C

An increase in viscosity has lead to a decrease in C as there is a decrease in the centrifugal forces. This viscosity increase would result in decreased shear rates and therefore an increase in fluid passing through the U/F as the magnitude of the inner vortex is decreased. However this is also dependent on the rheological properties of the slurry, as a dilatant suspension will exhibit decreased viscosities at decreased rates of shear and may result in a combined effect of an increased value of C as well in some cases.

2.12 Conclusions

The influence of viscosity on the performance of the hydrocyclone has been studied for many years. Many researchers have included viscosity terms in their empirical models as an alternative to the standard feed density term which was commonplace in the initial modelling stages. However the models have yet to make an impact in terms of application to changing rheological systems.

The measurement of the viscosity of actual hydrocyclone feed slurry remains an ongoing problem and the inclusion of a viscosity term will be fruitless unless this viscosity is correctly measured. It is for this reason that the trend has been to include a relative viscosity term which relates viscosity to the carrier fluid. It is indeed the carrier fluid which will control the viscosity in this environment, whether it is due to changes in slurry temperature or to an increase in the content of ultrafines in the suspension. The increase in viscosity due to solids concentration alone will only be important above 65% solids by mass and the accurate measurement of viscosity at these ranges is usually difficult due to particle settling.

The existence of the high pressure/flow feed to the cyclone and the high centrifugal force environment is advantageous in terms of rheology in that it eliminates the need to overcome the yield stresses if they exist, and it has been mentioned that the presence of any non-Newtonian fluids (pseudoplastics) should not be problematic due to the increased shear rate conditions.

The empirical models to date have been useful in predicting the performance of the hydrocyclone under specific conditions. However, when there is a departure from these specific conditions these models need their constants to be refitted to new data. It is believed that the theoretical models will still play a part in cyclone modelling in the future, especially with the development of non-invasive particle tracking techniques and their validity with the computational (CFD) model predictions.

3. HYPOTHESIS AND KEY QUESTIONS

This chapter introduces the hypothesis of the thesis and discusses the key questions that were looked at which arose out of the formulation and indeed the investigation of the hypotheses.

3.1 Hypotheses

The hypotheses that were proposed for this thesis were the following:

> *"A change in the hydrocyclone feed slurry viscosity will alter the efficiency of separation due to the influence of rheology on the fluid flow patterns inside the hydrocyclone". The separation is optimal under steady unhindered flow conditions and thus any resistance introduced to this flow will affect the performance.*
>
> *"The influence of viscosity will be more pronounced for larger cyclone diameters due to the decreased centrifugal forces and hence decreased tangential velocities".*

3.2 Key Questions

Various key questions arose from the proposed hypothesis:

- *How would a change in feed viscosity affect the sharpness of separation (α), water split to O/F (C) and the corrected cut-size (d_{50c})?*

  It has been mentioned previously that an increase in viscosity will lead to an increase in cut-size and a decrease in C, however the effect on alpha is not clearly understood. Different values of alpha can be obtained for different density components. The results from this work will seek to confirm previous researcher's findings.

- *Could a meaningful viscosity value be extracted for each rheological condition?*

  A different viscosity value will be obtained with each rheological change and the main aim will be to try and extract a meaningful value that can be useful in the validation of the new hydrocyclone models.

- *Castro (1990), made the observation that if a chart of apparent viscosity versus shear rate is drawn, different curves will be obtained for each condition, eg. % solids. These curves need to be compared between a specific range of shear rates and it should be determined if this is possible?*

The rate of shear in the hydrocyclone depends on many factors and it is not possible to quantify it for each condition tested in this work. However an approximate range of shear rates for each cyclone diameter can be chosen to compare the apparent viscosities mentioned above.

- *Would the efficiency curve be affected by certain viscosity altering factors more than others?*

  The carrier fluid viscosity will be altered by means of sucrose addition, and temperature modification. The slurry viscosity will also be changed by the increasing of feed solids concentration. It is expected that these changes will not have equal effects and it will be necessary to identify which variable will dominate for each ore type investigated.

- *Will a change in feed viscosity cause any appearance of the fish-hook effect?*

  The fish-hook phenomenon has been questioned by Nageswararao (2000). It will be of interest in this thesis to examine the efficiency curve data for the different rheological tests to see whether there is indeed any link between viscosity changes and fish-hook appearance (inclusion of β parameter).

- *Will the larger cyclone sizes be more affected when investigating viscosity effects, and can this be attributed to the decrease in centrifugal forces due to increased body diameter.*

  Particles fed into smaller cyclones experience larger centrifugal forces and tangential velocities. This will be beneficial when dealing with pseudoplastic slurry behaviour. If the behaviour is not pseudoplastic then a change in slurry viscosity would be expected to show similar trends with varying cyclone diameter (at the same operating conditions).

4. EQUIPMENT DESIGN & EXPERIMENTAL METHODOLOGY

This chapter explains the method that was used to characterise the slurries that were used for the test work. A method of excluding the lower shear rate values from the rheograms was used to eliminate the data where settling occurred in the pipe. The design and commissioning of the hydrocyclone test rigs used will then be described.

4.1 Tube rheometer calibration

As previously mentioned, measurement of slurry viscosity remains a problem when trying to characterise the rheology of a settling slurry. After doing some research into this area, the Centre for Minerals Research (CMR) at UCT commissioned Paterson and Cooke Consulting Engineers (PCCE) to design a special tube rheometer that would be suitable for characterising the rheology of settling slurries encountered in minerals processing. The manual process viscometer/rheometer (MPV) was thus purchased, Figure 4-1. Tube geometry is preferred when high concentration suspensions are to be characterised because the flow curves have been found to be dependent on the geometry, (Brown & Heywood, 1991).

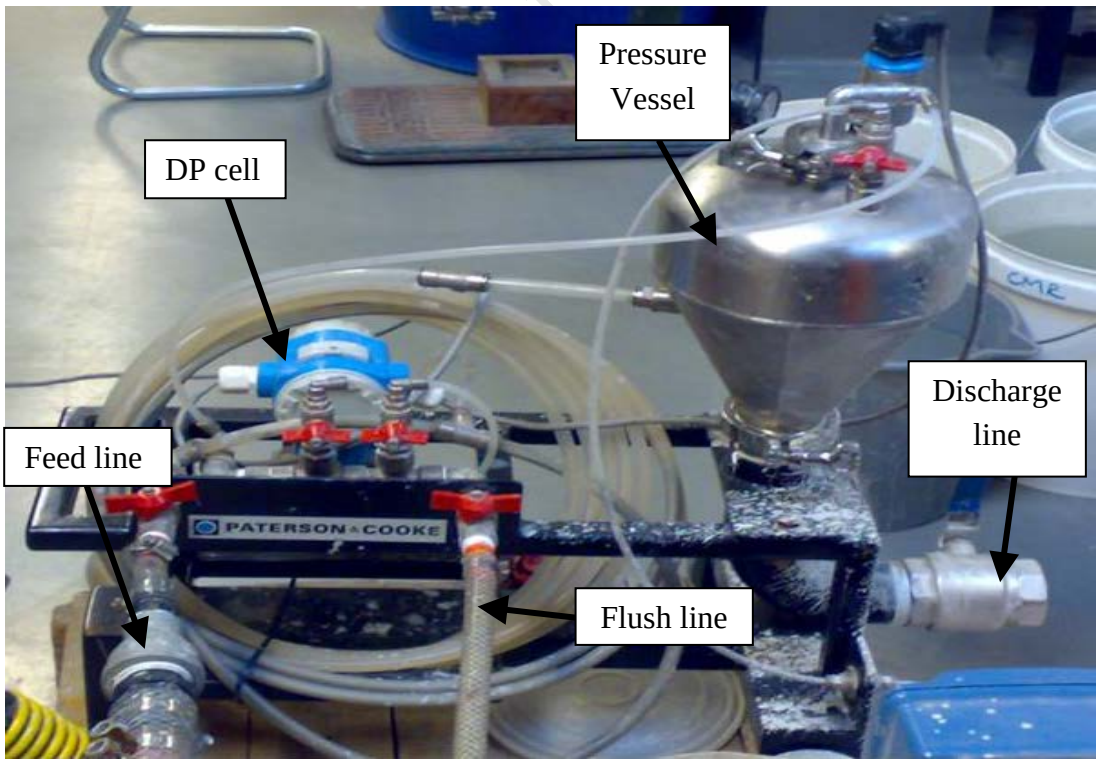

Figure 4-1. The Paterson & Cooke tube rheometer.

The rheometer consists of a long length of coiled tube 9.4 m in length and 9.9 mm internal diameter. A differential pressure (DP) cell measures the pressure drop between two sections of the tube. The tube is connected to an instrumented pressure vessel of known volume (5.72 litres) which is closed to the atmosphere. The slurry is pumped via a centrifugal pump through the tube and into the vessel and as it fills up, the slurry compresses the air and the pressure inside the vessel increases. Flow rate is calculated from the difference in vessel pressure according to Boyle's Law which states that the volume of gas is directly proportional to its pressure. DP cell and vessel pressure data are transmitted to a laptop computer via transmitter cables. Using the combined measurements of pressure drop in the pipe, pressure change in the vessel and slurry flow and equipment data, Labview MPV software calculates the wall shear stress (τ) and pseudo shear rate (γ) and plots the rheogram in real time. Data and configuration files are extractable to a spreadsheet program.

A user-friendly interface (Figure 4-2) allows the user to change many parameters such as sampling rate, sampling duration and sampling interval time. No rheometer is entirely suitable for settling slurries but the MPV allows a good comparison of a variety of sample types and its ease of use makes it suitable for plant and pilot plant studies.

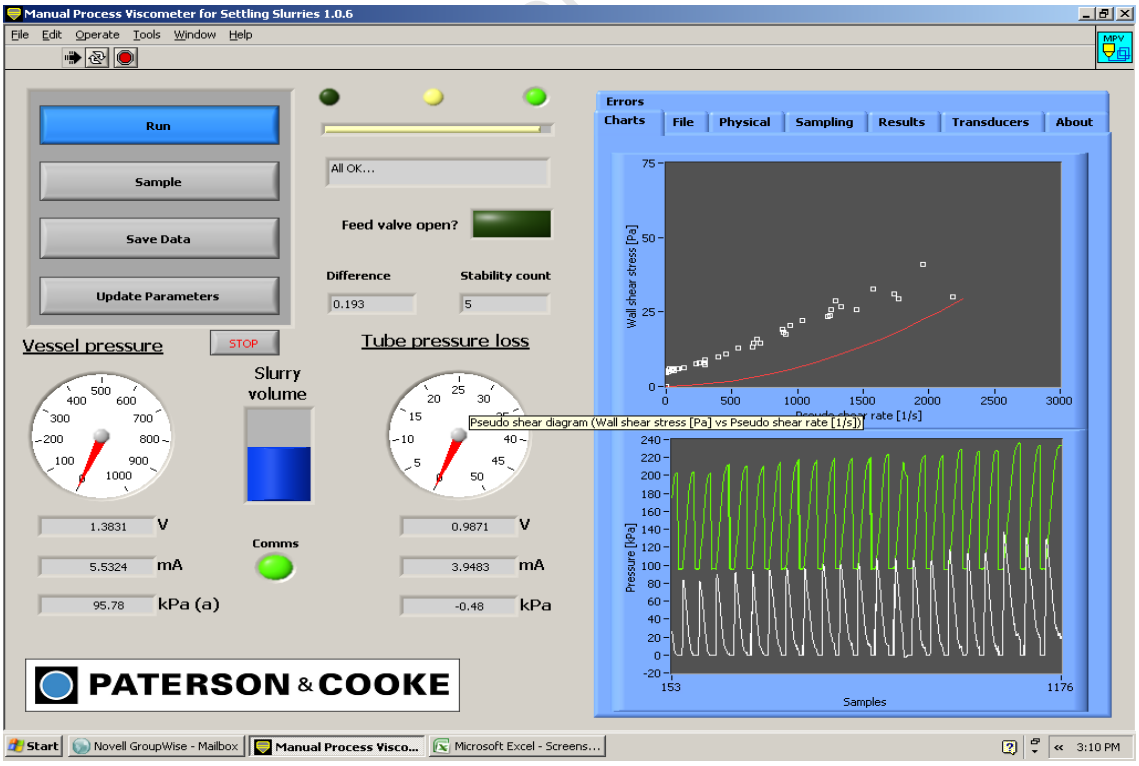

Figure 4-2. MPV user interface showing real-time plotting of rheogram.

The MPV was used as a standalone device and also connected online with the hydrocyclone test rigs. The hydrocyclone was simply bypassed when rheology measurements were required and the recycle lines on the test rigs were throttled slightly to enable the pump to generate a greater slurry flow rate at the rheometer inlet and hence a greater shear rate through the pipeline. Certain slurries settled in the pipeline as the pressure vessel filled up and lower shear rates were approached and this had to be carefully managed. If any settling behaviour was noticed the data below this point was not considered useful as no meaningful deductions can be made from the rheograms and the settled particles do not have a significant influence on the rheology of the suspension/slurry.

Water calibration tests were initially performed to ensure the equipment was working satisfactorily. All rheometer tests were performed in triplicate and the curves plotted against each other to check for reproducibility. If a curve was found to be significantly different from the others, it was excluded from the results.

Raw data from the resulting rheograms was obtained and evaluated. Data was exported to a Microsoft Excel spreadsheet in the form of wall shear stress and pseudo shear rate values. The wall shear stress (τ_w) could also be back calculated using the Hagen-Poiseuille Law as follows:

$$\tau_w = \left(\frac{D * \Delta P}{4 * L} \right) \quad \text{.....} \quad [4.1]$$

where: D = tube inside diameter, ΔP = pressure drop along pipe section, L= length of pipe.

The pseudo shear rate for Non-Newtonian suspensions (γ_w) is obtained by using the Rabinowitsch-Mooney equation, Govier & Aziz (1972):

$$\gamma_w = \left(\frac{8V}{D} \right) * \left(\frac{1 + 3n'}{4n'} \right), \; where: n' = \frac{d\left(\ln \tau\right)}{d\left(\ln \frac{8V}{D} \right)}, \; and \; V = \frac{4 * Q}{\pi * D^2} \quad \text{.....} \quad [4.2]$$

where: V = slurry velocity, n' =slope of a logarithmic plot of SS vs SR

In the case of Newtonian suspensions n' becomes one and the shear rate equation reverts back to 8V/D.

When analyzing the results it was found that the water calibration curve was offset by the onset of turbulence. The flow profile for a turbulent fluid is very different to that of one

exhibiting laminar flow and the result is an over prediction of apparent viscosity. A data correction procedure to account for this was devised using the Matlab software and this is described in APPENDIX B. Calibration tests were performed on water, sucrose solutions and kaolin suspensions.

4.1.1 Sucrose solutions (Newtonian)

Tests using sucrose (sugar) in water were conducted, as sugar dissolved in water is well known to be a standard Newtonian suspension used in rheology test work. Measurements were taken at a range of concentrations between 10 and 70% by volume (15 to 79% by mass) of sugar in solution. A solution of sucrose dissolved in water in measured in Brix, where 60 Brix is equivalent to 60% sugar by mass in solution. The tests were all performed under acceptable levels of sucrose saturation and the saturation point increases greatly when the temperature of the liquid is increased. Figure 4-3 shows an example of the raw data obtained from the rheometer for different solution concentrations. The straight lines passing through the origin indicate that the sucrose-water solution exhibited Newtonian behaviour at all concentrations.

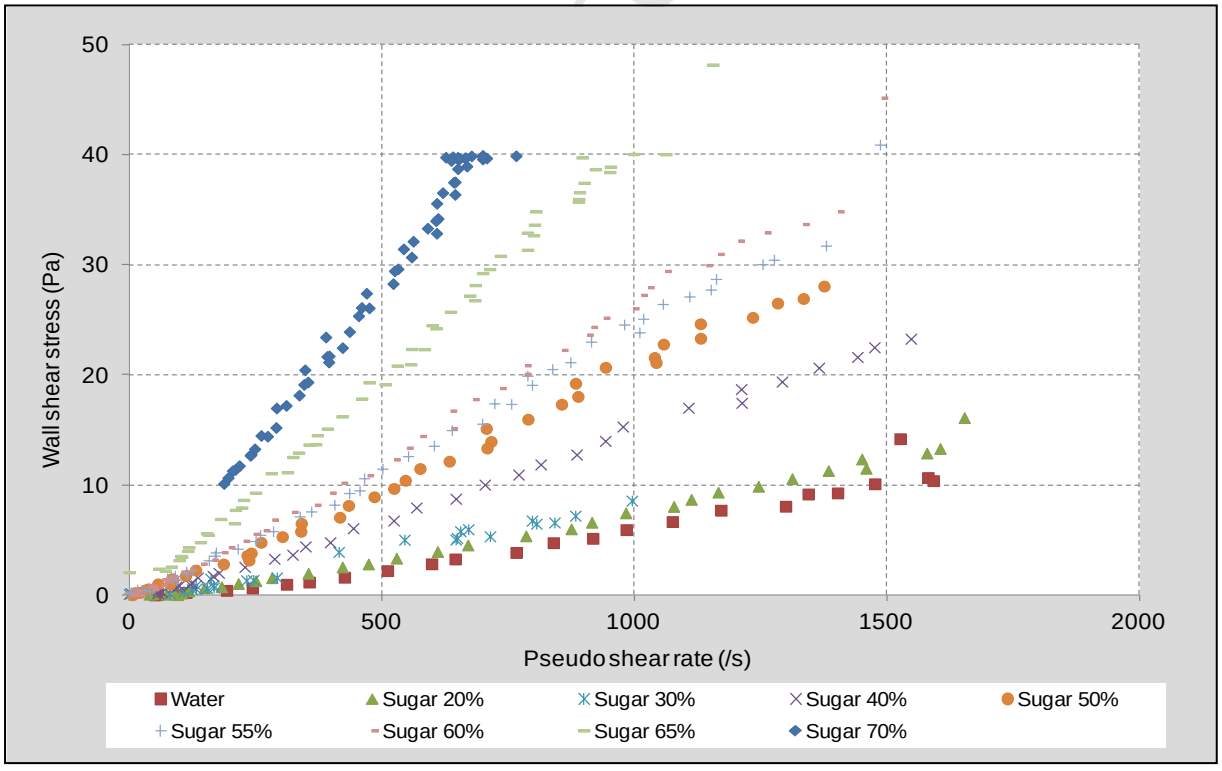

Figure 4-3. Raw data sucrose water flow curves, 20% to 70% by vol.

Figure 4-4 below is the corrected plot of the same data. The slope of the rheograms (and hence viscosity) increases as the concentration is increased from water (0%) to 70% sucrose by volume. The shear rate values were truncated at a shear rate of 1500/s.

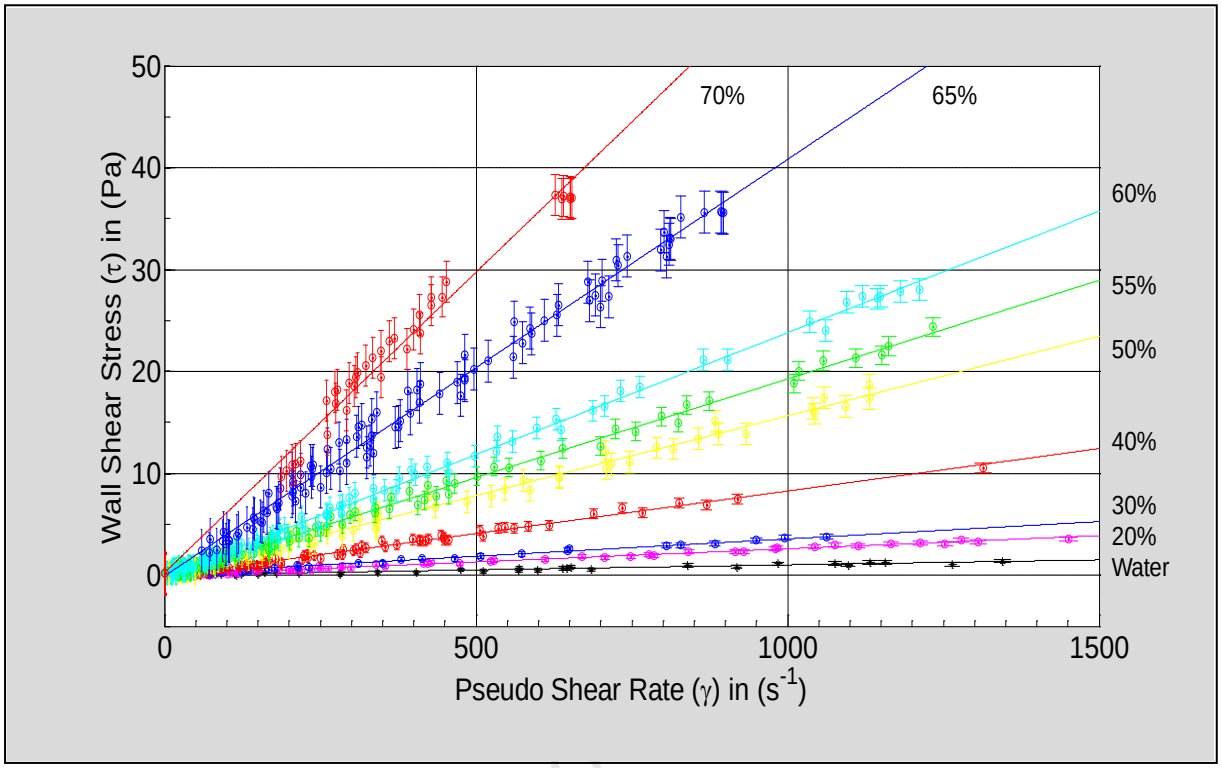

Figure 4-4. Corrected rheograms for sucrose solutions (vol.%).

4.1.2 Kaolin slurry (Non-Newtonian)

Kaolin or Kaolinite is a layered silicate mineral with the chemical composition $Al_2Si_2O_5(OH)_4$. It belongs to the class of Phyllosilicates and is a part of the clay group of minerals. A suspension of kaolin in water is well known to be a Non-Newtonian suspension and it is often used as a standard for rheology test work on rotational viscometers.

Tests were conducted to ensure that the tube viscometer could indeed provide accurate data using this material. Measurements were taken at a range of concentrations between 4% and 28% by volume (10% to 50% by mass) and comparisons were made to tests performed using kaolin in a standard rotational viscometer to verify the results obtained using the tube rheometer. Figure 4-5 and Figure 4-6 show the rheograms obtained using a standard rotational viscometer up to 25% by weight from Loginov *et al.* (2008), and the rheograms from tests performed using the tube rheometer respectively. Similar trends are observed above shear rates of 200/s. Kaolin is yield pseudoplastic at a given pH and its viscosity

decreases with an increase in shear rate. The fact that the tube rheometer is not accurate below a certain shear rate explains the fact that the curves do not show a drop in shear stress as in the rotational viscometer curves. Experiments were performed at the natural pH (7.5). The Herschel-Bulkley model was used to fit the data from the experiments shown in Figure 4-6.

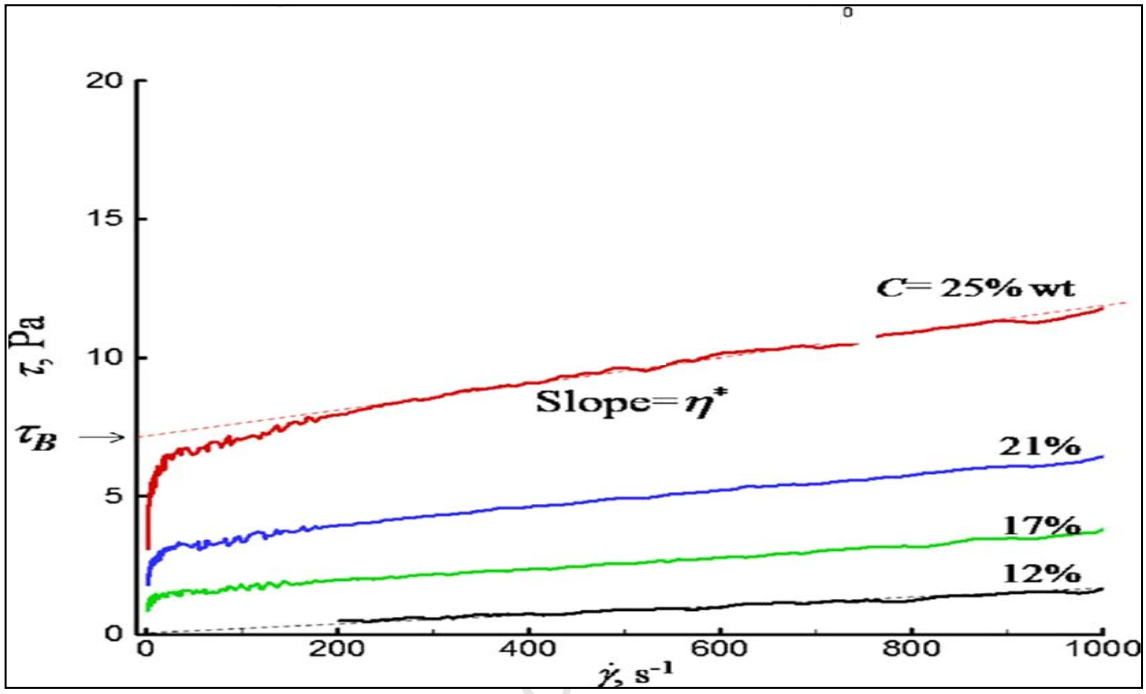

Figure 4-5. Rotational viscometer Kaolin curves, Loginov *et al.* (2008).

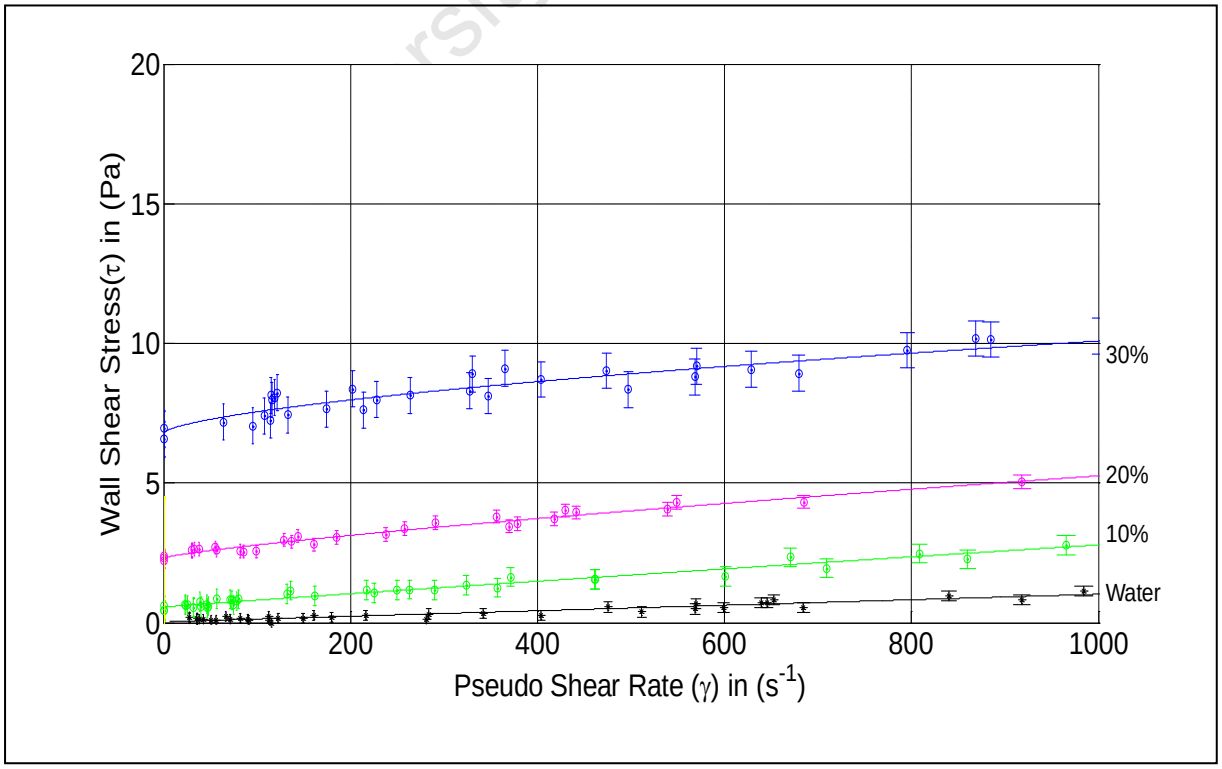

Figure 4-6. Rheograms from tube rheometer tests on different concentrations of Kaolin.

4.1.3 Platreef A slurry

Tests were then run on the tube rheometer using a Platreef A slurry at various concentrations ranging from 30 to 50% by mass (12 to 24% by volume). This was done to check whether the rheometer could provide meaningful results using real ore types. The ore sample used was from a secondary circuit cyclone feed stream and the size distribution for this material is shown in Figure 4-7. It had a P80 of 100 µm and 54% passing 75 µm. The particle size distribution is an important parameter when studying rheology as it has been shown that an increase in solids content can be achieved (at the same viscosity) when changing the particle size distribution, (Laskowski, 2001). The influence of rheology also becomes more significant at smaller particle sizes, (Yue & Klein, 2004).

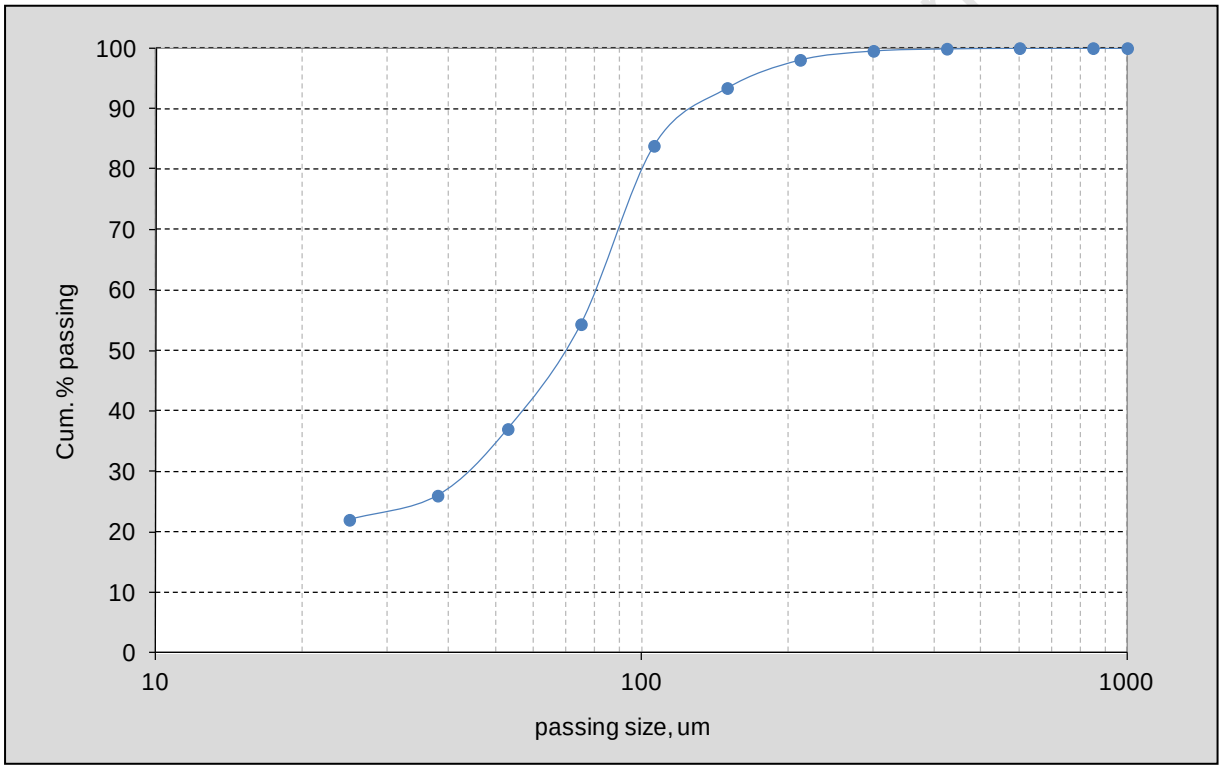

Figure 4-7. Platreef A sample size distribution.

Tests were performed in triplicate and then compared to check for any discrepancies. An example of the reproducibility of the rheograms for the 40% run is shown in Figure 4-8. The reproducibility of the equipment was good demonstrating that it was capable of providing repeatable results and thus gave us confidence in the data. Figure 4-8 shows the slurry to exhibit almost Newtonian like behaviour, with no evidence of a yield stress. The rheometer could however not provide accurate data below shear rates of approximately 200/s.

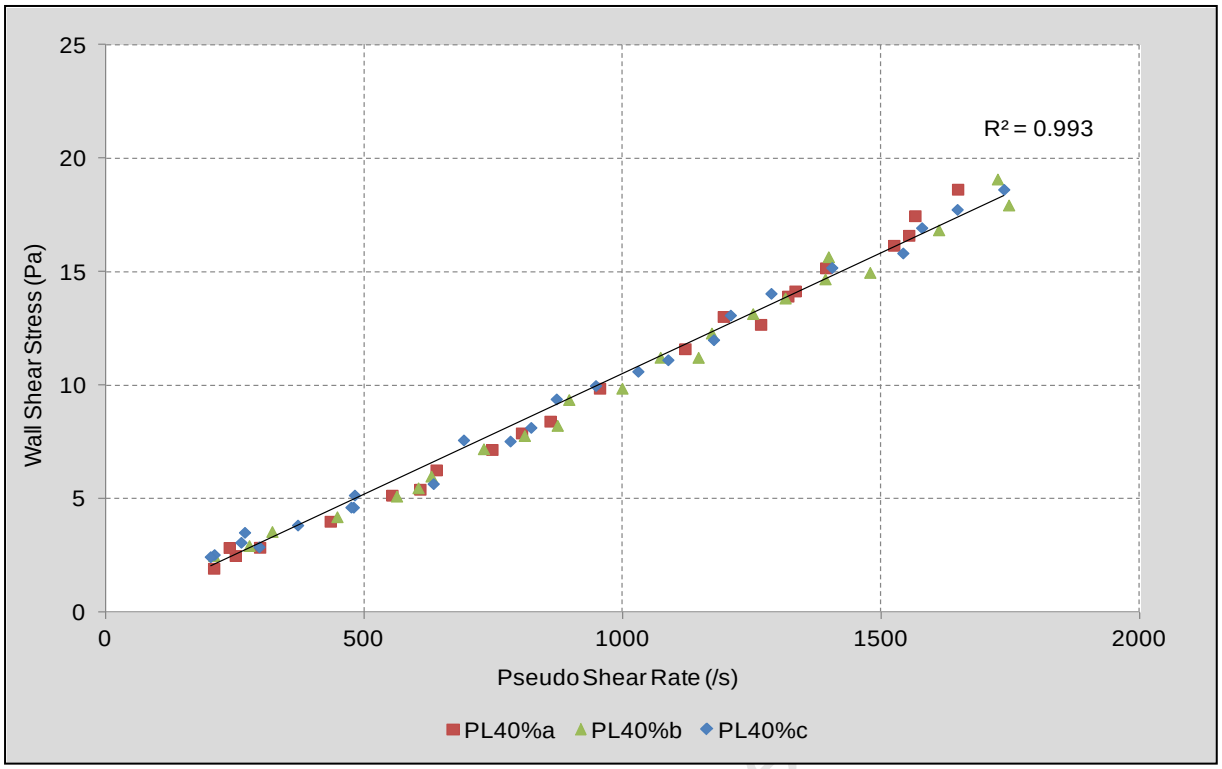

Figure 4-8. Reproducibility for tube rheometer data runs in triplicate.

To compare the results obtained using the tube rheometer with those using another method, tests were performed on the same sample using a pipe loop viscometer described in Section 4.2.1.

4.2 CPUT rheology test work

4.2.1 Pipe loop viscometer

A sample of the Platreef was taken to the Cape Peninsula University of Technology (CPUT) Flow Process Research Centre to be tested on their pipe loop viscometer shown in Figure 4-9, in order to test for the presence of wall slip. Pipe loop systems are standard test rigs used to characterise suspensions, particularly for pipeline design. Extensive work on pipe loop systems has been carried out by Shook *et al.* (1982), at the Saskatchewan Research Council Pipe Flow Technology Centre in Canada.

The pipe test loop rheometer at CPUT consisted of two pipelines of 27.2 mm and 34 mm internal diameter respectively. A diagram of the layout can be found in APPENDIX C. The two different diameter pipelines are used to indicate any presence of wall slip as the slurry is pumped through the pipelines. The loop was driven via a 50 mm Bredel peristaltic pump with a 4 kW motor and variable speed drive. Tests were conducted over a range of pump speeds to generate the range of shear rates required. The slurry was agitated in a 160 litre mixing tank and then pumped into the test loop through a set of dampers which absorbed any entrained air entering the system through the mixing tank. A Krohne Optiflux 4000 electromagnetic flowmeter and four Fuji electric FCX-CII series pressure transducers transmitted online flow rate and pressure drop data to the data processor. Custom designed software translated the measurements into shear stress and shear rate data.

Figure 4-9. CPUT pipe loop viscometer.

Water tests were initially performed for calibration of the test loop. The water results were within 10% of the theoretical prediction for both pipes using the Colebrook-White equation. An example of the calibration for the 27.2 mm pipe is shown in Figure 4-10.

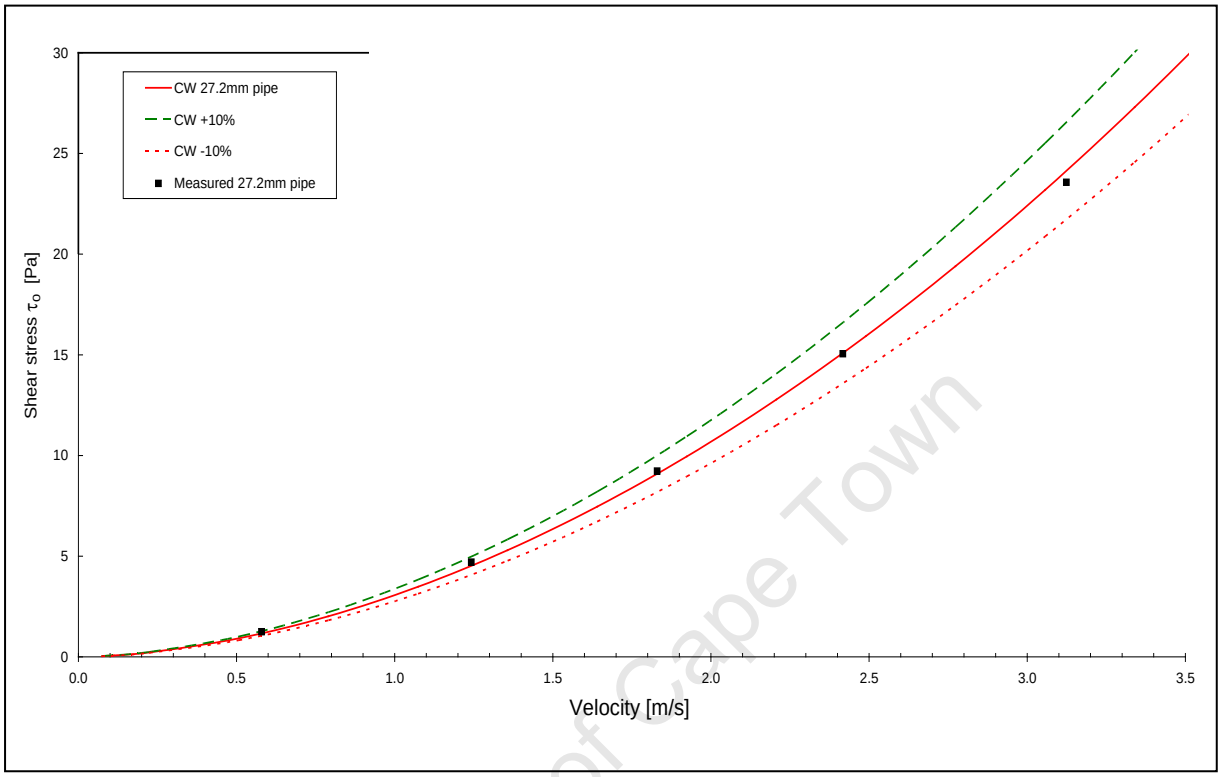

Figure 4-10. Water calibration curves in the 27.2 mm pipe, Fester (2009)

The hydraulic roughness values used were 8 µm and 20 µm for the 27.2 mm and 34 mm pipes respectively. Pipe loop tests are useful for helping to determine the flow regime that one is operating in with various ore types. A settling slurry will tend to show an upward curve at the lower shear rate range of a plot of shear rate vs shear stress (or pressure drop vs velocity), as shown in Figure 4-11 by Brown & Heywood (1991).

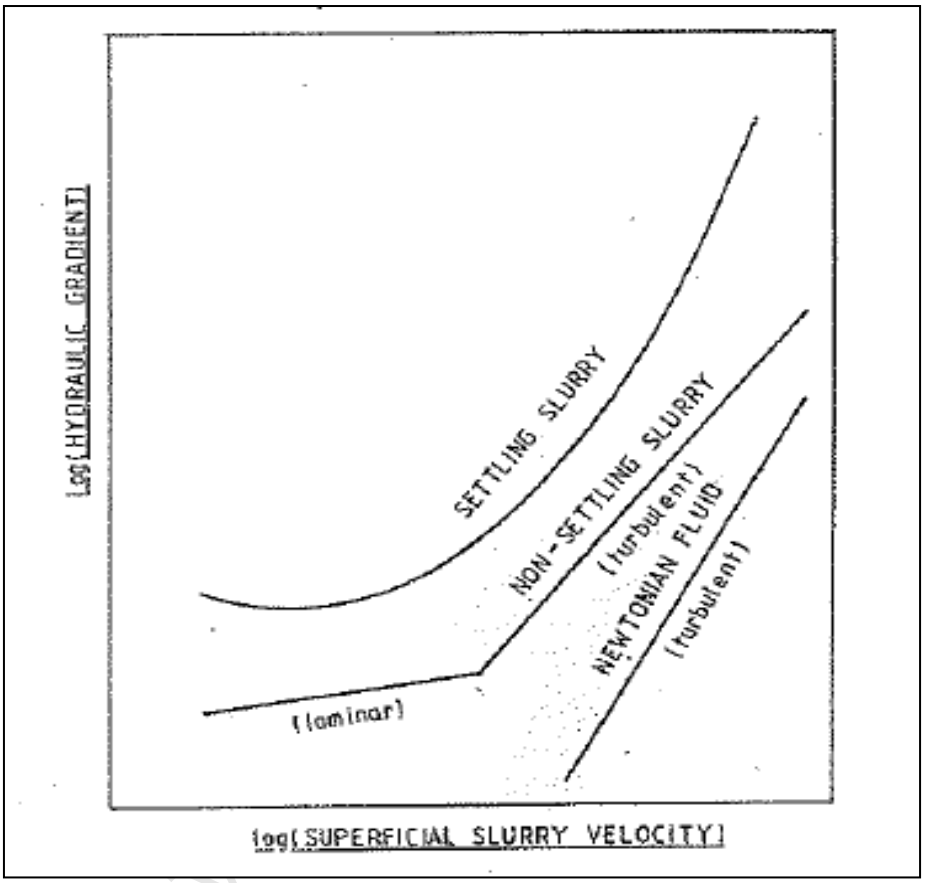

Figure 4-11. Hydraulic characteristics of slurries, Brown & Heywood (1991).

Results obtained are shown in Figure 4-12 and Figure 4-13 for the two pipe diameters at different concentrations (30, 35, 40, 43, 45, and 50% by mass – 12 to 24 % by volume). These graphs clearly show the presence of settling of the material in the pipelines at low velocity values – as depicted by the bending up of the curve below about 200/s. On a combined plot of pressure gradient versus velocity (Figure 4-14) the critical velocity is shown to be about 0.80 m/s for the 50% solids test. It is obviously slightly lower for the smaller diameter pipeline and will decrease for lower concentrations. This indicated that the pump was not able to keep the solids in suspension during the tests and that the slurry is in fact a settling slurry and not homogeneous in nature. These slurries cannot always have their apparent viscosity characterized using only standard rheograms, Fester (2009), and their

viscosity therefore needs to be expressed in terms of a relative viscosity (relative to the carrier fluid, which was water in this case).

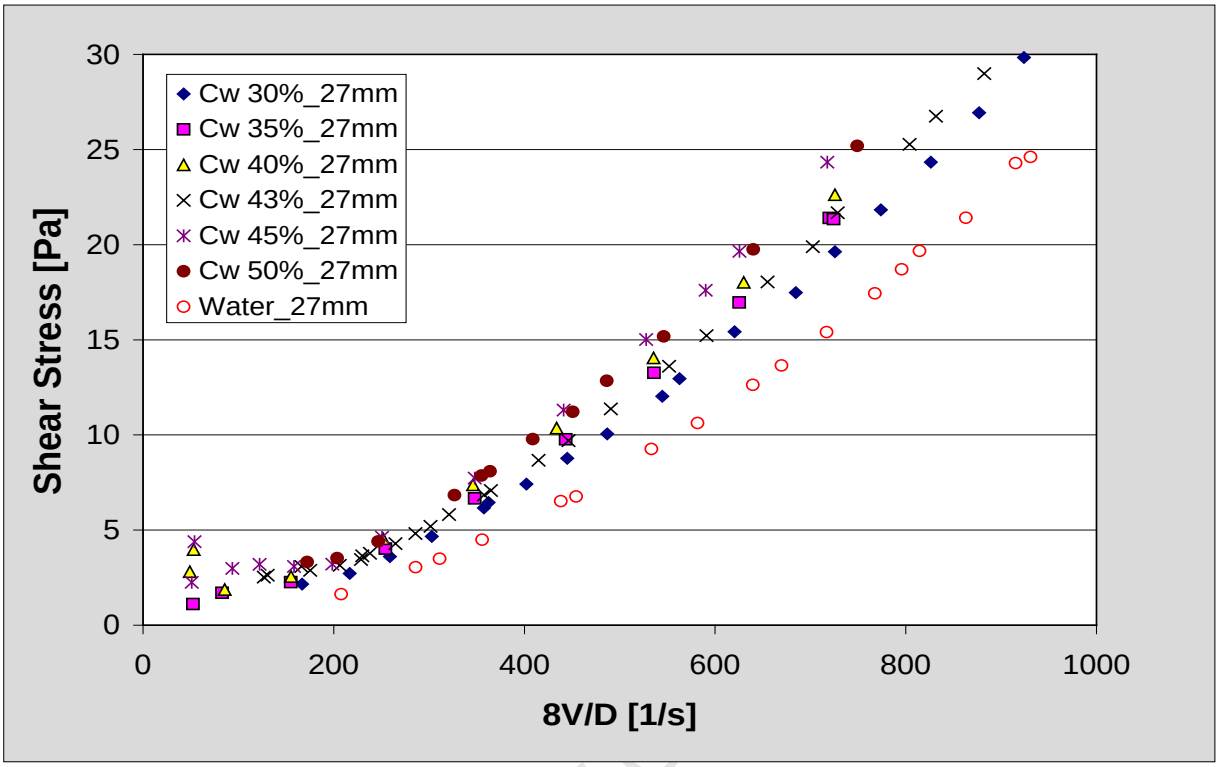

Figure 4-12. Platreef A sample in 27 mm pipe, exhibiting settling, Fester (2009)

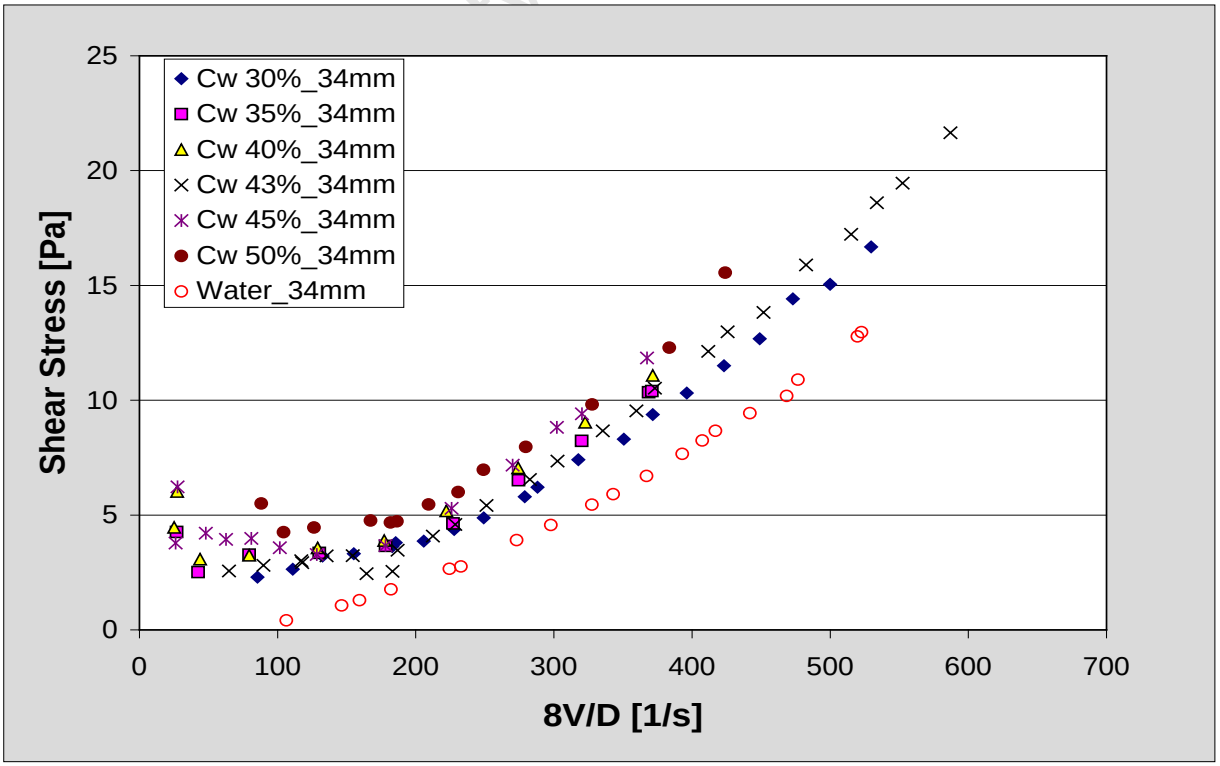

Figure 4-13. Platreef A sample in 34 mm pipe, exhibiting settling, Fester (2009)

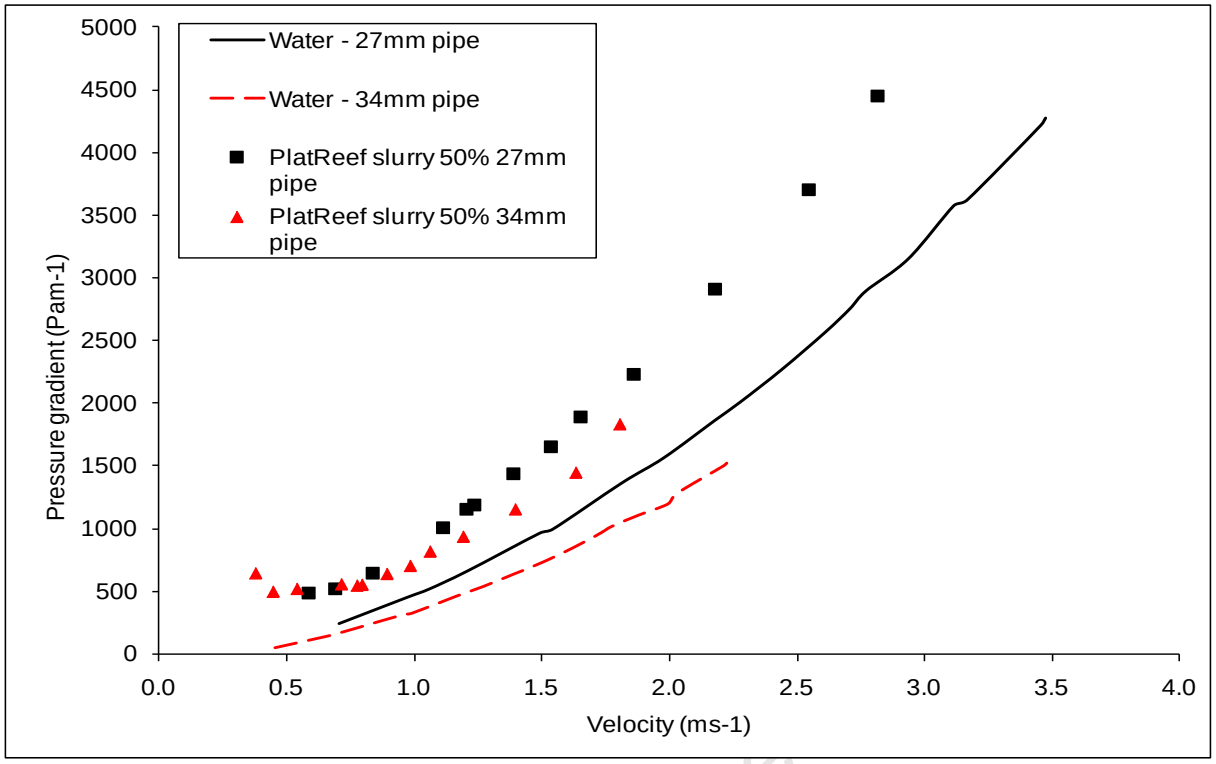

Figure 4-14. 50% solids test showing critical velocity for 27 and 34 mm pipes, Fester (2009).

Using this methodology the initial curves using the Platreef A slurry were then replotted on a log-log scale. Figure 4-15 shows the curves for the full PSD. Once these tests were completed the sample was screened to 100% passing 75 µm to try to see whether this had any significant effect on the rheology or the critical velocity. The rheograms obtained with the screened sample are shown in Figure 4-16. The settling is clearly visible below a certain shear rate (approximately 200/s) both for the full and the minus 75 µm sample, although for the finer sample settling occurs at a slightly higher concentration. This corresponds to the same approximate critical velocity as for the pipe loop tests. A calculation was then performed using the Turian equation to determine the exact critical velocity for the rheometer to make sure that it matched the experimental observations. The resultant critical velocity was determined to be 0.25 m/s (equivalent shear rate of about 202.5/s). This was determined at the maximum volume percent solids, which was found to be 25%. The critical velocity decreased above and below this value which corresponds with the findings of Turian *et al.* (1987).

As a result of this data the decision was made to exclude all rheogram data below a shear rate of 200/s for all the rheology tests going forward. This does not affect the viscosity/cyclone relationship as shear rates in the hydrocyclone tests were assumed to all be above this value; (Narasimha *et al*, 2010), (Suasnabar, 2002).

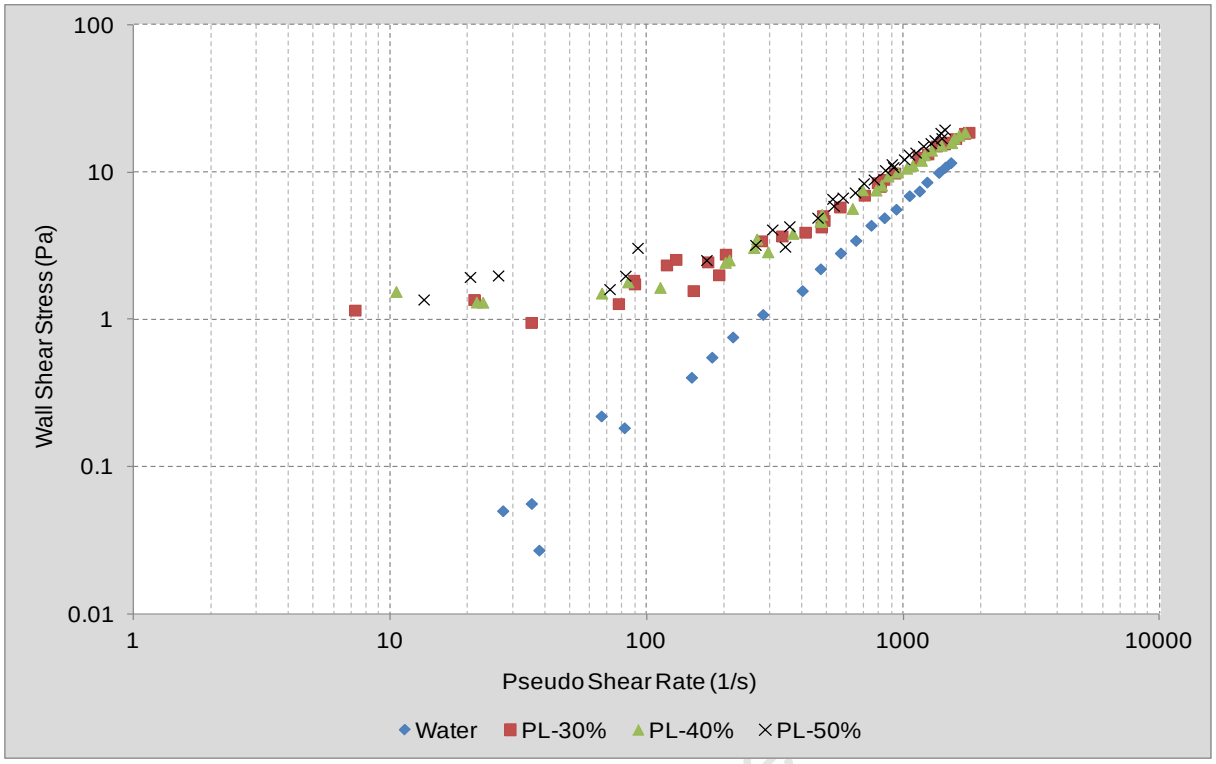

Figure 4-15. Platreef A full PSD sample showing settling.

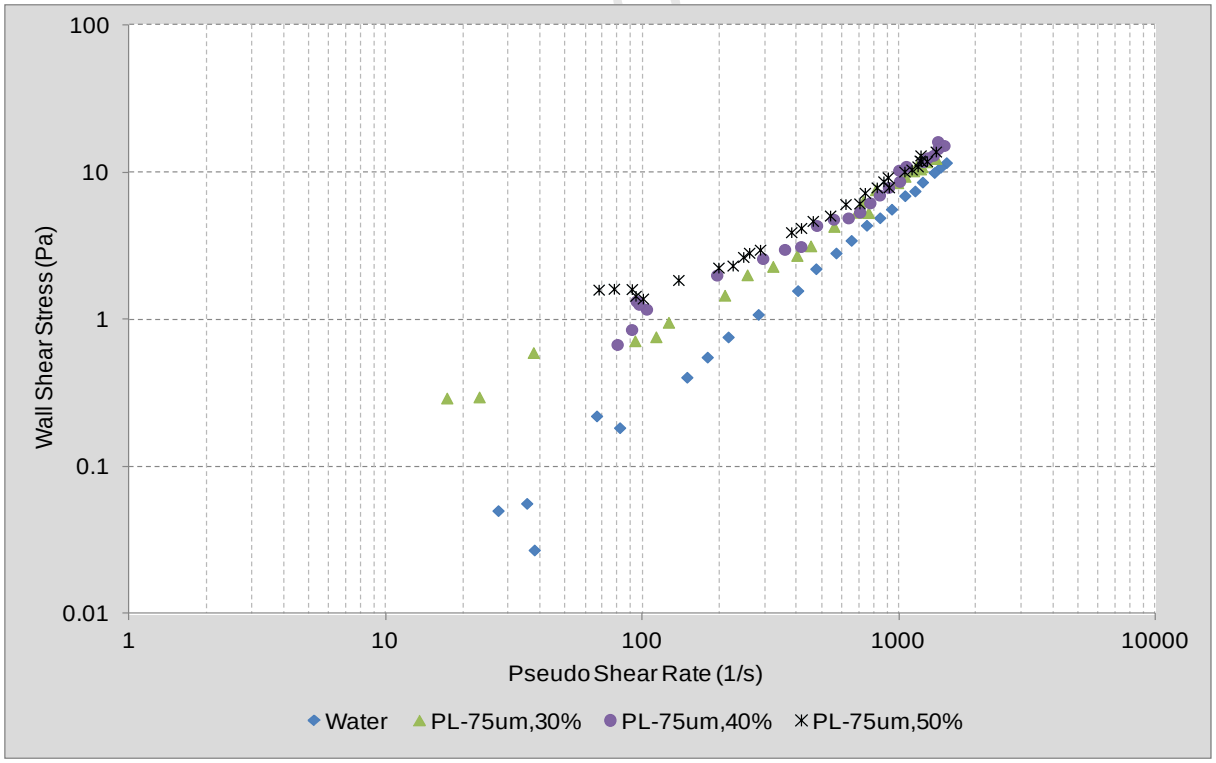

Figure 4-16. Platreef A minus 75 µm sample showing settling.

4.3 Hydrocyclone test rigs

4.3.1 75 mm & 100 mm cyclones

A considerable amount of time was spent by the author on the design, construction and commissioning of the hydrocyclone test rigs. The test rig designed for the 75 mm and 100 mm hydrocyclones was constructed at the CMR laboratory at the University of Cape Town and the 165 mm cyclone test rig was built at the University of Stellenbosch Process Engineering laboratory (see page 73). The CMR rig (Figure 4-17) is driven by a 3-phase 5.5kW Weir-Envirotech Centriseal centrifugal pump with a 180 mm rubber lined impeller. An Allen-Bradley variable speed drive coupled to the pump allows accurate viewing and control of frequency (speed) and pump power draw (Amps). The 75 mm and 100 mm cyclones used were Multotec type FC with dimensions as shown in Table 4-1. The rig was designed with an adjustable framework so as to accommodate different sizes of cyclone as well as to allow different conical lengths to be tested in future for each cyclone.

The products of the hydrocyclone are discharged into a common stainless steel conical sump with a fall angle of 49 degrees and a volume of 120 litres. A recycle line branching off the feed line to the hydrocyclone is allowed to discharge directly into the sump when the cyclone is not in use and the feed stream sample is taken from this part of the test rig. A Wika digital pressure gauge located at the cyclone inlet displays a continuous feed stream pressure drop reading.

Figure 4-17. UCT cyclone rig with 75 mm cyclone (left) and 100 mm cyclone (right).

An 'over the side' Hotflo 3 kW submersible heating element suspended in the sump is used to heat the slurry to the required temperature. The slurry temperature in the sump is monitored using a Wika Diwitherm resistance thermometer with a digital display. When cooling is required a custom made copper pipe cooling coil is used to keep the slurry temperature from reaching levels which may affect the rheological properties. In addition to this, the equivalent amount of ice could be added in place of water when water addition is necessary, and a cooling fan is positioned above the sump to further reduce the temperature.

The spigot and vortex finder combination chosen for this work ensured that the cone ratio was consistent for all three hydrocyclones. A minimum spigot size was also chosen to avoid roping conditions based on the criteria given in Napier-Munn *et al.* (1996) by Barrientos - using the ratio of apex to vortex finder diameter (0.56 < Du/Do for spray discharge). The specifications of the hydrocyclones used in this work are shown in Table 4-1.

Table 4-1. Dimensions of the cyclones used for the test work.

Cyc body - Dc (mm)	75	100	165
Cyc. Inlet - Di (mm)	23	30	46
Spigot - Du (mm)	23	28	45/35
Vortex finder - Do (mm)	32	41	64/53
Vortex finder length (mm)	70	120	180
Cylinder length - Lc (mm)	85	280	365
Cone length (mm)	185	480	440
Cone Angle (degrees)	5	20	15
Du/Do	0.72	0.68	0.70
Dc/Do	2.34	2.44	2.58

The test procedure followed was as follows (see Figure 4-18): V*alve numbers 1,2,5, were initially kept closed and valve numbers 3 and 4 were opened. The required amount of water was then added to the sump. Once the water was added valve 2 was opened and the pump VSD started. With the water circulating through the system, the required amount of solids was slowly added to the sump. Once the flow reached steady state and there was adequate*

mixing, valve number 5 was opened and valve number 4 was shut. The VSD was adjusted to achieve the required feed pressure. Once a new steady state condition through the cyclone was reached, sampling could begin. Samples of the feed, U/F and O/F were taken with a custom made pelican sample cutter at five minute intervals. Three increments were taken and were combined into the same bucket for analysis. These samples were used to calculate percentage solids values as well as for determining the full particle size distribution. Flow rate samples were taken for the U/F and O/F streams and these were combined to calculate a feed flow rate to obtain an accurate measure of the flow split within the cyclone. The U/F stream flow rate was measured directly using a bucket and stopwatch method. The O/F flow rate was measured by diverting the stream into a separate section of the sump (volume 40 litres, shown by dotted line in Figure 4-18), to be discharged into a separate measuring vessel. The MPV was connected online with the hydrocyclone rig and could be operated using the bypass line at valve #3 when required.

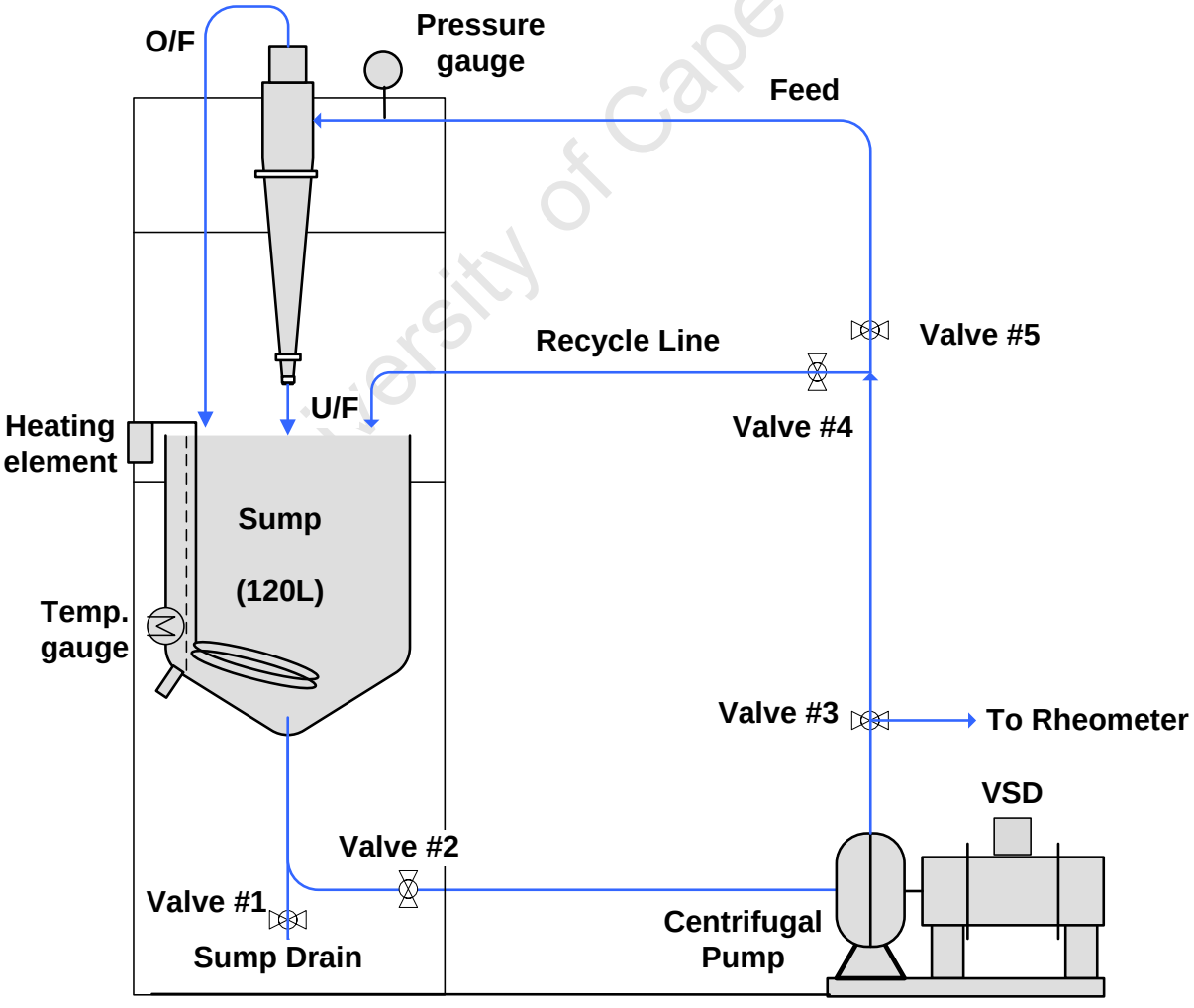

Figure 4-18. 75 & 100 mm cyclone rig schematic

When heating of the slurry was required, the recycle line was opened and the hydrocyclone feed line closed. When slurry cooling was required, the opposite procedure was followed as the free discharge of the U/F and O/F streams into the sump allowed the slurry to be air cooled. The test program was designed so as to ensure a minimum amount of heating and cooling during the day as this was time consuming, i.e. low temperature tests were performed back to back before the temperature was raised for the following test condition.

During the UCT hydrocyclone test rig operation on-line viscosity measurements were taken by opening a bypass line to the tube rheometer and throttling the recycle line where necessary. This was carefully controlled so that the solids density of the rig was not affected, the viscosity sample was replaced in the sump after each viscosity measurement and before subsequent cyclone samples were taken. Steady state conditions had to be re-established after this procedure.

Once the test work was complete, the resulting sample buckets were weighed on a hanging scale to obtain the total wet mass. The remaining slurry was drained into buckets by opening valve number 1 while circulating the slurry. After the sump was empty the entire system was flushed with water, taking care to ensure the valves were throttled to allow all the slurry to be recovered. The weighed samples were then filtered in a swing barrel filter press and the filter cake was placed in the oven for drying. After the samples were dry they were weighed to obtain the sample dry mass which was used to calculate the percentage solids values. The dry sample was then delumped over a 1.0mm sieve in preparation for sample splitting. The sample was then split on a 10-way rotary splitter in preparation for wet sieving. Once the split sub sample was obtained it was processed according to the standard CMR laboratory sizing procedure as described in APPENDIX D.

Sub-sieve analysis (minus 25 µm) was then performed. This was necessary as the O/F samples had a significant amount of sub 25 micron material and any differences in the size distributions would not be noticed if the sizing was not performed below this value. In addition, any evidence of a fish-hook effect would only be noticed at the finer sizes. Samples were thus split on a small 10-way sample splitter to obtain samples for the Malvern analysis. Laser sizing was done using a Malvern Mastersizer 2000 long bench laser sizing device located in the UCT Chemical Engineering analytical laboratory. The laser sizings and the sieve size analysis were combined to obtain the complete PSD curve for each sample.

4.3.2 165 mm cyclone

The test rig for the 165 mm and larger size cyclones (up to 250 mm) was constructed at the University of Stellenbosch (Figure 4-19). The rig is driven by a Weir-Envirotech 7.5 kW Centriseal centrifugal pump with a 250 mm rubber lined impeller. A Zest CFW+ VSD allows accurate monitoring and control of the pump speed and power draw. The 165 mm hydrocyclone was a Multotec type VV with dimensions as shown in Table 4-1.

Figure 4-19. 165 mm hydrocyclone test rig

The rig is also designed with an adjustable framework so as to accommodate a range of cyclone sizes if required as well as to allow different conical lengths to be tested. The rig consists of two stainless steel conical sumps, one for sample mixing and the other for flow rate measurement. The main sump has a fall angle of 54 degrees and a volume of 330 litres.

The flow rate sump has a fall angle of 59 degrees and a volume of 160 litres. A Wika Universal pressure transmitter was installed at the cyclone inlet to send a continuous pressure reading to a data processor, however during the cyclone tests the digital display panel was used for manual viewing of the feed pressure as well as feed slurry temperature. The U/F discharges directly into the main sump below the cyclone. The O/F reports to a smaller conical sump (O/F receiver - volume 50 litres) which is located above the point of feed entry to enable the stream to discharge freely at atmospheric pressure and avoid the possibility of the O/F stream having a siphoning effect on the cyclone. A pipe is installed from the small sump to discharge into the main mixing sump. This design was initially proposed by Trawinski (1976).

The feed line has a recycle line on it which passes over the flow rate tank into the main sump. The recycle line is used to mix the slurry in the main sump and could also be used to determine the pump flow rate measurements if required. A t-piece off the recycle line and the opening and closing of applicable valves enables a bypass flow to fill the graduated flow rate sump at any required moment and the volume and time can then be recorded. The valves used for switching between the recycle line and the hydrocyclone feed line are Saunders slurry valves with a soft rubber lining. The O/F stream flow rate is measured by diverting the pipe from the O/F sump to the flow rate sump. The U/F flow rate is measured directly using the bucket and stopwatch method. The flow rates of the U/F and O/F are then combined to give a feed flow rate, in the absence of an online flowmeter. An over the side 4 kW submersible heating element is used to heat the slurry to the required temperature if required. Test conditions were designed so as to minimise the amount of heating and cooling of slurry. The cyclone streams discharging into the main sump are shown in Figure 4-20.

Figure 4-20. Main sump with U/F and O/F streams

The procedure for running the rig was as follows (see Figure 4-21): V*alve numbers 1, 5, 6, 8 were initially kept closed and valve numbers 2, 3, 4 and 7 were opened. The required amount of water was then added to the main sump. Once the water was added the pump VSD was started. With the water circulating through the system, the required amount of solids was slowly added to the main sump. Once the flow reached steady state and there was adequate mixing, valve number 5 was opened and valve number 4 was shut. The VSD was adjusted to achieve the required feed pressure. Once a new steady state condition through the cyclone was reached, sampling could begin. Samples of the feed, U/F and O/F were taken with a custom made pelican sample cutter at five minute intervals. Three increments were taken and were combined into the same bucket for analysis. These samples were used to calculate percentage solids values as well as for determining the full particle size distribution.*

The O/F flow rate sample had to be carefully taken to minimise the disturbance to the system. When the flow rate was required, the O/F pipe was diverted into the flow rate tank at time zero and a volume of slurry was collected. Once the time was sufficient (greater than 5 seconds) the pipe was diverted back to the main sump, the stopwatch was stopped and the corresponding time interval was carefully recorded. The draining of the flow rate tank

required careful opening and shutting of valves simultaneously. Firstly valve number 8 was opened and valve number 2 was closed. Once the flow rate tank was almost empty the valves were reversed (valve 2 opened and valve 8 shut). It was important to ensure that the flow rate tank was never drained completely as this would entrain air into the system and would be detrimental to the stability as well as the pump performance, with the possibility of pump cavitation occurring, SAPMA (1991). For this reason a small amount of slurry was always left in the flow rate tank after the measurement and this was removed manually. After any flow rate measurements were taken a period of 5 minutes was allowed for the system to stabilise. Once the tests were completed the sump was drained by opening valve number 1. The system was then flushed with water to ensure all the slurry was recovered.

The resulting samples from the test work were processed in the same manner as described previously for the 75 mm cyclone rig. Sub-sieve analysis (minus 25 µm) was performed using a Malvern Mastersizer S long bench laser sizing device. The laser sizings and the sieve size analysis were combined to obtain the complete size distribution curve for each sample. In addition to the standard hydrocyclone rig setup the rig also had certain control aspects which were of interest to the University of Stellenbosch. The rig was to accommodate a camera which was positioned to record changes to the cone angle of the U/F and transmit images to a data processor for image analysis. The rig was a collaborative effort between UCT and US and offers both undergraduate and postgraduate students the advantage of studying the hydrocyclone in a variety of ways.

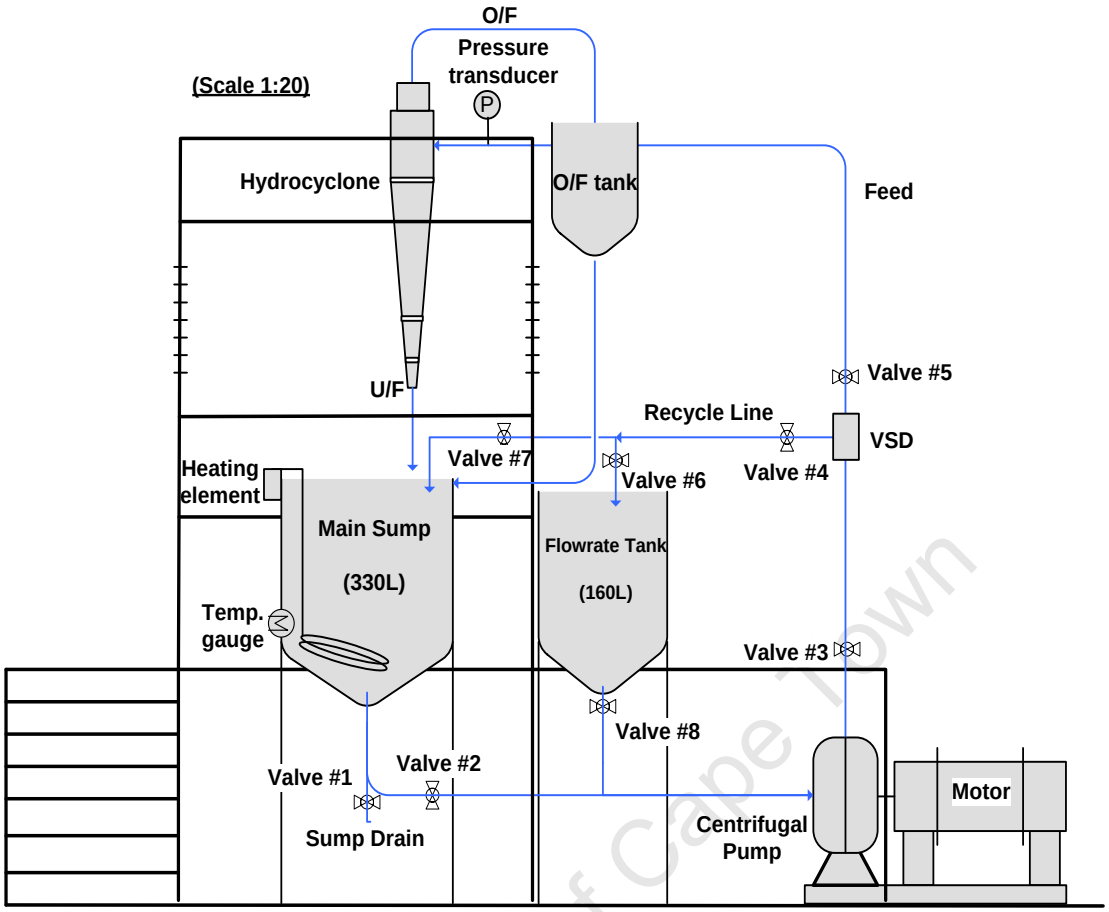

Figure 4-21. 165 mm hydrocyclone rig schematic.

5. RESULTS – VISCOSITY MEASUREMENTS

This thesis addresses the influence of viscosity on cyclone performance. This chapter discusses the results of the rheology test work performed to obtain the viscosity values associated with cyclone operations. The rheological characterization results include the correction procedure for the water curve and subsequent application to the data using slurry for both Platreef and copper ore. Although viscosity concentration is usually given in volume %, it is expressed as a mass percentage here in order to provide easier interpretation of the influence of viscosity on hydrocyclone performance where mass percentages are used.

5.1 Viscosity Characterisation – Standard

The procedure that was adopted during the experimental investigations in Chapter 4 was applied to two further ore types: a second Platreef ore from a different operation and a copper ore. The standard characterisation involved tests at increasing pulp concentration levels to provide data on the effect of solids content.

5.1.1 Platreef B Ore

A second Platreef ore was used for the rheological test work that was to provide the data for the effect on hydrocyclone operation. The particle size distribution for the ore used in the test work is shown in Figure 5-1. The ore had a F80 of 215 µm and 45% passing 75 µm. The size distribution was not a variable in this work and the feed samples were thus carefully prepared to ensure the feed distribution of each test was kept constant throughout the test programme.

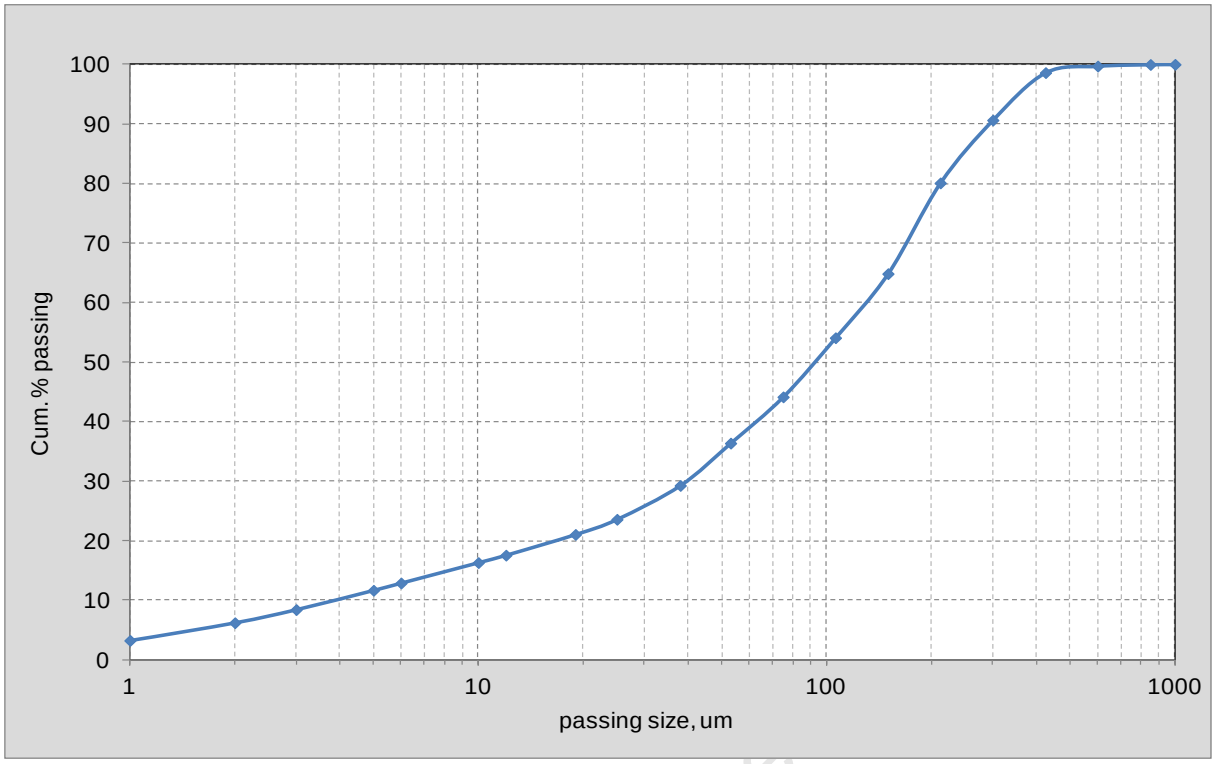

Figure 5-1. Particle size distribution for Platreef B ore.

It has been mentioned in Chapter 4 that all data that fell below the critical velocity was to be ignored as settling was definitely occurring at these low shear rates. The shear stress/shear rate data for the water calibration curve was corrected using the MATLAB procedure (APPENDIX B) to account for the turbulence and this ensured that an apparent viscosity of close to one was obtained for water at an operating temperature of 20 degrees Celsius. Viscosity tests were then performed with the Platreef B sample at various solids concentrations, at ambient temperature (25 degrees celcius). For each solids concentration test, the rheometer was first calibrated with water. Tests were run at 10, 20, 30, 40, 50, 60 and 70 % by mass of ore. The same correction was then applied to the data for increasing percentage solids and the resulting corrected curves obtained are shown in Figure 5-2.

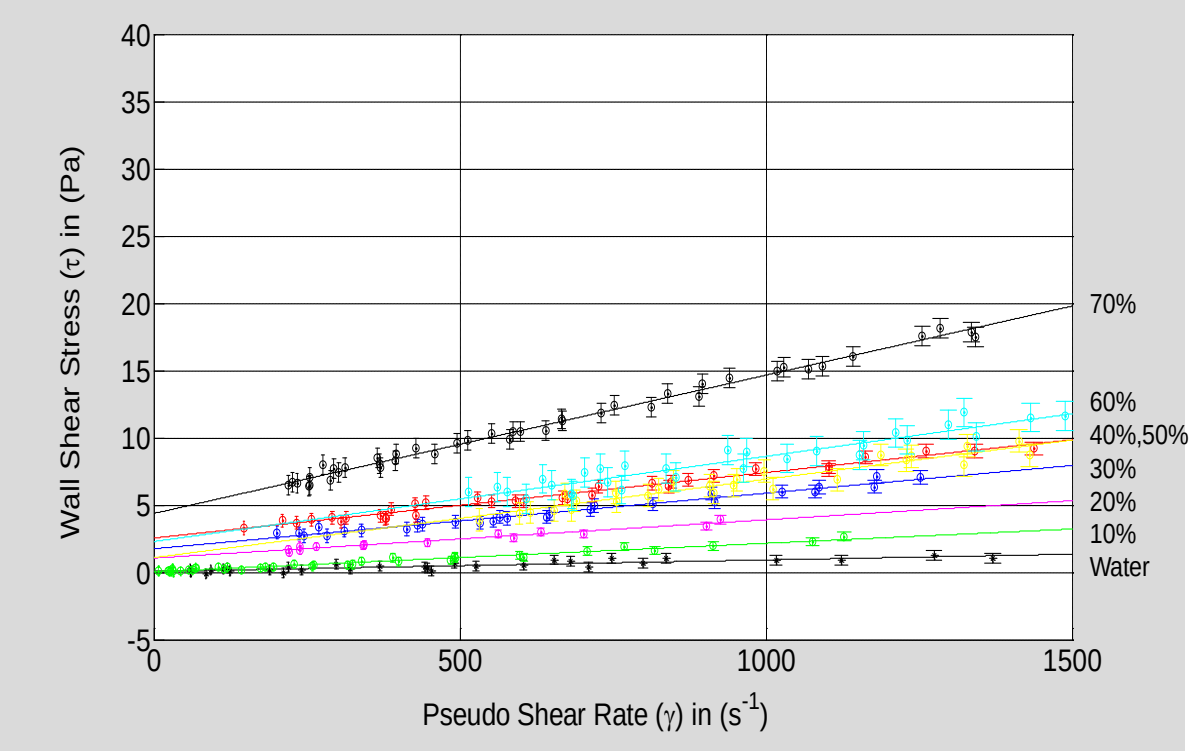

Figure 5-2. Rheograms for water and Platreef B ore at various mass solids concentration.

The data in Figure 5-2 shows a strong linear trend for each solids concentration. The magnitude of the slope gradually increases as the solids content is raised, due to particle-particle interaction. Several rheology models were fitted to the data and the Bingham Plastic model was found represent the data well. Extrapolated Bingham yield stress values are sometimes extracted from Bingham curves, but accurate yield stress values were not possible using the tube rheometer with the ore types under investigation as the data was inaccurate below shear rates of approximately 200/s. Since the material was processed in the hydrocyclone the yield stress value was not critical to this work and there was no need to use an extrapolated yield stress value which has been shown to be inaccurate, (Boger, 2009).

The increase in slope from 60 to 70% solids is evident in Figure 5-2. This is supported by the literature, Rutgers (1962), as the particle-particle contact becomes prohibitively high. The Bingham viscosity values were then extracted from the slope of the curves and these were plotted against the concentration (Figure 5-3) to obtain a viscosity/concentration relationship. This was effectively a relative viscosity relationship, corrected for water at 20 degrees Celsius.

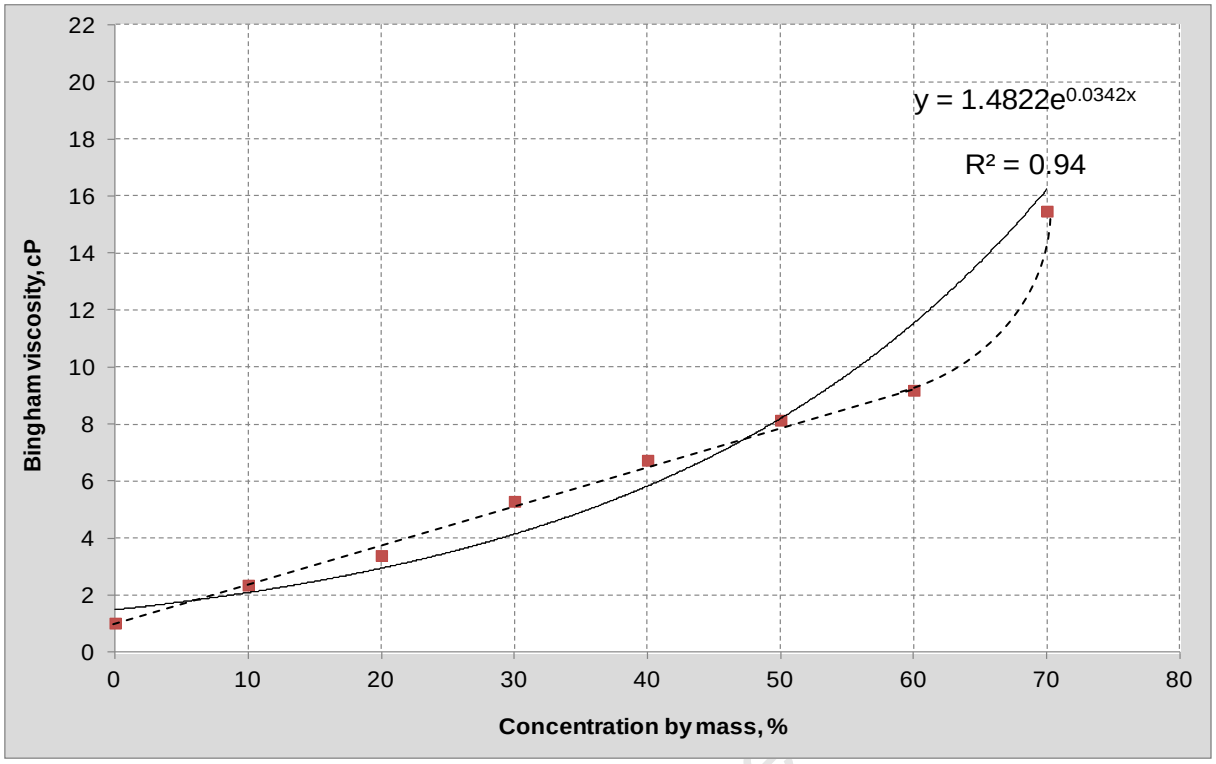

Figure 5-3. Viscosity vs concentration for Platreef B sample (fit is solid line).

Figure 5-3 shows that an exponential fit was obtained for viscosity versus concentration. A jump in viscosity was observed between 60% and 70% solids by mass. The model equation was therefore used to obtain a viscosity at a particular solids concentration. At times the rig cooling process was not adequate to maintain the slurry temperature at the desired value. The temperature increased gradually as the tests progressed and this was more pronounced for experiments performed at the increased solids content. This could explain the apparent decreased viscosity values at solids concentrations of 50% and above. The linear to exponential type curve of viscosity versus solids concentration is consistent with the observations of Cheng (1980). He states that "the viscosity increases at first linearly with concentration but as the concentration becomes medium, the viscosity-concentration relationship becomes nonlinear, with the rate of increase in viscosity accelerating as concentration increases". Similar observations have been reported by Rutgers (1962) and Thomas (1965).

5.1.2 Copper Ore

Rheological tests were conducted on a copper ore sample with a particle size distribution as shown in Figure 5-4. The ore had a F80 of 175 µm and 53% passing 75 µm. Compared to the Platreef B ore sample, the copper ore had a slightly finer size distribution but the difference was considered to be negligible for the purposes of this work.

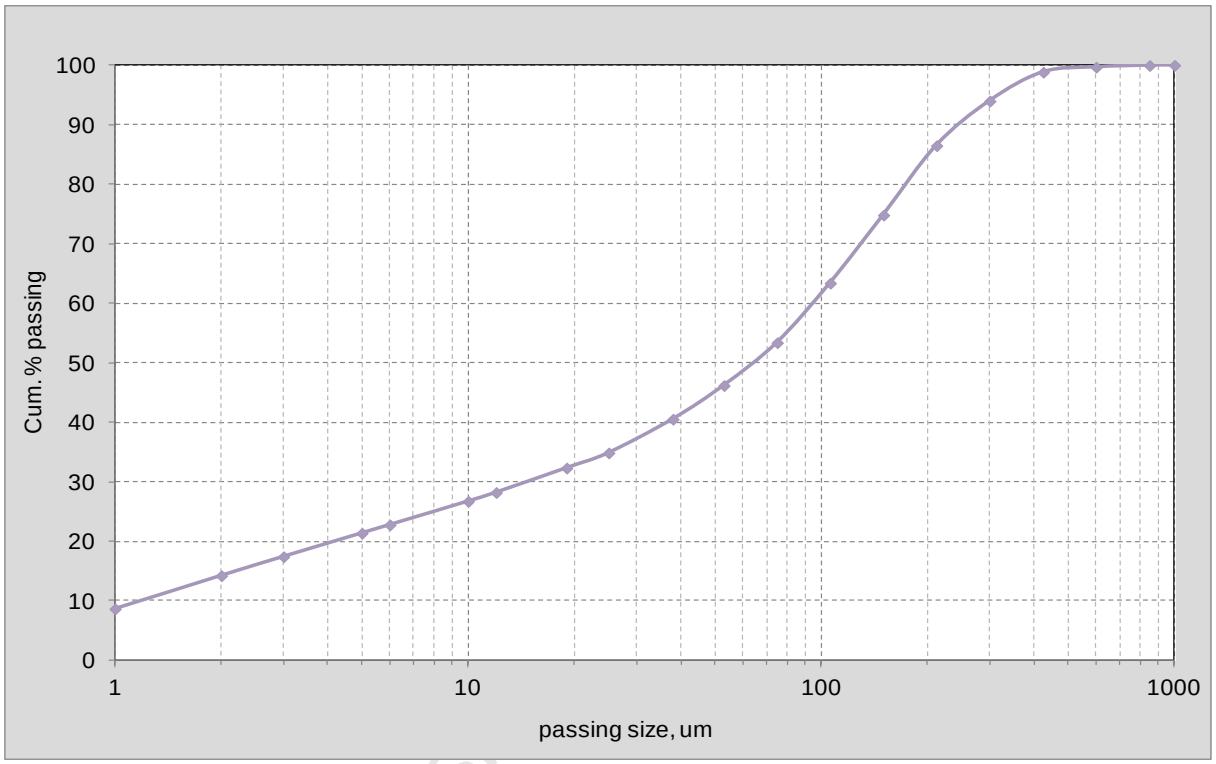

Figure 5-4. Particle size distribution for copper ore.

Tests were run at various concentrations (10, 20, 30, 40, 50, 60, 70% by mass). The procedure applied to the Platreef ore was followed for the copper ore. The rheograms from the copper rheology tests were corrected using the MATLAB procedure provided in APPENDIX B. Figure 5-5 shows that the rheograms also exhibited Bingham plastic behaviour. The steep increase in viscosity from 60% to 70% solids is also evident. The increase appeared more pronounced for the copper ore compared with the Platreef ore. The error bars are also much larger at the concentration of 70%, indicating that one may have less confidence in that data. The scatter is a result of the inability of the pump and equipment to provide accurate data above 70% solids by mass, especially for the more dense material.

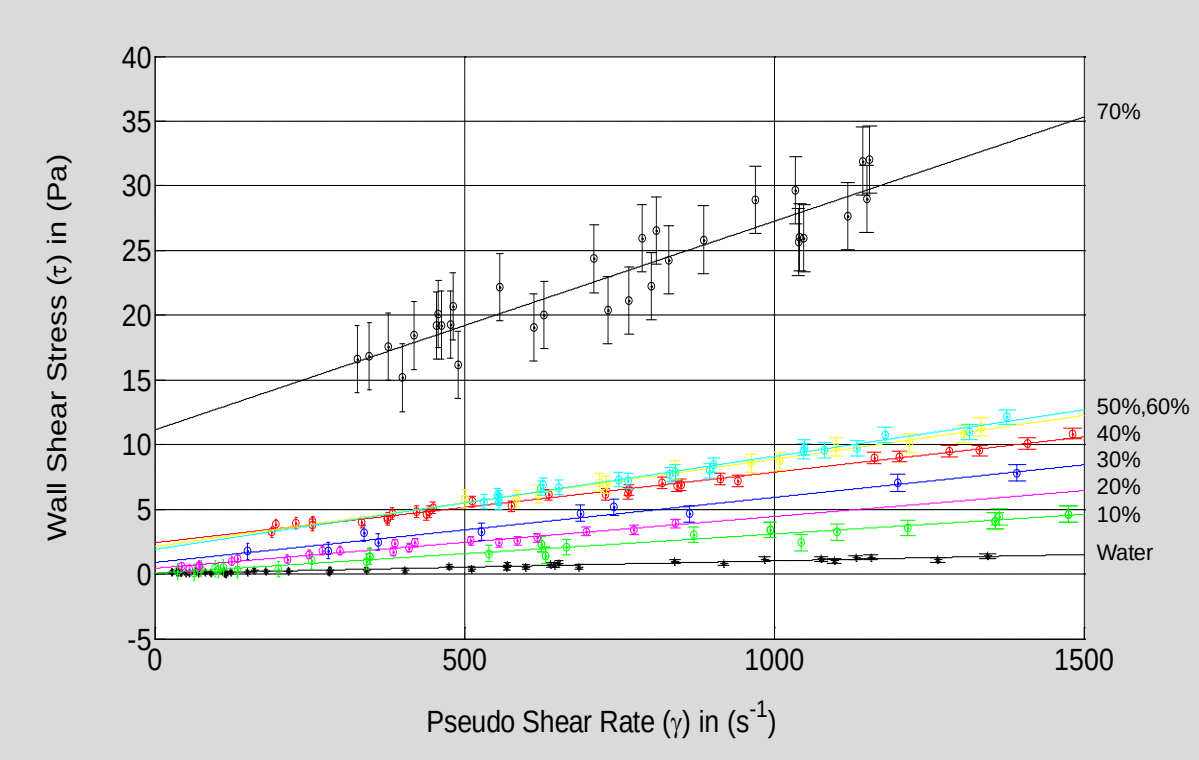

Figure 5-5. Rheograms water and copper ore at various mass solids concentration.

The viscosity values were extracted from the slope of the curves after fitting the Bingham model. These viscosity values were then plotted against concentration. Figure 5-6 shows the relationship between viscosity and solids concentration for the copper ore. This was effectively a relative viscosity relationship, corrected for water at 20 degrees Celsius.

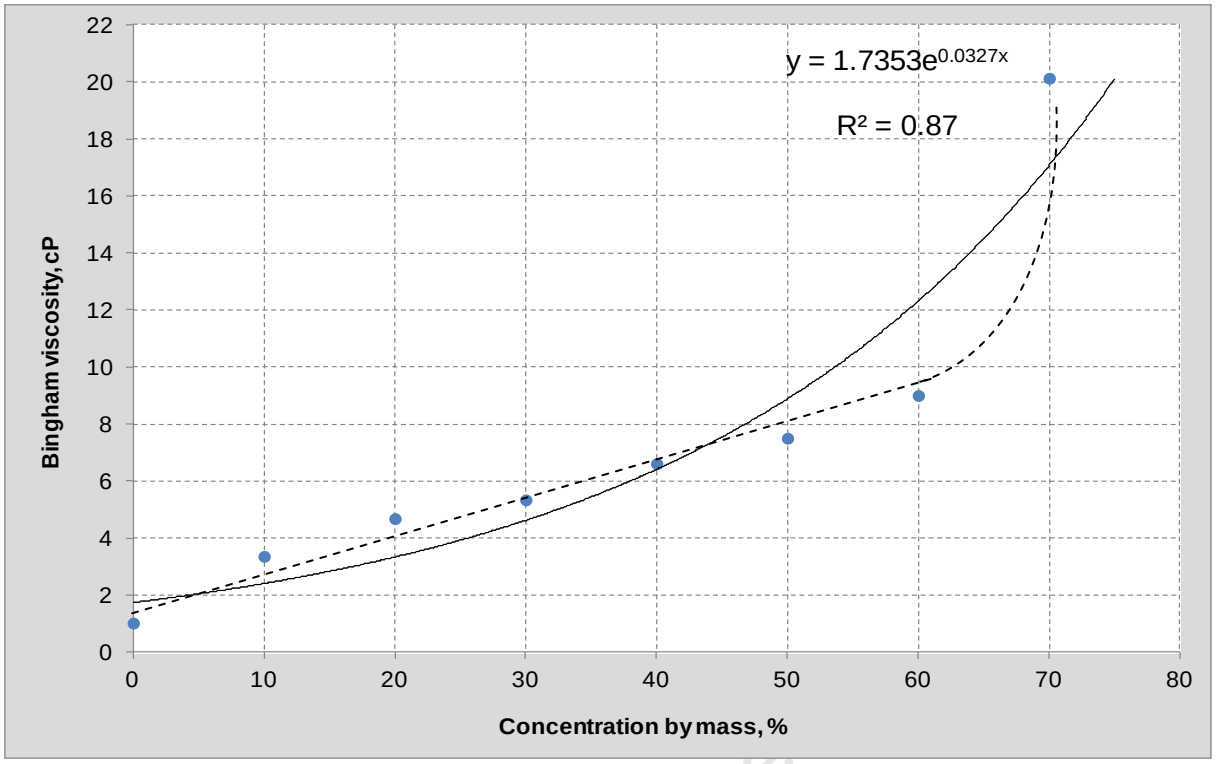

Figure 5-6. Viscosity vs concentration for copper ore sample (fit is solid line).

The trend in Figure 5-6 was similar to the curve for the Platreef B ore shown in Figure 5-3. It can be said that the fit is not as good, due to the lower R^2 value of 0.87 compared to 0.94 for the Platreef ore. The model equation could now be used to obtain a viscosity at any solids concentration used in the hydrocyclone test work. The gradual increase in slurry temperature could explain the slight decrease in the viscosity values at 50% and 60%.

The viscosity values extracted from the rheograms for the two ore types are compared in Figure 5-7. The viscosity values are alike between the solids concentration of 30% and 60%. The temperature was maintained between 24-27°C for all standard tests.

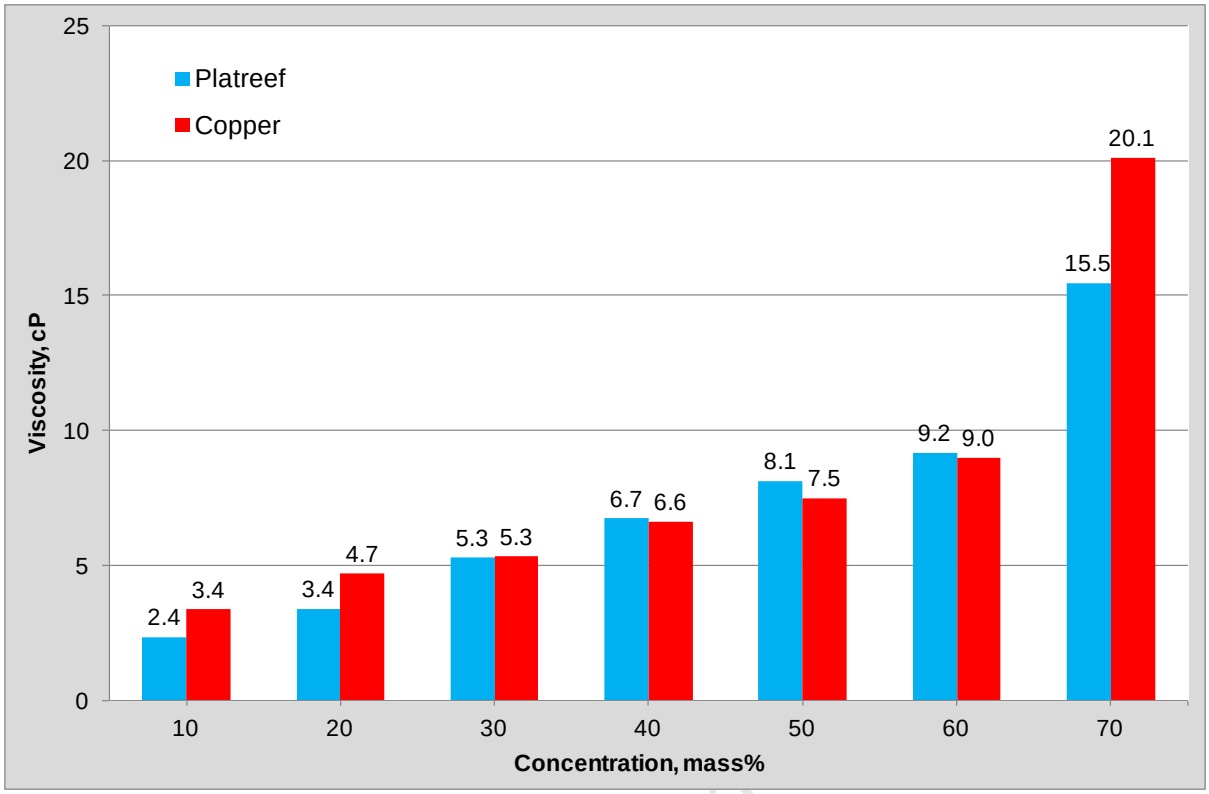

Figure 5-7. Viscosity values of the ore samples at various concentration levels.

As a result of their similarity in terms of rheology from 30% to 60% solids, it was decided to check whether they exhibited any marked differences in terms of particle shape and phyllosilicate content. This was done to ascertain if the rheology results were due to similar ore characteristics (besides the obvious differences in mineralogical make-up). The ore types have already been shown to possess a similar particle size distribution (Figure 5-1 and Figure 5-4).

5.2 Particle Shape

Shape pictures were taken of the two ore types using an optical microscope connected to a camera. The captured images were then downloaded to PC using the integrated software. The particles in the images were all above 25 µm as the image clarity was affected by the agglomerated fines, and thus the fines were screened out prior to taking the images. The resultant images for the Platreef B and copper ore in the size range -600 µm to +25 µm are shown side by side in Figure 5-8.

The images show that the two ore types exhibit similar particle shapes for the chosen portion of the size distribution. The particles appear to be mostly non-spherical. The sphericity (Ψ) of the particles was estimated using the ellipse model method as many of the particles appeared to conform to an ellipsoidal shape. To do this the dimensions of the major (longest) axis (A) and minor (shortest) axis (B) of 100 particles were calculated for each ore type. The sphericity was then determined using the semi-major (a) and semi-minor (b) values as shown in equation *5.10*. Average sphericity values of 0.72 and 0.76 were obtained for Platreef and copper ore respectively. These particles have been subjected to numerous stages of processing which could account for the lack of sharp edges, and a smooth edged appearance. The similarity in particle shape of the two ore types is confirmation that shape was not a variable in this work and suggests another reason for the similar rheological behaviour.

$$\Psi = \frac{2\sqrt[3]{ab^2}}{a + \frac{b^2}{\sqrt{a^2-b^2}}\ln\left(\frac{a+\sqrt{a^2-b^2}}{b}\right)} \quad [5.1]$$

, where a=A/2 and b=B/2.....

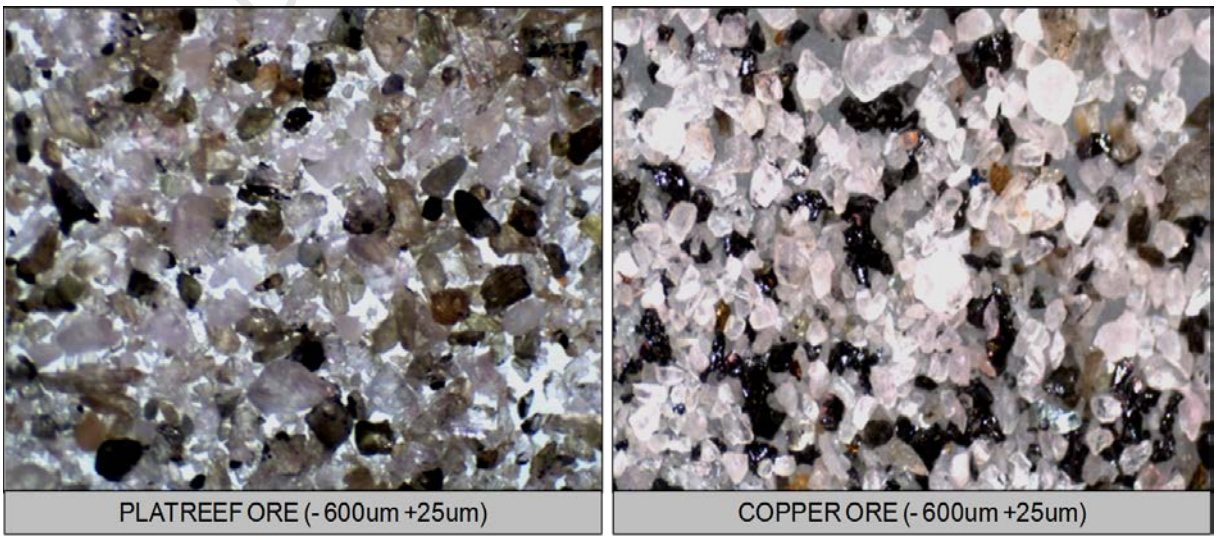

Figure 5-8. Shape images for Platreef B and copper ore.

5.3 Mineralogy

Mineralogy tests were conducted on the two ore samples to determine whether there were any significant proportions of minerals present that would influence the viscosity. Of particular interest was the amount of phyllosilicates present as these are known to create rheological complexities, (Ndlovu *et al.*, 2011). A sample of the feed material for both Platreef B and copper ores was separated into four size classes: -600 µm +150 µm, -150 µm +75 µm, -75 µm +25 µm, and -25 µm. Three analytical techniques were investigated – chemical assay by size using inductively coupled plasma optical emission spectrometry (ICP-OES), quantitative bulk x-ray diffraction (QXRD), and quantitative evaluation of minerals by scanning electron microscopy (QEMSCAN). The ICP-OES and QXRD results were used to validate what was measured using the QEMSCAN technique.

The mineralogical contents by size class and combined are shown in Figure 5-9 and Figure 5-10 for the Platreef B and copper ore respectively.

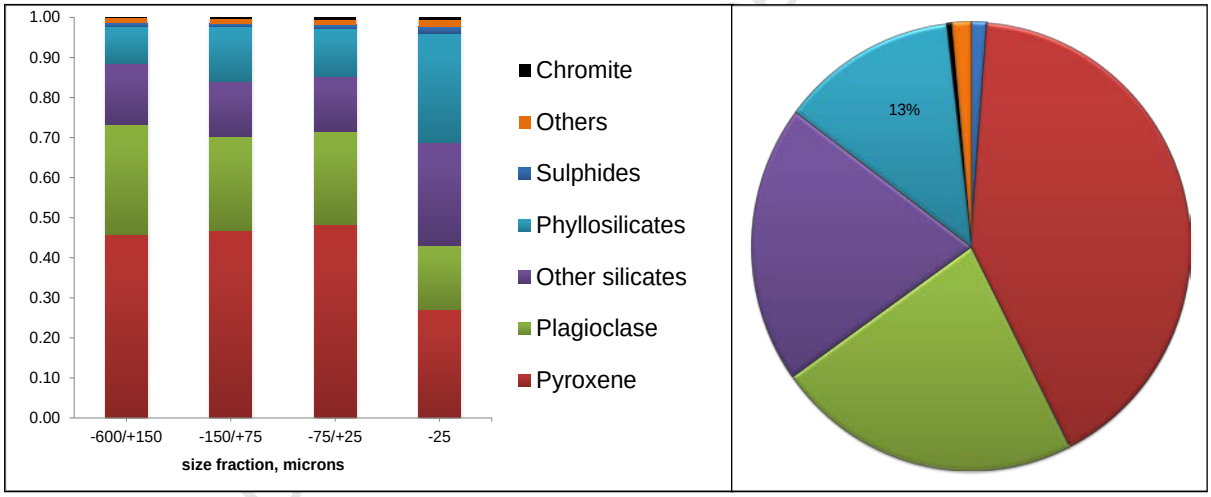

Figure 5-9. Mineralogy of Platreef B ore sample – mineral distribution by size class (LHS) and combined distribution (RHS).

Figure 5-9 shows that the Platreef sample is made up primarily of Pyroxene, Plagioclase, Phyllosilicates and other silicates (mainly Amphibole, Quartz and Epidote). The mineral distribution appears consistent throughout all four size fractions, although an increased amount of phyllosilicates are seen in the minus 25micron fraction, along with a decrease in the amount of Plagioclase and Pyroxene. The phyllosilicates content of the combined sample amounted to approximately 13% of the sample. The majority of these consisted of Chlorites, Talc and Serpentine.

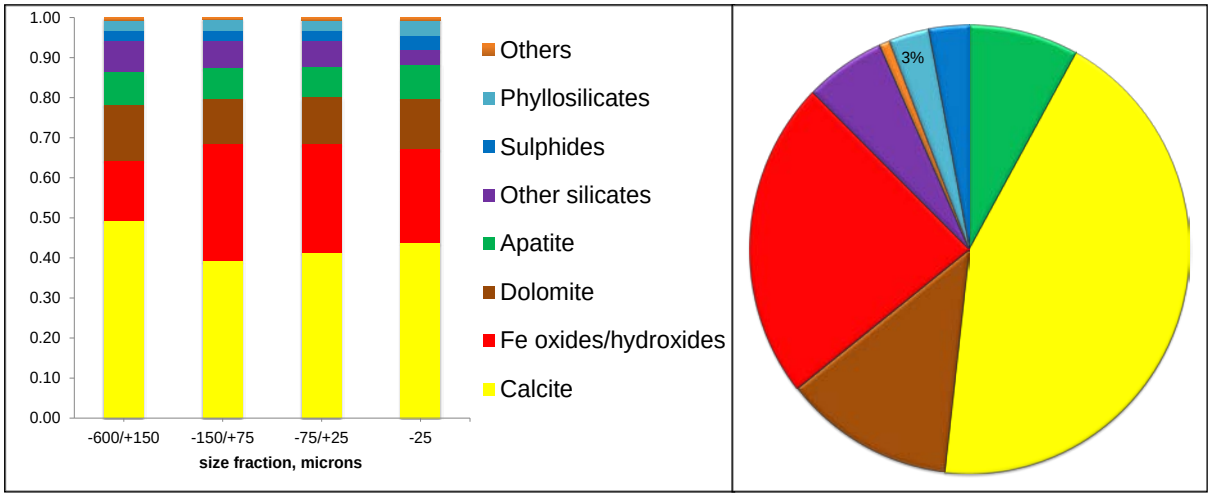

Figure 5-10. Mineralogy of copper ore sample - mineral distribution by size class (LHS) and combined distribution (RHS).

Figure 5-10 shows the copper ore sample consists primarily of Calcite, Dolomite and iron oxides. The mineral distribution seemed consistent once again across the size fractions, although slightly more dolomite and less iron oxides were present in the largest size fraction. The phyllosilicate content amounted to approximately 3% of the sample. The majority of these consisted of Serpentine and Chlorites. The other silicates refer mainly to Olivine, Pyroxene, Amphibole and Plagioclase.

The mineralogy results indicated that there were increased quantities of phyllosilicates in the Platreef B sample compared to the copper ore. Despite the fact that the Platreef sample contained at least 4 times the amount of phyllosilicates as the copper sample, the measured viscosities of the two ore samples were found to be similar between 30% and 60% solids. The difference in phyllosilicate content between the ore types is thus not considered to be significant enough to result in viscosity changes. Phyllosilicates have been found to have an effect on the yield stress of certain minerals; although once this stress is overcome the viscosity is affected by other physical parameters. The increased copper ore viscosity at 70% solids is most likely due to ore density effects.

5.4 Viscosity Characterisation – Modified fluid viscosity

In order to test the influence of a change in carrier fluid viscosity a series of tests were carried out on the two ore types under investigation. The tests involved changing the viscosity by the addition of sucrose, and the altering of the slurry temperature.

5.4.1 Platreef B Ore

Viscosity tests were run with the Platreef ore at 50% solids by mass (24% by vol.) with a sucrose addition of 30 and 50 Brix (%) to determine the effect of a change in carrier fluid viscosity on the suspension viscosity.

In addition to the sucrose tests, both sets of tests were run at a low (24-27 degrees Celcius) and a high (47-52 degrees Celcius) temperature to assess the effect of temperature on the rheology. The rheograms for Platreef are shown in Figure 5-11. The 50% sucrose tests exhibited greater viscosities than the 30% sucrose at both the low and high temperature conditions. The slope of the high temperature curves at 30% and 50% sucrose were reduced indicating a lower apparent viscosity. This is to be expected as the carrier fluid viscosity is reduced by the increased temperature. The low temperature tests however exhibit an increased slope at both 30% and 50% sucrose addition.

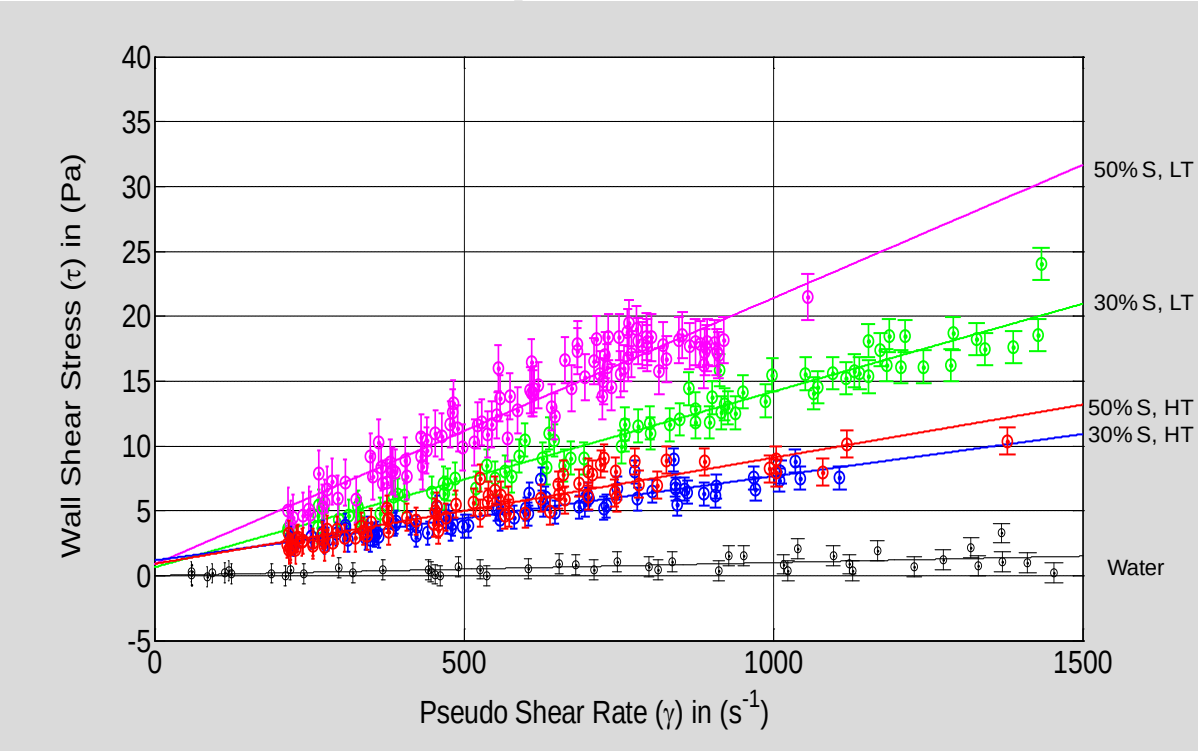

Figure 5-11. Platreef B at 50% with sucrose addition and temperature modification (S=sucrose addition, LT=low temp., HT=high temp.)

5.4.2 Copper Ore

Tests were conducted on the copper ore sample at 50% solids by mass (24% by vol.) with 30% and 50% sucrose addition at a low and high temperature. The rheograms from these tests are shown in Figure 5-12.

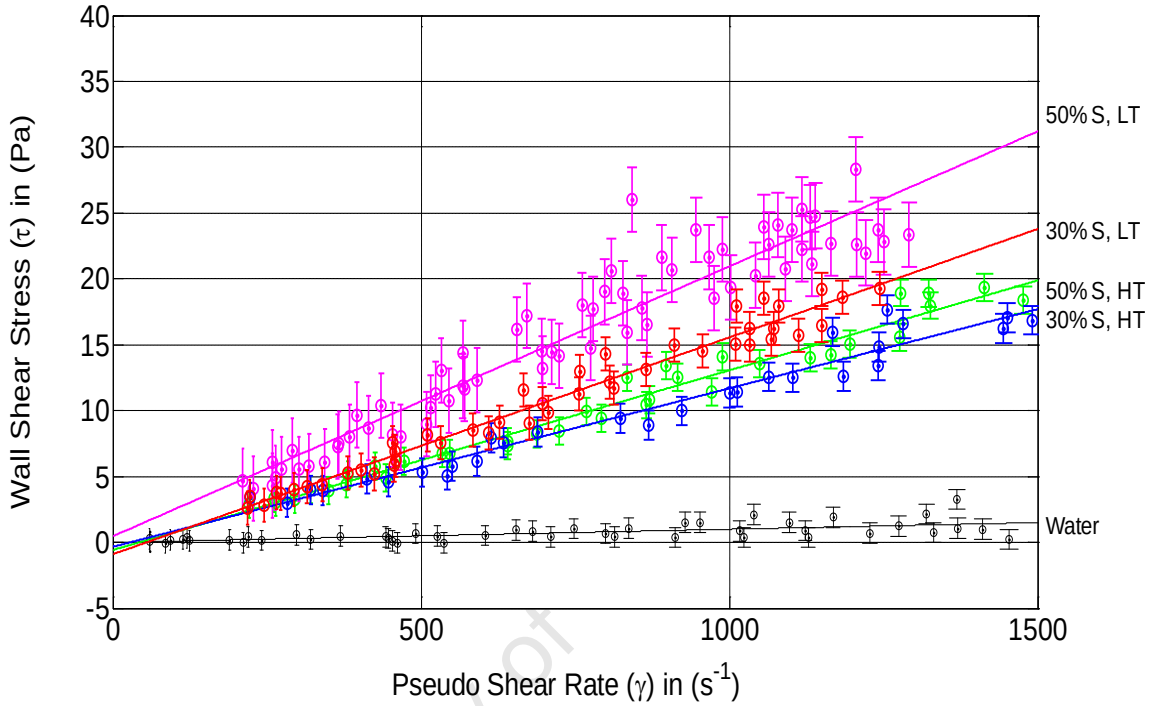

Figure 5-12. Copper ore at 50% with sucrose addition and temperature modification (S=sucrose addition, LT=low temp., HT=high temp.)

The 50% sucrose addition exhibits a steeper slope than the 30% condition for both low and high temperature tests. The slope of the high temperature tests is decreased, an indication of reduced fluid viscosity. It appears that the increased temperature did not affect the fluid viscosity to same degree as for the Platreef sample.

Figure 5-13 compares the apparent viscosities obtained for both ore types. The values were extracted from the curves for the tests performed at different test conditions in Figure 5-11 and Figure 5-12. The 'Std' condition refers to the 50% solids test result shown in Figure 5-7.

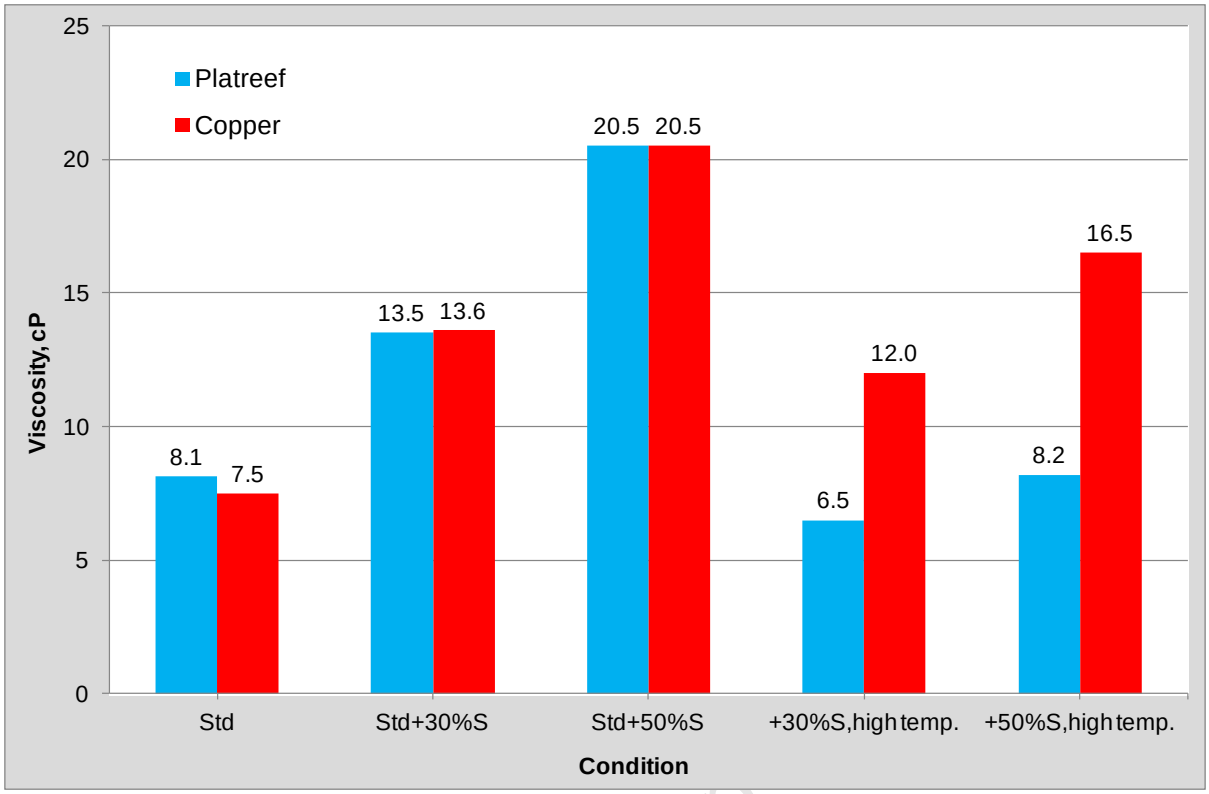

Figure 5-13. Viscosity values for the tests at modified fluid viscosity. S=sucrose addition.

When comparing the two ore types, Figure 5-13 shows that the viscosity for the slurry composed of copper ore particles is similar to that of the slurry containing Platreef for tests performed with 30% and 50% sucrose addition at low temperatures. However the high temperature tests seemed to have had a significant effect on the Platreef flow properties but did not reduce the viscosity of the copper ore to the same degree. This suggests that the influence of the sucrose in solution is different for the Platreef and copper ores.

The results of the rheology test work are consistent with the findings of Rutgers (1962) in terms of the effect of an increased solids concentration on viscosity. The influence of increased temperatures on the suspension viscosity are consistent with the findings reported in Jinescu (1974).

The range of viscosity data obtained in this chapter was combined with the hydrocyclone data in Chapter 6 to determine the effect of a change in pulp viscosity on cyclone performance. The rheological changes included altered slurry viscosities due to increased solids concentrations, and modified fluid viscosities due to sucrose addition and temperature changes.

6. HYDROCYCLONE RESULTS AND DISCUSSION

This chapter discusses the results of the hydrocyclone test work conducted for this thesis. The data was mass balanced using the JKSimMet simulator package. The data was fitted using the standard efficiency curve model developed by Whiten to extract values for cut-size, water split to fines, and sharpness of separation. The hydrocyclone test work data was then combined with the results from the viscosity characterisation test work to assess the effect of viscosity on the partition curve properties.

6.1 Hydrocyclone test results

A total of 65 cyclone tests were performed including repeats. A summary of the test conditions is shown in Table 6-1. Tests were performed using Platreef B ore on the 75 mm and 100 mm cyclone sizes and copper ore on the 75 mm, 100 mm and 165 mm cyclone sizes. The mineralogy of Platreef B ore is given in Section 5.3. The test variables included: slurry concentration, temperature, and altering viscosity by adding sucrose. The effect of solids concentration in terms of rheology has been well researched, Jinescu (1974), and is known to cause an increase in viscosity with increased levels of concentration. Temperature and sucrose were chosen in order to alter the viscosity of the carrier fluid, which is an important parameter for dense phase slurries. In addition to the tests at high pressure and low temperature (termed standard tests), low pressure tests were included to see if there was any effect on the partition curve parameters at reduced shear rates.

Table 6-1. Test conditions for hydrocyclone test work.

Cyclone size (mm)	75	100	165
Ore Type	P/Reef, Copper	P/Reef, Copper	Copper
Approx.% Solids (C_m)	30, 50, 70	30, 50, 70	50
Slurry Temp.	ambient, high	ambient, high	ambient, high
Feed Pressure	low, high	low, high	low, high
Sucrose Addition (%)	30, 50	30, 50*	30, 50

** For Platreef only*

All the unprocessed stream and size distribution data from the hydrocyclone tests was collated and checked for initial errors before mass balancing was performed to ensure self

consistency of the data. The mass balancing was carried out using MBal in the JKSimMet software package developed at the JKMRC in Australia. The mass balance would reflect any discrepancies in the experimental work and would indicate whether there was a problem with any of the flow rate or sizing data. Successful balances were achieved for all the data featured in the subsequent sections of this thesis. The data that was unreliable or was discovered to have irreconcilable errors was discarded.

6.1.1 Platreef B ore

Hydrocyclone tests were performed using the Platreef B ore. Table 6-2 and Table 6-3 contain a summary of the balanced results for the 75 mm and 100 mm cyclones respectively, at different rheological conditions. For the 75 mm hydrocyclone, Tests numbers (#) 1-9 involved tests at 30%, 50% and 70% solids at various pressures and temperatures. Tests 10-15 included the effect of modifying viscosity by sucrose addition. The test conditions were then repeated for the 100 mm cyclone.

The data in Table 6-2 and Table 6-3 show that operating at lower pressures resulted in reduced feed rates. The 100 mm cyclone operated at reduced inlet pressures as the centrifugal head was reduced. The underflow percentage solids values were consistently lower for the tests running at low feed pressures as the centrifugal forces and tangential velocities are reduced resulting in fewer solids recovered in the U/F. Tests 7-9 and tests 22-24 (70% solids tests) reflect the impact of solids overloading on the density of the product stream. The result is a significant increase in O/F density, accompanied by a significant coarsening of the O/F stream. This is reflected by a decrease in the percentage passing 75 µm from 98% to 60% for the 75 mm cyclone, and 90% to 50% for the 100 mm cyclone. This is an immediate indication of reduced cyclone performance in terms of separation efficiency. The U/F density was not affected to the same degree.

The majority of tests at increased slurry temperatures (hence reduced fluid viscosities) resulted in increased values of U/F density and therefore reduced O/F densities.

The tests at increased pulp viscosity (tests 10-15 and tests 25-30) showed reduced feed rates compared to the equivalent tests without sucrose addition. Interestingly the sucrose tests at 30% (tests 10-12 and tests 25-27) did not seem to have a significant effect on the product streams, besides the reduced flow rates. However, the increased sucrose addition tests (tests 13-15 and tests 28-30) were found to have a large effect on the U/F and O/F densities for both cyclone sizes.

Table 6-2. Balanced test data for 75 mm cyclone – Platreef B.

Test #	Feed P (kPa)	Slurry Temp. (℃)	Sucrose (%)	Feed			U/F			O/F		
				% solids	TPH	% pass. 75 µm	% solids	TPH	% pass. 75 µm	% solids	TPH	% pass. 75 µm
1	120	42.0		32.2	5.01	43.8	59.2	4.43	36.7	7.18	0.58	93.9
2	95	25.7		31.9	4.12	46.5	56.9	3.63	39.4	7.43	0.48	98.4
3	123	25.6		31.3	4.61	48.0	58.6	4.01	41.3	7.56	0.60	98.2
4	120	41.5		53.6	9.88	48.0	76.9	8.06	35.6	22.9	1.82	99.3
5	96	28.0		53.0	8.34	47.8	74.3	6.80	36.0	23.4	1.54	98.4
6	120	26.0		53.5	9.96	47.0	75.7	8.07	33.4	23.7	1.89	98.3
7	93	47.0		70.2	10.19	42.5	74.9	7.23	33.8	60.8	2.96	61.2
8	65	31.8		70.3	9.25	45.0	72.3	6.89	41.0	65.2	2.36	55.8
9	95	29.2		70.5	10.43	44.9	74.3	6.60	38.0	64.8	3.82	56.4
10	120	22.6	30	50.8	7.32	43.1	74.7	6.08	31.7	19.8	1.24	98.9
11	95	26.5	30	52.9	6.60	42.3	75.2	5.56	32.0	20.5	1.04	99.4
12	120	52.1	30	50.8	7.68	46.1	77.6	6.30	33.8	19.7	1.38	98.9
13	120	23.0	50	52.4	6.40	43.0	69.2	5.08	29.0	27.2	1.33	95.8
14	95	26.2	50	50.3	5.69	45.6	67.0	4.35	29.9	27.7	1.34	94.9
15	120	55.0	50	49.7	5.80	44.1	73.9	4.78	32.8	19.6	1.02	99.0

Table 6-3. Balanced test data for 100 mm cyclone – Platreef B.

Test #	Feed P (kPa)	Slurry Temp. (℃)	Sucrose (%)	Feed			U/F			O/F		
				% solids	TPH	% pass. 75 µm	% solids	TPH	% pass. 75 µm	% solids	TPH	% pass. 75 µm
16	88	21.5		31.6	6.49	40.4	62.4	5.56	30.3	7.98	0.93	97.8
17	68	23.4		31.8	5.65	41.7	61.3	4.85	30.6	8.12	0.80	97.9
18	88	49.1		32.4	6.57	45.2	61.4	5.57	34.9	8.95	1.01	98.0
19	100	23.0		54.4	16.09	46.9	75.5	10.81	22.7	34.7	5.28	89.4
20	75	27.4		54.1	13.44	45.5	74.8	9.38	24.3	33.0	4.06	89.0
21	100	50.5		54.1	15.11	45.8	77.9	10.56	23.8	31.6	4.55	92.7
22	80	28.0		69.7	18.07	45.3	73.6	9.26	37.5	66.0	8.82	53.7
23	50	30.3		69.3	14.16	45.7	70.1	8.57	43.5	68.1	5.59	49.4
24	80	50.0		70.2	15.44	45.6	70.8	8.54	44.1	69.6	6.90	47.6
25	92	22.8	30	50.7	10.08	37.2	74.5	8.16	24.1	21.5	1.92	93.3
26	70	26.0	30	50.1	9.02	37.2	72.1	7.31	25.0	21.7	1.71	92.4
27	91	53.5	30	50.9	10.65	39.4	78.3	8.54	26.3	21.1	2.11	95.1
28	92	52.7	50	48.0	8.63	43.7	72.3	6.15	25.4	26.2	2.48	89.2
29	72	29.5	50	47.4	7.73	34.8	57.8	5.04	24.6	38.8	2.70	53.9
30	80	29.0	50	51.1	8.46	43.8	62.6	5.12	27.2	39.8	3.34	67.3

6.1.2 Copper Ore

Similar tests were then performed using the copper ore on three cyclone sizes under variable rheological conditions. The balanced data from the tests performed using copper ore on the 75, 100 and 165 mm cyclone diameters are provided in Table 6-4, Table 6-5, and Table 6-6, respectively.

For the 75 mm hydrocyclone, Tests 31-39 involved tests at 30%, 50% and 70% solids at various pressures and temperatures. Tests 40-45 included the effect of sucrose addition. The test conditions were then repeated for the 100 mm cyclone, excluding the addition of sucrose.

All tests performed on the 165 mm hydrocyclone were done using the copper ore at the feed solids concentration of approximately 50% by weight. Tests 55-57 involved standard tests with altered pressures and temperatures. Tests 58 and 59 were two additional tests reducing the spigot size and vortex finder size respectively. This was done to assess whether the effect of these variables on the parameters extracted from the efficiency curve was similar to that obtained by changing viscosity. Tests 60-65 included the effect of sucrose addition.

Table 6-4 and Table 6-5 reflect similar trends as for the Platreef ore. The tests at reduced feed pressures resulted in reduced feed rates as expected. The reduced inlet pressures also resulted in decreased underflow densities. However, the increase in feed slurry temperature resulted in an increase in the underflow densities due to decreased carrier fluid viscosity and thus improved separation of liquid to the O/F, (Yoshida *et al.,* 2004).

Like the Platreef ore, the tests run at the highest solids concentration using the copper ore did not affect the U/F densities but had a significant effect on the O/F density and the percentage passing 75 µm. This is an indication of solids crowding near the apex, and entrainment of coarse particles into the inner vortex flow, (Braun & Bohnet, 1990). The sucrose addition tests at 30% for the 75 mm cyclone (tests 40-42) did not seem to affect the product stream densities. Tests performed using sucrose at 30% on a 165 mm cyclone (tests 60-62) did however result in reduced underflow density. The sucrose tests at 50% (tests 43-45, 63-65) greatly affected the cyclone operation with significantly increased O/F densities and reduced U/F densities, particularly for the 165 mm cyclone.

Table 6-4. Balanced test data for 75 mm cyclone – Copper Ore.

Test #	Feed P (kPa)	Slurry Temp. (℃)	Sucrose (%)	Feed			U/F			O/F		
				% solids	TPH	% pass. 75 µm	% solids	TPH	% pass. 75 µm	% solids	TPH	% pass. 75 µm
31	120	21.5		34.1	4.88	45.7	59.3	4.33	38.9	7.90	0.56	99.5
32	90	23.4		34.6	1.46	50.4	56.1	1.28	43.4	9.36	0.18	99.4
33	120	51.0		34.3	4.95	48.6	61.4	4.30	40.9	8.81	0.66	99.3
34	140	51.0		54.0	11.14	52.5	79.9	8.78	39.8	24.5	2.35	99.8
35	105	22.5		53.9	9.35	52.5	76.9	7.18	38.4	27.0	2.17	99.6
36	140	23.7		54.0	11.24	52.5	78.5	8.71	38.8	26.0	2.53	99.6
37	120	30.0		76.1	15.86	53.3	79.4	9.38	45.2	71.7	6.48	65.1
38	90	30.2		76.1	13.86	53.2	78.9	8.98	45.9	71.3	4.88	66.7
39	115	51.9		76.2	14.93	53.2	78.9	9.08	46.0	72.4	5.85	64.4
40	130	23.7	30	52.9	8.02	46.6	77.0	6.52	34.5	22.4	1.50	99.4
41	100	26.0	30	53.0	7.06	47.3	75.8	5.74	35.4	22.9	1.32	99.3
42	130	53.0	30	53.3	8.10	48.4	80.2	6.56	36.4	21.9	1.54	99.5
43	120	52.0	50	52.6	7.11	51.3	70.7	5.46	37.2	28.5	1.65	97.9
44	90	22.2	50	53.0	6.20	53.8	64.1	4.35	38.9	37.7	1.85	88.9
45	120	24.0	50	52.9	7.23	54.7	67.0	4.97	37.4	36.3	2.26	92.9

Table 6-5. Balanced test data for 100 mm cyclone – Copper Ore.

Test #	Feed P (kPa)	Slurry Temp. (℃)	Sucrose (%)	Feed			U/F			O/F		
				% solids	TPH	% pass. 75 µm	% solids	TPH	% pass. 75 µm	% solids	TPH	% pass. 75 µm
46	90	19.5		32.1	6.93	47.6	61.6	5.69	36.1	10.0	1.24	98.0
47	70	25.0		31.7	5.96	46.4	58.5	5.04	36.1	9.0	0.92	98.6
48	90	54.0		31.8	6.46	49.5	60.4	5.45	40.1	8.9	1.01	98.8
49	92	52.0		51.6	14.28	50.8	79.3	10.91	35.0	24.3	3.37	97.7
50	70	25.0		51.9	12.29	53.2	76.3	8.44	33.7	30.5	3.85	95.3
51	92	25.4		51.9	14.06	52.7	77.7	9.71	32.4	29.8	4.35	96.4
52	100	31.0		71.0	21.96	52.7	79.7	11.72	37.3	63.1	10.24	70.2
53	80	31.0		69.7	18.76	50.7	79.3	11.40	33.1	58.7	7.37	77.0
54	95	57.2		70.2	24.15	53.5	71.4	10.84	51.3	69.3	13.31	55.8

Table 6-6. Balanced test data for 165 mm cyclone – Copper Ore.

Test #	Feed P (kPa)	Slurry Temp. (℃)	Sucrose (%)	Feed			U/F			O/F		
				% solids	TPH	% pass. 75 µm	% solids	TPH	% pass. 75 µm	% solids	TPH	% pass. 75 µm
55	75	26.5		49.9	25.88	51.3	75.6	17.51	29.1	29.1	8.37	97.8
56	55	28.5		49.4	18.97	52.7	73.2	13.00	31.8	28.9	5.97	98.2
57	75	49.0		50.0	23.71	53.9	76.6	15.77	31.4	29.5	7.94	98.5
58 (<Du)	45	28.5		50.0	17.98	52.9	77.7	11.27	26.9	31.3	6.71	96.6
59 (<Do)	75	28.0		49.9	20.50	52.6	73.5	14.74	35.0	27.5	5.77	97.8
60	70	26.5	30	52.0	17.11	52.2	71.9	10.74	28.8	35.5	6.37	91.7
61	50	29.0	30	51.8	15.24	52.9	67.3	10.04	33.1	35.9	5.20	91.1
62	70	52.0	30	52.4	17.92	52.4	74.1	11.54	28.8	34.3	6.38	95.0
63	70	49.5	50	49.3	14.58	54.7	56.4	8.47	42.5	42.0	6.12	71.5
64	47	29.0	50	48.7	12.14	55.8	50.0	9.11	53.1	45.2	3.04	64.1
65	65	29.0	50	49.0	14.46	55.5	53.3	8.96	47.9	43.5	5.50	67.8

A comparison chart of the change in pulp density of the feed, underflow and overflow for all the high pressure, low temperature tests is shown in Figure 6-1.

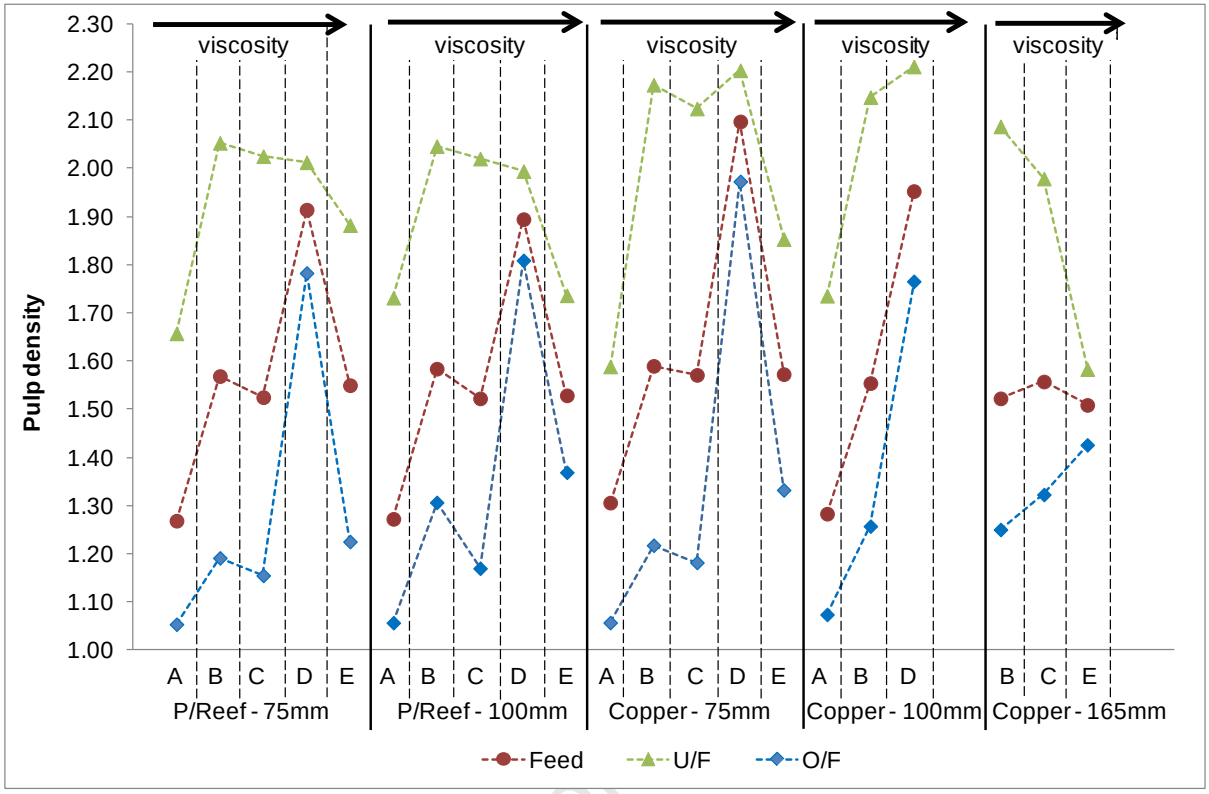

Figure 6-1. Comparison of stream densities.

X-axis notation: *A=30% solids* *B=50% solids*

C=50% solids + 30% sucrose *D=70% solids*

E=50% solids + 50% sucrose

With the exception of the tests performed using copper on a 165 mm cyclone, the peaks in the O/F densities correspond to the feed concentration of 70% by weight. A decrease in classification performance is expected for conditions where the product stream densities begin to approach that of the feed stream, as this indicates that the water split to O/F (C) is reduced resulting in inefficiencies, (Nageswararao, 2001). In this case it was for conditions of high feed densities and highest feed pulp viscosities. The high feed density condition does not correspond to the highest viscosity which is an indication that the poor performance is not merely a viscosity effect. The highest viscosity condition (high sucrose addition) thus results in decreased performance due to viscosity alone, especially for the 165 mm cyclone.

6.2 Hydrocyclone data analysis

After the flow and component data was balanced to an acceptable level of SSQ error, it was exported to MS Excel and the efficiency curves were constructed. The recovery to overflow was obtained using equation *6.1*:

$$E_{oa} = 100\left(\frac{W_{oi} * M_o}{W_{fi} * M_f}\right) \quad \text{.....[6.1]}$$

where: W_{oi}, W_{fi} = weight proportions of material of size i in overflow and feed solids

M_o, M_f = solids mass flow rates of overflow and feed streams

The actual efficiency curves reflected the uncorrected cut size (d_{50}) and water split to overflow (C). The corrected efficiency curve to overflow (E_{oc}) was then obtained by correcting for the bypass fraction (100-C) using equation *6.2*:

$$E_{oc} = \frac{E_{oa}}{C} \quad \text{.....[6.2]}$$

The initial estimate of the corrected cut size (d_{50c}) and water split was then obtained from the corrected efficiency curve to O/F.

The Whiten equation was then fitted to the partition curve and the fitted values of alpha, d_{50c} and C were extracted. The trends for these properties were then analysed in relation to changes in feed viscosity. A summary of the efficiency curve properties and capacity are tabulated in APPENDIX F.

6.3 Effect of carrier fluid viscosity on efficiency curve parameters

The effects of changing the viscosity of the slurry on the hydrocyclone partition curve parameters are discussed in this section. Standard tests on the charts (Std) are those conducted at low (ambient) slurry temperatures which ranged between 24 and 28 degrees Celsius, and high pressures.

6.3.1 Effect on cut-size (d_{50c})

The cut-size parameter is an important measure of classification efficiency. A coarser cut-size value would indicate a less efficient separation of the feed material to the required product stream. Figure 6-2 shows the effect of viscosity on the corrected cut size of the different cyclone diameters for **Platreef** ore. In this work viscosity was altered by changing the feed solids content (30, 50, 70%), and modifying the carrier fluid by increasing temperature and/or sucrose addition (30%, 50%).

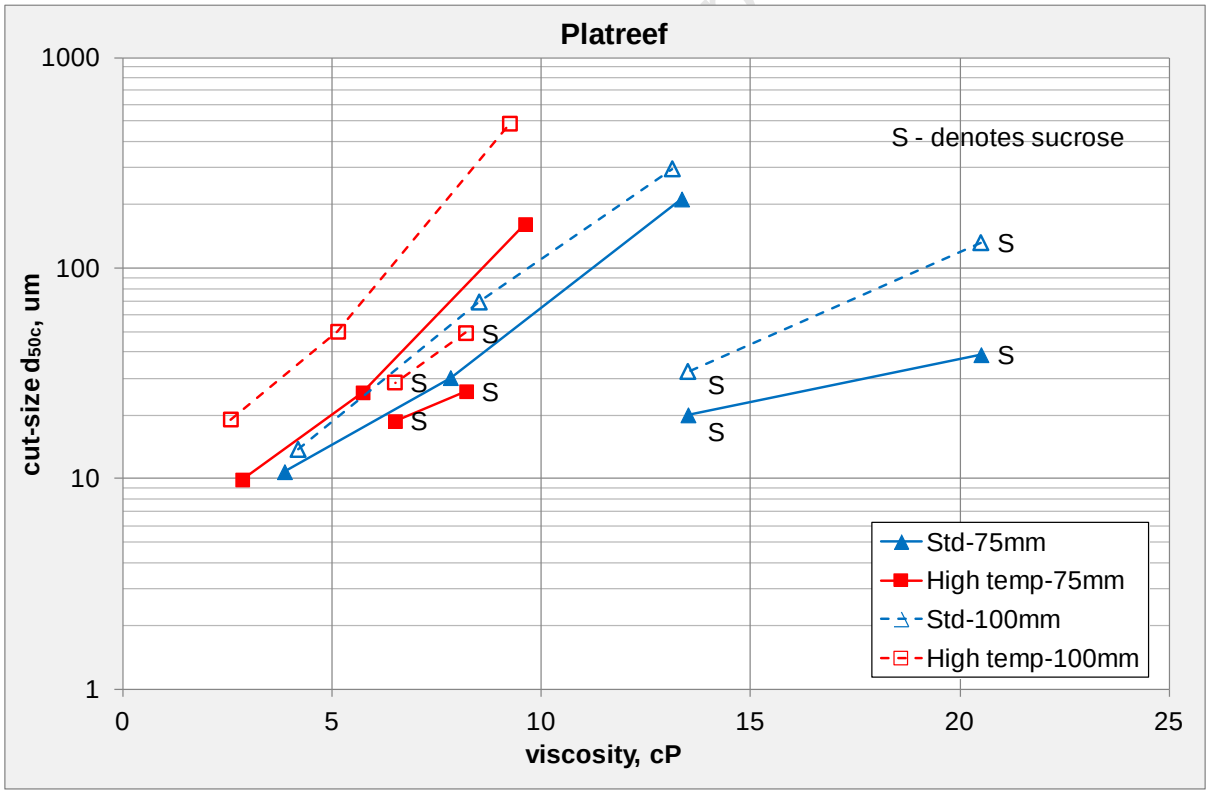

Figure 6-2. Effect of viscosity on corrected cut size – 75 mm and 100 mm cyclone, Platreef. 'S' denotes sucrose addition at 30%,50%.

Figure 6-2 shows that increasing viscosity resulted in increased cut sizes for both cyclone diameters tested. Lower cut sizes were obtained for the 75 mm diameter when compared to

the 100 mm diameter cyclone. Other authors have indicated that cut-size is directly related to cyclone diameter, (Napier-Munn et al., 1996).

The largest cut-sizes were obtained for the highest feed solids concentration, although this did not correspond to the largest viscosity values. This is an indication that the observed increase in cut size was not simply due to the influence of viscosity. There was indeed an increase in viscosity as the concentration increased from 50% to 70% solids, which in turn increased cut-size. However, it is believed that the cut-sizes at these solids concentration levels are due to hindered settling/hindered separation as the amount of particles in the hydrocyclone simply becomes prohibitively high. As a result the flow patterns are greatly affected resulting in not only more fine material being entrained with the coarse material to the U/F, but also more coarse material being 'dragged' into the inner vortex due to decreased tangential forces and solid overloading at the apex. It is worth mentioning here that tests were performed in such a way that roping conditions were avoided. The cyclone thus performed poorly but an inner vortex and air core were still present.

The increased viscosity values due to addition of sucrose did not affect the corrected cut-size initially. The sucrose addition at 30% resulted in cut-size values comparable to those tests at the same solids concentration without sucrose addition. Further increase in sucrose addition however increased the viscosity above 20 cP and this resulted in increased values for d_{50c} due to the increased carrier fluid viscosity which inhibits centrifugal flow formation.

The significant reduction in carrier fluid viscosity due to increased slurry temperatures generally resulted in reduced cut-sizes. The cut-sizes obtained for the sucrose addition tests in particular were greatly reduced with an increase in feed slurry temperature. The exception here were the tests conducted at 70% feed percentage solids for the 100 mm cyclone where large cut-sizes were still obtained even at viscosity values below 10 cP. This once again reiterates the fact that the increased cut-size value was not only viscosity related.

The effect of viscosity on the corrected cut size for **copper** ore on different cyclone diameters is shown in Figure 6-3. The test conditions were the same as for the Platreef ore but the sucrose tests were only performed on the 75 mm cyclone.

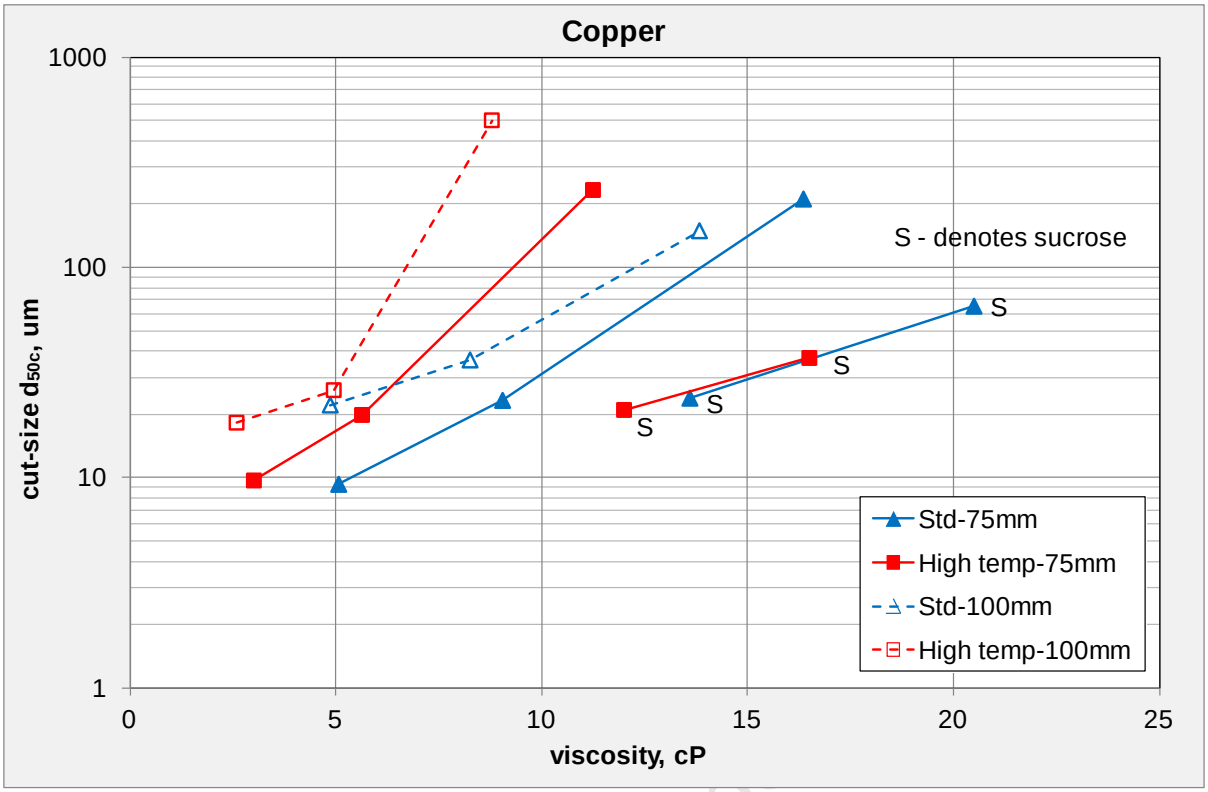

Figure 6-3. Effect of viscosity on corrected cut size – 75 mm and 100 mm cyclone, copper. 'S' denotes sucrose addition at 30%,50%.

Figure 6-3 shows that for the different ore type, the increased viscosity values resulted in increased cut-sizes due to solids content. Largest cut-sizes were obtained for the high feed solids concentrations even at reduced viscosities.

The addition of sucrose during the 75 mm cyclone tests increased the cut-size only for the high sucrose addition, due to increased carrier fluid viscosity. This corresponded to the highest pulp viscosity value of 21 cP, but larger cut-sizes were obtained for the high feed density experiments.

The high temperature tests resulted in a consistently reduced viscosity and corresponding reduced cut sizes, as the water viscosity was reduced. The exception though was the high feed solids tests which once again were not affected by carrier fluid viscosity, and the cut-size actually increased. This high feed solids result warrants some explanation.

The detrimental effects of the tests at highest concentration on the cyclone performance was described by Gaunt (1983). He conducted a theoretical study and stated that at 70% solids near the underflow the outer layer viscosity dominates and the shear stress at the wall increases as the feed concentration increases. After this the growth of the slurry at the wall

dominates and wall shear stress falls as the feed concentration increases. Gaunt offered an explanation for overloading of solids in the cyclone. He postulated that above a certain level of feed solids, the shear stress of the slurry falls below its yield stress resulting in the breakdown of flow in the boundary layer and the migrating of particles to the main flow. This leads to the dramatic loss of efficiency. If the shear stress is kept above the yield stress then the particles will return to the wall but as soon as the yield stress climbs above the shear stress the efficiency drops as the particles are entrained into the upward moving vortex to the O/F. This seems unlikely as the yield stress is the minimum force required for generation of flow, below this value the particles would effectively be stagnant. It does however provide an insight into the detrimental effects of increased feed density.

Braun & Bohnet (1990) also looked at the effect of feed solids concentration and stated that the deterioration of the cyclone efficiency appeared to result from the changes in the flow fields inside the cyclone as well as the re-entrainment of particles already separated by centrifuging action. Figure 6-1 shows that any further increase in feed solids density would not increase the U/F density as there is a physical limitation (spigot capacity) as to how much can be discharged by the U/F before the onset of roping. Fahlstrom (1963) studied the effects for his crowding theory postulation.

Viscosity effects on cut-size for the 165 mm cyclone are shown in Figure 6-4. Feed solids concentration was kept constant at 50% by weight as standard. The influence of spigot (Du) and vortex finder (Do) diameter were also investigated.

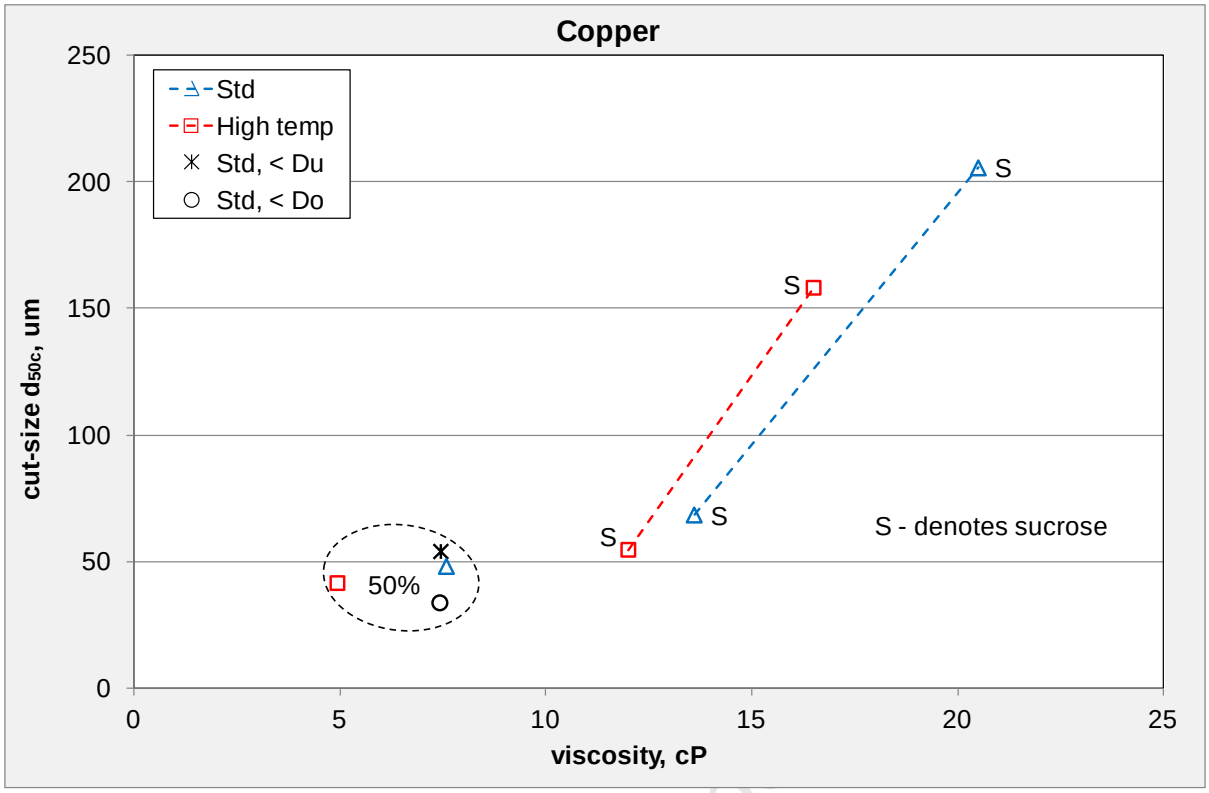

Figure 6-4. Effect of viscosity on corrected cut size – 165 mm cyclone, copper.
'S' denotes sucrose addition at 30%,50%.

Figure 6-4 shows a similar trend to that observed with smaller cyclones, where an increase in viscosity due to sucrose addition resulted in an increase in cut-size. However, relatively large increases in cut-size were observed at viscosity values above 15 cP.

An increase in slurry temperature reduced the cut-size due to a reduction in the carrier fluid viscosity. The increased temperature test for the high sucrose addition showed the greatest improvement in cut-size.

Two tests were performed at a modified spigot and vortex finder diameter. First the spigot size was reduced by 20% (from 45 mm to 35 mm). The decreased spigot diameter resulted in an increased cut size as more coarse material was sent to the O/F. The vortex finder was then reduced by about 17% (64 mm to 53 mm). The decreased vortex finder reduced the cut size under the same test conditions due to a reduction in the solids split to O/F. Despite these differences in cut-size, the effect on cut size was not nearly as significant as for when the viscosity was modified. The smaller spigot size resulted in close to roping conditions and therefore any further reduction in size was not possible under these conditions.

Previous work also showed that increasing viscosity results in increased cut-size. Kawatra *et al.* (1996) performed experiments on a 100 mm cyclone using silica sand, and altered viscosity using temperature and feed solids content. Tavares *et al.* (2002) performed experiments on a 50 mm cyclone using phosphate ore and modified viscosity by means of solids content and chemical environment (carrier fluid). The carrier fluid viscosity was altered either by the addition of a dispersant (polycarboxylic sodium salt), or a thickening agent (carboxymethylcellulose or glycerin).

6.3.2 Effect on water split to O/F (C)

The fraction of feed water reporting to the O/F stream is another important feature of the partition curve. In general good water split values are considered to be in the region of 70% to 80%, a poor split would be anything below about 60%, (Napier-Munn *et al.*, 1996). This effectively means that the U/F stream is too dilute which is undesirable, as fine material can often be included in the liquid (bypass fraction), and would be recirculated through the circuit. Figure 6-5 shows the effect of viscosity on the water split to O/F for Platreef ore from tests performed using 75 mm and 100 mm diameter cyclones. Viscosity was altered by changing the feed solids content (30, 50, 70%), and modifying the carrier fluid by increasing temperature and/ sucrose addition (30%, 50%).

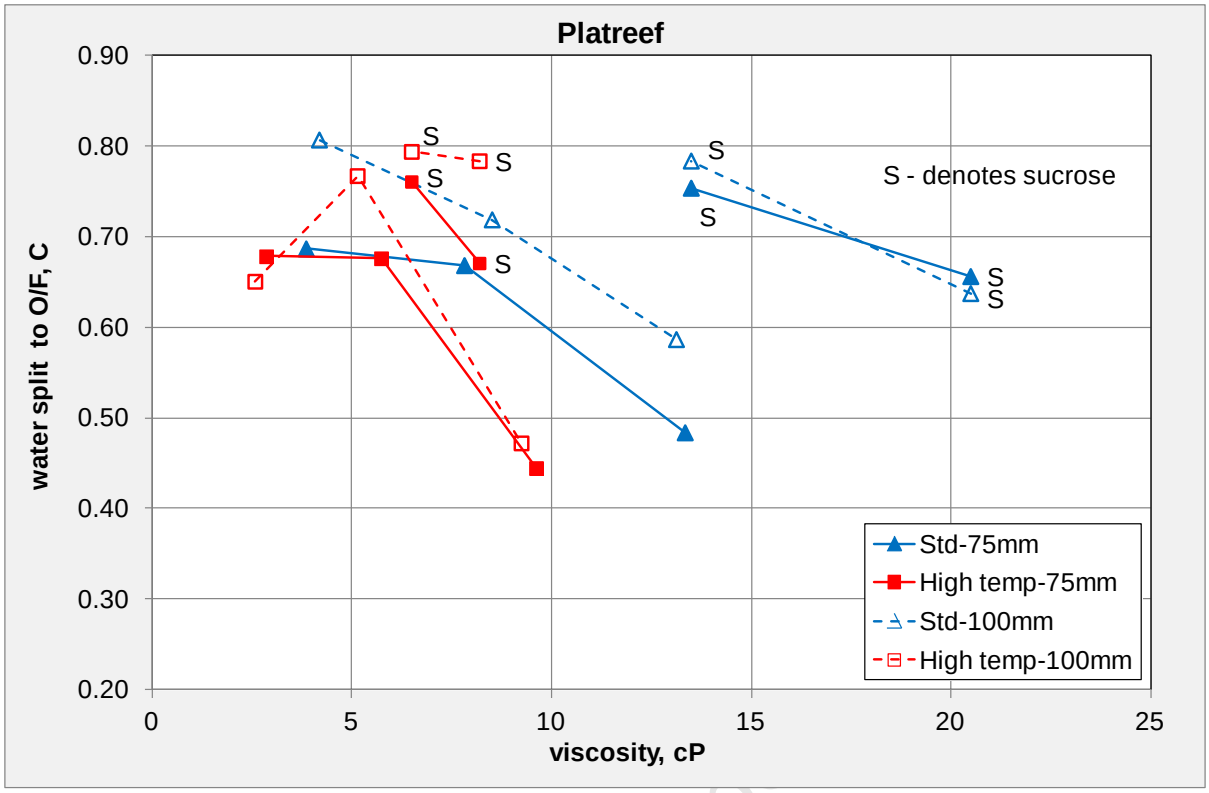

Figure 6-5. Effect of viscosity on water split to O/F – 75 mm and 100 mm cyclone, Platreef. 'S' denotes sucrose addition at 30%,50%.

Figure 6-5 shows slightly higher water split values for the 100 mm cyclone. A decrease in water split to O/F (C) is observed as the viscosity increases due to solids concentration. Significantly reduced water split values were obtained at the high feed solids concentration, with more than half the water reporting to the U/F stream which translates to poor cyclone performance, (Napier-Munn *et al.*, 1996). This is due to the overcrowding of particles which interferes with the flow fields inside the hydrocyclone, (Svarovsky, 1984).

The tests with 50% sucrose addition (highest viscosity) resulted in decreased water to the O/F. This decrease is most likely due to the fact that the centrifugal forces which contribute to the upward flow of liquid are reduced by the viscous pulp conditions.

An increase in the slurry temperature (reduced carrier fluid viscosity) resulted in improved water splits for the sucrose addition tests, particularly for the 100 mm cyclone at the maximum viscosity as the water reporting to the O/F increased from 64% to 78%. This is due to the higher temperature reducing the liquid viscosity which creates more optimal conditions for centrifugal motion.

The increased slurry temperature actually reduced the water split values for the tests at maximum solids concentration even though the viscosity was reduced. This was another indication that increased viscosity was not the only reason for the poor cyclone performance, as the excess feed solids resulted in hindered separation/particle overcrowding conditions inside the cyclone.

Figure 6-6 below shows the effect of viscosity on water split to O/F for copper ore from tests performed using 75 mm and 100 mm diameter cyclones.

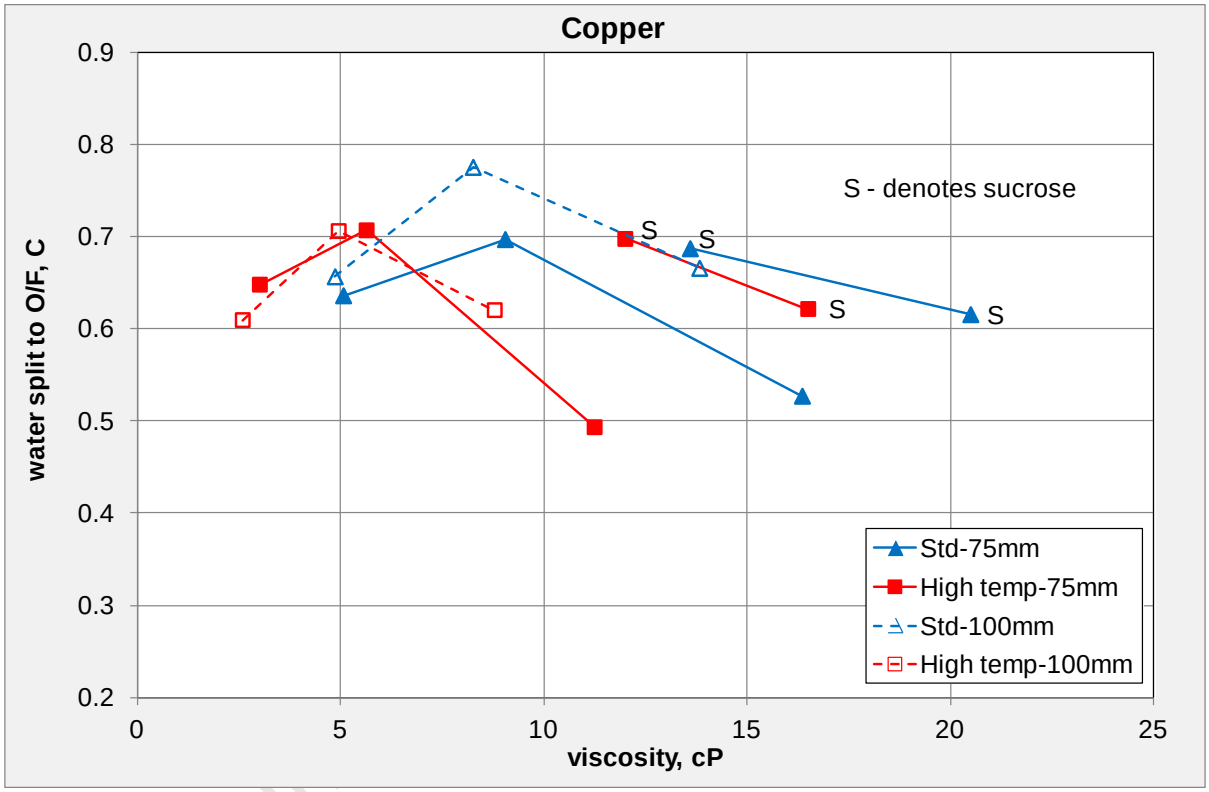

Figure 6-6. Effect of viscosity on water split to O/F – 75 mm and 100 mm cyclone, copper. 'S' denotes sucrose addition at 30%,50%.

A decrease in water recovery to O/F can be observed as viscosity is increased by increasing the solids concentration for both cyclone diameters. The high feed density experiments showed the detrimental effect to cyclone performance with a 50% water split to the O/F for the standard tests conducted on the 75 mm cyclone. Tests on the larger cyclone did improve the water split for the high feed solids concentrations. Interestingly the results indicated that the optimum water split was obtained at viscosity values between 5 cP and 10 cP for the copper ore suggesting that the feed concentration of 50% is where the optimum operating

point lies. This also suggests that there may be an optimum viscosity where the cut-size to water recovery to O/F relationship is most favourable.

The initial addition of sucrose to the copper ore pulp did not affect the water split, even at viscosities as high as 10 cP. A further increase however above 15 cP resulted in a decrease in water split due to increased carrier fluid viscosity.

The tests at increased slurry temperature did not seem to show a significant improvement in water split values for the copper pulp even though viscosities were reduced. The reduced carrier fluid viscosity due to temperature modification does not seem to have a major influence on the water split, as it did for the cut-size, for the 75 mm and 100 mm cyclones.

Figure 6-7 shows the effect of viscosity on the water split to the O/F for the copper ore for tests performed using the 165 mm diameter cyclone.

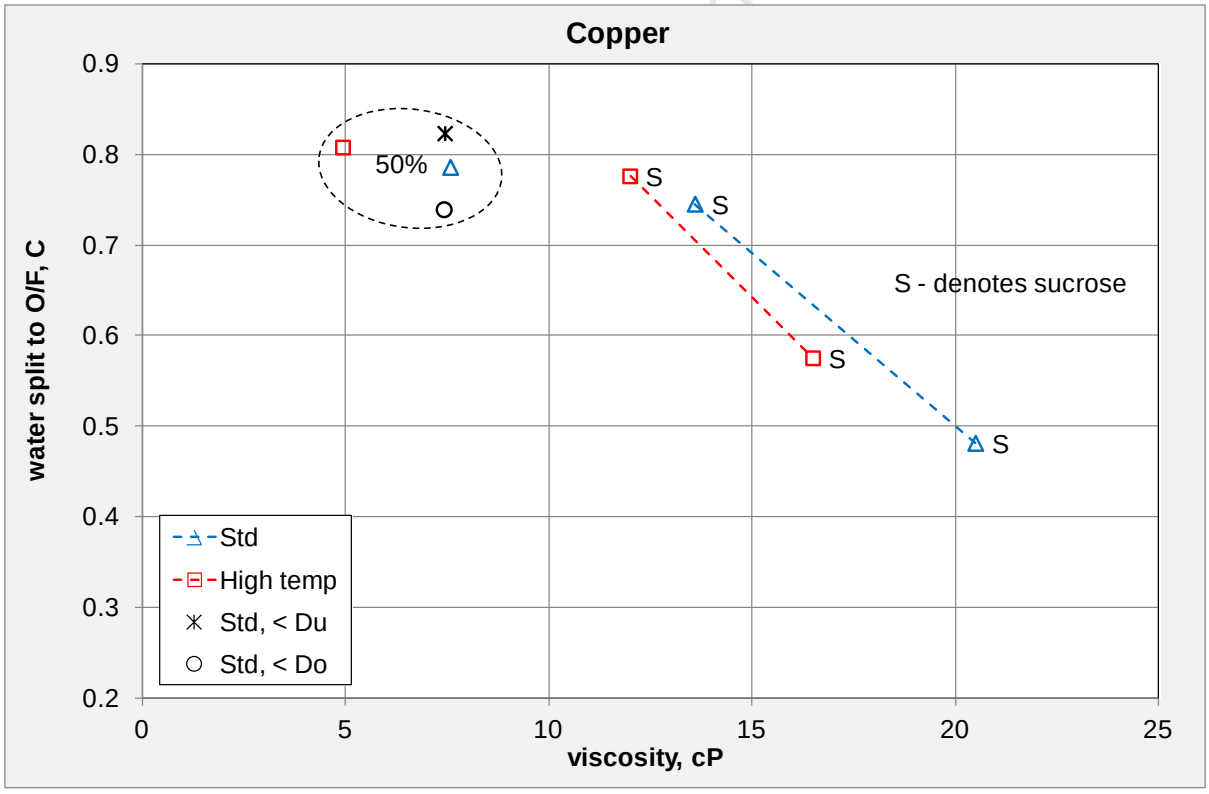

Figure 6-7. Effect of viscosity on water split to O/F – 165 mm cyclone, copper.
'S' denotes sucrose addition at 30%,50%.

The effect of a change in carrier fluid viscosity on the water split for the 165 mm diameter cyclone is apparent, and the difference does seem to be more pronounced for the larger

cyclone. Reduced water split values were observed with an increase in viscosity due to sucrose addition. The tests at highest sucrose addition of 50% resulted in a significantly reduced water recovery to the O/F, with the value decreasing from close to 80% for the standards tests, to below 50%.

The increase in temperature resulted in higher water split values to the O/F, particularly for the tests at highest sucrose addition. This can be attributed to the reduction in carrier fluid viscosity and thus improvement in the flow conditions inside the cyclone.

The reduced spigot diameter test (<Du) resulted in an increased water split as more water (along with solids) was sent to the O/F due to the restriction in the apex area. A reduced vortex finder diameter (<Do) resulted in a decrease in C due to the reduction of the inner vortex flow and hence less liquid leaving the O/F. The effects of the change in spigot and vortex finder diameter were not largely significant, compared to the viscosity effects.

Previous researchers have found a decrease in C with increased viscosity - Horsley & Allen (1987), Yopps et al. (1987), and Kawatra et al. (1996). These were all conducted on 100 mm cyclones using fine silica sand as the feed material.

6.3.3 *Effect on sharpness of separation, alpha (α)*

The slope of the partition curve (alpha) is another important feature when determining classification efficiency. It is however often unreliable in its nature. Alpha values range from 0.1 for very poor separation, up to values of 10 for very efficient separation. Figure 6-8 below shows the effect of viscosity on the alpha efficiency curve parameter for Platreef using the 75 mm and 100 mm diameter cyclones. Viscosity was altered by changing the feed solids content (30, 50, 70%), and modifying the carrier fluid by increasing temperature and/or sucrose addition (30%, 50%).

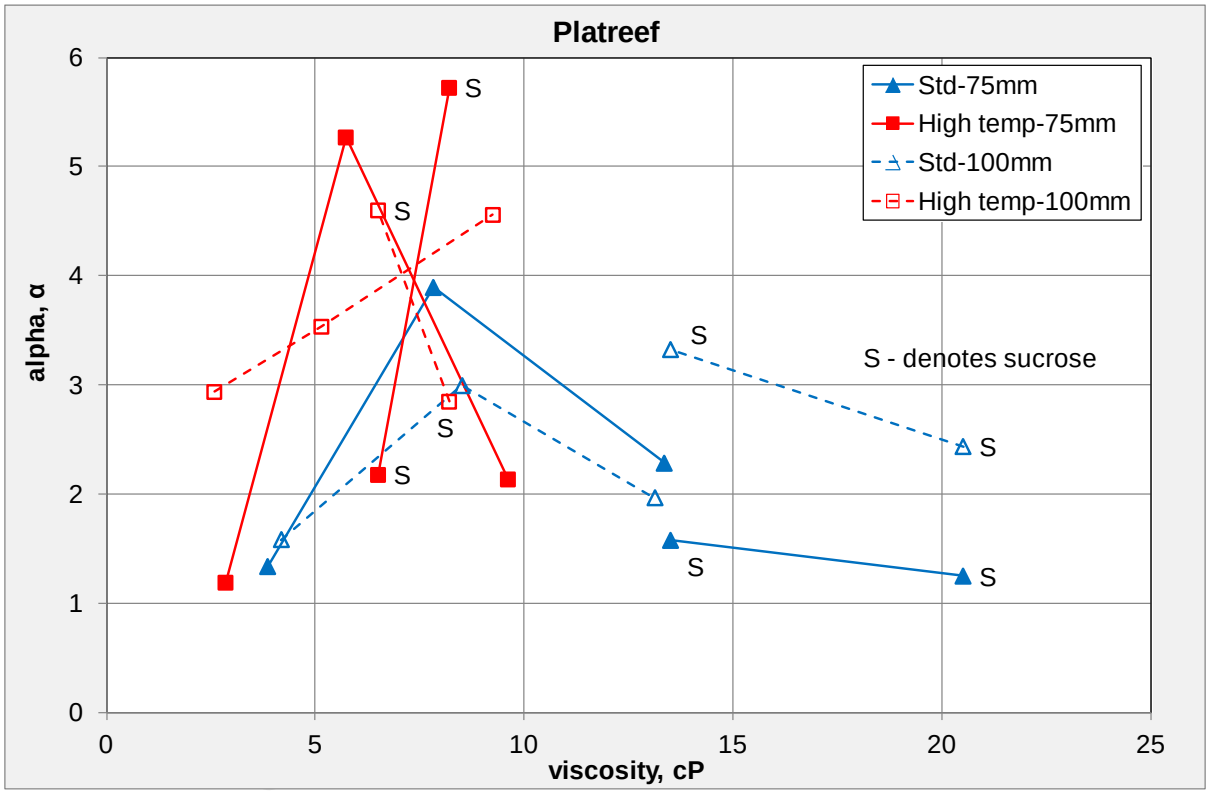

Figure 6-8. Effect of viscosity on sharpness of separation – 75 mm and 100 mm cyclone, Platreef. 'S' denotes sucrose addition at 30%,50%.

Figure 6-8 shows that values of α ranged from 1 to 5, for a range of viscosities. There did appear to be a low sharpness of separation when running at the lowest viscosity, again indicating that there might be an optimum viscosity at which to run the cyclone. An optimum value for alpha was obtained for the tests corresponding to 50% solids by weight. The standard tests at highest feed solids concentration resulted in reduced values of alpha.

The addition of sucrose resulted in decreased values of alpha, particularly for the 75 mm diameter cyclone where low alpha values of between 1 and 2 were obtained. The further addition of sucrose did not seem to have a large effect on alpha.

An increase in slurry temperature consistently improved the value of alpha for the tests corresponding to 50% solids for both cyclone diameters, as the carrier fluid viscosity was reduced. The increased temperature had no effect for the tests at highest concentration for the 75 mm cyclone, but the high temperature test on the 100 mm diameter cyclone increased the value of alpha at the reduced viscosity. The modification of temperature for the sucrose addition tests improved the values of alpha at both levels of sucrose addition for both cyclone diameters. The highest value of alpha was obtained for the highest sucrose addition test at reduced carrier fluid viscosity due to increased temperature.

Figure 6-9 shows the effect of viscosity on the alpha efficiency curve parameter for copper ore on the 75 mm and 100 mm diameter cyclones.

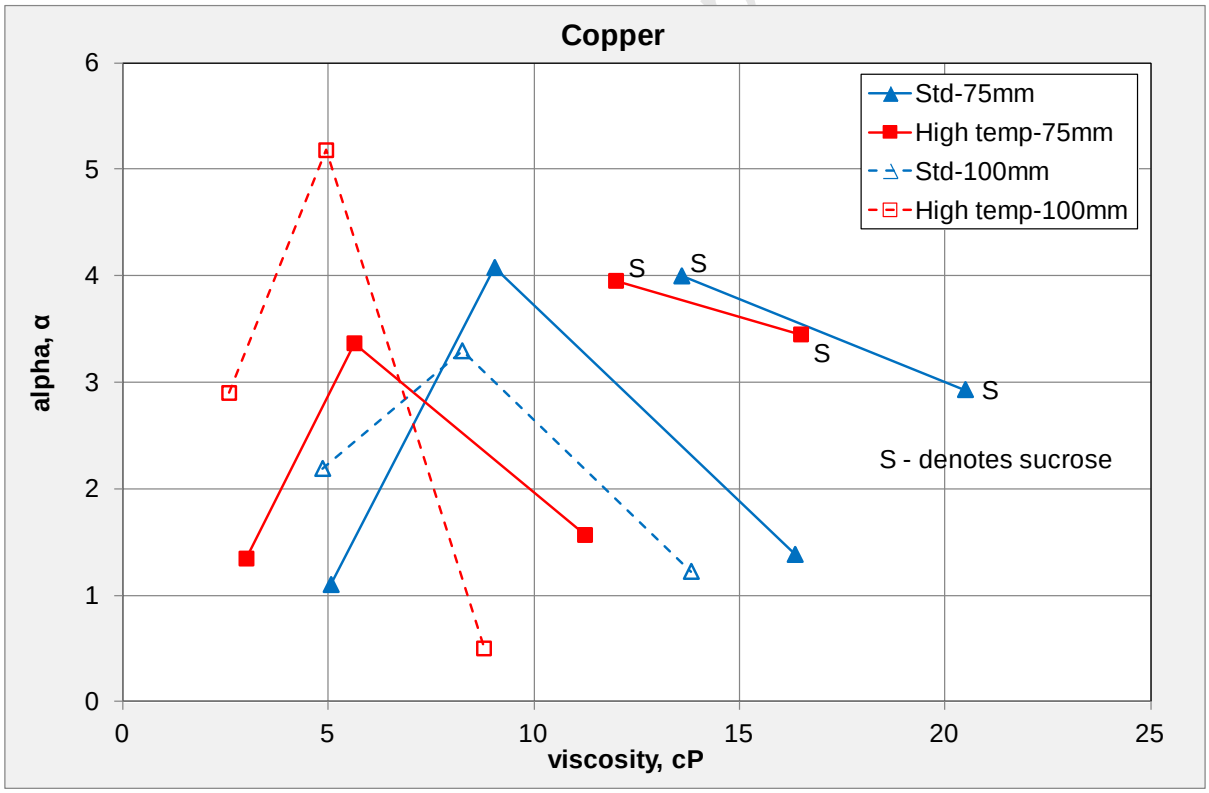

Figure 6-9. Effect of viscosity on sharpness of separation – 75 mm and 100 mm cyclone, copper. 'S' denotes sucrose addition at 30%,50%.

The chart for copper shows an optimum value for alpha at the 50% solids condition for both cyclone diameters. Above and below 7 cP there seemed to be a drop in the sharpness of

separation for the standard tests. This value is reduced for the tests at high temperature to about 5 cP. The tests at highest solids concentration resulted in reduced values of alpha for all test conditions.

The effects of sucrose addition to the copper pulp did not seem to be detrimental in terms of alpha, with the values obtained similar to those obtained for the standard tests. Alpha values of close to 3 were obtained even at the highest viscosities of above 20 cP.

The increase in slurry temperature did not have a large effect on alpha for the 75 mm diameter cyclone, but an improved value of alpha was obtained for tests on the 100 mm cyclone with the exception of the test at highest concentration.

The effect of viscosity on alpha for the copper ore tests performed on the 165 mm diameter cyclone is shown in Figure 6-10.

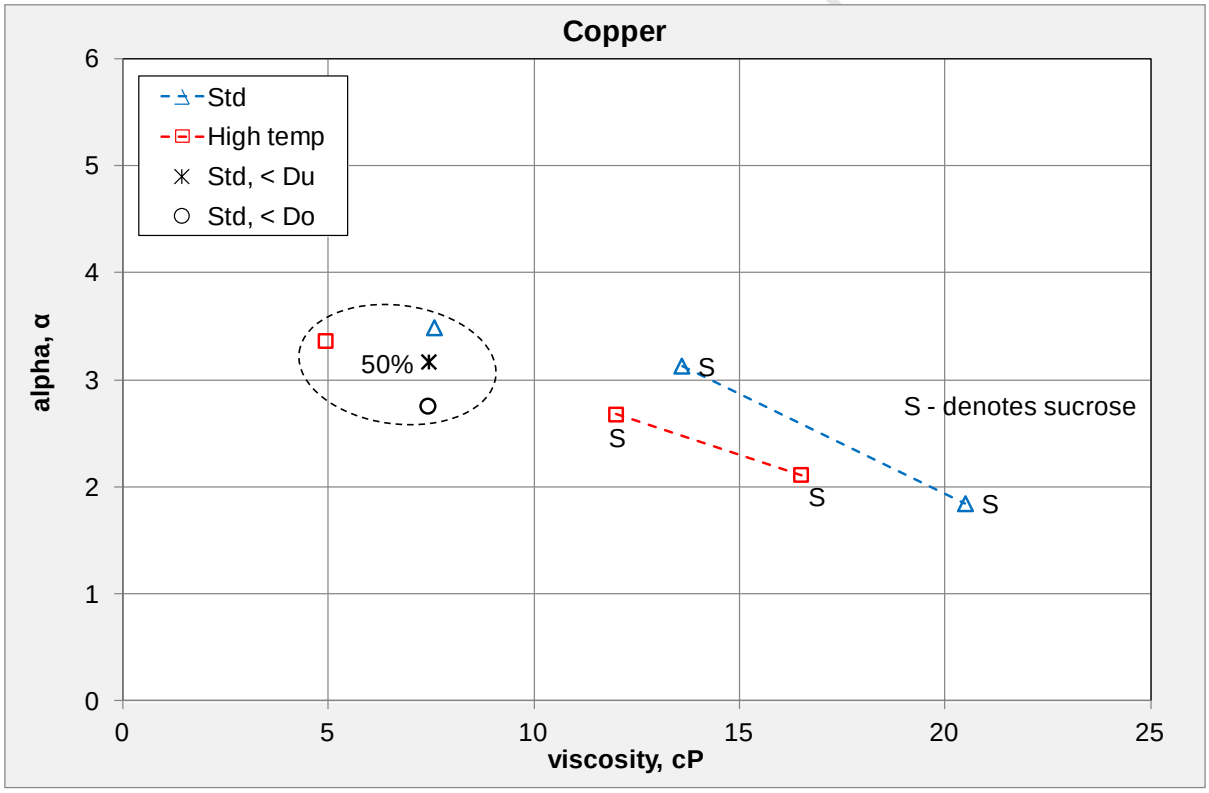

Figure 6-10. Effect of viscosity on sharpness of separation – 165 mm cyclone, copper. 'S' denotes sucrose addition at 30%,50%.

Figure 6-10 shows a consistent decrease in alpha with an increase in slurry viscosity. The increase in viscosity due to sucrose addition was detrimental to the slope of the efficiency curve, particularly at viscosities of above 20 cP.

Reduced carrier fluid viscosity due to increased pulp temperature resulted in an increased value of alpha for the test at highest sucrose addition.

The reduction in both spigot (<Du) and vortex finder (<Do) diameter resulted in slightly reduced values for alpha compared to the standard test condition. The effect is not nearly as significant compared to when the pulp viscosity is increased.

Overall the alpha value is sometimes a difficult parameter to obtain, either from a model fit perspective or directly from the partition curve, as these curves sometimes exhibit unusual characteristics. Different values of alpha may also be obtained for minerals of different density, (Weedon *et al.*, 1990). It is important to obtain a reliable measure of alpha to determine its true potential in identifying the efficiency of classification of the hydrocyclone.

Previous research on the subject of the effects of viscosity on alpha has mostly shown the effect to be negligible – (Kawatra et al., 1996), (Tavares et al., 2002). Others have found a decrease in alpha at an increased viscosity, (Yopps et al., 1987) and (Castro, 1990).

6.4 Effect of feed Pressure

After performing experiments involving altered viscosity conditions, additional tests were conducted at a lower feed pressure. These tests were performed at ambient pulp temperatures and no heating of slurry was involved. The aim was to identify if the reduction in feed flow rate would affect the efficiency due to reduced centrifugal forces inside the cyclone. Figure 6-11 shows the low pressure trends for Platreef ore in terms of corrected cut-size for the 75 mm and 100 mm diameter cyclones.

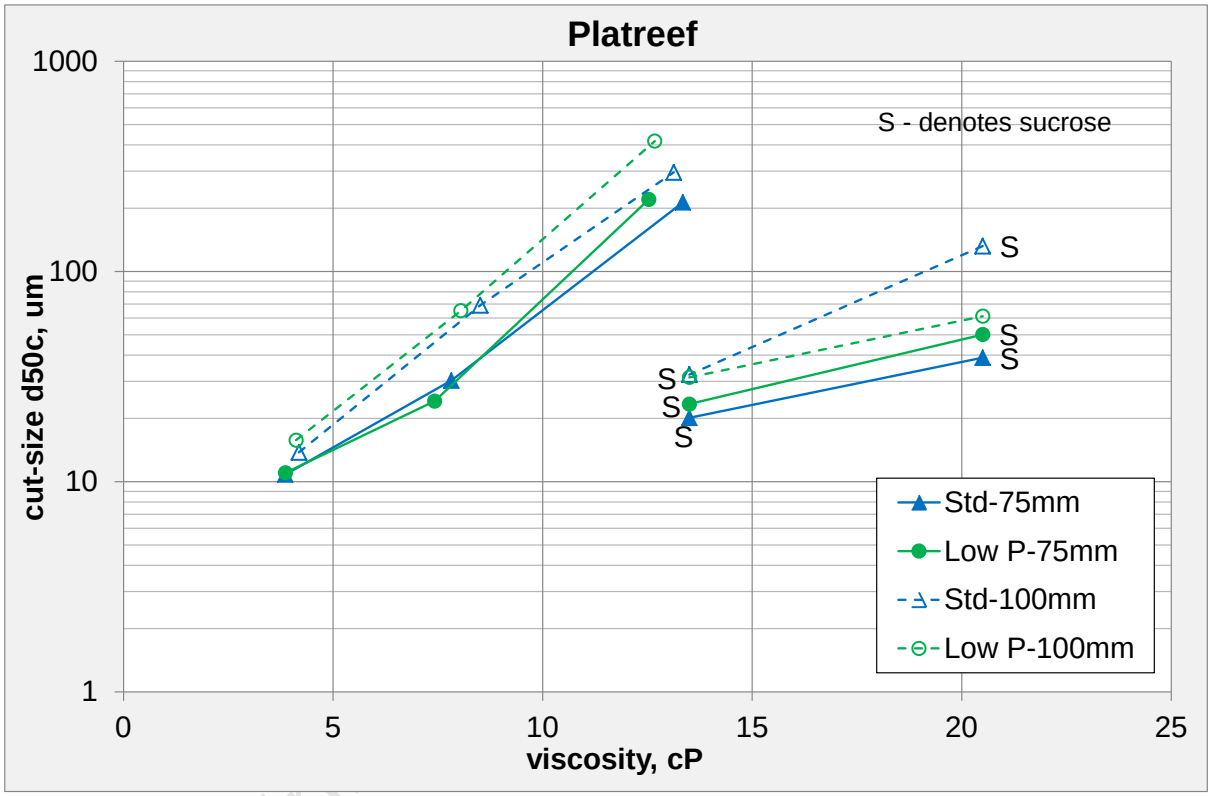

Figure 6-11. Effect of feed pressure on corrected cut-size for Platreef ore.

Figure 6-11 shows slight differences in d_{50c} when the tests were run at lower pressures. The cut-size increased for the maximum feed concentration condition for Platreef in both diameter cyclones. Tests at maximum sucrose addition for Platreef on a 100 mm cyclone showed a decreased cut-size with a decrease in feed pressure.

Figure 6-12 shows the low pressure trends for copper ore in terms of corrected cut-size for the 75 mm, 100 mm and 165 mm diameter cyclones.

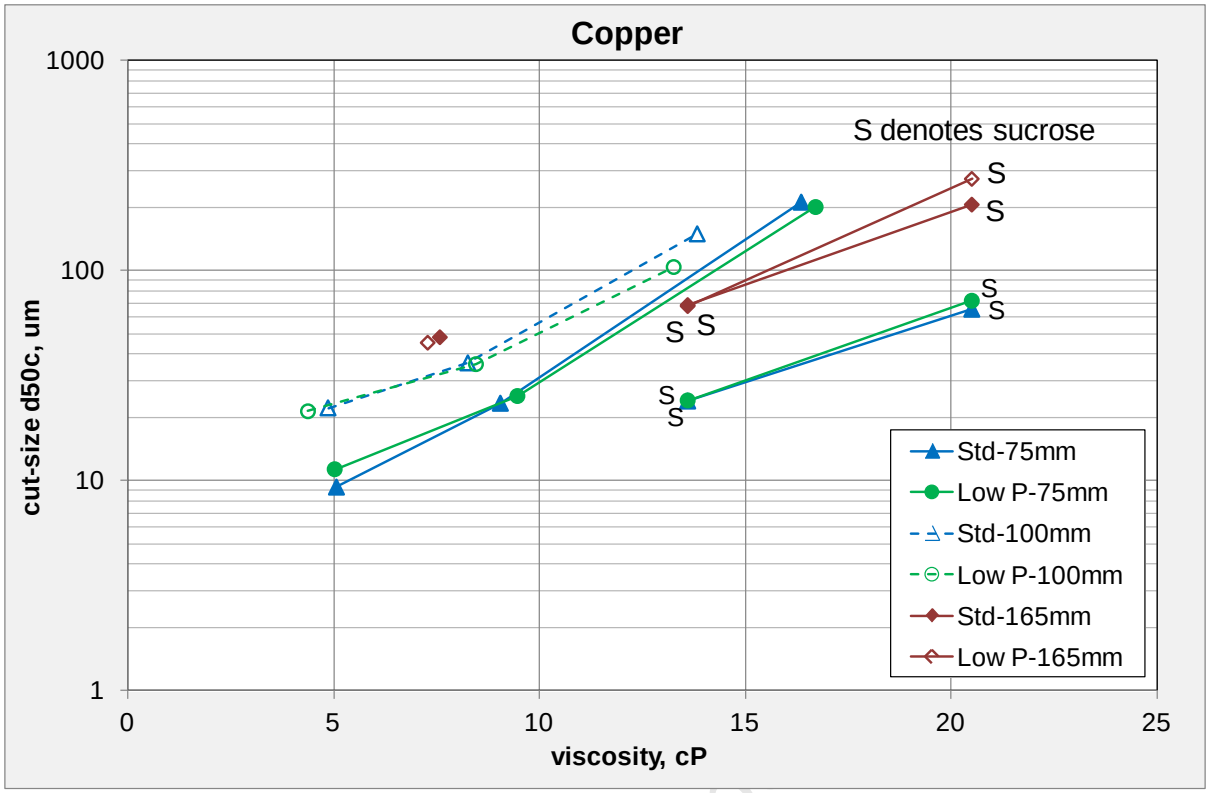

Figure 6-12. Effect of feed pressure on corrected cut-size for copper ore.

Tests using copper ore in Figure 6-12 showed a slight increase in cut-size under all conditions. The decreased pressure (and hence decreased flow rate) results in reduced centrifugal forces and therefore reduced tangential velocities. The reduced velocities affect the separation of coarser particles and a greater number of these report to the O/F.

Figure 6-13 shows the low pressure trends for Platreef ore in terms of the water split to O/F for the 75 mm and 100 mm diameter cyclones.

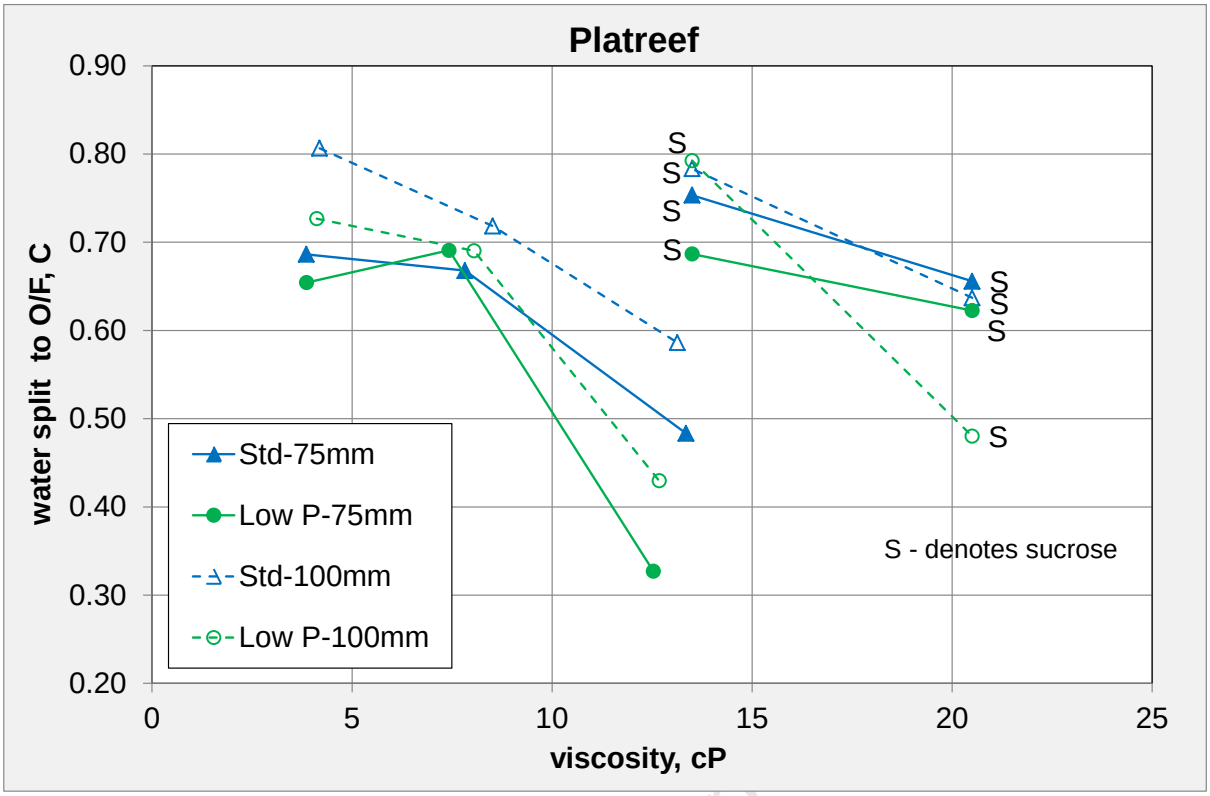

Figure 6-13. Effect of feed pressure on water split to O/F for Platreef ore.

The effect of reduced feed pressure on water split to O/F (Figure 6-13) shows that lower pressures resulted in decreased water split values for Platreef ore on the 75 mm and 100 mm cyclones. The low pressure tests at maximum solids concentration resulted in the lowest recovery of water to the O/F.

Figure 6-14 shows the low pressure trends for copper ore in terms of the water split to O/F for the 75 mm, 100 mm and 165 mm diameter cyclones.

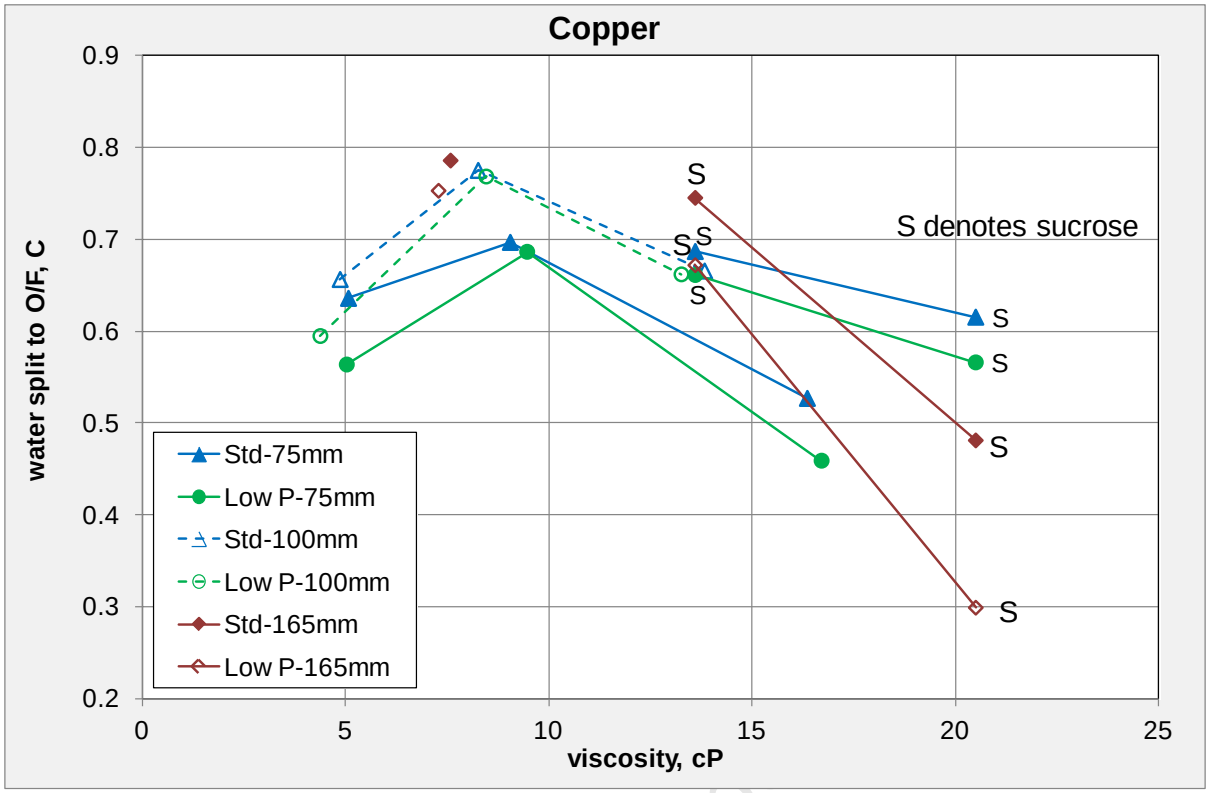

Figure 6-14. Effect of feed pressure on water split to O/F for copper ore.

Figure 6-14 shows that lower pressures resulted in decreased water split values for all cyclone sizes. The tests using copper ore with sucrose addition on the 165 mm cyclone resulted in significantly reduced water recovery to the O/F (as low as 30% for highest sucrose addition). In this case, the internal forces become diminished to such an extent that there is not sufficient flow of liquid in an upward direction, particularly at the largest viscosity when the pulp is simply too viscous. This is an indication of the importance of an appropriate feed pressure to generate the vortices required for particle/fluid separation, (Bradley, 1965).

Figure 6-15 shows the low pressure trends for Platreef ore in terms of alpha values for the 75 mm and 100 mm diameter cyclones.

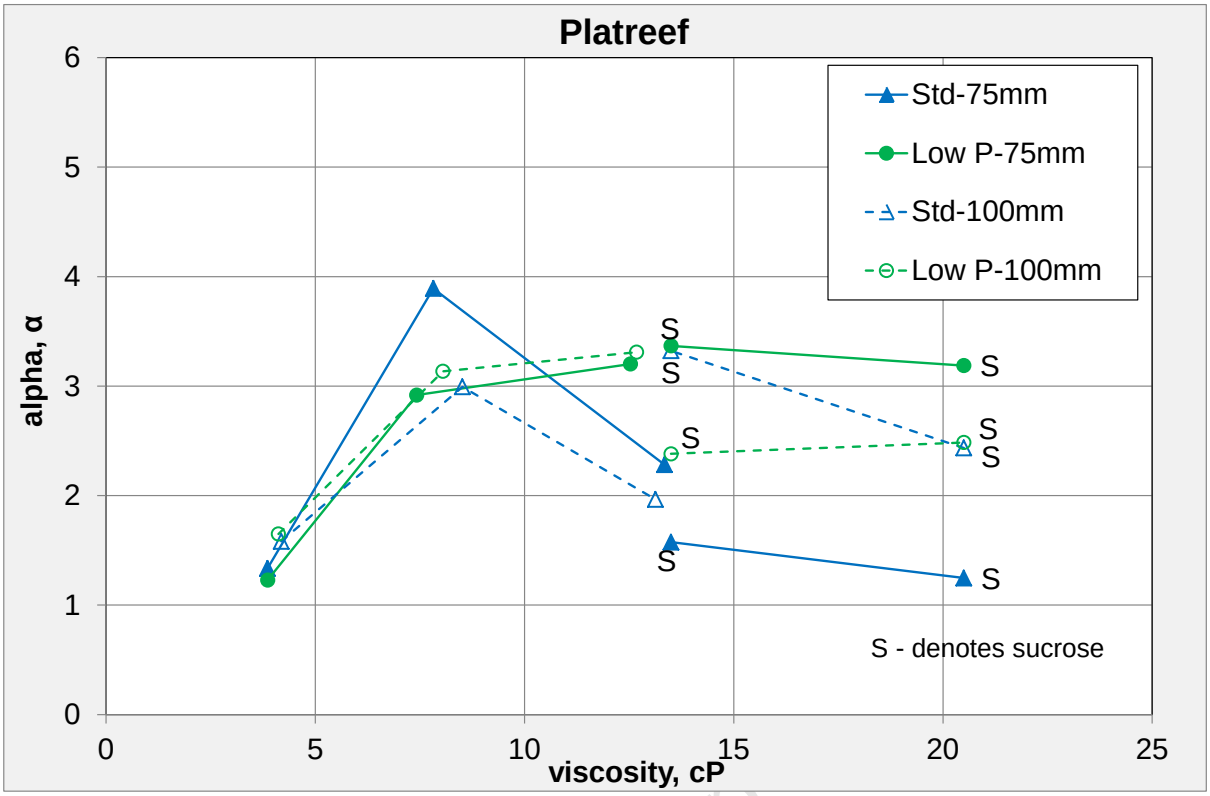

Figure 6-15. Effect of feed pressure on alpha for Platreef ore.

No clear trends were evident from Figure 6-15 in terms of the reduced feed pressure. The peak in the alpha can be seen at the conditions corresponding to tests at 50% solids, even at the reduced pressures.

Figure 6-16 shows the low pressure trends for copper ore in terms of alpha values for the 75 mm, 100 mm and 165 mm diameter cyclones.

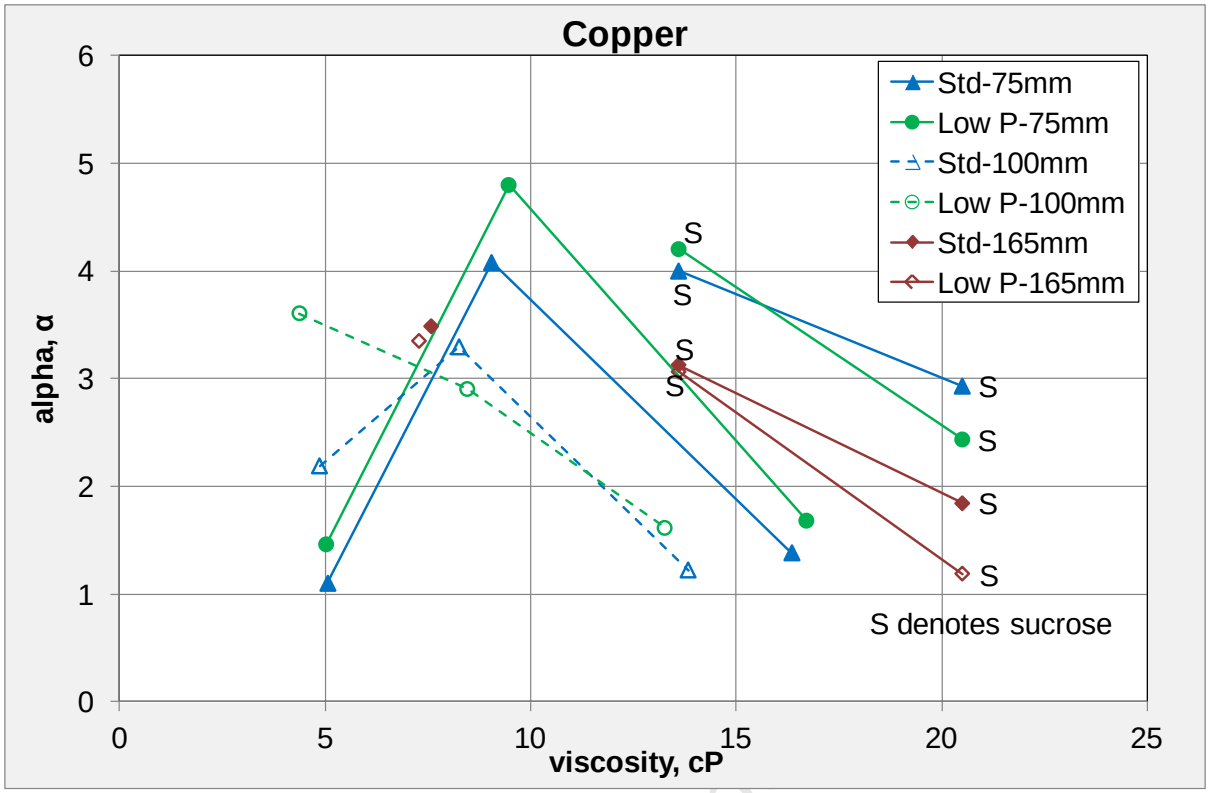

Figure 6-16. Effect of feed pressure on alpha for copper ore.

The tests performed at maximum sucrose addition for the copper ore tests showed a decrease in alpha at the reduced pressure conditions.

The fact that the reduced feed pressure and flow rate did not have a major difference on the cut-size and alpha parameters when viscosity is considered could be due to the suspensions Bingham plastic nature of flow, and are therefore not affected by shear rate (certainly above shear rates of 200/s). True pseudoplastic slurries are expected to exhibit increased viscosity at reduced shear rates, resulting in decreased cyclone performance, (Upadrashta *et al.*, 1987).

The effect of a reduced feed pressure on hydrocyclone operation has been established, (Napier-Munn *et al.*, 1996), (Wills & Napier-Munn, 2006). The effect of a reduced feed pressure for tests involving Newtonian or Bingham plastic suspensions appears to conform to the same result in that a reduced feed pressure results in reduced separation. The effect is related to the flow patterns and not related to the viscosity of the fluid.

6.5 Reduced efficiency curves

It has been well documented by Lynch & Rao (1975b), Nageswararao (1978), that reduced efficiency curves are insensitive to cyclone size, feed size distribution and cyclone cone angle. There has not been much mention of the effect of ore type or viscosity on these normalised curves. The reduced efficiency curves were plotted for all 65 cyclone tests (APPENDIX G). The curves were found to be fairly consistent in their appearance; however deviations from the general shape of the curve are noticeable.

The effects of ore type and slurry viscosity on the reduced efficiency curve are plotted in Figure 6-17 and Figure 6-18 respectively. Comparisons for ore type are made at a constant solids content of 50%.

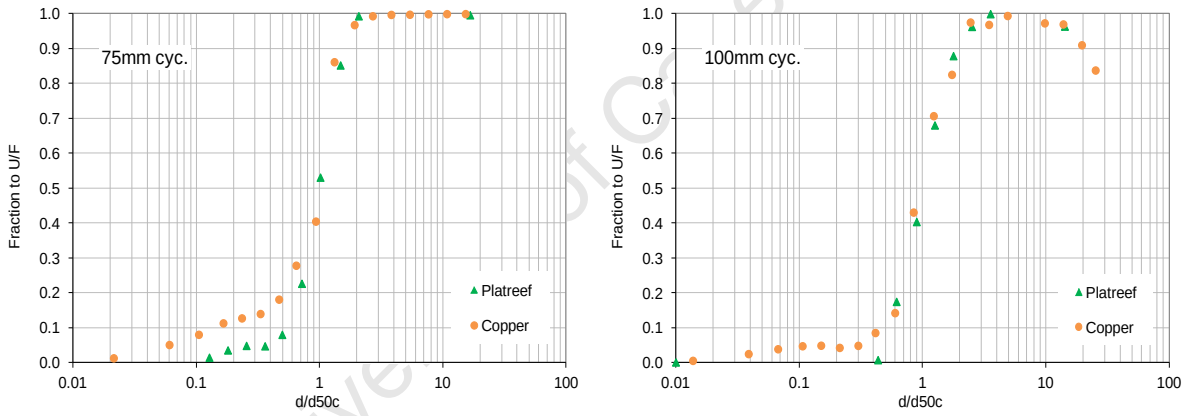

Figure 6-17. Effect of ore type on the reduced efficiency curve.

Figure 6-17 shows that the different ore types possess similar curve shapes, the only deviation being at the lower end of the x-axis where the curve for copper indicates a higher fraction reporting to the U/F than for the Platreef, for both cyclone diameters. The slope (or α) could be considered the same.

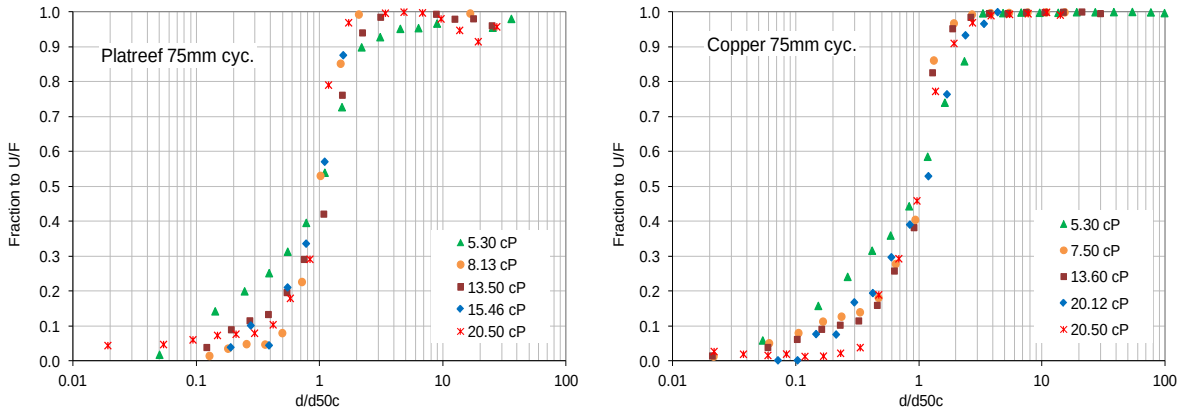

Figure 6-18. Effect of viscosity on reduced efficiency curve.

The modified viscosity of both ore types shown in Figure 6-18 did not appear to have a major influence on the reduced efficiency curves. A deviation from the general shape can be seen for the lowest viscosity conditions of 5 cP for both ore types, which corresponded to the tests conducted at the lowest feed solids concentration of 30%.

The effect of viscosity on alpha is shown to be inconsistent, possibly due to the difficulty of obtaining a meaningful value for alpha under different rheological conditions. An accurate measure of the sharpness of separation of the partition curve is still an important parameter for hydrocyclone modelling purposes and work will continue in this area.

6.6 Discussion of key questions

From the results of the testwork conducted, the key questions in Section 3.2 will now be addressed -

- *How would a change in feed viscosity affect the sharpness of separation (α), water split to O/F (C) and the corrected cut-size (d_{50c})?*

An increase in viscosity of the feed was found to increase the cut-size, decrease the water split to O/F, yet there was no clear effect on the alpha parameter.

- *Could a meaningful viscosity value be extracted for each rheological condition?*

Viscosity values were determined for each pulp rheological condition - changes in solids concentration, sucrose addition and temperature modification.

- *Castro (1990), made the observation that if a chart of apparent viscosity versus shear rate is drawn, different curves will be obtained for each condition, eg. % solids. These curves need to be compared between a specific range of shear rates and it should be determined if this is possible?*

The Platreef and copper ores that were used in the study exhibited Bingham Plastic behaviour. The determination of an accurate yield stress was not possible with the tube rheometer equipment due to settling conditions. In excluding the data below a certain shear rate (200/s) the rheological behaviour was effectively a straight line and the apparent viscosities would not change with increase in shear rate. The comparison of different apparent viscosity versus shear rate curves is therefore only necessary when non-Newtonian (pseudoplastic, dilatants) behaviour is observed.

- *Would the efficiency curve be affected by certain viscosity altering factors more than others?*

The addition of 50% sucrose to the feed slurry had the greatest effect on the hydrocyclone efficiency. This corresponded to the highest viscosity values. Temperature modification was shown to be influential during the cyclone tests. An average increase in slurry temperature of approximately 20-25 degrees Celsius counteracted the negative effects of the sucrose addition for the majority of the test work. However, the data tend to suggest that there is an optimum temperature at which to run the cyclone (about 50 degrees Celsius), and a further increase above this value had a negative influence on the centrifugal pump performance.

- *Will a change in feed viscosity cause any appearance of the fish-hook effect?*

Abnormalities in the efficiency curves due to an increase in the slurry viscosity were found in certain cases. These were not consistent with fish-hook appearance and appeared at coarser size ranges than one would expect for the fish-hook phenomenon. This indicates that a fish hook phenomenon was not observed. In this work a viscosity increase did not result in the fish-hook appearance as both fine and coarse size ranges were affected by the change in rheological properties of the slurry.

- *Will the larger cyclone sizes be more affected when investigating viscosity effects, and can this be attributed to the decrease in centrifugal forces due to increased body diameter.*

The performance of the larger (100 mm, 165 mm) cyclone diameters appeared to be more affected by an increase in pulp viscosity, especially when one considers the cut-size. Since the rheological behaviour of the ores was Bingham at higher rates of shear, one cannot state that the increased shear rates in the smaller cyclones were the reason for the improved performance as this would only be viable when pseudoplastic material is treated. However it is believed that the decreased tangential velocities in the larger cyclones would contribute to the decrease in efficiency for more viscous suspensions, as the flow patterns and vortices become affected. This would need validation on cyclone sizes as large as 1 meter in diameter. The increased fluid viscosity compounds the effect as coarser particles are less likely to travel as easily to the wall, and fine particles are less likely to migrate to the inner vortex without hindrance, (Svarovsky, 1984).

7. CONCLUSIONS & RECOMMENDATIONS

This chapter presents the outcomes of the thesis with regard to the influence of rheology on hydrocyclone performance. A summary of key findings and conclusions are provided before recommendations for future work on the subject are proposed.

A range of hydrocyclone experiments were performed on 75, 100 and 165 mm cyclones, using a Platreef ore and a copper ore sourced from mineral processing operations. An on-line tube rheometer was used to characterize the rheology of slurry for each test condition. The viscosity of the slurry was modified in three ways – varying the feed solids content, addition of sucrose, and changing the slurry temperature. The rheological characterisations were then combined with the hydrocyclone data to obtain relationships between feed slurry viscosity and the efficiency curve parameters.

7.1 Summary of findings

7.1.1 Rheology testwork

- The rheometer used in the thesis (MPV) was found to adequately characterise the viscosity of real slurries at concentrations up to 70% by mass, however accurate measurement of dense phase (settling) slurries is only possible above a shear rate of 150-200/s. A suitable turbulence correction procedure should also be applied. Successful calibration was performed on a standard Newtonian fluid (sucrose solution) and non-Newtonian fluid (kaolin suspension).
- The characterisation of yield stress for dense phase slurries is not possible using the MPV device, unless an extrapolation is performed. This extrapolation is to be practised with caution as non-Newtonian suspensions often exhibit nonlinear behaviour at low shear rate ranges. However it is regarded as a useful tool for studying rheology for ‘real’ ore types in terms of their apparent viscosities under medium to high shear rate conditions, such as those existing in hydrocyclones.
- Both the Platreef and copper ore used for testwork in this thesis exhibited Bingham plastic behaviour above shear rates of 200/s. The yield stress was not characterised but was not required in this work as the cyclone feed flow was above the minimum shear rate required.

7.1.2 Rheological influence on hydrocyclone performance

- The effect of increased viscosity due to increased solids concentration from 30% to 50% resulted in an increase in cut-size, increased water split fraction to O/F for the copper ore but decreased fraction for Platreef, and an increased alpha value for all cyclone diameters tested. Tests at concentrations as high as 70% solids resulted in significantly decreased performance - for example for the 75 mm cyclone running with Platreef slurry at a viscosity of 13 cP (corresponding to 70 % solids by mass) the d_{50c}, C and alpha values were 213 µm, 0.48 and 2.28 respectively. This is compared to tests at 7.8 cP (corresponding to 50% solids by mass) having values of d_{50c}, C and alpha of 30 µm, 0.67 and 3.9 respectively.
- Tests at the highest feed solids concentration of at least 70% resulted in the poorest cyclone operation. The fact that these tests were not at the highest viscosity conditions on occasion is evidence that viscosity was not the only contributing factor. Separation is hindered by the physical conditions of the pulp in the cyclone, particularly near the apex. Despite the absence of roping (close to roping conditions were observed but true roping was avoided), the cyclone effectively becomes a t-piece under these conditions. Operation at feed densities this high should be avoided unless deemed necessary for some reason other than classification.
- Increased carrier fluid viscosity due to sucrose addition resulted in decreased cyclone performance, although only at the highest levels of sucrose addition (50%). The effects were an increase in cut-size and reduced water split to O/F. Values for d_{50c}, C and alpha for Platreef ore in the 100 mm cyclone at the highest viscosity of 20.5 cP (50% solids and 50% sucrose addition) were 132 µm, 0.64 and 2.43 respectively. This is compared to tests at 8.5 cP (corresponding to 50% solids by mass) having values of d_{50c}, C and alpha of 69 µm, 0.72 and 2.99 respectively.
- Decreased carrier fluid viscosity by an increase in the slurry temperature counteracted the effect of increased viscosity due to sucrose addition. The decreased viscosities decreased cut-sizes and increased the amount of water reporting to the O/F stream. Cut-size values for Platreef ore in the 100 mm cyclone at the highest viscosity of 20.5 cP (50% solids and 50% sucrose addition) were reduced from 132 um to 49 µm by an increase in temperature of 20 degrees Celcius. The increased temperature reduced the pulp viscosity value to 8.2 cP at the same condition. Likewise the water split to O/F

fraction was improved from 0.64 to 0.79 and the value of alpha improved from 2.43 to 2.84, for the same temperature change. The high solids concentration conditions did not benefit from increased slurry temperature.

- Decreased values of alpha with increased slurry viscosities were obtained for tests on the largest cyclone diameter. The difficulty in obtaining an accurate single value of alpha when the partition curve exhibits unusual properties is likely to contribute to inconclusive results in some cases.
- Evidence exists that there may be an optimum viscosity to run a hydrocyclone for improved water split to O/F. In this work this was found to be between 5 cP and 8 cP where values for C of 0.77 to 0.81 were obtained. Optimal cut-sizes were achieved at the lowest viscosities.
- The two ore types under investigation did not show marked differences in their behaviour in terms of the effect on partition curve parameters.

7.2 Conclusions

In addressing the hypotheses, the following conclusions were drawn from the thesis:

1. At a constant feed solids concentration, an increase in pulp viscosity achieved by high levels of sucrose addition results in decreased hydrocyclone performance, attributed to an increased cut-size, reduced water split to O/F and reduced alpha value.
2. At a constant feed solids concentration, a decrease in pulp viscosity attained by increased slurry temperatures results in improved hydrocyclone performance, attributed to a decreased cut-size, increased water split to O/F and increased alpha value. Increasing the pulp temperature counteracts the effects of sucrose addition.
3. An increased feed solids concentration causes an increase in pulp viscosity, but has dissimilar effects for the three properties of the partition curve used for quantifying hydrocyclone performance. An optimum point is reached for the water split to O/F and alpha values, however cut-sizes are lowest for the lowest feed concentration and viscosity.
4. Although testwork in this thesis was limited to small hydrocyclone body diameters, rheological effects on cyclone performance became more pronounced as this diameter increased from 75 mm to 165 mm. This can be attributed to the decrease in tangential velocities in the cyclone in the case of pseudoplastic and plastic fluids. In the case of

dilatant fluids operating a larger cyclone diameter could prove beneficial to the process.

The data arising from this thesis will prove useful in the continuing research efforts focussed on the development of more accurate hydrocyclone models, particularly those focussed on the inclusion of viscosity.

7.3 Recommendations

The following is recommended for the advancement of the subject of rheology in hydrocyclones:

- It is recommended that further tests are conducted on 'real' ore types varying the amount of fine (minus 38 micron) material present to assess the effect of particle size which was not looked at in this work.
- Ore types containing a high proportion of clay-like material should be included in future cyclone testwork. This will enable one to predict or determine the influence of variability in ore type as more clay-like material is processed. This in combination with the rheology of the ore will be a valuable source of information for future concentrator operations.
- Hydrocyclone testwork under variable rheological conditions should be performed on cyclone diameters larger than 165 mm (ideally up to 1000 mm in diameter), to identify any issues that may arise on concentrator operations with large cyclones.
- The effect of variability of ore particle shape on rheology and the resultant influence on the behaviour of the hydrocyclone should be investigated further, to quantify an additional ore parameter that could have an influence on certain classification circuits.

All data arising from the above suggestions will be useful in validating the new semi mechanistic hydrocyclone models that are currently being developed.

8. REFERENCES

Agar, G. E. and Herbst, J. A. (1966). "The effect of fluid viscosity on cyclone classification." Trans. Society of Mining Engineers of AIME **235**: 145-149.

Akroyd, T. J. and Nguyen, Q. D. (2003). "Continuous on-line rheological measurements for rapid settling slurries." Minerals Engineering **16**: 731-738.

Asomah, A. K. and Napier-Munn, T. J. (1997). "An empirical model of hydrocyclones, incorporating angle of cyclone inclination." Minerals Engineering **10**(3): 339-347.

Asomah, I. (1996). Improved Models of Hydrocyclones. Department of Mining and Metallurgical Engineering. JKMRC, University Of Queensland. **PhD**.

Bloor, M. I. G. and Ingham, D. B. (1975). "Turbulent Spin in a Cyclone." Trans. Instn. Chem. Engrs. **53**: 1-6.

Bloor, M. I. G., Ingham, D. B. and Laverack, S. D. (1980). An analysis of boundary layer effects in a hydrocyclone. Int. Proc. Int. Conf. on Hydrocyclones, Cambridge.

Boger, D. V. (2009). "Rheology and the resource industries." Chemical Engineering Science **64**: 4525-4536.

Bradley, D. (1965). The Hydrocyclone, Pergamon Press.

Bradley, D. and Pulling, D. J. (1959). "Flow Patterns in the Hydraulic Cyclone and their Interpretation in Terms of Performance." Trans. Instn. Chem. Engrs. **37**: 34-45.

Braun, T. and Bohnet, M. (1990). "Influence of feed solids concentration on the performance of hydrocyclones." Chemical Engineering Technology **13**: 15-20.

Brennan, M. S., Narasimha, M. and Holtham, P. N. (2007). "Multiphase modelling of hydrocyclones – prediction of cut-size " Minerals Engineering **20**(4): 395-406.

Brown, N. P. and Heywood, N. I. (1991). Slurry Handling: Design of solid-liquid systems, Elsevier Applied Science.

Castro, O. (1990). An investigation of pulp rheology effects and their application to the dimensionless type hydrocyclone models. JKMRC. **MSc**.

Chan, C. W., Seville, J. P. K., Fan, X. and Baeyens, J. (2009). "Particle Motion in CFB Cyclones as Observed By Positron Emission Particle Tracking." Ind. Eng. Chem. Res. **48**: 253-261.

Chang, Y. F., Ilea, C. G., Aasen, O. L. and Hoffman, A. C. (2011). "Particle flow in a hydrocyclone investigated by positron emission particle tracking." Chemical Engineering Science **66**: 4203-4211.

Cheng, D. C.-H. (1980). "Viscosity concentration equations and flow curves for suspensions." Chemistry and Industry **17**: 403-406.

Chryss, A. and Pullum, L. (2007). A new viscometric technique to successfully measure shear thickening behaviour, if and when it occurs. Hydrotransport 17. The 17th Int. Conf. on the Hydraulic Transport of Solids, SAIMM & BHR Group.

Clarke, B. (1967). "Rheology of coarse settling suspensions." Trans. Instn. Chem. Engrs. **45**: T251-T256.

Criner, H. E. (1950). The Vortex Thickener. International conference on Coal Preparation, Paris.

Dahlstrom, D. A. (1954). "Fundamentals and applications of the liquid cyclone." Chemical Engineering Progress Symposium Series **50**(15): 41-61.

Delgadillo, J. A. and Rajamani, R. K. (2007). "Exploration of hydrocyclone designs using computational fluid dynamics." Int. J. Miner. Process. **84**: 252-261.

Driessen, M. G. (1951). "Review of Industrial Mining." Special Issue **4**: 449-461.

Durand, R. (1953). Proceedings of the Minnesota International Hydraulics Convention.

Fahlstrom, P. H. (1963). Studies of the hydrocyclone as a classifier. 6th Int. Min. Proc. Congress, Cannes.

Fester, V. (2009). Final Report - Rheology of Platreef A sample, Cape Peninsula University of Technology - Flow Process Research Centre.

Finch, J. A. (1983). "Modelling a Fish-hook in Hydrocyclone Selectivity Curves." Powder Technology **36**.

Flintoff, B. C., Plitt, L. R. and Turak, A. A. (1987). "Cyclone Modelling: A Review of Present Technology." CIM Bulletin: 39-50.

Fontein, F. J., Van Kooy, J. G. and Leniger, H. A. (1962). "The influence of some variables upon hydrocyclone performance." British Chemical Engineering **7**(6): 410-421.

Franks, G. V., Yates, P. D., Lambert, N. W. A. and Jameson, G. J. (2005). "Aggregate size and density after shearing, implications for dewatering fine tailings with hydrocyclones." International Journal of Mineral Processing **77**(1): 46-52.

Gaunt, G. N. (1983). "Effect of high particle concentration on the boundary layer flow in a hydrocyclone." Chem. Eng. Research and Design **61**: 271-281.

Govier, G. W. and Aziz, K. (1972). The flow of complex mixtures in pipes, Robert E. Krieger Publishing.

He, Y. B., Laskowski, J. S. and Klein, B. (2001). "Particle movement in non-Newtonian slurries: the effect of yield stress on dense medium separation." Chemical Engineering Science **56**: 2991-2998.

Holland-Batt, A. B. (1980). "A bulk model for separation in hydrocyclones." Trans. Instn Min. Metall. (Sect. C: Mineral Process Extr. Metall.) **91**.

Horsley, R. R. and Allen, D. W. (1987). The effect of yield stress on hydrocyclone performance in the mining industry. 3rd International Conference on Hydrocyclones, Oxford, England.

Hudson, D. R. (1949). "Density and packing in an aggregate of mixed spheres." Journal of Applied Physics **20**: 154-162.

Jinescu, V. V. (1974). "The rheology of suspensions." International Chemical Engineering **14**(3): 397-420.

Kawatra, S. K. and Bakshi, A. K. (1996). "On-line measurement of viscosity and determination of flow types for mineral suspensions." Int. J. Miner. Process. **47**: 275-283.

Kawatra, S. K., Bakshi, A. K. and Eisele, T. C. (1999). "An on-line pressure vessel rheometer for slurries." Powder Technology **105**: 418-423.

Kawatra, S. K., Bakshi, A. K. and Rusesky, M. T. (1996). "The effect of slurry viscosity on hydrocyclone classification." International Journal of Mineral Processing **48**: 39-50.

Kawatra, S. K. and Eisele, T. C. (1988). "Rheological effects in grinding circuits." International Journal of Mineral Processing **22**(1-4): 251-259.

Kawatra, S. K., Eisele, T. C., Zhang, D. and Rusesky, M. (1988). "Effects of temperature on hydrocyclone efficiency." International Journal of Mineral Processing **23**(3-4): 205-211.

Kelly, E. G. and Spottiswood, D. J. (1982). Introduction to Mineral Processing, John Willey & Sons.

Kelsall, D. F. (1953). "A further study of the hydraulic cyclone." Chemical Engineering Science **2**: 254-273.

Kelsall, D. F. (1952). "A study of the motion of solid particles in a hydraulic cyclone." Trans IChemE. **30**: 87-108.

Klimpel, R. R. (1981). "The Influence of a chemical dispersant on the sizing performance of a 24-in. Hydrocyclone." Powder Technology **31**(2): 255-262.

Kraipech, W., Chen, W., Parma, F. J. and Dyakowski, T. (2002). "Modelling the fish-hook effect of the flow within hydrocyclones." International Journal of Mineral Processing **66**: 49-65.

Kraipech, W., Nowakowski, A., Dyakowski, T. and Suksangpanomrung, A. (2005). "An investigation of the effect of the particle-fluid and particle-particle interactions on the flow within a hydrocyclone." Chemical Engineering Journal **111**: 189-197.

Lambert, S. (2010). Personal Communication. Cape Town.

LaPlante, A. R. and Finch, J. A. (1984). "The origin of unusual cyclone performance curves." Int. J. Miner. Process. **13**: 1-11.

Laskowski, J. S. (2001). Rheological Measurements in mineral processing related research. IX Balkan Mineral Processing Congress, Beril Ofset, Istanbul, Turkey.

Lilge, E. O., Fregren, T. E. and Purdy, G. R. (1957). "Apparent viscosities of heavy media and the Driessen Cone." Trans IMME. **67**: 229-249.

Lilge, E. O. and Plitt, L. R. (1968). The cone force equation and hydrocyclone design. InterAmerican Conference on Materials Technology, San Antonio.

Loginov, M., Larue, O., Lebovka, N. and Vorobiev, E. (2008). "Fluidity of highly concentrated kaolin suspensions: Influence of particle concentration and presence of dispersant." Colloids and Surfaces A: Physicochemical and Engineering Aspects **325**: 64-71.

Lynch, A. J. and Rao, T. C. (1975a). The development and use of a simulation model for hydrocyclones, JKMRC Report.

Lynch, A. J. and Rao, T. C. (1975b). Modelling and scale-up of hydrocyclone classifiers. IMPC, Cagliari.

Mainza, A. N. (2006). Contribution to the understanding of the three-product cyclone on the classification of a dual density platinum ore. Centre for Minerals Research. Cape Town, University of Cape Town. **PhD**.

Majumder, A. K., Yerriswamy, P. and Barnwal, J. P. (2003). "The fish-hook phenomenon in centrifugal separation of fine particles." Minerals Engineering **16**: 1005-1007.

Malvern. (2009). "10 Ways to control rheology by changing particle properties (Size, Zeta potential and Shape)." Inform - A series of white papers providing advice on material characterisation issues, from www.malvern.co.uk.

McFarlane, A., Bremmell, K. and Addai-Mensah, J. (2006). "Improved dewatering behavior of clay minerals dispersions via interfacial chemistry and particle interactions optimization" Journal of Colloid and Interface Science **293**: 116-127.

Mizrahi, J. and Cohen, E. (1966). "Studies of some factors influencing the action of hydrocyclones." Institute of Mining and Metallurgy: C318-C330.

Mular, A. L. and Jull, N. A. (1980). The selection of cyclone classifiers, pumps and pump boxes for grinding circuits, Krebs Engineers**:** 376-403.

Multotec (2010). Personal Communication.

Nageswararao, K. (2000). "A critical analysis of the fish hook effect in hydrocyclone classifiers." Chemical Engineering Journal **80**: 251-256.

Nageswararao, K. (2001). Flow Split and water split in industrial hydrocyclones. American Filtration and separation society.

Nageswararao, K. (1978). Further developments in the modelling and scale up of industrial Hydrocyclones, University of Queensland. **PhD**.

Napier-Munn, T. J., Morrell, S., Morrison, R. D. and Kojovic, T. (1996). Mineral Comminution Circuits: their operation and optimisation, JKMRC Monograph series, Vol.2.

Narasimha, M., Sripriya, R. and Banerjee, P. K. (2004). "CFD modelling of hydrocyclone—prediction of cut size." Int. J. Miner. Process. **75**: 53-68.

Narasimha, M., Brennan, M.S., Mainza, A., Holtham, P. N., (2010).Towards improved hydrocyclone models - Contributions from computational fluid dynamics. XXV International Mineral Processing Congress, Brisbane, Australia.

Ndlovu, B., Becker, M., Forbes, E., Deglon, D. and Franzidis, J.-P. (2011). "The influence of phyllosilicate mineralogy on the rheology of mineral slurries." Minerals Engineering **24**(12): 1314-1322.

Neesse, T., Gerhart, C. and Bickert, G. (1997). Hydrocyclone separation curves with fishhook. XX IMPC, Aachen, Germany.

Nowakowski, A. F., Cullinan, J. C., Williams, R. A. and Dyakowski, T. (2004). "Application of CFD to modelling of the flow in hydrocyclones. Is this a realizable option or still a research challenge?" Minerals Engineering **17**: 661-669.

Obeng, D. P. (2003). The three-product cyclone – separation performance, potential applications and modelling, JKMRC. **PhD**.

Olhero, S. M. and Ferreira, J. M. F. (2004). "Influence of particle size distribution on rheology and particle packing of silica-based suspensions." Powder Technology **139**: 69-75.

Patil, D. D. and Rao, T. C. (2001). "Studies on the fishhook effect in hydrocyclone classification curves." Minerals & Metallurgical Processing **18**(4): 190-194.

Peronius, N. and Sweeting, T. J. (1985). "On the correlation of minimum porosity with particle size distribution." Powder Technology **42**: 113-121.

Plitt, L. R. (1976). "A mathematical model of the Hydrocyclone Classifier." CIM Bulletin: 114-123.

Reeves, T. J. (1985). "On-line viscometer for mineral slurries." Trans. Instn. Min. Metallurgy: 201-208.

Richardson, J. F. and Zaki, W. N. (1954). "The sedimentation of a suspension of uniform spheres under conditions of viscous flow." Chemical Engineering Science **3**(65).

Rietema, K. (1961). "The Mechanism of the Separation of Finely Dispersed Solids in Cyclones." Cyclones in Industry **4**: 45-63.

Rietema, K. (1960). "Performance and design of hydrocyclones - II." Chemical Engineering Science **15**: 303-309.

Roldan-Villasana, E. J., Williams, R. A. and Dyakowski, T. (1993). "The origin of the fish-hook effect in hydrocyclone separators." Powder Technology **77**: 243-250.

Rutgers, R. (1962). "Relative viscosity and concentration." Rheologica Acta **2**: 305-348.

SAPMA (1991). Pumps - Principles and Practice. South African Pump Manufacturers Association.

Schubert, H. (2003). "On the origin of 'Anomalous' shapes of the separation curve in hydrocyclone separation of fine particles - Above all on the so called fish-hook effect." Aufbereitungs Technik **44**(2): 5-17.

Schubert, H. and Neesse, T. (1980). A Hydrocyclone Separation Model in Consideration of the Turbulent Multi-Phase Flow. Int. Proc. Int. Conf. on Hydrocyclones, Cambridge.

Shi, F. N. and Napier-Munn, T. J. (1996a). "Measuring the rheology of slurries using an on-line viscometer." Int. J. Miner. Process. **47**: 153-176.

Shi, F. N. and Napier-Munn, T. J. (1996b). "A model for slurry rheology." Int. J. Miner. Process. **47**: 103-123.

Shook, C. A., Gillies, R., Haas, D. B., Husband, W. H. W. and Small, M. (1982). "Flow of coarse and fine sand slurries in pipelines." Journal of Pipelines **3**: 13-21.

Suasnabar, D.J., Fletcher, C.A.J., (2003). A CFD model for dense medium cyclones. 3rd International Conference on CFD in the Minerals and Process Industries, CSIRO, Melbourne, Australia.

Svarovsky, L. (1996). A critical review of hydrocyclone models. Hydrocyclones '96, London.

Svarovsky, L. (1984). Hydrocyclones, Technomic Publishing.

Tangsathitkulchai, C. and Austin, L. G. (1988). "Rheology of concentrated slurries of particles of natural size distribution produced by grinding." Powder Technology **56**: 293-299.

Tavares, L. M., Souza, L. L. G., Lima, J. R. B. and Possa, M. V. (2002). "Modelling classification in small-diameter hydrocyclones under variable rheological conditions." Minerals Engineering **15**: 613-622.

Thomas, D. G. (1965). "Transport characteristics of suspension: VIII. A note on the viscosity of Newtonian suspensions of uniform spherical particles." Journal of Colloid Science **20**: 267-277.

Trawinski, H. (1976). "Theory, applications and practical operation of hydrocyclones." Engineering and Mining Journal **September**: 115-127.

Tromp, K. F. (1973). "New methods of computing the washability of coal." Colliery Guardian **CLIV**.

Turian, R. M., Hsu, F. L. G. and Ma, T. W. (1987). "Estimation of the critical velocity in pipeline flow of solids." Powder Technology **51**: 35-47.

Upadrashta, K. R., Ketcham, V. J. and Miller, J. D. (1987). "Tangential velocity profile for Pseudoplastic power-law fluids in the hydrocyclone - a theoretical derivation." Int. J. Miner. Process. **20**: 309-318.

Van Duijn, G. and Rietema, K. (1983). "Performance of a large cone angle hydrocyclone -I." Chemical Engineering Science **38**(10): 1651-1661.

Van Kooy, J. G. (1958). The influence of the Reynold's Number on the operation of a hydrocyclone, Chapter 5 in "Cyclones in Industry". 2nd Symposium on cyclones, Utrecht, Elsevier.

Van Wazer, J. R., Lyons, J. W., Kim, K. Y. and Colwell, R. E. (1963). Viscosity and Flow Measurement - A laboratory handbook of Rheology, Interscience Publishers.

Weedon, D. M., Napier-Munn, T. J. and Evans, C. L. (1990). Studies of mineral liberation performance in sulphide comminution circuits. Sulphide deposits: their origin and processing. P. M. J. Gray. London**:** 135-154.

Wills, B. A. and Napier-Munn, T. J. (2006). Mineral Processing Technology, Elsevier Science.

Yang, H.-G., Li, C.-Z., Gu, H.-c. and Fang, T.-N. (2001). "Rheological behaviour of titanium dioxide suspensions." Journal of Colloid and Interface Science **236**: 96-103.

Yopps, S. W., Spottiswood, D. J., Bull, W. R. and Pillai, K. J. (1987). A study of the effect of slurry rheology on hydrocyclone performance. 3rd International Conference on Hydrocyclones, Oxford, England.

Yoshida, H., Takashina, T., Fukui, K. and Iwanaga, T. (2004). "Effect of inlet shape and slurry temperature on the classification performance of hydro-cyclones." Powder Technology **140**(1-2): 1-9.

Yoshioka, N. and Hotta, Y. (1955). "Liquid Cyclone as a Hydraulic Classifier." Chemical Engineering Japan **19**: 632-640.

Yue, J. and Klein, B. (2004). "Influence of rheology on the performance of horizontal stirred mills." Minerals Engineering **17**(11-12): 1169-1177.

APPENDIX A

Alteration of water viscosity with temperature

According to the Andrade Equation (Andrade, 1930): $\mu = A \exp B/T$

Where A and B are constants: $A = 2.414 \times 10^{-5}$ *Pa·s,* $B = 247.8$ *K. T is the absolute temperature.*

Temperature (°C)	Viscosity (cP)
10	1.305
15	1.140
20	1.005
25	0.893
30	0.800
35	0.721
40	0.653
45	0.595
50	0.546
55	0.502
60	0.464
70	0.401
80	0.352
90	0.312
100	0.279

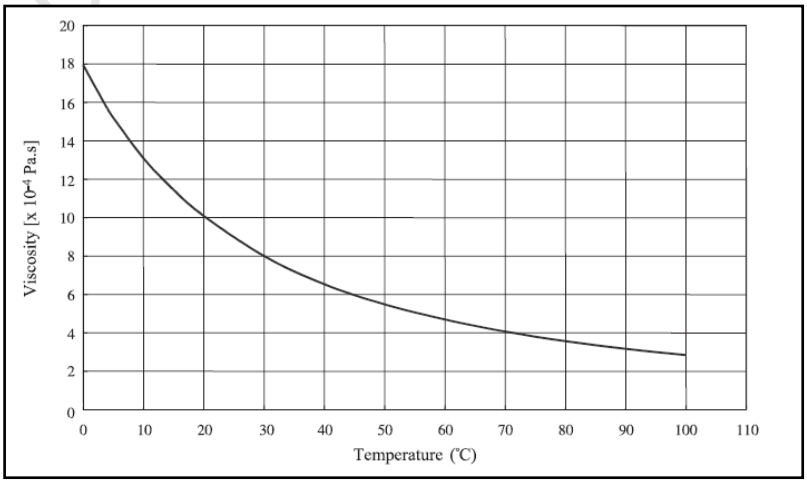

Relationship between water temperature and viscosity, Yoshida *et al.* (2004)

APPENDIX B

Correction of systematic error in rheological measurements

The correction to measured rheological data was obtained by subtracting the theoretical curve for water at room temperature (20°C), $\tau = (1x10^{-3})\gamma$, from the best fitting curve for the tube rheometer water raw data. A rheogram for water (Newtonian fluid) at constant temperature should be a straight line through the origin, although an upward trend arises when the flow regime shifts to the turbulent zone. This results in an over- prediction of water viscosity. For the range of solids concentrations used, the best fitting curve was a polynomial of order 2, i.e. a quadratic. In this regard, the following procedure was applied:

1. A straight line and a quadratic were fitted to the water rheogram and the "goodness of fit" was compared.

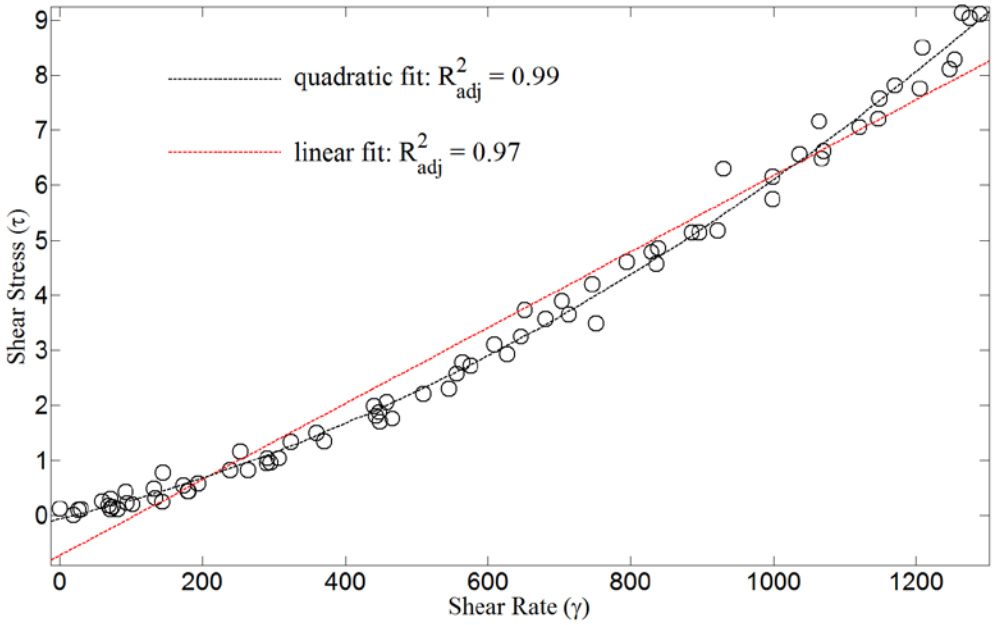

2. The theoretical curve, $\tau = (1x10^{-3})\gamma$, was subtracted from the best fitting curve, $a\gamma^2 + b\gamma + c$, yielding the required correction:

$$\tau_c = a\gamma^2 + b - (1x10^{-3})\gamma + c \quad (1)$$

3. Provided that the measured shear stress (τ_m), for C*m* = 0%, 10%, 20%, 30%, 40%, 50%, 60%, and 70% solids concentrations, did not deviate significantly from the quadratic, the measured shear stress values were corrected by subtracting the corresponding correction (τ_c):

$$\tau_n = \tau_m - \tau_c \quad (2)$$

- *where τ_n is the corrected shear stress.*

4. Motivated by literature, Govier & Aziz (1972), and experimental observations that the rheology appeared to be Bingham-Plastic, a Bingham model (a straight line) was fitted to the corrected rheological data for the slurry conditions. This model appeared to fit the majority of the test conditions well, as most of the data exhibited linear behaviour.

Furthermore, to remove any distinct outliers from the adjusted data the following method was used -

Using a 99% confidence interval for the fitting process, standard deviation error bars were applied to the adjusted data. The difference between the fitted 'y' and the measured 'y' was then determined and the mean of all these differences were taken. The data points that were greater than this mean were then excluded. The data was then replotted and refitted.

APPENDIX C

CPUT pipe loop viscometer rig layout - from Fester (2009)

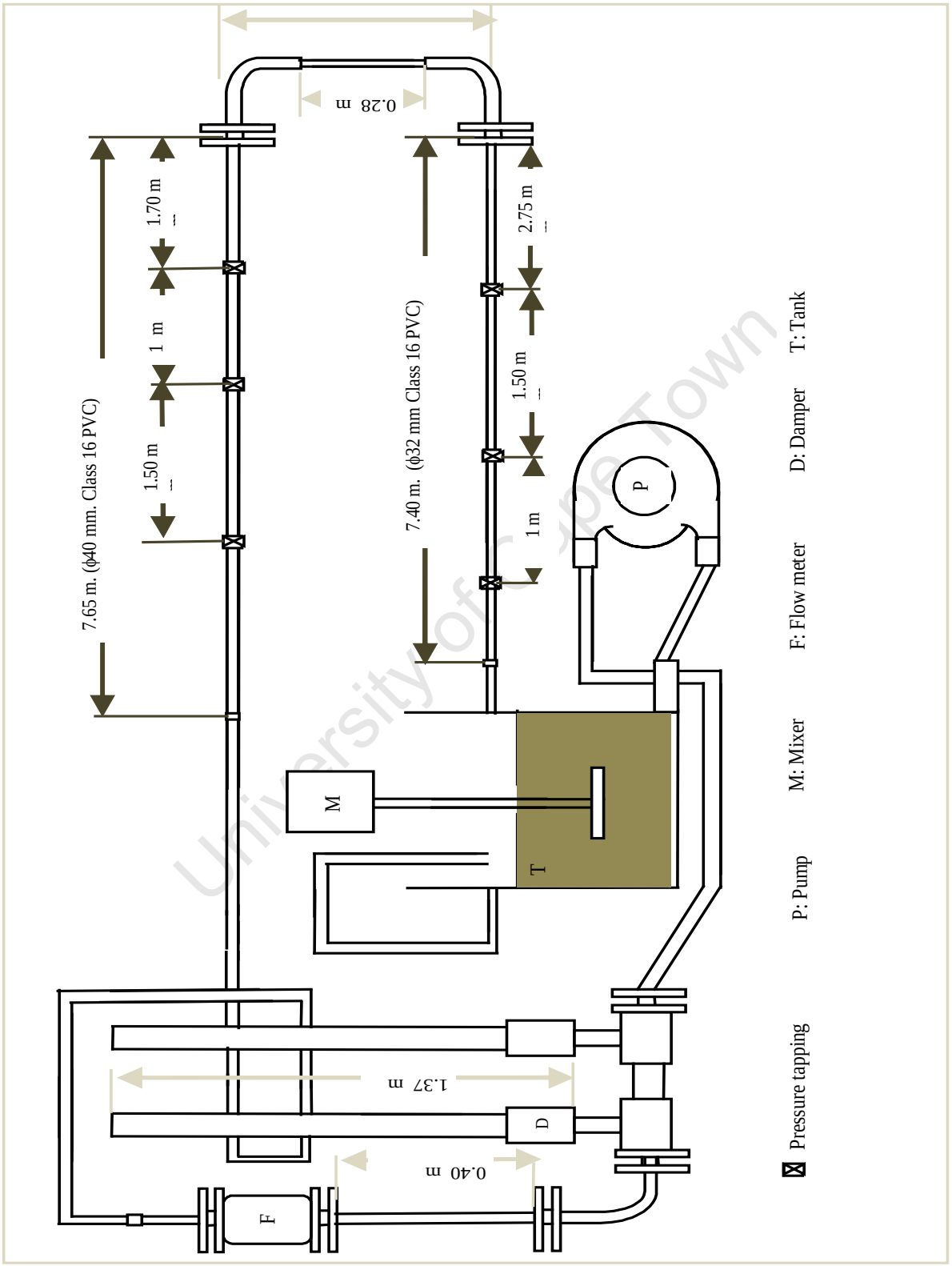

APPENDIX D

Sample sizing procedure (sub 1 mm)

The procedure developed by Powell and Mainza at UCT was applied. Sizing was done on the sub sample after it had passed through a 1.00 mm screen and had then been split on a 10-way rotary sample splitter. The split sample should be about 200 g when using a 200 mm wet screen shaker or approx. 300 g when using a 300 mm wet screen shaker. The dry split sample was first placed in a beaker and mixed with water to obtain a slurry. The sample was then screened using a 300 mm single sieve wet shaker as follows:

Wet Screening

- The sample was slowly poured onto a 25 µm sieve and spray water was manually added as required. Undersize sample was collected in a large diameter bucket. Screening continued until all water passing the sieve was clear. The sub 25 µm material (fines) was kept in the buckets for filtering. (If agglomerated material was discovered on the sieve during this stage, it was first placed in a beaker in an ultrasonic bath and then poured over the sieve once more).
- The +25 µm material retained on the 25 µm sieve was then washed onto a 53 µm sieve and the screening procedure was repeated. The material that was retained on the 53 µm sieve was washed into a dish for drying.
- After decanting some of the clear water from the undersize bucket, the minus 53 µm material was poured onto a 38 µm sieve and sieving was repeated once more. The +38 µm material was then washed into a dish for drying.
- The minus 38 µm material was again poured over a 25 µm sieve to ensure that all the minus 25 µm material had passed through the 25 µm sieve. The +25 µm material was then washed into a dish for drying.
- Any resultant minus 25 µm material from this stage was added to the initial minus 25 µm material and the sample was filtered in a swing barrel filter press. After filtering was complete the filter cake was placed in the oven along with the other size fractions.
- After drying, all size fractions were weighed and the masses recorded.

Dry Screening

- The dry +53 µm size fraction was dry screened on a 200 mm shaker deck for approx. 20 minutes using an 850,600,425,300,212,150,106,75, and 53 µm screen deck. Any sub 53 µm material was allocated to the +38 µm size fraction.
- All size fractions were then weighed, and a total mass integrity check was done to identify any screening losses. The size fractions were all kept in case of any sample issues arising at a later stage during the mass balancing.

APPENDIX E

Efficiency Curves – Mass balanced, unfitted data.

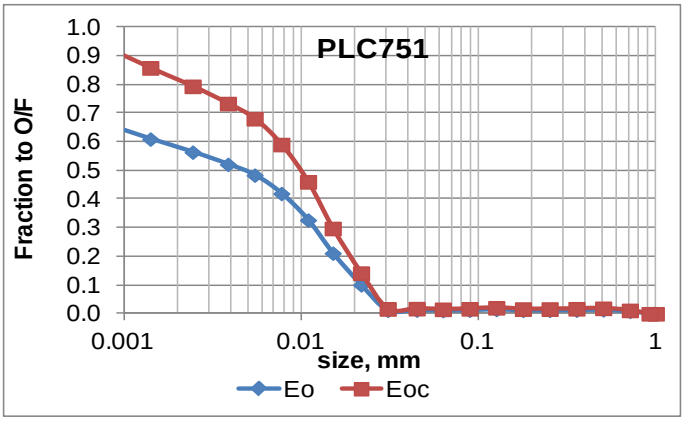

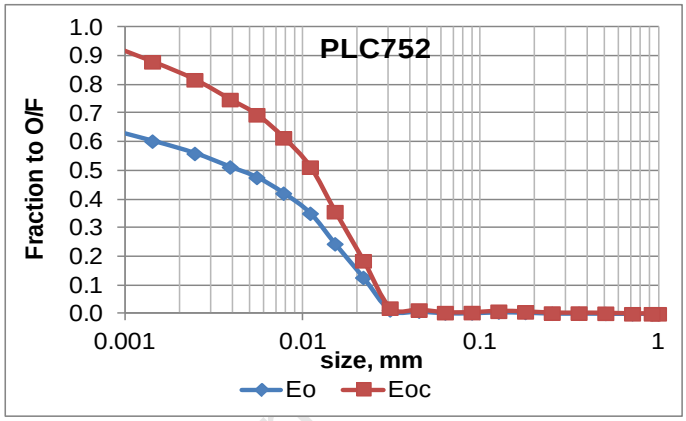

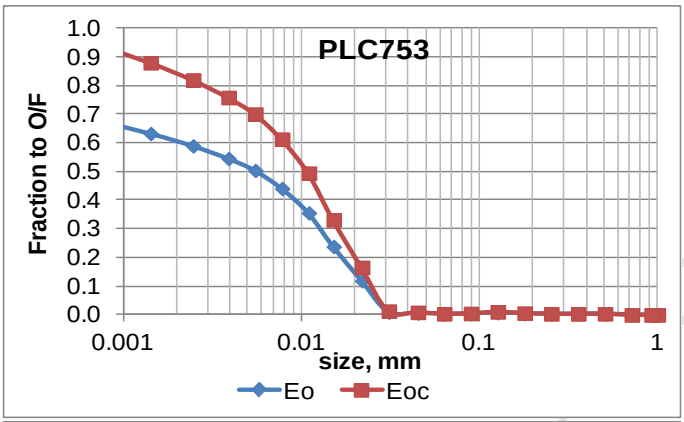

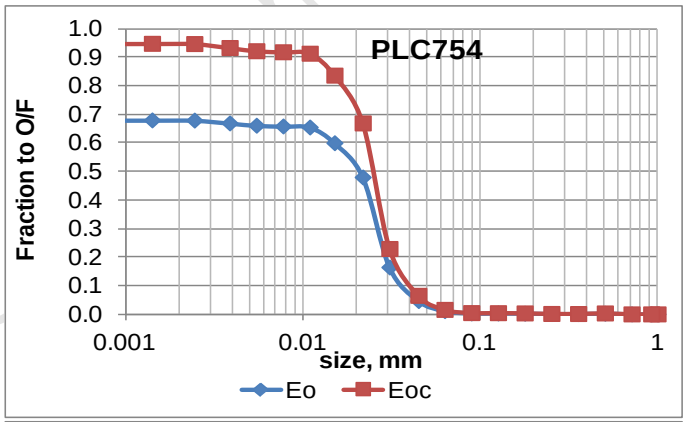

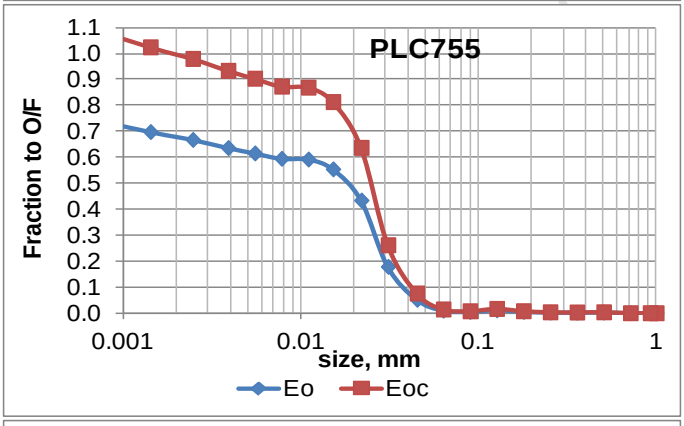

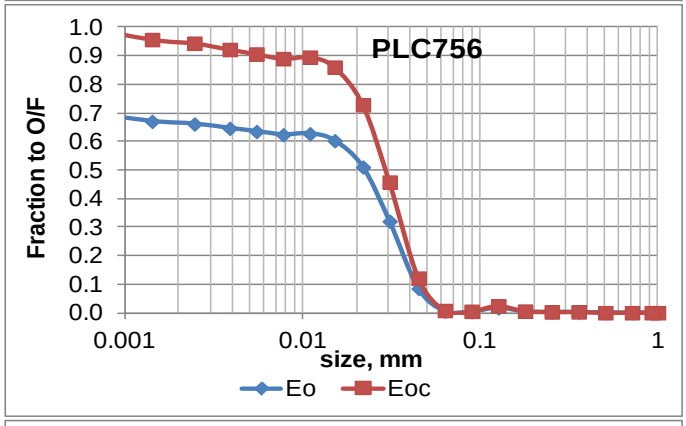

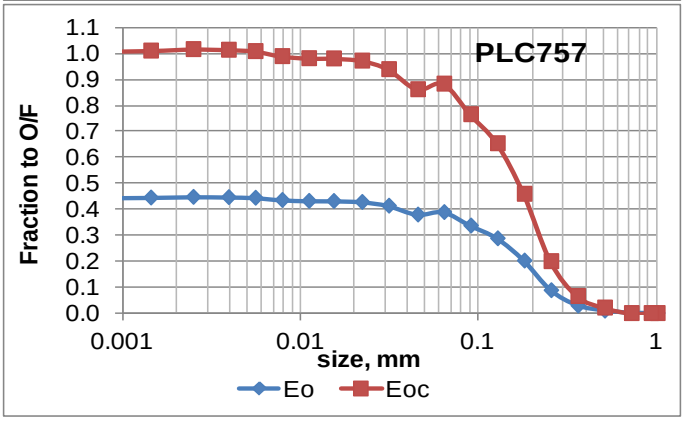

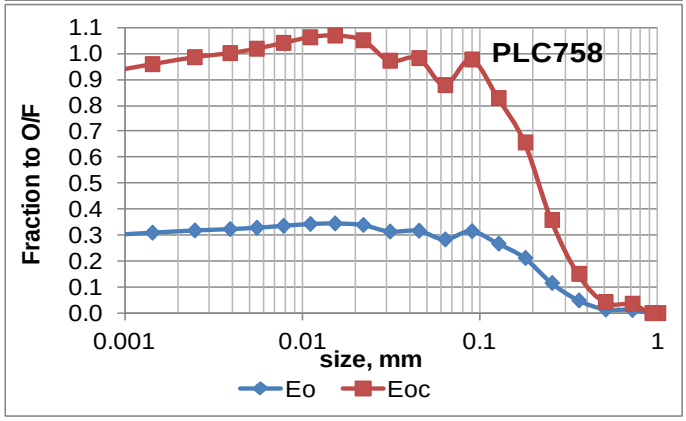

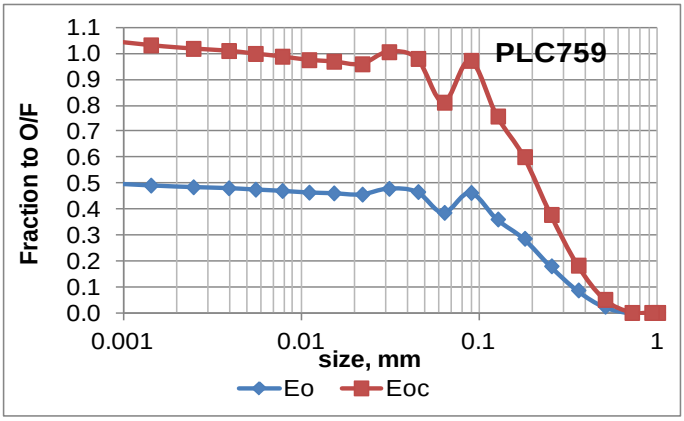
PLC759
Fraction to O/F
size, mm
Eo
Eoc

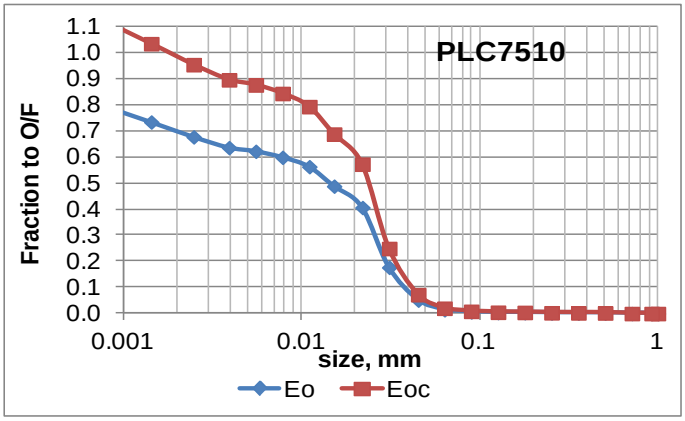
PLC7510
Fraction to O/F
size, mm
Eo
Eoc

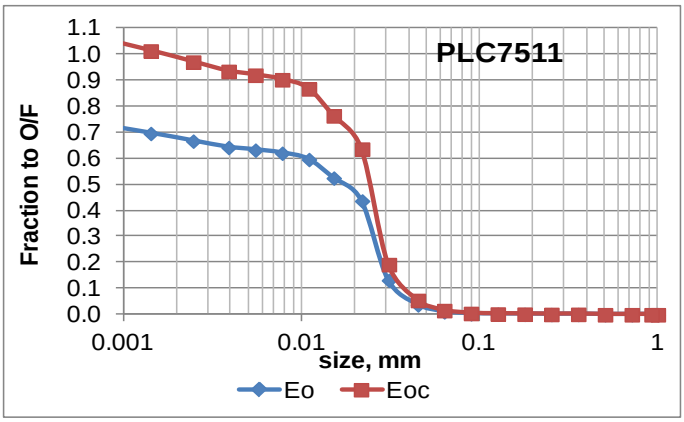
PLC7511
Fraction to O/F
size, mm
Eo
Eoc

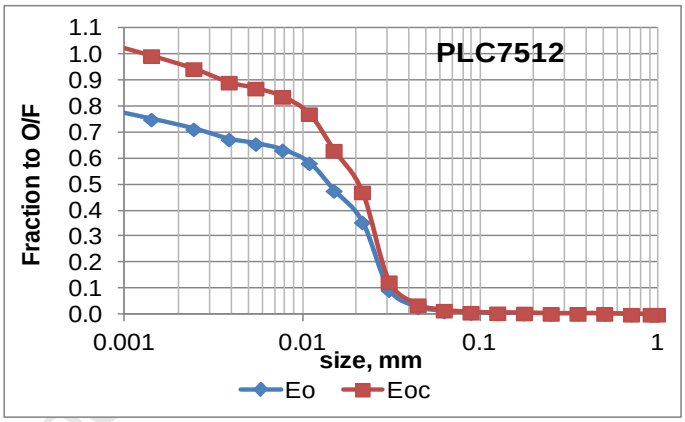
PLC7512
Fraction to O/F
size, mm
Eo
Eoc

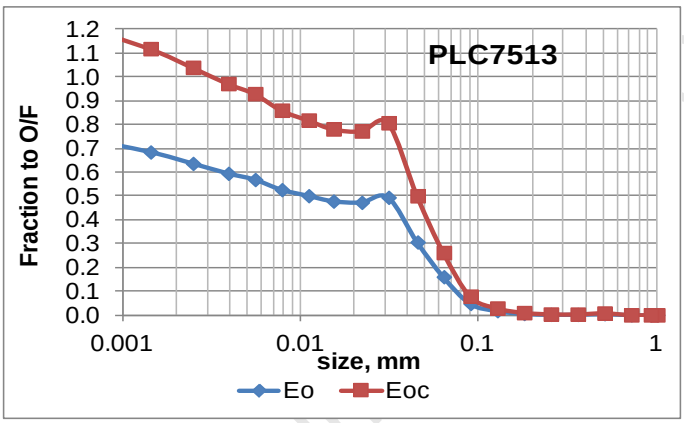
PLC7513
Fraction to O/F
size, mm
Eo
Eoc

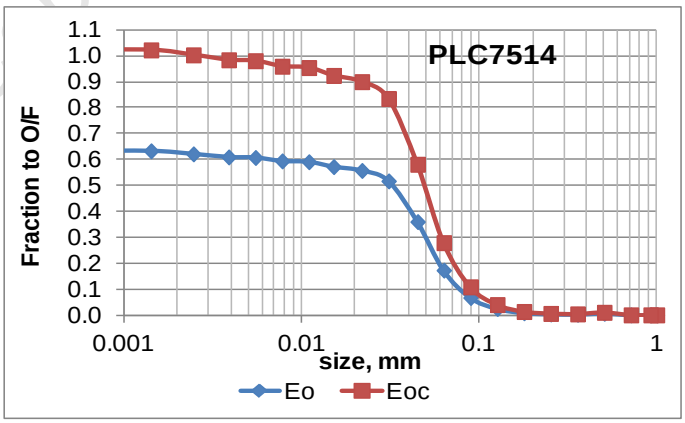
PLC7514
Fraction to O/F
size, mm
Eo
Eoc

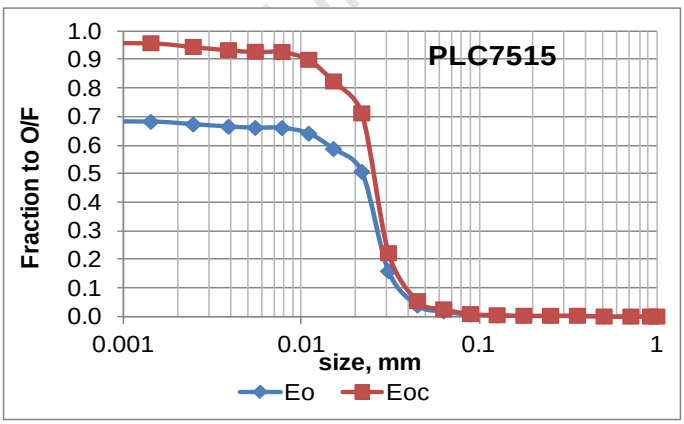
PLC7515
Fraction to O/F
size, mm
Eo
Eoc

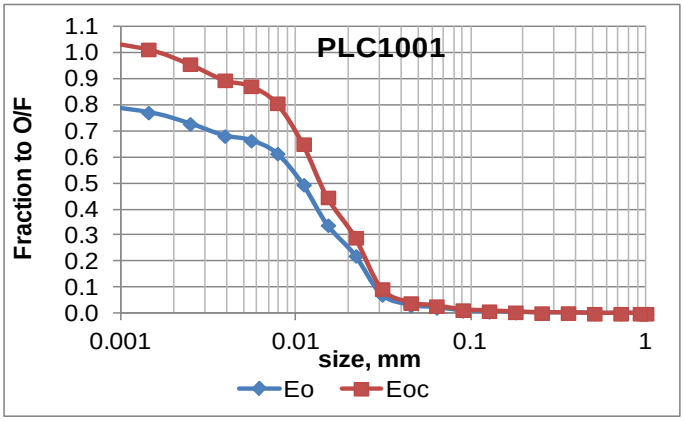
PLC1001
Fraction to O/F
size, mm
Eo
Eoc

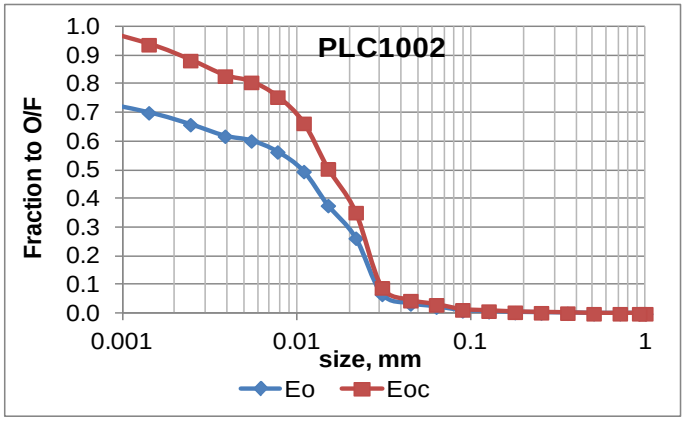
PLC1002
Fraction to O/F
size, mm
Eo
Eoc

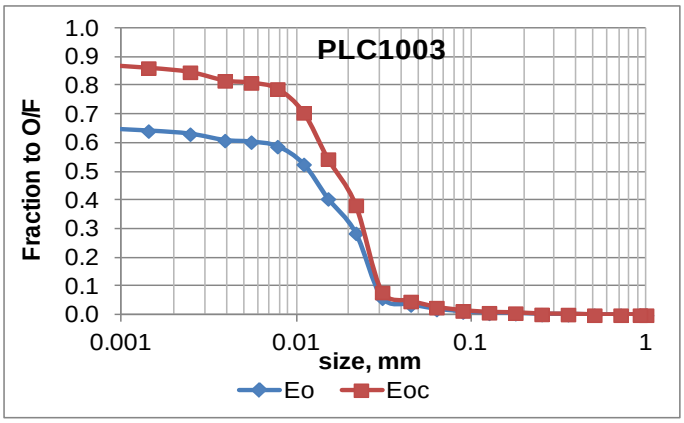
PLC1003
Fraction to O/F
size, mm
Eo
Eoc

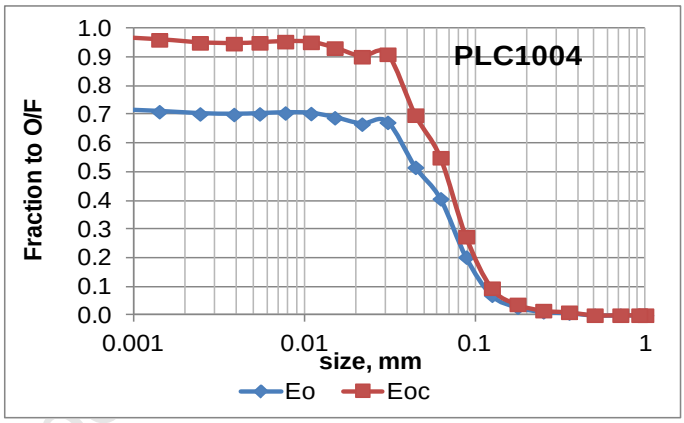
PLC1004
Fraction to O/F
size, mm
Eo
Eoc

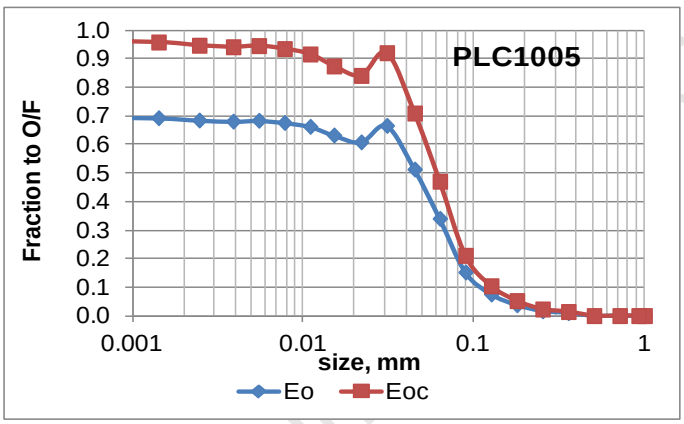
PLC1005
Fraction to O/F
size, mm
Eo
Eoc

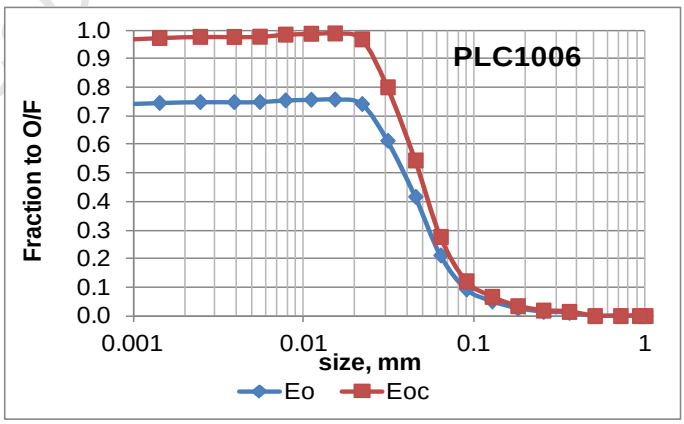
PLC1006
Fraction to O/F
size, mm
Eo
Eoc

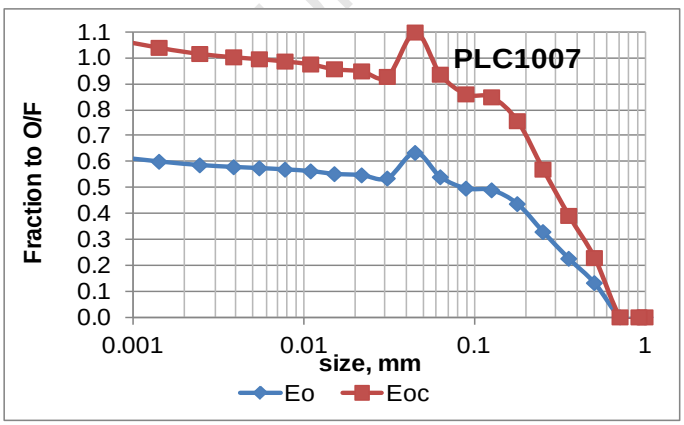
PLC1007
Fraction to O/F
size, mm
Eo
Eoc

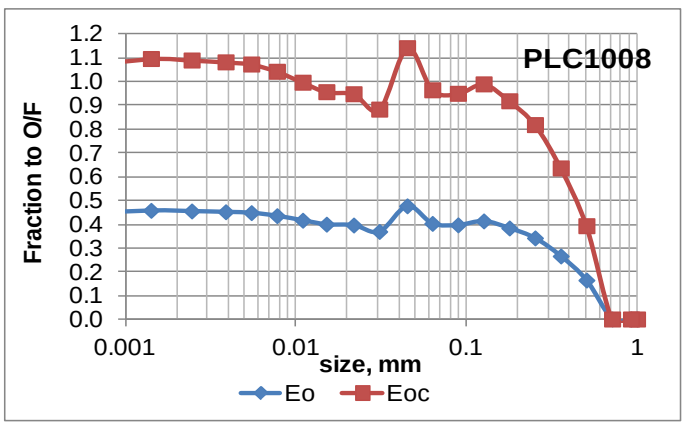
PLC1008
Fraction to O/F
size, mm
Eo
Eoc

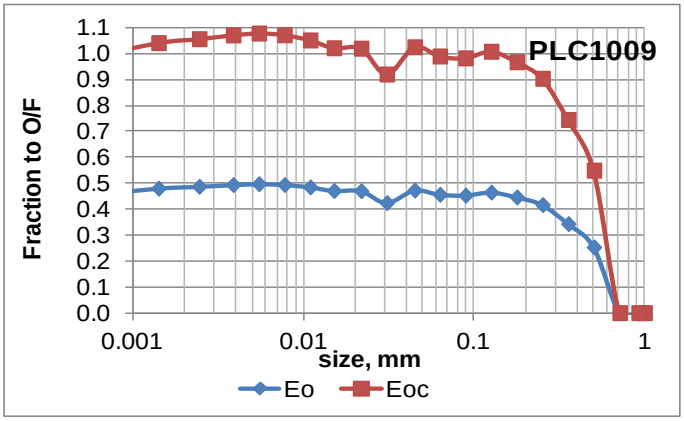
PLC1009
Fraction to O/F
size, mm
Eo
Eoc

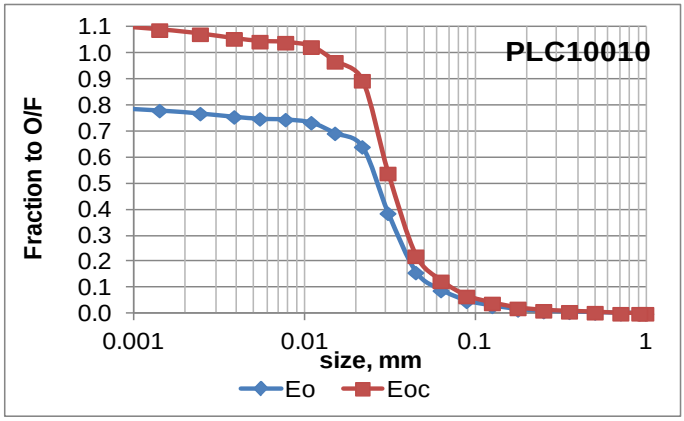
PLC10010
Fraction to O/F
size, mm
Eo
Eoc

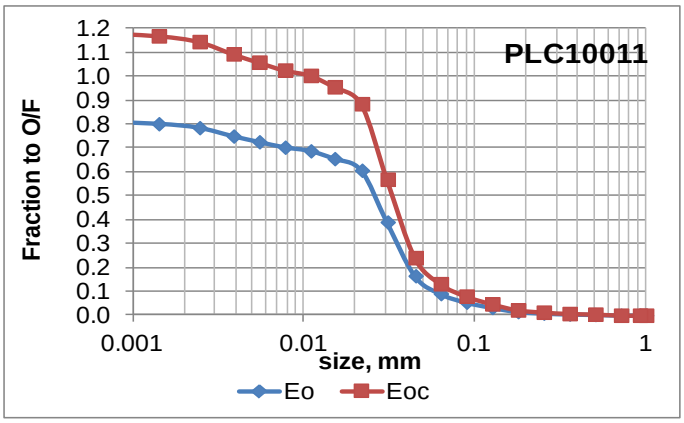
PLC10011
Fraction to O/F
size, mm
Eo
Eoc

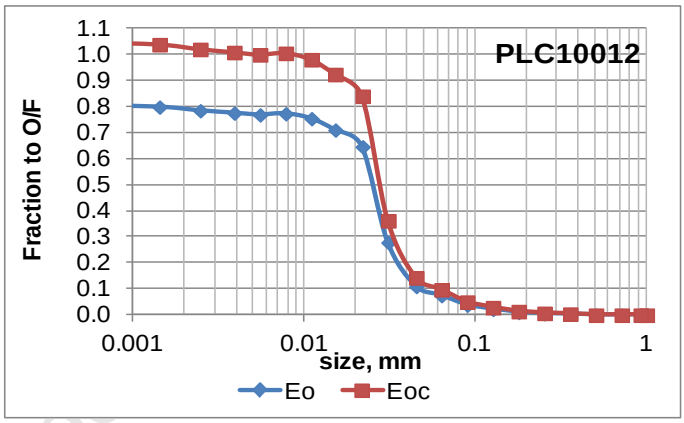
PLC10012
Fraction to O/F
size, mm
Eo
Eoc

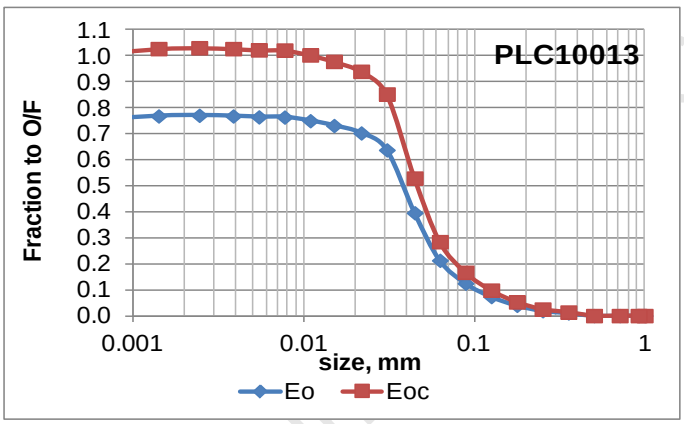
PLC10013
Fraction to O/F
size, mm
Eo
Eoc

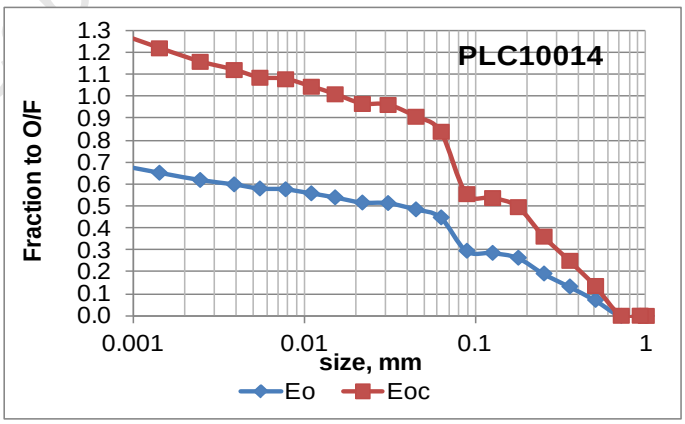
PLC10014
Fraction to O/F
size, mm
Eo
Eoc

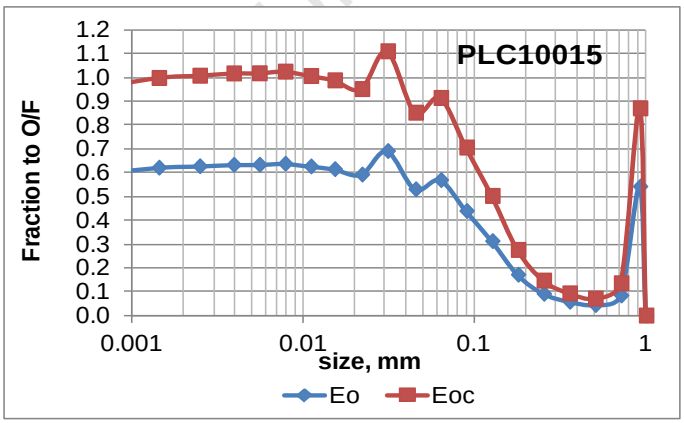
PLC10015
Fraction to O/F
size, mm
Eo
Eoc

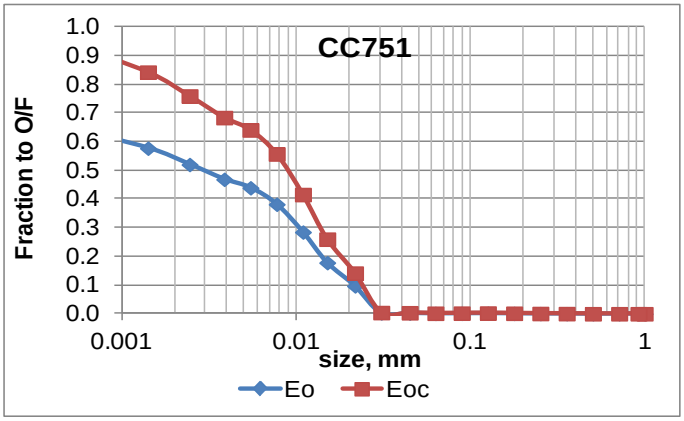
CC751
Fraction to O/F
1.0
0.9
0.8
0.7
0.6
0.5
0.4
0.3
0.2
0.1
0.0
0.001
0.01
0.1
1
size, mm
Eo
Eoc

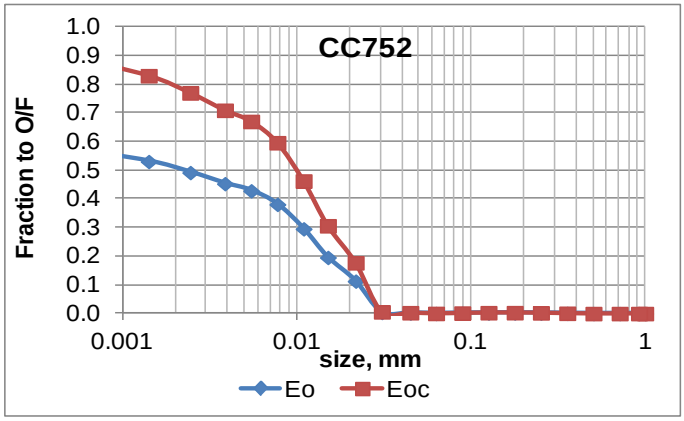
CC752
Fraction to O/F
1.0
0.9
0.8
0.7
0.6
0.5
0.4
0.3
0.2
0.1
0.0
0.001
0.01
0.1
1
size, mm
Eo
Eoc

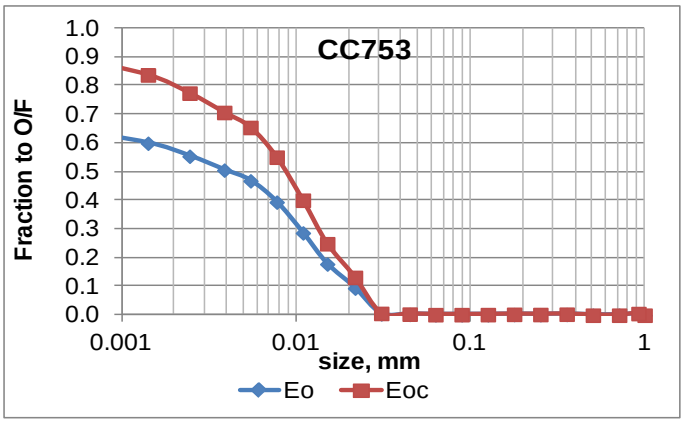
CC753
Fraction to O/F
1.0
0.9
0.8
0.7
0.6
0.5
0.4
0.3
0.2
0.1
0.0
0.001
0.01
0.1
1
size, mm
Eo
Eoc

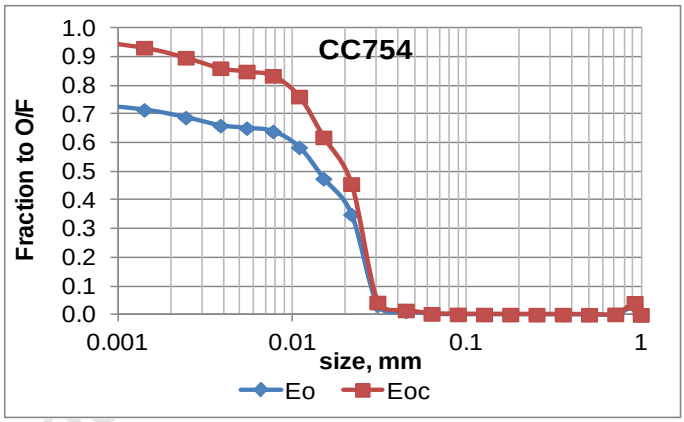
CC754
Fraction to O/F
1.0
0.9
0.8
0.7
0.6
0.5
0.4
0.3
0.2
0.1
0.0
0.001
0.01
0.1
1
size, mm
Eo
Eoc

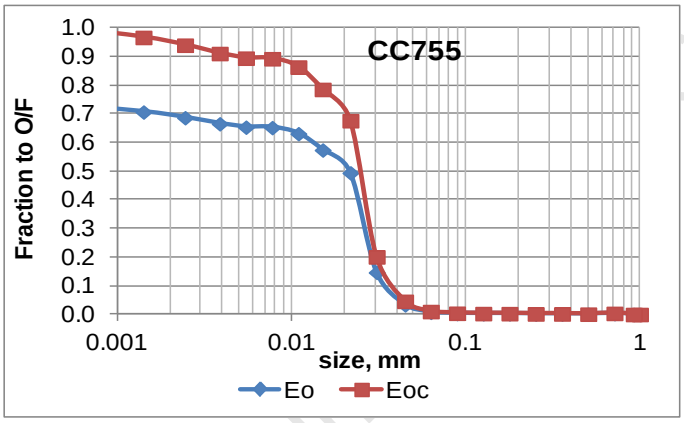
CC755
Fraction to O/F
1.0
0.9
0.8
0.7
0.6
0.5
0.4
0.3
0.2
0.1
0.0
0.001
0.01
0.1
1
size, mm
Eo
Eoc

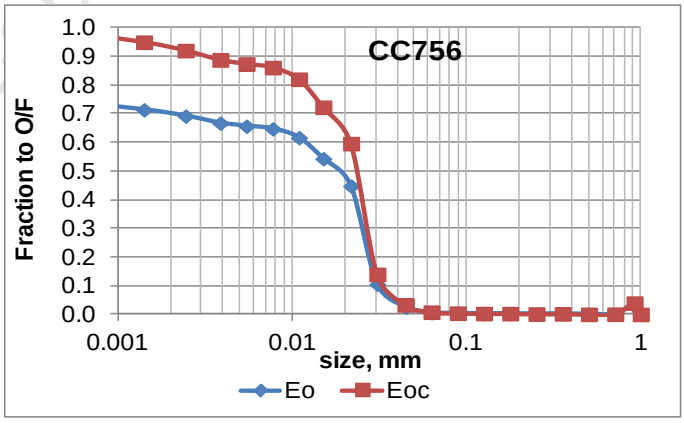
CC756
Fraction to O/F
1.0
0.9
0.8
0.7
0.6
0.5
0.4
0.3
0.2
0.1
0.0
0.001
0.01
0.1
1
size, mm
Eo
Eoc

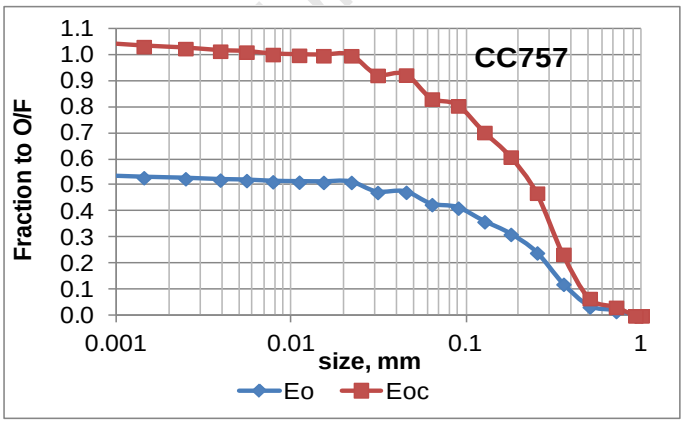
CC757
Fraction to O/F
1.1
1.0
0.9
0.8
0.7
0.6
0.5
0.4
0.3
0.2
0.1
0.0
0.001
0.01
0.1
1
size, mm
Eo
Eoc

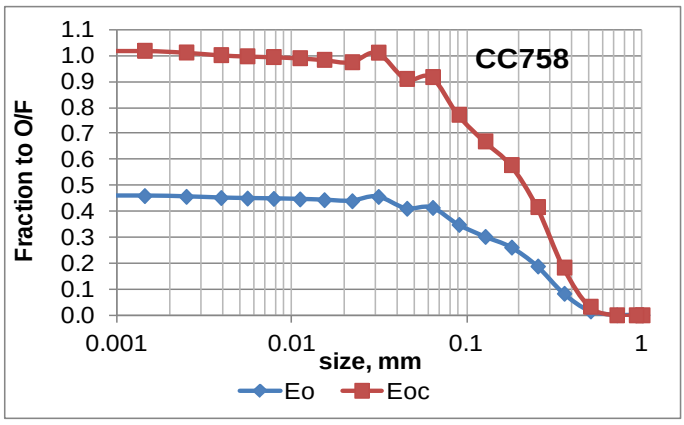
CC758
Fraction to O/F
1.1
1.0
0.9
0.8
0.7
0.6
0.5
0.4
0.3
0.2
0.1
0.0
0.001
0.01
0.1
1
size, mm
Eo
Eoc

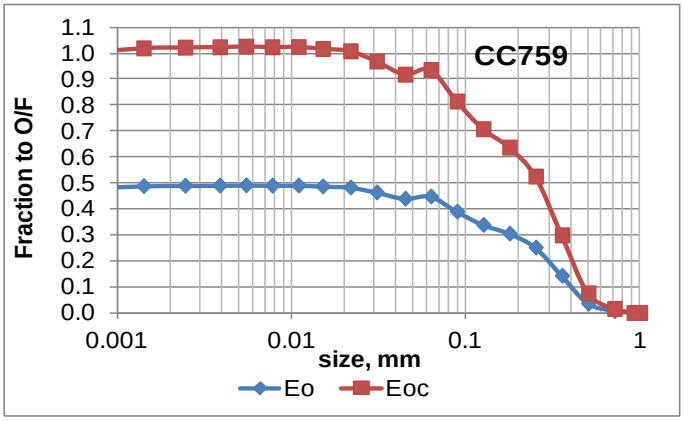
CC759
Fraction to O/F
size, mm
Eo
Eoc

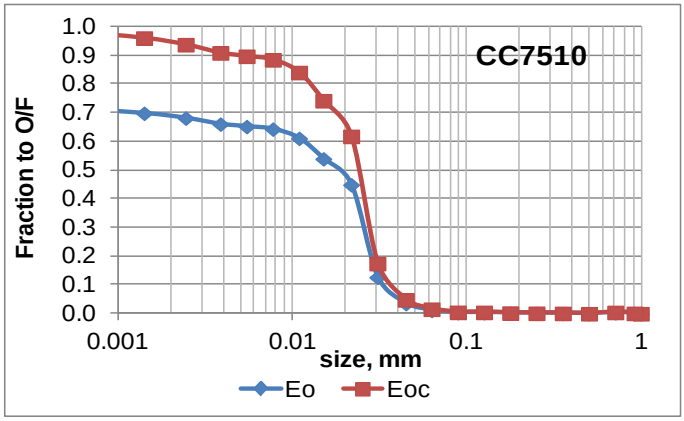
CC7510
Fraction to O/F
size, mm
Eo
Eoc

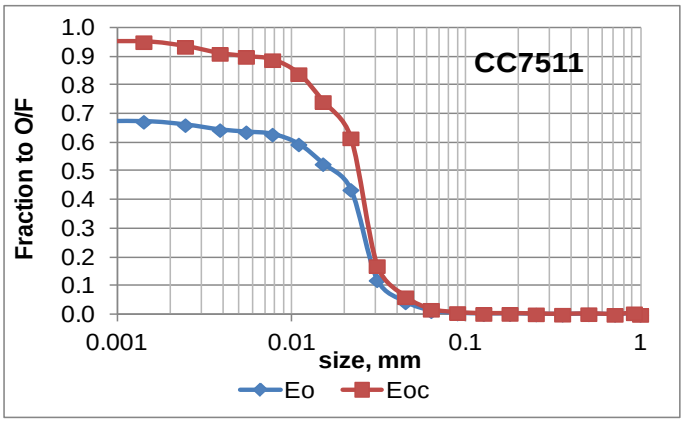
CC7511
Fraction to O/F
size, mm
Eo
Eoc

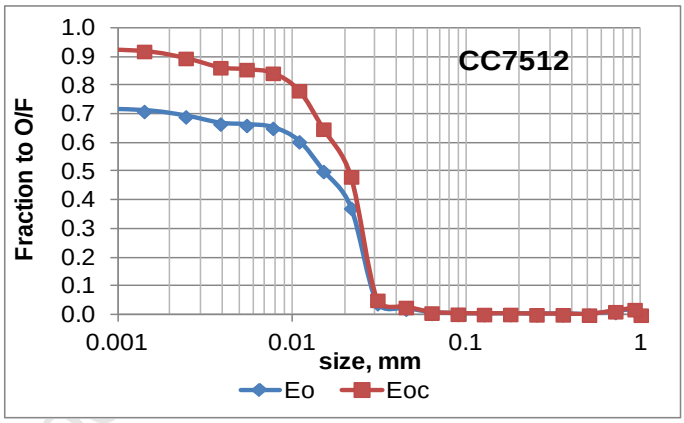
CC7512
Fraction to O/F
size, mm
Eo
Eoc

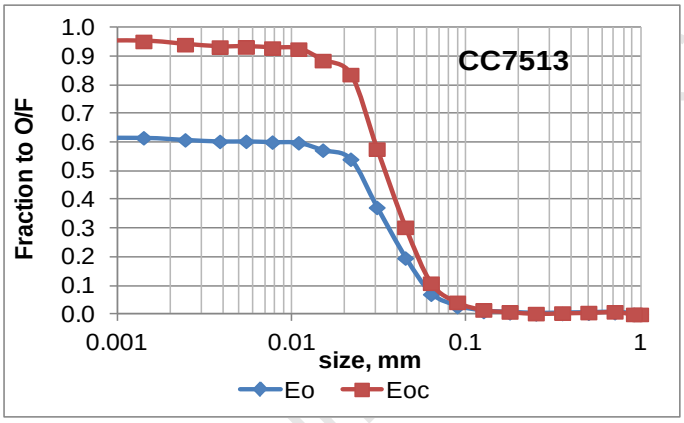
CC7513
Fraction to O/F
size, mm
Eo
Eoc

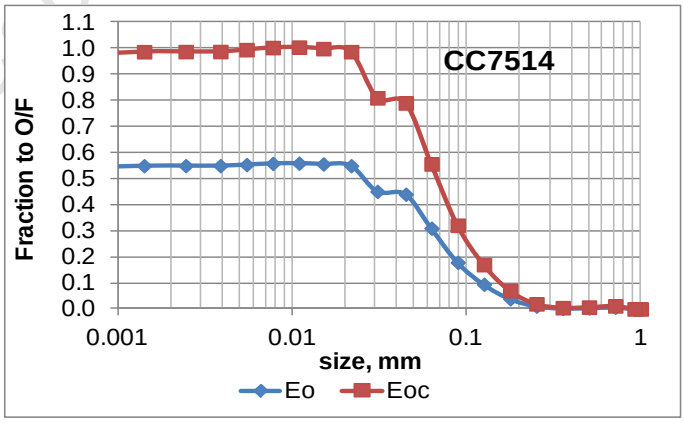
CC7514
Fraction to O/F
size, mm
Eo
Eoc

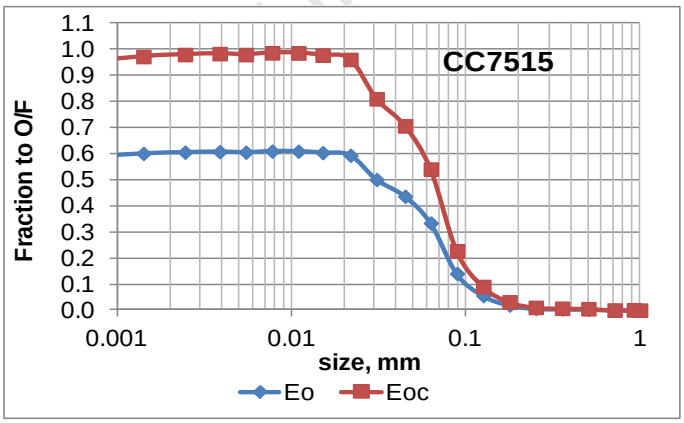
CC7515
Fraction to O/F
size, mm
Eo
Eoc

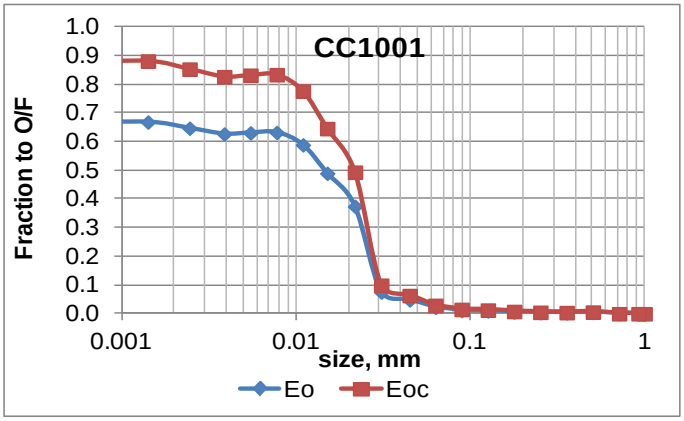
CC1001
Fraction to O/F
1.0
0.9
0.8
0.7
0.6
0.5
0.4
0.3
0.2
0.1
0.0
0.001
0.01
0.1
1
size, mm
Eo
Eoc

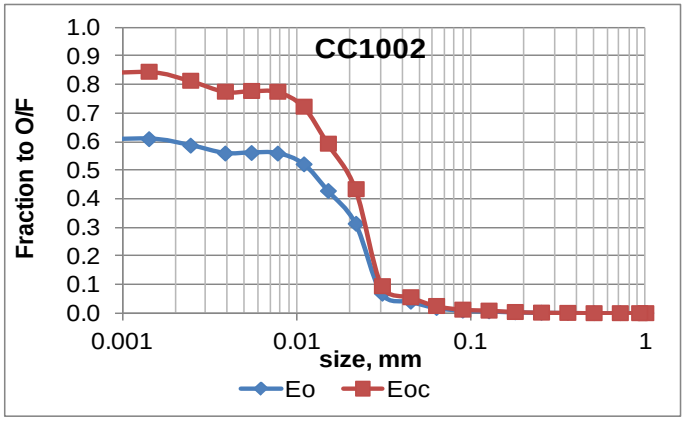
CC1002
Fraction to O/F
1.0
0.9
0.8
0.7
0.6
0.5
0.4
0.3
0.2
0.1
0.0
0.001
0.01
0.1
1
size, mm
Eo
Eoc

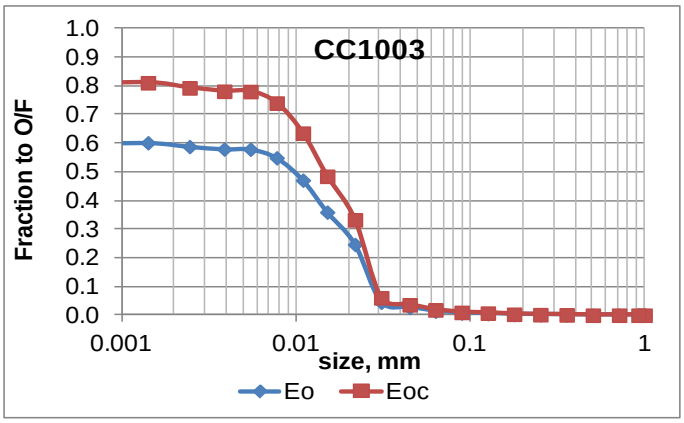
CC1003
Fraction to O/F
1.0
0.9
0.8
0.7
0.6
0.5
0.4
0.3
0.2
0.1
0.0
0.001
0.01
0.1
1
size, mm
Eo
Eoc

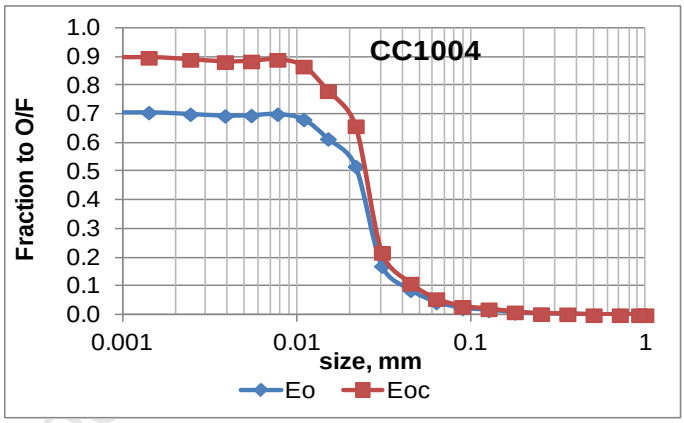
CC1004
Fraction to O/F
1.0
0.9
0.8
0.7
0.6
0.5
0.4
0.3
0.2
0.1
0.0
0.001
0.01
0.1
1
size, mm
Eo
Eoc

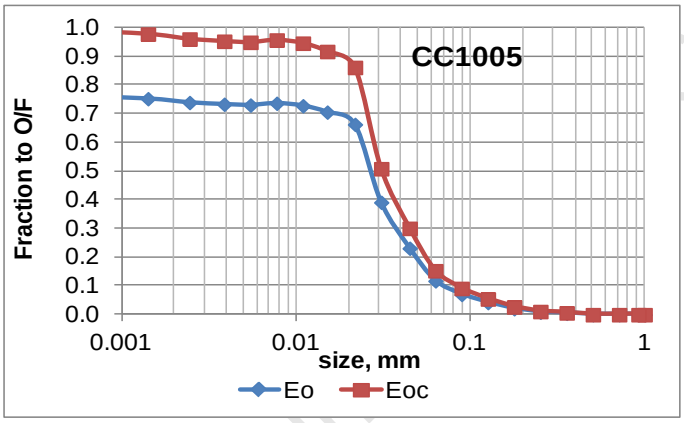
CC1005
Fraction to O/F
1.0
0.9
0.8
0.7
0.6
0.5
0.4
0.3
0.2
0.1
0.0
0.001
0.01
0.1
1
size, mm
Eo
Eoc

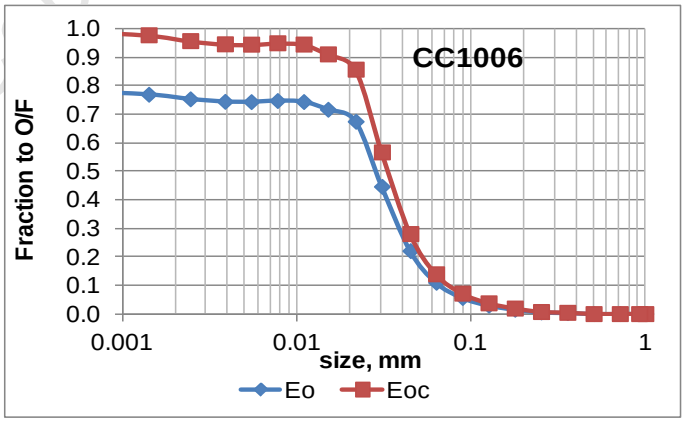
CC1006
Fraction to O/F
1.0
0.9
0.8
0.7
0.6
0.5
0.4
0.3
0.2
0.1
0.0
0.001
0.01
0.1
1
size, mm
Eo
Eoc

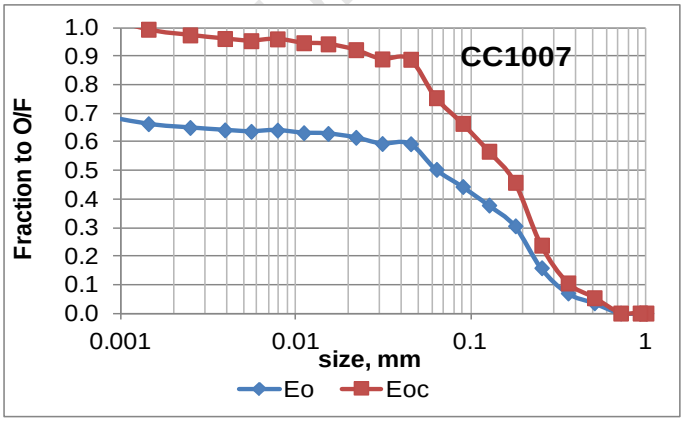
CC1007
Fraction to O/F
1.0
0.9
0.8
0.7
0.6
0.5
0.4
0.3
0.2
0.1
0.0
0.001
0.01
0.1
1
size, mm
Eo
Eoc

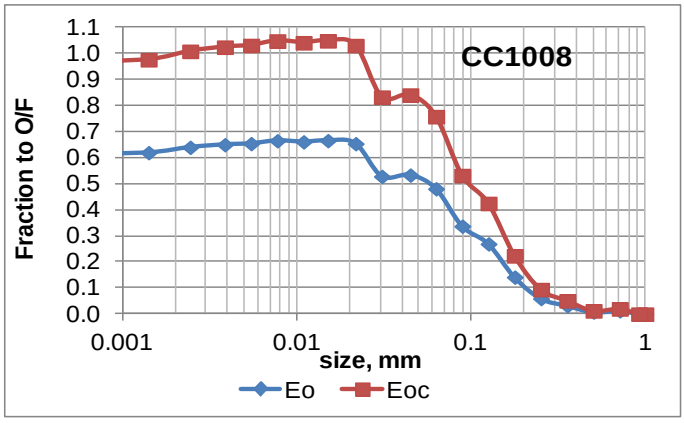
CC1008
Fraction to O/F
1.1
1.0
0.9
0.8
0.7
0.6
0.5
0.4
0.3
0.2
0.1
0.0
0.001
0.01
0.1
1
size, mm
Eo
Eoc

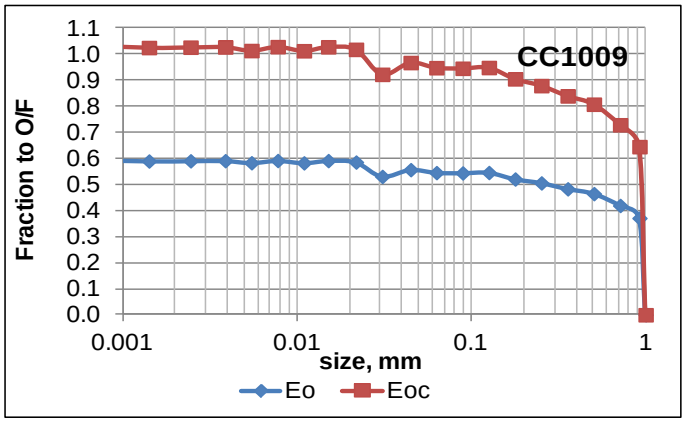

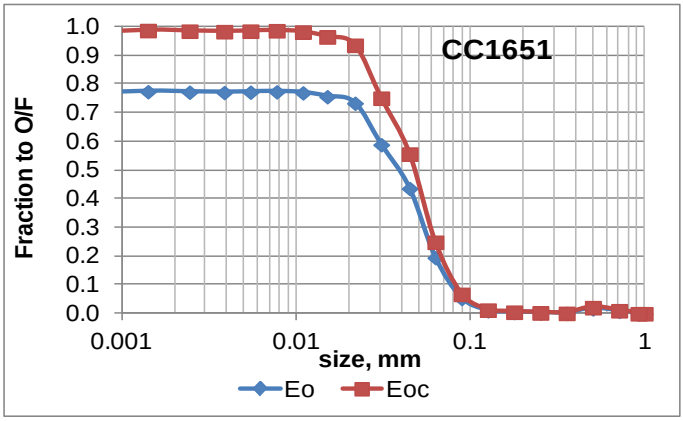
CC1651
Fraction to O/F
size, mm
Eo
Eoc

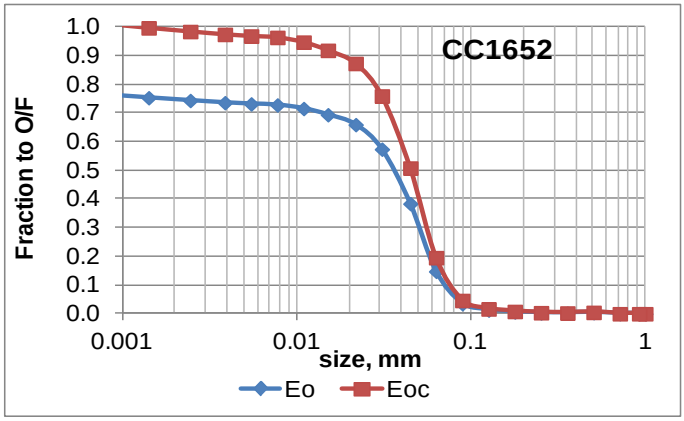
CC1652
Fraction to O/F
size, mm
Eo
Eoc

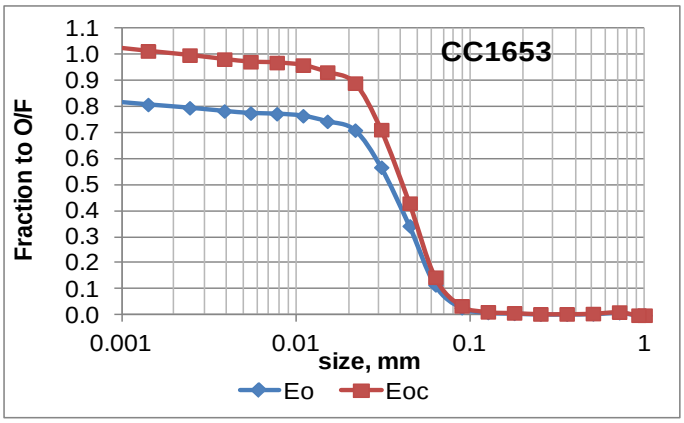
CC1653
Fraction to O/F
size, mm
Eo
Eoc

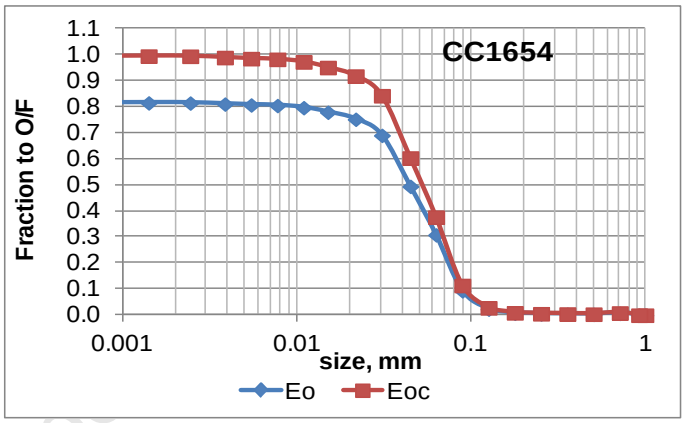
CC1654
Fraction to O/F
size, mm
Eo
Eoc

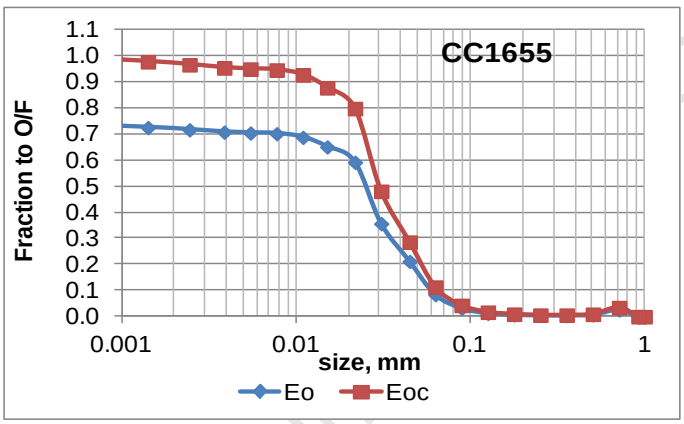
CC1655
Fraction to O/F
size, mm
Eo
Eoc

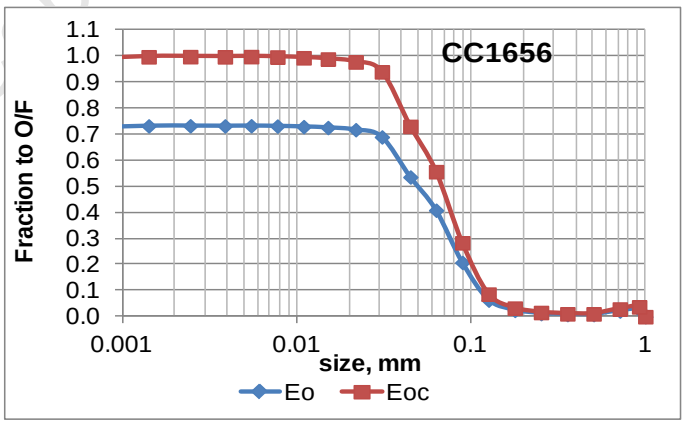
CC1656
Fraction to O/F
size, mm
Eo
Eoc

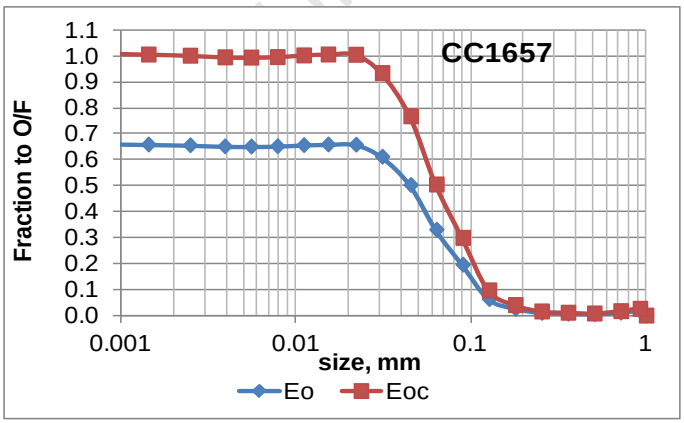
CC1657
Fraction to O/F
size, mm
Eo
Eoc

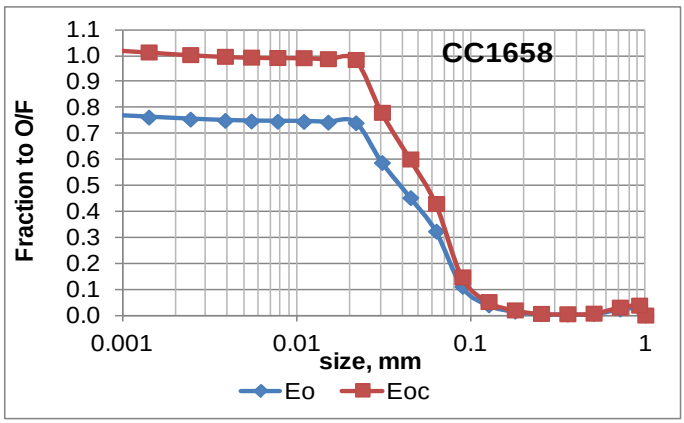
CC1658
Fraction to O/F
size, mm
Eo
Eoc

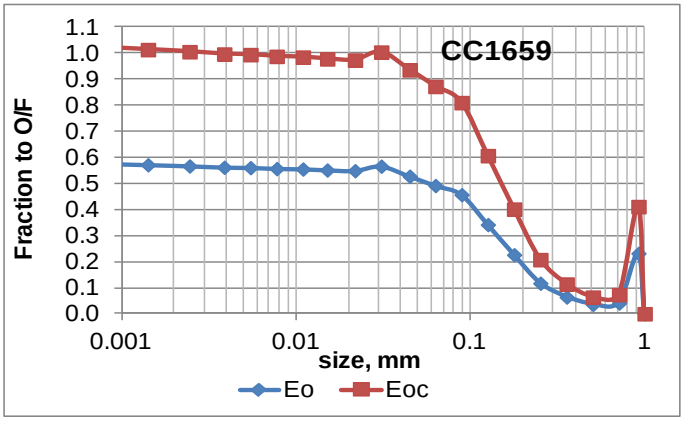

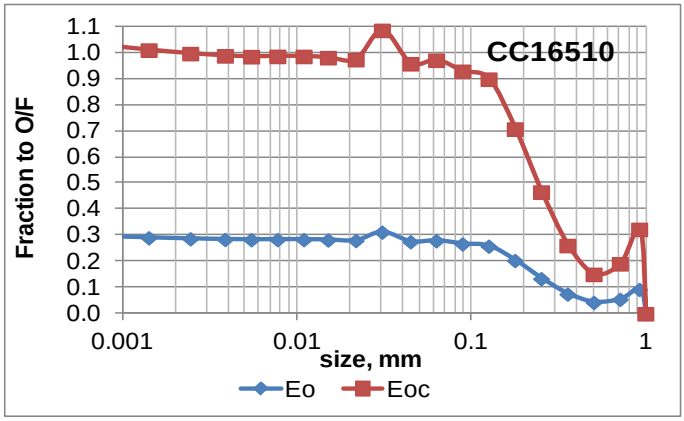

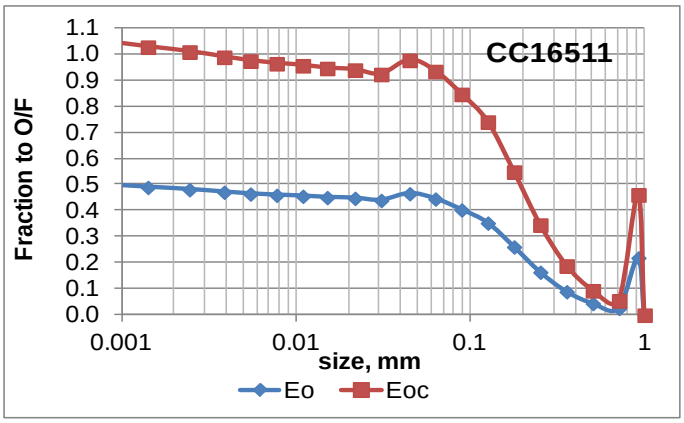

APPENDIX F

Efficiency curve parameters from Whiten fit

Test #	Test ID	Q (tph)	Feed P (kPa)	d_{50c}, µm	C	α
1	PLC751	5.01	120	9.9	0.68	1.19
2	PLC752	4.12	95	11.0	0.65	1.23
3	PLC753	4.61	123	10.8	0.69	1.33
4	PLC754	9.88	120	25.7	0.68	5.27
5	PLC755	8.34	96	24.2	0.69	2.92
6	PLC756	9.96	120	30.3	0.67	3.89
7	PLC757	10.19	93	162.0	0.44	2.13
8	PLC758	9.25	65	220.0	0.33	3.20
9	PLC759	10.43	95	213.2	0.48	2.28
10	PLC7510	7.32	120	20.1	0.75	1.57
11	PLC7511	6.60	95	23.4	0.69	3.37
12	PLC7512	7.68	120	18.8	0.76	2.17
13	PLC7513	6.40	120	38.9	0.66	1.25
14	PLC7514	5.69	95	50.1	0.62	3.19
15	PLC7515	5.80	120	26.1	0.67	5.72
16	PLC1001	6.49	88	13.8	0.81	1.58
17	PLC1002	5.65	68	15.8	0.73	1.65
18	PLC1003	6.57	88	19.1	0.65	2.93
19	PLC1004	16.09	100	69.0	0.72	2.99
20	PLC1005	13.44	75	65.0	0.69	3.14
21	PLC1006	15.11	100	49.9	0.77	3.53
22	PLC1007	18.07	80	296.1	0.59	1.97
23	PLC1008	14.16	50	416.9	0.43	3.31
24	PLC1009	15.44	80	485	0.47	4.56
25	PLC10010	10.08	92	32.3	0.78	3.32

Test #	Test ID	Q (tph)	Feed P (kPa)	d_{50c}, µm	C	α
26	PLC10011	9.02	70	31.3	0.79	2.38
27	PLC10012	10.65	91	28.6	0.79	4.60
28	PLC10013	8.63	92	49.1	0.78	2.84
29	PLC10014	7.74	72	110.5	0.63	0.27
30	PLC10015	8.46	80	132.1	0.64	2.43
31	CC751	4.88	120	9.3	0.64	1.10
32	CC752	1.46	90	11.3	0.56	1.46
33	CC753	4.95	120	9.7	0.65	1.34
34	CC754	11.14	140	19.9	0.71	3.37
35	CC755	9.35	105	25.2	0.69	4.80
36	CC756	11.24	140	23.3	0.70	4.08
37	CC757	15.86	120	211.1	0.53	1.38
38	CC758	13.86	90	200.1	0.46	1.68
39	CC759	14.93	115	233.1	0.49	1.57
40	CC7510	8.02	130	23.9	0.69	4.00
41	CC7511	7.06	100	24.0	0.66	4.20
42	CC7512	8.10	130	21.0	0.70	3.95
43	CC7513	7.11	120	37.0	0.62	3.45
44	CC7514	6.20	90	71.6	0.57	2.43
45	CC7515	7.23	120	65.3	0.62	2.93
46	CC1001	6.93	90	22.1	0.66	2.19
47	CC1002	5.96	70	21.3	0.59	3.61
48	CC1003	6.46	90	18.2	0.61	2.90
49	CC1004	14.28	92	26.0	0.71	5.18
50	CC1005	12.29	70	35.7	0.77	2.90
51	CC1006	14.06	92	36.2	0.77	3.29
52	CC1007	21.96	100	149.2	0.67	1.22

Test #	Test ID	Q (tph)	Feed P (kPa)	d_{50c}, µm	C	α
53	CC1008	18.76	80	103.7	0.66	1.61
54	CC1009	24.15	95	500	0.62	0.50
55	CC1651	25.88	75	48.0	0.79	3.49
56	CC1652	18.97	55	45.2	0.75	3.35
57	CC1653	23.71	75	41.4	0.81	3.49
58	CC1654	17.98	45	53.9	0.82	3.17
59	CC1655	20.50	75	33.6	0.74	2.75
60	CC1656	17.11	70	68.3	0.74	3.13
61	CC1657	15.24	50	67.6	0.67	3.06
62	CC1658	17.92	70	54.6	0.78	2.68
63	CC1659	14.58	70	158.1	0.57	2.11
64	CC16510	12.14	47	272.5	0.30	1.19
65	CC16511	14.46	65	205.5	0.48	1.84

APPENDIX G

Reduced efficiency curves for all tests

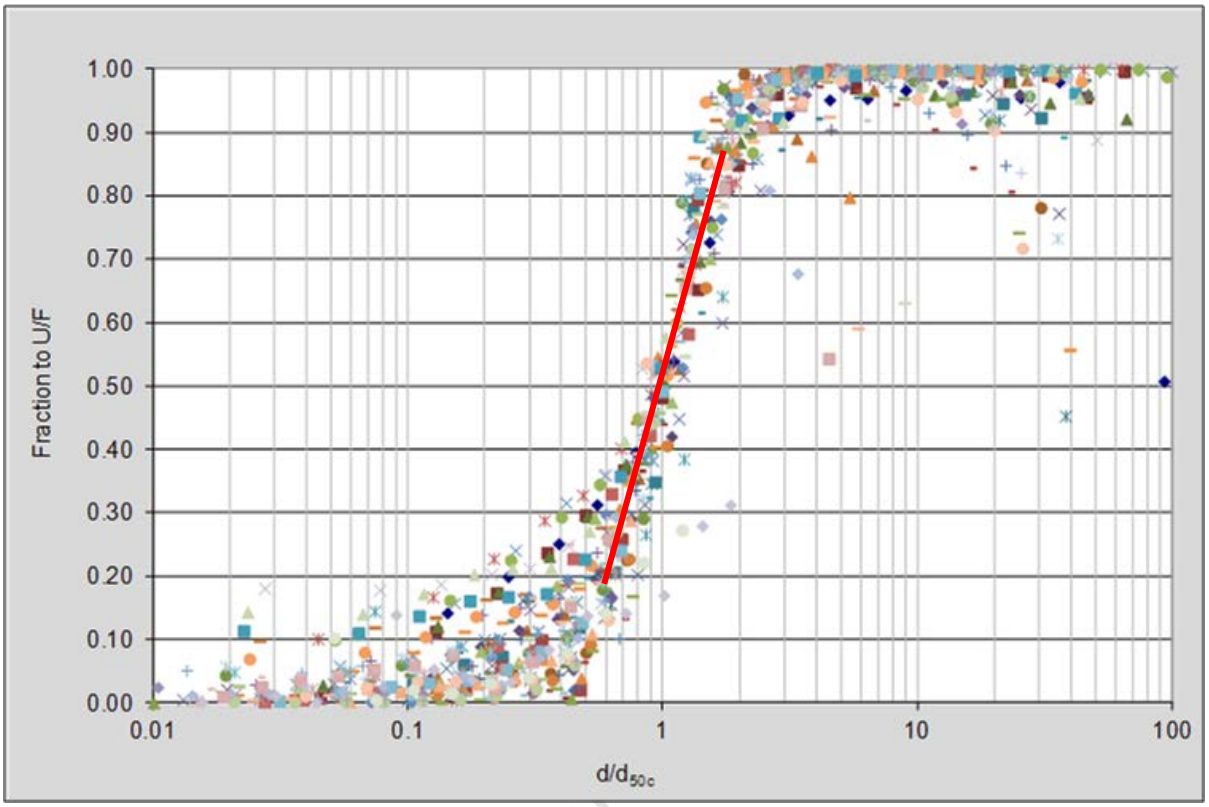

Reduced efficiency curves for 65 tests - including 2 ore types and 3 cyclone sizes.